UNIVERSIDADE
BEIRA INTERIOR

Biomarkers in Barrett's Esophagus

Understanding the disease and supporting clinical decisions

Marta Catarina da Piedade Sirgado Mesquita

Tese para obtenção do Grau de Doutor em
Biomedicina

Janeiro 2021

Biomarkers in Barrett's Esophagus: understanding the disease and supporting clinical decisions

Marta Catarina da Piedade Sirgado Mesquita

Tese para obtenção do Grau de Doutor em
Biomedicina
(3º ciclo de estudos)

Orientadora: Prof. Doutora Paula Chaves
Co-orientadora: Prof. Doutora Mónica Bettencourt Dias

Provas de doutoramento:
18 de Dezembro de 2020

Júri:
Presidente: Prof. Doutor Miguel Castelo Branco Craveiro de Sousa
1ª arguente: Prof. Doutora Maria de Fátima Machado Henriques Carneiro
2ª arguente: Prof. Doutora Joana Cancela de Amorim Falcão Parede
Prof. Doutor José Crespo Mendes de Almeida
Prof. Doutora Maria Paula Guerreiro Chaves Pascoal
Prof. Doutora Sílvia Cristina da Cruz Marques Socorro
Prof. Doutora Diana Raquel Fernandes Martins

janeiro de 2021

Dedicatória

A todos aqueles que me acompanham nesta aventura que é a vida

e que me mostram continuamente que apesar de haver dias menos bons

há sempre motivos para sorrir, agradecer e prosseguir viagem.

A vós, minha família e amigos, com todo o meu amor e carinho.

Uma intenção de vida:

"... Fazer da interrupção um caminho novo.
Fazer da queda um passo de dança,
do medo uma escada, do sono uma ponte,
da procura um encontro."

FERNANDO SABINO

Uma das aprendizagens na vida:

"O Perfeito é desumano"

"Adoramos a perfeição,
porque não a podemos ter;
repugná-la-íamos, se a tivéssemos.
O perfeito é desumano,
porque o humano é imperfeito."

FERNANDO PESSOA

Agradecimentos

Este trabalho contribuiu não só para o meu crescimento profissional e científico como também numa vertente mais pessoal para me conhecer melhor, trazendo ao de cima todas as minhas fragilidades e inseguranças. Saio por isso desta aventura uma pessoa mais forte e com uma maior autoconsciência dos meus limites verdadeiros e não daqueles que a minha mente foi produzindo ao longo do tempo. Foi um caminho longo, tortuoso, muitas vezes penoso, cheio de obstáculos e dificuldades e só foi possível chegar até aqui porque não fiz o caminho sozinha. Ao longo do projeto fui sempre acompanhada por pessoas que me apoiaram e deram uma palavra de incentivo para continuar. Por isso quero agradecer:

. Às minhas orientadora e coorientadora Paula Chaves e Mónica Bettencourt-Dias por me terem incentivado a participar neste projeto e pelo seu contributo científico, orientação e apoio constantes.

. Aos meus dois anjos da guarda: Carla Lopes, por ter sido a minha mentora científica e me ter apoiado incondicionalmente, em todos os momentos, por saber dizer a palavra certa no momento exato e acima de tudo por acreditar em mim quando eu não acreditava; à Raquel Tomás porque me ter ajudado até ao último minuto a concluir esta tese, e não me ter deixado desistir nestes últimos momentos de loucura.

. A todas as pessoas com quem colaborei diretamente neste projeto, que partilharam comigo o seu saber e com as quais aprendi muito, Carla Lopes, Joana Cardoso, António Dias Pereira, José Pereira Leal, Paula Chaves e Mónica Bettencourt Dias.

. João Matos pela sua paciência, compreensão e apoio durante as últimas semanas e à Inês Conchinha pela seu contributo como Web Designer na realização da capa.

. A todas os meus colegas e amigos do serviço de Anatomia Patológica do IPOLFG pelo apoio e incentivo constantes ao longo destes anos.

. À minha família e amigos do coração (não consigo escrever o nome de todos porque felizmente a lista é demasiado extensa) porque estão sempre lá quando preciso, nos bons e maus momentos.

. A todas as pessoas (sem exceção) que fizeram e fazem parte da minha vida porque eu sou o resultado das minhas vivências e foi com elas que chego hoje ao final desta etapa.

Resumo

O esófago de Barrett (EB) é uma reconhecida condição pré-maligna que surge no esófago distal associada ao refluxo gastroesofágico crónico e constitui o maior factor de risco para o desenvolvimento do adenocarcinoma esofágico (AE). Apesar da taxa de progressão maligna do EB ser baixa, a incidência de ambos tem aumentado drasticamente nas últimas décadas. Como agravante, esta neoplasia em estadios avançados está associada a taxas elevadas de morbilidade e mortalidade a menos que diagnosticada e tratada em estadios iniciais, pelo que todos os doentes com EB são integrados em programas de vigilância com vista à detecção precoce de progressão neoplásica. Contudo, esta prática clínica tem-se mostrado ineficaz para reverter este cenário epidemiológico e um dos factores limitantes relaciona-se com o facto da displasia continuar a ser o único marcador de risco de progressão maligna e não haver marcadores moleculares e clínicos que possam predizer e estratificar o potencial maligno do EB. É assim urgente encontrar biomarcadores sensíveis e específicos capazes de guiar a prática médica, melhorar a relação custo-benefício dos programas de vigilância, mas principalmente a qualidade de vida dos doentes com EB.

O objectivo principal desta tese foi descobrir novas vias moleculares subjacentes à progressão maligna do EB de forma a identificar biomarcadores fidedignos passíveis de serem aplicados à clínica apoiando o diagnóstico, prognóstico e manejo destes doentes, e assim contribuir para aprofundar o conhecimento relativo ao processo de cancerigénese desta doença e potencialmente melhorar a abordagem clínica aos doentes com EB.

Para tal foram seguidas duas linhas de investigação diferentes. De modo a encontrar biomarcadores com potencial preditivo para progressão maligna em doentes com EB foi realizada uma meta-análise de dados de transcriptomas previamente publicados, seguida de uma validação experimental utilizando amostras de EB de doentes acompanhados no programa de vigilância do Instituto Português de Oncologia Francisco Gentil. Esta estratégia permitiu identificar dois promissores biomarcadores, o CYR61 e o TAZ, capazes de estratificar o risco de progressão maligna do EB, não só pela sua expressão diferencial ser a mais significativa na análise bioinformática mas porque a validação experimental revelou que estes dois genes se encontravam sobre-expressos logo na primeira biopsia (vários anos antes do desenvolvimento de cancro) onde foi feito o diagnóstico de EB dos doentes que progrediram comparativamente com

a expressão detetada no EB dos não progressores. Adicionalmente, foram ainda identificados outros genes diferencialmente expressos em EB associados a progressão maligna, cujas funções estão associadas a fenótipos de células estaminais e fenómenos de transição epitélio-mesenquimal (TEM) em cancro. Assim, foi também descoberto um potencial novo processo molecular associado ao desenvolvimento de cancro em EB.

Paralelamente, e considerando que alterações numéricas dos centrossomas podem estar presentes ao longo da progressão maligna em EB e assim contribuir para o seu processo de cancerigénese, decidimos explorar quando e como surgem as alterações numéricas dos centrossomas ao longo da progressão do EB, desde a condição pré-maligna até às metástases ganglionares, tanto em amostras de doentes como em linhas celulares, usando um método de dupla marcação por imunofluorescência para identificar e quantificar fidedignamente o número de centrossomas por célula. Esta análise revelou a existência de células com centrossomas supranumerários logo na fase de metaplasia dos doentes que progrediram para cancro, e que a sua incidência aumenta significativamente na fase de displasia, a qual é dependente da perda de função do gene supressor tumoral p53, estando também depois presentes ao longo das restantes fases de progressão. Estes resultados sugerem assim que a desregulação dos centrossomas pode contribuir para a iniciação e progressão neoplásica do EB. No futuro será importante aprofundar o contributo dos centrossomas na cancerigénese do EB e tentar perceber qual o seu impacto no diagnóstico, prognóstico e tratamento destes doentes. Uma vez que tanto as alterações numéricas dos centrossomas como a perda de função do p53 são achados prevalentes em cancro, os resultados deste estudo poderão ser relevantes para outros modelos tumorais.

Em conjunto, os resultados obtidos sugerem que a propensão maligna não é igual em todos os EB. Logo muito cedo no processo, aqueles cujo risco de virem a desenvolver cancro é maior sofrem alterações moleculares e celulares passíveis de serem detetadas e utilizadas como biomarcadores preditivos estratificando o risco de progressão maligna, e desta forma orientar as decisões clínicas, adequar tempos de vigilância e melhorar a abordagem terapêutica.

Palavras-chave

Esófago de Barrett;displasia;adenocarcinoma esofágico;biomarcadores;CYR61;TAZ;transição epitélio-mesenquimal (TEM); centrossomas;p5

Resumo Alargado

O esófago de Barrett (EB) é uma reconhecida condição pré-maligna que confere risco aumentado de progressão neoplásica para o adenocarcinoma esofágico (AE). O EB surge no esófago distal como uma complicação associada a uma contínua agressão da mucosa esofágica pelo refluxo gastroesofágico. Caracteriza-se pela substituição metaplásica do epitélio pavimentoso estratificado, que normalmente reveste o esófago, por um epitélio colunar do tipo intestinal, confirmado pela presença de células caliciformes. Apesar do risco de progressão neoplásica do EB ser baixo, este risco é significativo, e por isso não pode ser desvalorizado. Como agravante, esta neoplasia em estadios avançados está associada a taxas elevadas de morbilidade e mortalidade a menos que diagnosticada e tratada em estadios precoces. É por isso que todas as diretrizes internacionais recomendam a integração dos doentes com EB em programas de vigilância com vista à deteção precoce de progressão neoplásica que possibilite o tratamento endoscópico curativo. No entanto, esta prática clínica tem-se mostrado pouco eficaz uma vez que a incidência do EA tem aumentado drasticamente nas últimas décadas, principalmente nos países ocidentais desenvolvidos. Um dos fatores limitantes apontados relaciona-se com o facto da displasia continuar a ser o único marcador de risco de progressão maligna e não haver marcadores moleculares e clínicos que possam predizer e estratificar o potencial maligno do EB. Presentemente, esta falta de marcadores para identificar os doentes em risco de progressão para cancro implica a vigilância endoscópica de todos apesar da grande maioria nunca vir a desenvolver cancro. Assim, urge encontrar biomarcadores sensíveis e específicos capazes de guiar a prática médica e melhorar a relação custo-benefício dos programas de vigilância, mas principalmente a qualidade de vida dos doentes com EB.

O objetivo principal desta tese foi descobrir novas vias moleculares subjacentes à progressão maligna do EB de forma a identificar biomarcadores fidedignos passíveis de serem aplicados à clínica apoiando o diagnóstico, prognóstico e manejo destes doentes. O trabalho desenvolvido pretende contribuir para aprofundar o conhecimento relativo ao processo de cancerigénese desta doença e potencialmente melhorar a abordagem clínica aos doentes com EB.

Para tal foram seguidas duas linhas de investigação diferentes. Com o objetivo de encontrar biomarcadores com potencial preditivo para progressão maligna em doentes com EB foi realizada uma meta-análise, com recurso a uma *pipeline* bioinformática

inovadora, em que se combinaram dados de expressão génica (transcriptomas) previamente publicados de doentes de EB que progrediram para cancro *versus* doentes que não progrediram. Com esta estratégia pretendeu-se identificar genes diferencialmente expressos durante a fase de metaplasia entre os dois grupos de doentes e perceber se haveria uma assinatura genética associada à progressão maligna do EB. Desta análise bioinformática foram selecionados dois genes candidatos com potencial capacidade preditiva e estratificação do risco de cancro em EB, o CYR61 e o TAZ, não só pela sua expressão diferencial ser a mais significativa (significativamente sobre-expressos em EB que progrediu comparativamente com EB que não progrediu), mas também tendo em conta o seu reconhecido envolvimento em outros modelos de cancerigénese. Seguiu-se depois um processo de validação experimental utilizando amostras de EB de doentes acompanhados no programa de vigilância do Instituto Português de Oncologia Francisco Gentil (IPOLFG). Para isso foi avaliada a expressão génica (por PCR quantitativo) e expressão proteica (por imunocitoquímica), do CYR61 e do TAZ em EB de doentes que progrediram para cancro no decurso do seu seguimento versus doentes com EB cujo diagnóstico se manteve negativo para displasia até ao momento do estudo. Este processo de validação não só confirmou os resultados obtidos por bioinformática como revelou que estes dois genes se encontram sobre-expressos logo na primeira biopsia (vários anos antes do desenvolvimento de cancro) onde foi feito o diagnóstico de EB dos doentes que progrediram comparativamente com a expressão detetada no EB do grupo dos não progressores, reforçando o potencial poder preditivo e precoce do CYR61 e do TAZ como marcadores de risco de progressão maligna no EB. Adicionalmente, foi ainda explorado o seu possível contexto funcional no processo de cancerigénese do EB. Na análise bioinformática foram também identificados outros genes diferencialmente expressos em EB associado a progressão para cancro, que já tinham sido previamente detetados em assinaturas moleculares relacionadas com fenótipos de células estaminais e fenómenos de transição epitélio-mesenquimal (TEM) em cancro. Dado que tanto o CYR61 como o TAZ regulam funções celulares relevantes para o desenvolvimento de ambos os fenótipos investigou-se bioinformaticamente se haveriam outros marcadores de TEM também diferencialmente expressos, e de facto, foi encontrado um gene, TWIST1, cuja expressão era significativamente aumentada em EB associado a progressão, a qual foi depois validada por PCR quantitativo logo na biopsia diagnóstica de EB em doentes que progrediram para cancro. Uma vez que um dos eventos moleculares no processo de TEM é a perda de adesão celular, foi ainda avaliada a expressão proteica da E-caderina e verificou-se uma perda focal de expressão desta proteína no EB dos doentes que progrediram, tanto na biopsia diagnóstica como na biopsia associada com a progressão

para displasia/adenocarcinoma, mas não no EB em doentes que não progrediram. Estes resultados sugerem que desde muito cedo, anos antes da progressão neoplásica, ocorrem alterações moleculares relacionadas com TEM em EB que podem potencialmente contribuir para a sua propensão para desenvolvimento de cancro. Assim, para além da identificação do CYR61 e do TAZ como potenciais biomarcadores capazes de estratificar o risco de progressão maligna em EB foi também descoberto um potencial novo processo molecular associado ao desenvolvimento de cancro em EB. No futuro seria crucial conseguir validar o potencial preditivo destes dois biomarcadores em amostras com mais doentes e também aprofundar o contributo de ambos, juntamente com o processo de TEM, na carcinogénese do EB.

A segunda linha de investigação baseou-se no facto de a progressão neoplásica do EB resultar da acumulação de anomalias em processos celulares regulados pelo centrossoma, que em células animais é o principal organizador de microtúbulos, e também em evidências prévias que demonstram que as alterações do número de centrossomas são um achado prevalente em vários modelos neoplásicos, tanto em estadios iniciais como em estadios avançados. Tomando como ponto de partida este conhecimento, elaborou-se uma hipótese em que alterações numéricas dos centrossomas podem estar presentes ao longo da progressão maligna em EB e assim contribuir para o seu processo de cancerigénese. Para confirmar esta hipótese decidimos explorar quando e como surgem as alterações numéricas dos centrossomas ao longo da progressão do EB, desde a condição pré-maligna até às metástases ganglionares, tanto em amostras de doentes como em linhas celulares. Para tal, desenvolveu-se um método de dupla marcação por imunofluorescência de forma a identificar ambas as componentes que constituem um centrossoma (centríolos e material pericentriolar) e assim quantificar fidedignamente o número de centrossomas por célula. Esta análise revelou que de facto existem células com anomalias numéricas dos centrossomas logo na fase de metaplasia e que a sua incidência aumenta significativamente na fase de displasia, estando também depois presentes ao longo das restantes fases. Verificámos também que o número de centrossomas por célula se encontra desregulado ao longo da progressão. Ao relacionar as alterações encontradas com as alterações moleculares características deste modelo de progressão tumoral, verificámos que o aumento da incidência das anomalias dos centrossomas na transição de metaplasia para displasia coincidia com a perda de função do gene supressor de tumores p53. Através de estudos mecanísticos nas linhas celulares demonstrámos que o aumento de células com centrossomas supranumerários depende da perda de função deste gene e que muito provavelmente durante a fase de metaplasia o número de

células com extra centrossomas está a ser reprimido pela função normal do p53. Em conjunto, ao mostrar que as alterações numéricas dos centrossomas antecedem a progressão maligna, estão sempre presentes nos restantes estadios da doença, e surgem exclusivamente nos doentes que desenvolveram cancro, não se observando naqueles sem progressão tumoral, os nossos resultados sugerem, tal como foi inicialmente formulado, que a desregulação dos centrossomas pode contribuir para a iniciação e progressão neoplásica do EB. Assim, no futuro será importante aprofundar o contributo dos centrossomas na cancerigénese do EB e tentar perceber qual o impacto na diagnóstico, prognóstico e tratamento destes doentes. Uma vez que tanto as alterações numéricas dos centrossomas como a perda de função do p53 são achados prevalentes em cancro, os resultados deste estudo poderão ser relevantes para outros modelos tumorais.

Em conjunto, os resultados obtidos nas duas linhas de investigação sugerem que a propensão maligna não é igual em todos os EB. Logo muito cedo no processo, aqueles cujo risco de virem a desenvolver cancro é maior sofrem alterações moleculares e celulares passíveis de serem detetadas e utilizadas como biomarcadores preditivos estratificando o risco de progressão maligna, e desta forma orientar as decisões clínicas, adequar tempos de vigilância e melhorar a abordagem terapêutica.

Palavras-chave

Esófago de Barrett;displasia;adenocarcinoma esofágico;biomarcadores;CYR61;TAZ;transição epitélio-mesenquimal (TEM); centrossomas;p53

Abstract

Barrett's esophagus (BE) is a recognized premalignant condition of the distal esophagus that constitutes the major risk factor for the development of esophageal adenocarcinoma (EA). Despite the known low rates of BE progression to EA, the incidence of both has increased profoundly over the last decades and esophageal malignancy remains to be a deadly cancer with high morbidity and mortality unless diagnosed at early stages. Current BE clinical management has revealed unsuccessful in reverting this worrisome epidemiological picture and a major hurdle has been the incapacity to discriminate among BE patients those who have a higher risk of malignant progression. In fact, to this date, besides dysplasia none of the existing clinical and histologic criteria could anticipate malignant progression. It is therefore imperative to find reliable molecular biomarkers to guide medical practice and improve the standard of care for BE patients.

The global aim of this thesis was to better understand the pathways underlying BE malignant progression and thereby identify reliable biomarkers relevant for the diagnosis, prognosis and management of BE patients thus contributing to an improved understanding of BE biology and an optimized support for clinical decisions.

To accomplish these challenging goals an unbiased and a hypothesis-driven strategies were followed. Through the unbiased approach, a meta-analysis of transcriptome datasets and subsequent experimental validation in a cohort BE patients in follow-up was used to define a gene set associated with BE cancer development and, therefore, identify early biomarkers predictive of BE malignant progression. *In silico* analysis singled out two genes, CYR61 and TAZ as candidate predictive markers for BE malignant progression and experimental validation using quantitative PCR and immunohistochemistry revealed that both genes are upregulated and overexpressed in non-dysplastic BE index biopsies from progressors years before cancer development when compared with index biopsies from BE patients that did not progressed. We also found that EMT and stemness-related genes were also significantly over represented in BE associated with progression. Together, these results support that CYR61 and TAZ are promising early biomarkers to stratify BE patients according to their cancer risk and suggest a novel mechanist route for BE neoplastic progression.

Using an hypothesis-driven approach, we explored when and how centrosome abnormalities arise along BE malignant pathway, from the early premalignant

condition stage to metastatic disease, by establishing an accurate method to identify and score centrosomes, at the single-cell level, in patient samples and cell lines. We found that centrosome amplification arises as early as the premalignant condition of patients that progress to malignancy and significantly expands at dysplasia stage, which is dependent of p53 loss of function, being then present along cancer progression, namely in EA and metastasis. So, these finding suggest that centrosome amplification could contribute to BE initiation and malignant progression. Considering that centrosome amplification is specific of patients that progress to cancer, this could be further explored to be translated into useful tools to be used in the clinical setting and potentially improve its diagnosis, prognosis and treatment. Moreover, given widespread occurrence of both p53 mutations and centrosome abnormalities in human tumors, our findings are likely to be extended to other cancers.

Collectively, both research avenues suggest the existence of different cellular and molecular abnormalities dictating different pathological propensity for malignant progression in BE, right from the beginning, and this could be further explored to trace a cancer risk profile for every patient and guide medical decisions and improve patient care.

Keywords

Barrett's esophagus;esophageal adenocarcinoma;early biomarkers;risk prediction;CYR61;TAZ;centrosomes

Table of Contents

List of Figures

List of Tables

Lista de Acrónimos

ACG	American College of Gastroenterology
AGA	American Gastroenterological Association
APC	Adenomatous polyposis coli
ARID1A	AT-Rich Interaction Domain 1A
BA	Barrett's adenocarcinoma
Bcl-2	B-cell lymphoma 2
BE	Barrett's esophagus
BMI	Body mass index
BMP4	Bone morphogenic protein 4
BRCA1	BRCA1 DNA repair associated
BSG	British Society of Gastroenterology
CCN	CYR61, CGTF and NOV family
CDX1	Caudal type homeobox 1
CDX2	Caudal type homeobox 2
CEP135	Centrosomal protein 135
CEP152	Centrosomal protein 152
CEP192	Centrosomal protein 192
CEP63	Centrosomal protein 63
CEP97	Centrosomal protein 97
CI	Centrosome index
CIN	Chromosomal instability
CIN I, CIN II, CIN III	Cervical intraepithelial neoplasia progression stages
CLE	Columnar lined esophagus with no intestinal features
CP110	Centriolar coiled-coil protein 110
CPAP	CENPJ, centromere protein J
CRBs	Centrosome related bodies
CYR61	Cysteine-rich angiogenic inducer 61
DAS-1	Dst1-delta 6-Azauracil Sensitivity
DNA	Deoxyribonucleic acid
DOCK2	Dedicator of cytokinesis 2
EA	Esophageal adenocarcinoma
EGFR	Epidermal growth factor receptor
ELMO1	Engulfment and cell motility 1
EM	Electron microscopy
EMR	Endoscopical mucosal resection
EMT	Epithelial-to mesenchymal transition
ESCC	Esophageal squamous cell carcinomas
ESMR	Endoscopical submucosal resection
FFPE	Formalin-fixed paraffin-embedded
FISH	Fluorescence in situ hybridization
G1, G2 Phase	Gap phases of the cell cycle
GATA4	GATA binding protein 4
GATA5	GATA binding protein 5
GEJ	Gastro-esophageal junction
GERD	Gastroesophageal reflux disease
GI	Gastrointestinal
HER-2	HERBB2, human erb-b2 receptor tyrosine kinase 2
HGD	High- grade dysplasia
HGIN	High-grade intraepithelial neoplasia

Hh	Hedgehog
Hp	Helicobacter pylori
HPP1	Hyperpigmentation, progressive, 1
HPV	Human papilloma virus
IF	Immunofluorescence
IHC	Immunohistochemistry
IM	Intestinal metaplasia
IPOLFG	Instituto Português de Oncologia Francisco Gentil
KRAS	KRAS proto-oncogene, GTPase
LGD	Low-grade dysplasia
LGIN	Low-grade intraepithelial neoplasia
lncRNAs	Long noncoding RNAs
LOH	Loss of heterozygosity
M Phase	Mitosis phase of the cell cycle
miRNAs	MicroRNAs
mRNA	Messenger Ribonucleic acid
MT	Microtubule
MTOC	Microtubule-organizing center
MUC-2	Mucin 2
MYC	MYC proto-oncogene, bHLH transcription factor
NF-kB	Nuclear factor kappa B
NGS	Next generation sequencing
NKX2.1	NK2 homeobox 1
NOS	Nitric oxide
p16/CDKN2A	Cyclin dependent kinase inhibitor 2A
p53	TP53, tumor protein p53
p63	TP63, tumor protein p63
PCM	Pericentriolar material
PCR	Polymerase Chain Reaction
PIK3CA	Phosphatidylinositol-4,5-bisphosphate 3-kinase catalytic subunit alpha
PLK1	Polo like kinase 1
PLK4	Polo like kinase 4
pRb	Rb protein
pSMAD	Phospho-SMAD
qRT-PCR	Quantitative Reverse Transcription PCR, qPCR
RA	Retinoic acid
Rb	RB1, RB transcriptional corepressor 1
RFA	Radiofrequency ablation
RNA	Ribonucleic acid
ROS	Reactive oxygen species
RUNX3	RUNX family transcription factor 3
S Phase	Synthesis phase of the cell cycle
SAC	Spindle assembly checkpoint
SAS-6	SAS-6 centriolar assembly protein
SFED	French Society of Digestive Endoscopy
Shh	Sonic Hedgehog
SMAD	Mothers against decapentaplegic homolog 4
SMARCA4	SWI/SNF related, matrix associated, actin dependent regulator of chromatin, subfamily a, member 4
SNP	Single nucleotide polymorphism
SOX2	SRY-box transcription factor 2
SOX9	SRY-box transcription factor 9
Src	SRC proto-oncogene, non-receptor tyrosine kinase
STIL	STIL centriolar assembly protein
TAZ	Transcriptional coactivator with PDZ-binding motif
TGFα	Transforming Growth Factor Alpha

TLR4	Toll like receptor 4
TWIST1	Twist family bHLH transcription factor 1
UK	United Kingdom
USA	United States of America
WWTR1	WW domain-containing transcription regulator protein 1

CHAPTER 1:
General Introduction

1.1 Definition and clinical relevance of Barrett's esophagus

Barrett's esophagus (BE) is a pathological condition of the distal esophagus whose definition still remains controversial. It is broadly regarded as the replacement of the normal stratified squamous lining by a columnar-lined metaplastic epithelium, which is detectable by endoscopy and confirmed histologically. It is clinically relevant because it correlates with long standing gastroesophageal reflux disease (GERD) and it is a premalignant condition that increases the risk of developing esophageal adenocarcinoma (EA), also known as Barrett's adenocarcinoma (BA).[1-4] This neoplasia develops through a sequence of molecular and histologic events reflected morphologically by the multistep process of metaplasia, dysplasia (low/high grade) and adenocarcinoma.[3]

1.1.1 Definition of Barrett's esophagus

Despite the histologic features of Barrett's columnar mucosa being well described, the morphological criteria for BE diagnosis are still a matter of worldwide discussion. Whereas the American Gastroenterological Association (AGA) and the American College of Gastroenterology (ACG) claim that the presence of intestinal metaplasia (IM) is required, the British Society of Gastroenterology (BSG) argues that a columnar epithelium, with no goblet cells, is enough for the diagnosis. Despite the recognition of three distinct epithelia in BE, namely cardiac, oxyntic-cardiac and intestinal, the AGA and the ACG only consider the intestinal type for diagnosis. [5-9]

Underlying this discussion are the different perspectives regarding the risk of malignant progression of the distinct metaplastic phenotypes. Actually, the rationale behind BE definition diverges between USA and UK scientific societies. The former support that BE is clinically important because it predisposes to cancer so the definition should only include the histologic features that significantly increases the risk of cancer development; the latter advocate that BE definition should be merely a description of the acquired metaplastic condition irrespective of its malignant potential.[3] The BSG claim that the evaluation of risk in BE patients must be addressed separately, taking into account the current knowledge and several factors (endoscopic, histological and molecular) specific of each patient in order to determine the best individual management strategy.[10]

The USA perspective stems from early retrospective cohort studies demonstrating that most EA arises in the background of columnar mucosa with intestinal features [11-15], and large population-based studies demonstrating that the cancer risk is significantly higher in patients with IM versus patients with columnar epithelium without goblet cells.[16, 17] North American medical societies therefore consider IM as the columnar type of epithelia that clearly

predisposes to EA and recommend that BE diagnosis implies the histological identification of this epithelium in biopsies before recommendation for surveillance. [7, 18]

In favor of the British point of view there are retrospective studies showing a similar risk of progression for patients with IM or columnar epithelium without goblet cells. [6, 19, 20] There is also a growing conviction among BE experts that the columnar lined esophagus with no intestinal features (CLE) is a previous step in BE pathway, and thus the development of IM is a time related event.[6] Accordingly, evidence from two follow-up studies where patients with columnar epithelium without IM at index biopsy were included in surveillance programs and prospectively followed support this: in a cohort (n=322) studied by Gatenby and colleagues (2008), IM was documented in 54.8% of the patients after 5 years of surveillance and in 90.8% after 10 years [19]; and in our cohort (n=15), Dias Pereira and Chaves (2012) reported the presence of specialized columnar epithelium in 60% of the cases after a mean follow-up of 7.1 years.[21]

Another important issue is related to the fact that the absence of goblet cells in a biopsy could be due to a sampling error, and thus lead to an erroneous diagnosis (non-IM CLES instead of CLES with IM). A study by Chandrassoma and colleagues (2012), where a systematic collection of biopsies was conducted, revealed that IM was detected in most of the cases (87.4%), including those with dysplasia or adenocarcinoma. In the cases with only cardiac-type mucosa there was no dysplasia or invasive neoplasia. In the group where a systematic biopsy sampling was not applied, a substantial number of cases with dysplasia or EA exhibited exclusively neoplasia in the biopsy material. Thus, the authors concluded that many adenocarcinomas, with no documented adjacent residual IM, could be explained by tumor overgrowth or by insufficient sampling instead of a real absence of IM. They also supported that when an adequate and systematic protocol of biopsies was followed, the cases without IM have an insignificant risk of malignant progression.[22, 23] This raises an important question since inadequate sampling could, erroneously, exclude from follow-up risk patients (when USA criteria is applied) that if deprived of an early BE diagnosis could have a later presentation and a worst prognosis.

Moreover, there is accumulated evidence that non-goblet columnar metaplasia exhibits cryptic features of intestinal differentiation. In accordance, diverse studies have shown expression of intestinal markers, CDX2 [24-26], DAS-1 [24, 27, 28], HepPar1 [29], villin [24, 30], MUC-2 [24], and a quite similar cytokeratin expression pattern [27] not only in areas of BE with typical goblet cells but also in non-goblet columnar epithelium from BE and CLEs, favoring a common origin. In addition, several reports also disclosed similar molecular abnormalities, such as microsatellite instability [31], chromosomal instability [31, 32] and DNA content alterations [33] in columnar mucosa with no goblet cells, both in BE and CLE patients. These data support that esophageal non-globlet columnar epithelium, along with IM, is clearly abnormal and at risk of malignant progression. In line with this, and questioning the North American guidelines, a report from Riddel and Odze came out in 2009 supporting the exclusion of intestinal metaplasia

from BE definition.[6] This fact points out that even the USA experts are not consensual regarding this issue.

Nevertheless, USA medical societies argue that, up to now, there is not strong evidence supporting the inclusion of patients without IM in follow-up. Although they recognize that non-goblet columnar epithelium could predispose to malignancy, they argue that the level of risk remains unclear. Until then they maintain that it is not possible to make substantiated management guidelines for those patients. [7, 34] Indeed, given the low risk of malignant progression, the cost-benefit of surveillance and treatment programs, even for patients with IM whose cancer risk is well defined, has been questioned. [7] [34, 35]

There is convincing evidence in favor of both perspectives supporting the need of future research to clarify the most appropriate definition and the best strategy for BE patient management. Curiously, the controversy concerning BE definition extends to other countries beyond the USA and the UK. Europe, other than the UK, follows the American definition while in Japan, as in the UK, BE is diagnosed in the context of columnar metaplasia lacking goblet cells. Actually, Japanese experts were the first to propose that the diagnosis of BE could be performed in the context of columnar epithelium without goblet cells. [6, 36]

Another important and controversial issue is the anatomical landmarks used at endoscopy to define the limits of the distal esophagus, thereby identifying the gastro-esophageal junction (GEJ) since an accurate diagnosis of BE requires the precise detection of red velvet mucosa (columnar epithelium) proximal to that junction.[34, 37] While the Western world uses the proximal end of the gastric longitudinal folds, in the East the distal end of the lower esophageal palisade vessels is the reference for the GEJ.[34, 38] Conceptually, the two landmarks should co-localize but there are factors that may affect this co-localization including diverse pathological conditions. [10] These limitations are responsible for inter-observer variability and can lead to false positive or false negative BE diagnosis, namely in short or ultra-short segments. Current scientific evidence does not favor a universally endoscopic landmark and without a validated gold standard any choice will have always an arbitrary component.[7, 34] In the lack of substantiated evidence advocating alternative markers, both UK and USA guidelines support that “the proximal limit of the longitudinal gastric folds with minimal air insufflation is the easiest landmark to delineate the GEJ”, despite its limitations.[7, 10, 34] In Asian countries, however, endoscopists continue to support the use of distal end of palisade vessels as the best reference point. Particularly in Japan they use this landmark to identify the GEJ since the proximal end of gastric folds is impaired by the prevalence of severe *Helicobacter pylori* atrophic gastritis. [39]

In conclusion, the histologic features for the diagnosis of BE and the anatomic landmarks for the identification of the GEJ remain inconsistent requiring more research to reach an adequate consensual definition.

1.1.2 Brief history of Barrett's esophagus

Although the concept of BE has been discussed for more than one century, the diagnostic criteria remains controversial, reflecting the lack of a clear understanding of the disease. Indeed, the history of BE is full of misunderstandings, uncertainties, and controversies. A summary chronological overview of the key events that conducted to the present understanding of the entity is crucial to stress the ever-existing misinterpretations and the progressive clarification of BE biopathology.

Even though he was not the first to refer the entity, the eponymous "Barrett's esophagus" stayed after the publication in 1950 by Norman Rupert Barrett, a recognized British surgeon who brought the focus on the condition.[40] In his report he supported that an organ should be defined by its mucosal lining rather than by its anatomic location and sustained that the esophagus should be regarded as "that part of the foregut, distal to the cricopharyngeal sphincter, which is lined by squamous epithelium". Therefore, he argued that the previously described ulceration, similar to chronic gastric ulcer observed in a tubular organ, appearing at the distal esophagus, are in fact located in the stomach. In favor of his argument, he noticed that the ulcerated columnar lining was "gastric in type".[40] Norman Barrett's misinterpretation, based on the assumption that the squamous-columnar transition defines the gastroesophageal junction, sustained that the lesion was congenital and located at stomach. Despite defining an incorrect biopathology, the eponymous persisted. Actually, before Norman Barrett many authors have already described clinical conditions framing the spectrum of BE. [41, 42]

Almost fifty years before Barrett, Tileston reported the entity, described its morphology, clarified the epidemiology and, in striking contrast to Barrett, suggested the correct etiology. The first morphologic description of the condition is attributed to Wilder Tileston in 1906.[41] He described a "simple ulcer of the esophagus" located in the esophageal lowest part, near to the cardia that resembles, grossly and microscopically a "simple ulcer of the stomach. He stated that it is more frequent in middle age males and that "the cardia should be insufficient, allowing regurgitation of the gastric juice into the esophagus".[41] Almost simultaneously with Norman Barrett, in 1951 in France, Lortat-Jacob described the "endo-brachyesophagus", an endoesophageal ascent of gastric type mucosa in patients with reflux and with no alteration of GEJ topography.[43-45] Lortat-jacob's interpretation was closer to the present understanding of BE than Barrett's first description. In respect to BE etiology, Norman Barrett regarded the lesion as congenital while Tileston and Lortat-Jacob as associated to reflux.[40, 41, 43]

The discussion on the nature of the lesion, congenital vs. acquired, parallels the controversy about its histological characterization. Tileston, Norman Barrett and Lortat-Jacob described a gastric type mucosa adjacent to the ulcer.[40, 41, 43] Bosher and Taylor's, in 1951, described a "lower esophagus completely lined by gastric mucosa with intestinal-type goblet elements but no parietal cells", which they considered a heterotopia. [46] This was the first reference to an intestinal phenotype in the esophageal lining, although it was regarded as a heteropia. The

second reference to an intestinal phenotype came in 1952 by Morson and Belcher who reported a case of esophageal adenocarcinoma arising in a “glandular mucous membrane” showing “chronic inflammatory and atrophic changes, with a tendency towards an intestinal type containing many goblet cells”.[47] Despite the reference to a previous report of adenocarcinoma in the esophagus (by Carie in 1950), their work was the first detailed description of an adenocarcinoma arising in a distal esophagus lined by columnar epithelium, clearly corresponding to the entity, currently, designated as Barrett’s adenocarcinoma.

In 1959, the report by Moersch and colleagues about patients with reflux esophagitis referred to a “deep ulceration in columnar epithelium-lined esophagus” which they already named as “Barrett’s ulcer” suggesting that the eponym was been retained. Remarkably, the authors described “cells resembling young columnar cells were seen occasionally, and thus the question of inflammatory metaplasia had to be considered.” [48] This was the first suggestion of a metaplastic process associated to long standing GER. Nevertheless, the question regarding BE etiology was clarified only in 1970 with the experimental work of Bremner et al. They demonstrated that in the absence of GER the removal of distal esophageal lining in dogs was followed by squamous re-epithelialization, but inducing GER, a new columnar epithelium arose. [49] This study corroborated the association between GER and the columnar lining of the distal esophagus and discarded the congenital hypothesis.

The histological picture of the columnar lining was another polemic and challenging issue. Paralleling the debate on BE etiology, several histological descriptions emerged using different designations. [50-55] It was Paul and colleagues in 1976, who clarified the histological spectrum of the columnar lined mucosa.[56] Using a multilevel esophageal biopsy protocol in 11 patients, the authors described three different types of columnar epithelium: the atrophic “gastric fundic” type with parietal and chief cells; the junctional type with cardiac type mucous glands and no parietal cells; and the “specialized columnar epithelium”, a unique type of intestinal metaplasia, with a villiform surface, mucous glands, Alcian-blue positive goblet cells and no parietal or chief cells. The first two types were similar to normal gastric mucosa and the third one was only analogous to some types of intestinal metaplasia observed in the stomach. A distinctive pattern on their topographic distribution was also prominent. The intestinal type was always proximally located, adjacent to the squamous epithelium, followed by the junctional type, being the atrophic gastric fundic type distally located. Therefore, they concluded that BE columnar lining is highly heterogeneous which could explain the previous existent discrepancies. Another relevant issue in this report was the recognition, in one case, of dysplastic features within specialized columnar epithelium. Pointing out this, the authors perceived the importance of this columnar epithelium in malignant transformation. [56] This work was an important piece in the puzzle of BE discussion considering their focus on three crucial points regarding the disease: morphology, heterogeneity and risk. Actually, it contributed to the understanding of the complex columnar epithelium morphology raising for the first time the concept of cellular

heterogeneity in BE and reporting the development of cancer associated to intestinal metaplasia.

The debate regarding BE association with EA matched the discussion on BE etiology and histology. Despite previous reports describing adenocarcinomas arising in columnar epithelium with intestinal features, it was in 1978 that Haggitt and colleagues who clearly demonstrated the biopathological association.[11, 47, 57, 58] The authors described 12 out primary esophageal adenocarcinoma arising in the setting of a columnar mucosa, 10 of which with a continuum of lesions from columnar epithelium to invasive adenocarcinoma. They concluded that "esophageal adenocarcinoma is one complication of a columnar epithelium-lined esophagus", and suggested that the "invasive carcinoma evolves through a sequence of epithelial dysplasia and carcinoma in situ". So, they recommended a surveillance program with biopsy and cytology as effective methods to detect precursor lesions and to prevent invasive neoplasia. [11] Likewise, Skinner and colleagues aiming at identifying etiological and prognostic factors associated to malignancy, compared BE patients with and without associated neoplasia. [12] Their work stressed the role of GER on BE, highlighted the value of specialized intestinal epithelium featuring goblet cells, as a hallmark of BE, namely in risk patients and suggested dysplasia, mainly associated with the intestinal phenotype, as the most serious indicator of malignant potential.[12]

In the last decades of the 20th century, BE and the intestinal phenotype reached a widely acceptance between experts as a premalignant condition and as a risk marker, respectively. In 1998, the ACG proposed a definition that stands until nowadays, despite the controversies and lack of consensus. It was recommended that BE should be defined as "a change from the normal esophageal squamous mucosa to columnar mucosa of any length that is visible endoscopically and that on biopsy demonstrates intestinal metaplasia". [59, 60]

Nowadays, it is consensual that BE is a lesion of the distal esophagus, acquired as a consequence of long standing GER and widely accepted as the premalignant condition for esophageal adenocarcinoma. However, several points remain ambiguous, namely, which are the BE features really associated with malignancy, which are the patients that are going to progress, and would in fact benefit from surveillance and in what frequency. Also the actual biological meaning of the different cellular lineages, namely the gastric phenotype is still a matter of controversy.

These ambiguities are responsible for different approaches that bring limitations with detrimental effects not only in the clinical setting but also in research, giving rise to an unclear interpretation of the literature.

Actually, the Barrett's esophagus concept seems like "a never-ending story" with the last chapter still completely unrevealed.

1.1.3 Epidemiology and risk factors of Barrett's esophagus and Esophageal Adenocarcinoma

The clinical relevance of Barrett's esophagus (BE) disease relates to its establishment as the major risk factor for development of esophageal adenocarcinoma (EA), a malignancy whose incidence has been rising at an alarming rate, especially in western countries during the last decades.[61-63]

1.1.3.1 Epidemiology

Barrett's esophagus (BE) normally develops in the background of chronic gastroesophageal reflux disease (GERD), which is a highly common clinical disorder with prevalence rates varying from 8 to 40% worldwide.[64] BE is approximately 10 times more frequent among persons with manifestations of GERD, with studies reporting a prevalence between 5-20% in patients undergoing upper endoscopy for reflux symptoms.[64-69] However, many BE patients are asymptomatic, which means they have silent reflux, do not seek medical care and remain undiagnosed.[70, 71]

The overall prevalence of BE remains quite difficult to estimate due to the significant number of cases that are clinically undetected.[67, 72] In 1999, Cameron and colleagues found that BE was five times more prevalent in autopsies when compared to BE prevalence retrieved from endoscopic series in the same geographic area. This suggested that only a minority of the cases were clinically recognized [73], and that for every diagnosed BE patient probably 20 more remain unidentified in the overall population [71]. Additionally, two studies in individuals undergoing screening colonoscopy, in which endoscopy and biopsies were done to evaluate BE prevalence, revealed that BE was also present in patients without GERD symptoms. [74, 75] In the first study the overall prevalence of BE was 6.8%. BE was diagnosed in 5.6% of the patients with no history of heartburn and in 8.3% of the patients with reflux symptoms.[74] In the second study, 16.7% of the population studied was diagnosed with BE. Once more, clinical GERD symptoms were a poor predictor for detecting BE that was found in 19.8% of the symptomatic cases and in 14.9% of patients who denied having reflux symptoms.[75] It is important to note that these two studies were conducted in tertiary care centers and selection bias needs to be considered since age is a risk factor for BE and older patients are more prone to have GERD when compared to a truly unselected sample of the adult population.[67] Thus the prevalence of BE in the aforementioned studies was likely overestimated and the overall incidence and prevalence rates are expected to be smaller in the general population.[37, 76]

The most accurate estimates are derived from endoscopic surveys of random samples of the adult population, regardless of clinical indication, with the single purpose of detecting BE. Since this condition can only be diagnosed through endoscopic evaluation and histologic confirmation, there are few population-based studies assessing the prevalence and incidence in unselected overall population.[1, 77] The best data were probably derived from three different studies named Kalixanda, Loiano-Monghidoro and SILC studies, which overcame the logistic

challenge of doing an endoscopic survey on a large scale at random in the communities.[78-80] In the Kalixanda study, upper endoscopy on 1,000 randomly selected Swedish adults revealed a BE prevalence of 1.6%.[78] The Loiano-Monghidoro study of 1,033 Italian individuals revealed a prevalence of 1.3%.[79] Finally, in the SILC study of 1,029 endoscopies of individuals in Shanghai BE was found in 1.8% of the subjects.[80] It is noteworthy that the Swedish and Italian studies confirmed histologically the presence of intestinal metaplasia to diagnose BE whereas in the SILC study the investigators were less restrictive and used endoscopically suspected BE as diagnostic criterion. Thus, estimates on BE have to be interpreted with caution since global epidemiological differences could vary widely depending on the endoscopic diagnostic criteria and definition used, apart from geographic, demographics, genetics and lifestyle factors.[38, 81-84]

BE is globally recognized as the premalignant condition for EA, a tumor whose incidence has been rising over the past decades, at a rate faster than any other type of cancer, mainly in western nations, becoming also the fastest growing cause of death from cancer.[9, 84-86] In the USA there was a seven-fold increase on EA incidence rate, from 0.36 to 2.56 per 10,000 cases, between 1973 and 2006.[87] This same trend was noticed in several European countries and Australia. Thus, EA evolved from being a rare neoplasia to become the most frequent esophageal malignancy in the USA and most Western countries in the late 1990s.[83] In 2014, 18,170 new cases of esophageal cancer were documented in the USA of which 59.9% were EA.[88] However some recent data show evidence that the rate of this increase has leveled off or even plateaued.[87, 89, 90]

The causes for the dramatic increase of this neoplasia incidence are not fully elucidated but it is conceivable that one of the reasons might be the rising incidence of BE and its underlying condition, GERD, in the last decades.[39] In fact, GERD incidence has been increasing in many developed countries and in the USA it became the leading diagnosis for gastrointestinal disorders in the outpatient setting.[91, 92] While some authors claimed the increasing BE incidence might be partially explained by a greater awareness of the disease among clinicians, and consequently by a higher number of endoscopies and biopsies performed, there is evidence that the incidence of BE is rising independently of these factors suggesting a real occurrence rather than a higher detection rate.[64, 72] For example, a study based on data from the Northern Ireland registry reported an increase of 93% in BE incidence between 1993 and 2005. A similar study was conducted in the Netherlands and the same upward trend was found. Notably, this rising incidence was more pronounced in patients younger than 60 years.[93-95] Other hypotheses about BE increasing incidence are related with the increased prevalence of other known risk factors such as abdominal obesity and smoking, and also with the decreased prevalence of *Helycobacter pylori* infection.[63, 72, 96]

Patients with BE are at an increased risk of developing EA, with estimates ranging from 10 to 125 times the risk of the general population.[94, 97-100] Early progression rates reports tended

to overestimate the cancer risk since they were performed mainly at reference centers and derived from small cohort studies with a short length of follow-up.[7, 71, 101] Recent better-quality studies, based on larger cohorts, longer surveillance follow-up and more stringent criteria, such as, more robust BE definition and exclusion of cases with prevalent dysplasia (either present just in the index biopsy or in the first year of follow-up), showed a considerable lower cancer incidence. These large population-based BE follow-up studies reported an absolute annual risk of progression to EA of 0.12-0.14%. [17, 95, 102, 103] Moreover, a recent large meta-analysis of 57 studies demonstrated that the pooled annual incidence of EA in this BE cohort was of 0.33% (95% CI 0.28–0.38%).[35, 104] So, in the light of these studies, only a small minority of the BE patients will progress to malignancy.

However, the risk of progression to invasive neoplasia increases significantly with dysplasia.[77]. The rate of progression to EA ranged from 0.5 to 26.5% for LGD and from 6 to 19% for high-grade dysplasia.[105-108] Low-grade dysplasia was traditionally considered as harboring a low risk of progression. Recent studies showed that when the diagnosis of low-grade dysplasia was confirmed by an expert pathologist the risk of progression was high. So high-grade dysplasia and confirmed low-grade dysplasia are the best risk markers of progression to EA. [109, 110]

In conclusion, BE is the main risk factor for the development of EA. The risk of progression among BE patients is low but significant. Furthermore, dysplasia is the only validated marker that increases significantly the risk of progression to EA. So, international guidelines recommend targeting and screening the population at higher risk of BE and endorse these patients to endoscopic surveillance programs in order to detect malignant progression at an early and curable stage cancer.

1.1.3.2 Risk factors

Despite being a common disorder, BE is not equally distributed among the overall population and the risk of progression of BE patients is different between regions. It is therefore envisioned that BE is a disease with a multifactorial etiology resulting from the interaction of several risk factors, such as demographic, environmental and clinical factors, with the unique genetic background and susceptibility characteristic of each individual. However, the knowledge about the contribution of these interactions in the development and progression of BE is still scarce.[1, 111-114]. Since BE is a premalignant condition of EA, it is conceived that, along with BE itself, risk factors beyond this precursor lesion also contribute to neoplastic progression.[115]

BE segment length - Most studies report that the risk of developing dysplasia/EA is higher as the extent of BE segments increases. [10, 116] However, there is no cut-off length at which the risk of malignant progression is significantly higher. [62, 95] On the other hand, as short segment BE are more frequent than long segments, it is conceivable that most EA occur in the former ones.[115]

Gastro-esophageal reflux disease (GERD) is a chronic disorder associated to continued esophageal exposure to gastric or bile acids driven by a defective lower esophageal sphincter.[83, 111] Currently, GERD is defined according to the Montreal consensus as "a condition that develops when the reflux of stomach contents causes troublesome symptoms and/or complications".[117] Long-standing GERD is tightly associated with BE and EA being considered the major risk factor for BE and to play a role in BE malignant progression. [83]

Hiatal hernia is an anatomical alteration resulting from the protrusion of part of the stomach upwards throughout the diaphragm. This decreases the efficiency of lower esophageal sphincter against reflux predisposing to GERD and BE.[69, 118] The size of hiatal hernia also seems relevant [119], with some studies showing association between larger hiatal hernia, severe reflux and higher risk of malignancy.[95, 120, 121]

Obesity, measured as total body mass index (BMI), has long been accepted as a risk factor for BE and EA.[69, 122] It deserves special attention since obesity is becoming globally epidemic.[123] Not only BMI, but also the location where fat accumulates, namely the abdominal/visceral adiposity is a stronger risk factor for BE and EA.[124, 125] Several hypotheses were raised to support the obesity involvement in the pathogenesis of GERD, BE and EA, including mechanical features as increased intra-abdominal pressure and metabolic factors such as secretion of high levels of proinflammatory cytokines.[124] Also, abdominal obesity increases the likelihood of having hiatal hernia, which *per se* also fosters reflux.[126] Interestingly, an association between visceral adiposity and higher risk of 9p loss of heterozygosity (LOH), 17p LOH and aneuploidy, the main molecular changes in BE progression was also reported.[95]

Gender - Most studies show that BE and EA is more common in men.[34, 62, 111, 112] Although the prevalence of GERD is similar in both sexes, a meta-analysis showed a male:female ratio of 1.96:1 in BE and of 5:1 in EA. These differences have been explained by a protective role of women hormonal behavior [111], or by a different body fat distribution since men have predisposition to develop central obesity whereas women to develop peripheral obesity.[125] However, prospective studies do not prove this gender ratio.[34, 62] Nevertheless, the prevailing evidences still show male gender as a risk factor for BE and for the malignant progression to EA.[62]

Age is accepted as a risk factor for BE and EA by many investigators.[61, 127] Despite the fact that in older individuals it is clinically more frequent the need for endoscopies, therefore being higher the chance of BE diagnosis, these studies argue that, in the patients with GERD symptoms, the probability of having BE is also amplified, as age increases. [7]

Ethnicity - The prevalence of BE varies between different ethnic origins and geographic regions being more frequent in white Caucasian than Asian, Middle Eastern, African, Caribbean and South American.[1, 111, 128] In fact, several cohort studies demonstrated that most BE

patients are white when compared with other ethnic groups and that this variation in prevalence increases with malignant progression. There is not a clear explanation for these findings but these differences could derive from studies bias, because they rely on the demographics of people who attend for endoscopy, unidentified genetic variants in non-Caucasian, or may also result from distinctive environmental background (dietary and lifestyle habits) and differences in the rates of obesity and GERD among countries. [34, 61, 111]

Smoking is considered a moderate risk factor for BE and to a higher extent for EA albeit the results in this field being inconsistent.[63] This may be due to different methodologies and sample sizes in studies and variable BE definition. [62, 83, 112] There is a suggestion that smoking alone may not be a risk factor but when associated with visceral obesity, GERD symptoms, and with long segment BE, it should be considered. [111, 129]

***Helicobacter pylori* (*Hp*)** is a Gram-negative bacterium that commonly infects the human stomach and its chronic infection is strongly associated with an increased risk of developing gastric cancer.[130, 131] Inversely, several authors argue that *Hp* infection, mainly CagA positive strains, seems to have a protective role against BE and EA.[35, 132] In fact, some epidemiologic studies have shown that *Hp*(+) individuals have half the risk of developing BE and EA when compared with *Hp*(-).[83, 133, 134] This protective role could be explained by the capacity of these bacteria to cause gastritis, which results in reduced gastric acid production and decreased GERD.[115, 135] Since the prevalence rates of *Hp* infection is falling, mainly in developed countries, it has been proposed that could be, at least in part, the reason for the increasing incidence of BE and EA.[115, 136, 137]

Diet - Since the incidence of BE and EA varies considering sex, ethnic and geographic characteristics, it is conceivable that different dietary habits could be one of the factors involved in this difference.[83] Nevertheless, the current data only results from observational studies and still lacks randomized trials to confirm the role of diet in BE.[138]

Most of these risk factors have already been translated to the clinical setting. In fact, recent guidelines from AGA, ACG and BSG advocate that, additionally to GERD, other risk factors (at least two or multiple depending on the guideline) should be considered, namely male gender, age ≥50, white race, hiatal hernia, obesity (high BMI and/or intra-abdominal adiposity) and smoking habits, to select patients to be endorsed to endoscopic screening in order to detect BE.[7, 10, 139]

1.2 Barrett's esophagus malignant progression to esophageal adenocarcinoma: pathogenesis and carcinogenesis

The prevailing rational is that Barrett's esophagus (BE) is the result of a metaplastic process, defined as the replacement of one cell type by another, that appears as an adaptive response to

gastro-esophageal reflux disease (GERD). Chronic exposure to reflux damages the esophageal squamous cells and leads to esophagitis. In some individuals the healing process is accompanied by a cellular reprogramming triggered by a change in the expression of key developmental transcription factors, which dictates a shift in the cell's phenotypic commitment. This results in the replacement of the damaged squamous epithelium by columnar cells that are able to secrete mucus and are more resistant to acid and bile reflux. However, what determines whether BE develops or not remains elusive. Actually, to this day, the cell of origin of BE is still matter of debate, a problem that is urgent to solve since it is crucial for understanding the molecular mechanisms underlying the metaplastic conversion. [3, 114, 140]

On the same line of thinking, and despite decades of research, we are still far from knowing when, how and which BE patients will progress to cancer. Current knowledge suggests that in the setting of chronic injury, due to recurrent reflux episodes and repeated healing of the Barrett's mucosa, together with chronic inflammation, in some individuals BE cells could acquire physiological properties that enable them to become cancer cells.[2, 141, 142] In fact, several factors have already been implicated in the molecular pathways involved in BE malignant progression to EA, namely those involved in regeneration, cell cycle, apoptosis, cell adhesion, chromosomal instability (CIN), aneuploidy and invasion, events that have already been linked in general with tumorigenesis.[143] By definition, the process of carcinogenesis involves the acquisition of genetic and epigenetic abnormalities in key molecular pathways, allowing normal cells to develop anomalous functional properties that lead to the development of cancer cells. In 2000, Hanahan and Weinberg proposed that six essential changes must occur in order for a cell to become malignant and denominated these changes as "cancer hallmarks" [144]. Cancer cells must: be independent from exogenous mitotic stimulation or being self-sufficient in growth signals, evade growth inhibitory signals, resist cell death by avoiding apoptosis, have limitless replicative capacity becoming immortal, induce angiogenesis in order to sustain their own growth, and be able to invade local tissues and metastasize, this is, spreading and proliferating in distant locations. Later in 2011 the authors proposed two additional cancer hallmarks: reprogramming of the energy metabolism to enhance further proliferation of cancer cells (e.g. switch to aerobic glycolysis) and the ability to evade destruction by the immune system. Furthermore, according to the same authors, underlying the acquisition of these cancer hallmarks, there are genetic instability and mutations, which provide cancer cells with genetic changes that drive tumor progression, and inflammation that triggers a tumor-promoting microenvironment.[144-146]

Similar to other types of cancer, the process of carcinogenesis in BE is also characterized by a succession of genetic and epigenetic alterations, which confer a selective advantage to neoplastic cells through the acquisition of these cancer hallmarks.[147] The progressive sequence of these molecular changes goes along with histologic events, morphologically expressed on the multistep process of metaplasia, dysplasia (low/high grade) and adenocarcinoma.[3]

1.2.1 Histologic features of Barrett's metaplasia, dysplasia and carcinoma sequence

BE is a pathological condition of the distal esophagus. Four layers compose the esophageal wall: mucosa, submucosa, muscularis propria and adventitia/serosa. (Fig. 1)

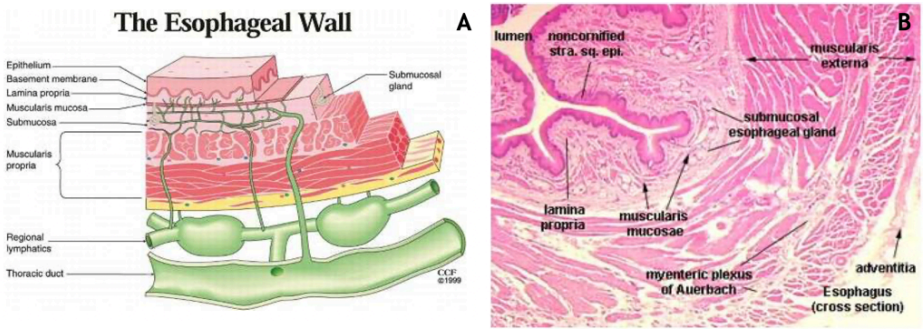

Figure 1. Cross-section of the esophageal wall. A) Schematic anatomical view. **B)** Histological sagittal section displaying the multiple layers. (Retrieved from [466, 467])

The mucosal lining of the esophagus is a non-keratinized stratified squamous epithelium supported by a thin layer of loose connective tissue called lamina propria containing stromal cells, blood and lymphatic capillaries, nerve fibers and scattered inflammatory cells. In the distal esophagus, near the gastro-esophageal junction (GEJ), the lamina propria also contains cardiac glands that secrete neutral mucins for protection of the esophagus against the acidic gastric juices. The lamina propria invaginates into the squamous epithelium giving rise to papillae that usually extend to one third/one half of the epithelial thickness. Histologically, this epithelium is characterized by the presence of multiple layers of epithelial cells organized in a deeper proliferative and a thicker superficial differentiated zone. The proliferative zone has a basal layer of cuboidal dividing cells, adherent to the basement membrane and occupying 10% to 15% of the total thickness. From the deepest layer, cells differentiate moving upwards to the surface becoming flat and larger keratinocytes (cells with small nuclei and eosinophilic cytoplasm, being the clear look due to the presence of glycogen) and continuously replacing the outer superficial cells that were sloughed off [148, 149]. The esophageal mucosa contains a third layer of longitudinally oriented smooth muscle fibers, the muscularis mucosa. The submucosa of the esophagus is highly vascular and is composed of connective tissue with abundant blood vessels and lymphatics, nerve cells, and occasional lymphocytes and plasma cells. Similar to salivary glands it also has mucous glands that produce mucins in order to lubricate the esophagus, commonly called esophageal glands. Deeper, the esophagus is covered by an inner circular and an outer longitudinal layers of muscle cells, the muscularis propria. The outermost stratum is composed by a layer of loose connective tissue (adventitia or serosa, if located above or below the diaphragm) containing blood and lymphatic vessels, and nerve fibers.

As a result of chronic tissue injury due to GERD, BE develops in the distal esophagus by the metaplastic replacement of the native squamous epithelium by a columnar epithelium with

gastric and intestinal features. [140] Currently, and according to observational studies in human BE samples and animal models as well as molecular data, currently, not only the progression to EA but also the development of IM has been progressively recognized as a multistep process. (Fig. 2)

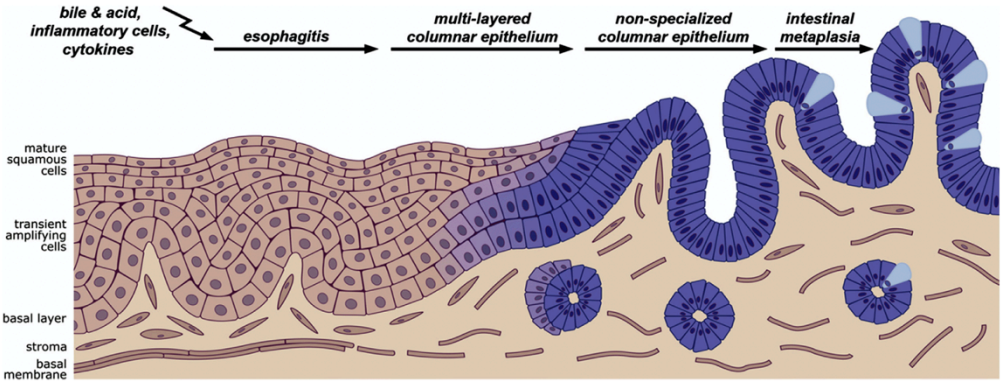

Figure 2. Stepwise process in the development of intestinal metaplasia. Chronic tissue injury of squamous epithelium is followed by the development of a multi-layered epithelium, which further develops into a columnar epithelium, culminating in intestinal metaplasia. (Retrieved from [150])

Preceding the appearance of columnar metaplasia, the injured squamous epithelium is first substituted by an "intermediate" epithelium, commonly named as multilayered epithelium. It is regarded as a hybrid epithelium that exhibits features of both squamous and columnar epithelia. Histologically, it is composed by flattened squamoid cells containing small round or oval nuclei, small centrally located nucleolus and ample eosinophilic cytoplasm in its basal layers and by cells with a cumulative degree of columnar differentiation (with a basal nucleus and clear cytoplasm containing vacuoles of mucus) in its suprabasal and superficial layers. Nuclear pseudostratification is usual and there are no perceptible intercellular bridges.[30, 151] The next step in the BE process is the development of a gastric type columnar epithelium, which undergoes a further differentiation reprograming, resulting in an intermediate non-goblet columnar epithelium with cryptic intestinal differentiation and finally in IM, recognized by the presence of goblet cells. So, the different entities previously regarded as independent metaplastic phenotypes, namely the junctional/cardiac, the atrophic gastric-fundic/ oxyntocardiac type and the specialized columnar/IM are now recognized, according to most recent data, as being interrelated and part of the stepwise process of BE development.[3, 150, 151]

Barrett's esophagus (BE) comprises two epithelial compartments, the surface/crypt epithelium, and the glandular portion underneath (Fig. 3A). The metaplastic epithelium is composed by a mixture of different columnar cells, with mucinous elements resembling gastric foveolar cells, goblets cells (characteristically having a barrel-shaped configuration and a nucleus compressed due to distended cytoplasmic containing acid mucin vacuoles), enterocytic cells and, in a smaller proportion, by Paneth and endocrine cells.[152, 153] Cellular elements with features of different cell types are also present, namely with combined gastric/intestinal or

intestinal/squamous (e.g. multilayered epithelium) mixed phenotypes.[154] The proportion of each cell type in the metaplastic lining depends on patient's age, length and age of the BE segment, biopsies location (proximal vs. distal), and presence or absence of neoplasia. The cellular composition of the glandular compartment also depends on the segment location: whereas in the distal portion there is normally a higher proportion of oxyntic glands, mucous glands are more frequent in the proximal BE mucosa, namely in areas where goblets cells are prominent. Nevertheless, the most common pattern is an assortment of mucous (cardiac) and oxyntocardiac glands along the BE segment.[3] Additionally to epithelial changes, BE also presents mesenchymal and stromal alterations: lamina propria commonly has increased blood and lymphatic vessels, nerve fibers, and displays features associated to chronic inflammation; and muscularis mucosa is rearranged with a thick single layer or, frequently, with a double layer.[155] However, the remaining structural components of the esophagus remain unchanged, namely the submucosal elements. So the recognition of submucosal mucous glands could be crucial as an evidence of esophageal location of the columnar epithelium and the establishment of BE diagnosis.[156]

BE without dysplastic features presents surface maturation compared to the underlying basal glands. Indeed, the nuclear:cytoplasmic ratio is lower in the surface epithelial elements than in the deep glands lining. Lamina propria surrounding the glands is prominent. The metaplastic columnar epithelium retains cell polarity with basal nuclei location, regular nuclei with smooth membranes and small nucleoli. Mitotic figures are confined to the basal compartment of the glands.[8] Since BE is a metaplastic epithelium associated to an inflammatory background, some degree of atypia could be present as a result of reactive changes but it is confined to basal glands of the mucosa maintaining surface maturation.[157] Recently, it was suggested that the recognition of the "four lines" in the superficial BE epithelia is indicative of preserved polarity of epithelial cells and could help to reduce equivocal diagnosis of "indefinite for dysplasia, discharging many cases as reactive. The first, or top line, matches to the apical mucin cap and the second line to the base of the cap. The third line corresponds to the aligned eosinophilic cytoplasm and the fourth or the bottom line to the row of nuclei.[158, 159] Along the carcinogenic pathway, BE cells acquire several molecular changes becoming neoplastic. Morphologically, these abnormalities are reflected as an uncontrolled cell growth, and a progressive degree of cytological and architectural atypia, recognized as dysplasia.[23]

Dysplasia is a "neoplastic epithelium that is confined to the basement membrane."[156] There are several types of dysplasia already associated to BE. The first and best characterized is the intestinal type dysplasia even though, more recently, two others types were described, namely gastric (foveolar) and serrated dysplasia.[3] Irrespectively of the type, dysplasia is graded into low-grade and high-grade according to several criteria: degree of cytoarchitectural atypia, nuclear stratification, nuclear:cytoplasmatic ratio, nuclear hypercromasia, cellular and nuclear pleomorphism, number of mitoses and presence of atypical mitoses.[3, 143] **Low-grade dysplasia (LGD)** is characterized by having slight absence of surface maturation (Fig. 3B).

Atypical cells are present not only in the basal compartment but also at the luminal surface. Cytological abnormalities include nuclear enlargement, elongation, hypercromasia and nuclear pseudo-stratification, although with maintained or minimal loss of nuclear polarity. Minor architectural changes are present with glands appearing crowded but with evident surrounding lamina propria and no complex architectural forms. Mitoses are increased, but typically normal.[8, 23, 156]

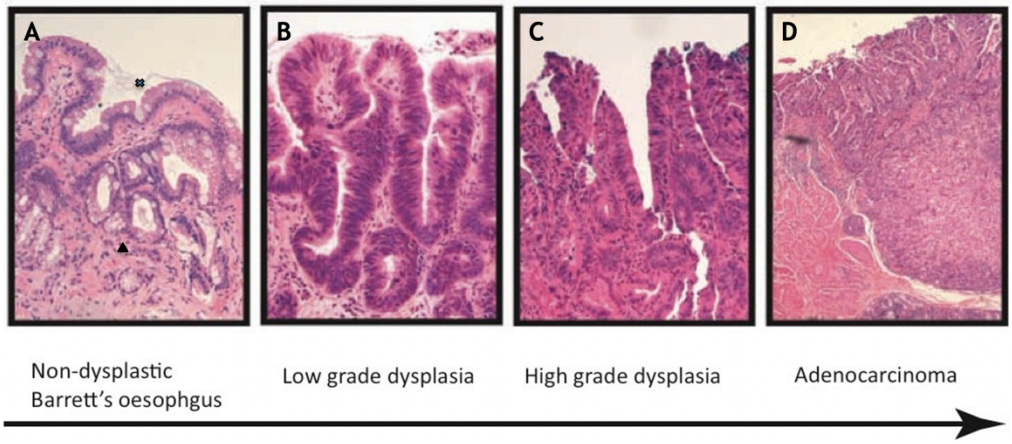

Figure 3. **BE multistep pathway of progression.** A) Barrett's esophagus without dysplastic features. The cross indicates the surface/cript compartment and the arrowhead indicates the glandular components of the epithelium. **B)** Low grade dysplasia**. C)** High grade dysplasia **D)** Esophageal adenocarcinoma (Retrieved from [160]).

In **high-grade dysplasia (HGD),** cytological and architectural changes are more prominent (Fig. 3C). Surface maturation is absent and cytologic atypia involves the entire length of the epithelium. Nuclei enlargement is more striking, displaying marked pleomorphism, hypercromasia, anisocytosis and irregular membranes. Round vesicular nuclei with conspicuous nucleoli are common features. Nuclear polarity is lost and mitotic figures, including atypical forms, are frequent even at the luminal surface. The epithelium shows striking architectural abnormalities such as villiform surface configuration and glandular distortion with focal budding, cribriform appearance and crowded glands with loss of lamina propria. Dilated glands with luminal necrotic debris could be present. In the setting of a diagnosis of HGD the pathologist should look for evidence of coexisting EA. However, in biopsy the differential diagnosis can be difficult and the exclusion of intramucosal adenocarcinoma may be impossible. [23, 156, 157]

In **esophageal adenocarcinoma (EA)**, the neoplastic cells are no more restrict to the epithelium and infiltrate the lamina propria, the muscularis mucosa and/or submucosa, frequently eliciting a characteristic desmoplastic stromal reaction (Fig. 3D). Among the histological types of EA, the most common is the intestinal pattern but diffuse, signet ring or mixed types, despite less frequent, can also be observed. Invasive neoplasia normally exhibits high-grade cytological and architectural features with crowed and small angulated glands, fused or syncytial growth of tumor cells and single cells infiltrating the lamina propria. Dilated tubules

containing necrotic debris and a pronounced neutrophilic infiltrate in the epithelium may be present. Pagetoid spread of neoplastic cells, when present, is always a feature of invasive neoplasia.[8, 23, 143]

Importantly, the well-known morphologic progression of BE through the sequence of metaplasia, LGD, HGD and adenocarcinoma is the phenotypic expression of a complex progressive biopathogenic process. Dysplasia is a challenging morphological concept. Despite the precise definition and the strict and well-defined criteria, the agreement between pathologists when classifying dysplasia is poor. In fact, graduation of dysplasia remains highly subjective and frequently inaccurate, especially if not performed by experts in gastrointestinal (GI) pathology. Since graduation of dysplasia remains the gold standard for clinical BE management, guidelines recommend that two pathologists should evaluate the diagnosis of any dysplasia and at least one should have expertise in GI pathology.[34, 35, 65]

Furthermore, differential diagnosis between BE negative for dysplasia and LGD could be very difficult and highly variable, particularly in the presence of reactive changes related to inflammation/regeneration. Therefore, the concept of diagnostic uncertainty led to the creation of a provisional diagnosis, **BE "indefinite for dysplasia"**. This category do not constitute a step on the spectrum of BE malignant progression. Oppositely, it means that there are no criteria to discriminate the nature, regenerative vs neoplastic, of the morphological changes observed. In that sense, indefinite for dysplasia represents a holding diagnosis until the treatment reduces inflammation and a new biopsy is performed. [8, 156, 159]

1.2.2 Barrett's esophagus pathogenesis

Despite extensive research, the cellular origin of BE remains a mystery and a controversial issue. At least five hypotheses are currently under discussion. One proposal is that BE could arise from a trans-differentiation process wherein mature squamous cells transform into columnar cells through an epigenetic effect without requiring proliferation. Another theory proposes that BE originates from a reprogramming or commitment of the pluripotent stem cells responsible for the continued replacement of the esophageal lining that undergo columnar rather squamous differentiation, a process named trans-commitment.[114] These stem cells could be from the basal layer of the native squamous epithelium, the submucosal esophageal glands or from the neck region (ductal lining) of these glands.[161] Another hypothesis suggests that a small population of embryonic columnar cells, maintained at the GEJ until adulthood, is able to migrate and proliferate after chronic injury and erosion of the squamous epithelium, giving rise to BE. It has also been proposed that bone marrow stem cells could be involved, migrating and seeding in the area of epithelial injury and later differentiating into columnar cells.[114] Lastly, some authors argue that BE development may be related to stromal cells modulation, namely by alterations on the regulatory signals that affect the stromal component of the mucosa (e.g. myofibroblasts and inflammatory cells). Stromal cells could either send signals that would influence and shift the differentiation program of epithelial cells, or directly originate columnar

cells through mesenchymal-to-epithelial transition [149] As there is reliable scientific evidence favoring or rejecting each of these proposals under specific contexts, there is no winning theory to this day. More research is crucial to elucidate the molecular mechanisms essential for the BE metaplastic process. Until then, some authors argue that is plausible to consider that more than one BE cellular origin could exist, and that perhaps the source could be different from patient to patient. This could be a possible explanation for the fact that only few BE patients progress to EA. In contrast, if we consider the hypotheses that neoplastic risk would not be dependent on the cell of origin, then the cell type giving rise to BE could dictate different cancerigenesis pathways and result in diverse subtypes of EA, each of which may need particular clinical management. [114, 161, 162]

Whilst the BE progenitor cell remains unknown, current evidence indicates that long-term exposure to acid and bile reflux creates an inflammatory environment that triggers genetic and/or epigenetic changes, and contribute to the activation or inactivation of signaling pathways that are crucial to BE development and eventually progression to EA.[149, 163] In fact, experimental data obtained from *in vitro* and *in vivo* animal models have allowed significant progress regarding the comprehension of the aberrant signaling events involved in the onset of BE and its malignant progression.[164-167] The existing hypothesis implicates the involvement of several signaling pathways that normally participate in the development and maintenance of the gut, and other organs, during embryogenesis: the Hh (Hedgehog) and BMP4 (Bone morphogenic protein 4) pathways, activated to develop and maintain the simple columnar epithelium of the embryonic esophagus and not expressed in the adult esophagus; the RA (Retinoic acid) signaling, crucial for the development of the esophagus and the squamous mucosa; and the Wnt (wingless-related integration site) and Notch pathways, responsible for the development and differentiation of the intestine including regulation of intestinal stem cell homeostasis. [2, 114, 150]

The embryological esophagus develops from the dorsal half of the foregut being initially covered by a columnar lining that, as the embryo matures, is replaced by a squamous epithelium that remains until adulthood. The above signaling pathways regulate this shift in the differentiation program through the expression of different transcription factors: NKX2.1 expression induces the columnar differentiation, whereas SOX2 and p63 are involved in the development and maintenance of the squamous epithelium.[72, 168] With continuous exposure of this epithelium to acid and bile reflux, the ensuing inflammation and tissue injury lead to the expression of different transcription factors that promote a shift towards an intestinal phenotype. First, there is an activation and upregulation of Hh signaling, which acts as an inducer of BMP4 signaling pathway, resulting in a renewed expression of epithelial Shh (Sonic Hedgehog), one of the three ligands of Hh, and stromal BMP4 proteins. These signals lead to increased expression of pSMAD and SOX9, which drive columnar differentiation. Then, the interaction of pSMAD and CDX2 transcription factors, and later, the Notch and Wnt signaling, dictate the further development and homeostasis of intestinal type of BE metaplasia.[150] Of note, the phenotypic

expression of intestinal features by columnar cells precedes the morphologic appearance of goblets cells, suggesting that CDX2 plays an early role in the intestinalization process.[3] Regarding Wnt signaling, which involves stabilization and nuclear re-localization of β-catenin, there are contradictory opinions regarding its role on BE pathogenesis. Since nuclear β-catenin is not expressed in human BE samples, some authors argue that this pathway plays either a minor or no role at all in BE development.[169, 170] Surprisingly, RA signaling, responsible for squamous differentiation, is also activated in BE and appears to have a role in its pathogenesis. This apparently contradictory finding may be related with the fact that the effect of RA on cellular differentiation is dependent on the specific retinoid receptor subtype activated, which may result in different responses to RA signaling.[168] In fact, a study using primary human esophageal keratinocytes cultured in vivo demonstrated that RA is able to induce the expression of the intestinal differentiation marker MUC2.[171] Furthermore, another study also showed that an increase in RA activity induces a glandular phenotype in human squamous mucosa *ex vivo* and suppress squamous differentiation.[172] Some of these signaling pathways have also been associated with BE neoplastic progression. Although data from human samples point to a further increase in the Hh signaling along the progression sequence, its role in EA development is not clear.[168] Notch signaling activation is associated with progression from BE to EA [163]and Wnt signaling seems to be an important driver during BE malignant transformation, as revealed by a progressive increase of nuclear β-catenin in the metaplasia-dysplasia-carcinoma sequence [72]. On the other hand, RA signaling appears to have a dual role in BE tumorigenesis. Despite being increased in BE, its signaling decreases in dysplasia and EA. As RA can function as an inhibitor of cell proliferation in several cancer cell lines and triggers apoptosis in a BE cell line, activation of this pathway could have a tumor suppressor effect. [168]

Inflammation is known to play an important role in both BE and EA pathogenesis. GERD triggers an acute and chronic inflammatory process characterized by the recruitment of different immune cells and by the release of inflammatory mediators, such as cytokines, chemokines and growth factors. For example, the transcription factor NF-kB (nuclear factor kappa B), a pivotal mediator in inflammatory response, induces the expression of CDX1 and CDX2, important transcription factors for intestinal differentiation in BE development. Furthermore, immune cells and inflammatory mediators also contribute to tumor development through the secretion of inflammatory factors, by promoting proliferation and angiogenesis, and by creating an immunosuppressive environment that helps tumors evade the host response.[173, 174] Exposure of esophageal tissue and cultured cells to acid and bile salts also generates reactive oxygen species (ROS) and the production of nitric oxide (NOS), both responsible for oxidative stress, DNA damage and double-strand breaks. Bile and acid reflux also change BE cells kinetics allowing cells with DNA damage to escape apoptosis through the activation of NF-kB pathway. DNA damage, in turn, is associated with telomere dysfunction, activation of telomerase and p53 mutation. All these events are not only observed along the BE malignant sequence, but are also thought to contribute to the process of BE carcinogenesis. [91, 122, 175-177]

Bile and acid reflux has also been associated with deregulation of microRNAs (miRNAs), a class of small non-coding RNAs with key roles in regulation of cell growth, differentiation and migration.[91, 178] Given that diverse miRNAs were already found to be deregulated in BE within the context of signaling pathways underlying BE pathogenesis and carcinogenesis as Hh, Notch, Wnt and NF-kB, they could also play a role in BE initiation and carcinogenesis [178]. BE and EA have a different miRNA profile from that of the normal esophagus, with at least 34 differentially expressed miRNAs in BE/EA when compared to native squamous epithelium.[179] Moreover, BE patients who progressed have a miRNA profile distinct from non-progressors, with four miRNA (miR-192, miR-194, miR-196a, and miR-196b) having a higher expression in the first group comparatively to the second group of patients.[180] As miRNAs are stable and identifiable in blood, they could be used in a near future as an important diagnostic tool.[178] Long noncoding RNAs (lncRNAs) are also associated with BE malignant progression. They have key roles as regulators of chromatin dynamics and gene expression, and in the control of cell growth, differentiation and migration.[91, 181] A recent study identified a specific lncRNA, AFAP1-AS1, that is hypomethylated and overexpressed in BE an EA. This work also demonstrated that *in vitro* silencing of this lncRNA inhibited cell migration, invasion capacity and promoted apoptosis, showing that its aberrant overexpression could contribute to tumor development and progression.[182]

1.2.3 Molecular changes underlying Barrett's esophagus progression to Esophageal Adenocarcinoma

The genomic instability that characterizes the process of carcinogenesis in BE fosters the occurrence of molecular alterations affecting tumor suppressors, oncogenes, and cell cycle checkpoints, which in turn contribute to oncogenic behavior and neoplastic progression.[163] Given the availability of BE samples over time from patients in follow up, and the presence of BE and dysplasia adjacent to EA in esophagectomy specimens, this cancer model was soon considered ideal to characterize the molecular defects in the prior steps before advanced cancer, to chronologically order those events along the cancer pathway and to identify those that could be associated with an increased risk of developing cancer.[113] With that in mind, several studies have addressed the relationship between genetic abnormalities and disease stage. Thus far, several types of DNA abnormalities have been described in BE and EA, namely structural genomic changes (amplifications, deletions and translocations), DNA sequence modifications, and epigenetic alterations (DNA methylation and miRNA expression).[183, 184] Currently, the prevailing evidence points to molecular events such as loss of heterozygosity (LOH), aberrant methylation of tumor suppressor genes, specific genetic mutations, clonal diversity, whole-genome doubling and large scale copy number changes, as relevant mechanisms in BE initiation and/or progression to EA.[185]

Recent large-scale sequencing studies revealed that EA is one of the most mutated epithelial cancers, with high somatic mutation rates exceeded only by melanoma and lung cancer.[185] This is not surprising given that EA develops in a highly genotoxic background associated with

continuous injury triggered by GERD, inflammatory environment and sometimes by tobacco smoke, which are all mutagenic factors. [186] Surprisingly however, the mutational burden in non-dysplastic BE, although inferior to that of dysplasia and EA, was found to be higher than some types of invasive tumors such as multiple myeloma, breast and colorectal cancers.[146, 187] In fact, genomic studies have shown that despite being a benign condition, BE is not a simple metaplastic epithelium but rather it already presents several abnormalities, part of which could also be identified in dysplasia and EA. [183]

The starting point of understanding the genomic profile of BE and EA as well as the process of clonal evolution within BE carcinogenesis began many years before the advent of genomics revolution, with the use of techniques like flow cytometry, FISH (fluorescence in situ hybridization), array comparative genomic hybridization and the analysis of the methylation, LOH and mutational status of specific known genes. [188-190] That research revealed that cell cycle and genetic abnormalities are not exclusive of EA but occur early in the premalignant condition and accumulate during malignant progression, thus laying the groundwork in tracing the major molecular events involved in BE malignant progression.[186, 187] Early studies in EA uncovered a high prevalence of cell cycle and genetic abnormalities such as increased G1, S phase and 4N fractions, as well as aneuploidy and LOH at multiple chromosomes.[188, 191] BE was found to be hyperproliferative in relation to normal esophageal and gastric epithelium, with a high mitotic index, decreased generation time, and increased proliferation very early in the progression process.[188, 192-194] Prospective studies showed that a minority of BE patients also develops increased 4N (G2/tetraploid) cell populations, genetically unstable intermediates with a predisposition for subsequent development of aneuploidy, and that those patients had a higher propensity to progress to dysplasia or EA and could be considered high-risk patients.[188, 195, 196]

Those early studies also revealed that loss of p16/CDKN2A and p53 tumor suppressor genes was highly prevalent, and among the most common somatic genetic abnormalities found in EA.[197] In general, tumor suppressor genes in cancer are inactivated by the conjugation of three different mechanisms: deletion of the chromosomal region where the gene is located (LOH), mutation, and methylation of the promoter region. In EA, p53 and p16 inactivation result from 17p LOH and mutation of the remaining allele, and 9p21 LOH and mutation or promoter methylation of the second allele, respectively [197, 198]. As tumor suppressor genes are normally responsible for controlling cell proliferation and inhibiting tumor expansion, their inactivation allows cells to avoid growth inhibitory signals and to proliferate without restrictions contributing to tumor development. Moreover, since p53 also has an important pro-apoptotic function, its loss can promote cancer progression by suppression of cell death through apoptosis. Retrospective studies in patients that progressed to EA showed that abnormalities in p16 and p53 are early genomic evens in BE malignant progression and precede the development of aneuploidy and cancer.[199, 200] p16 lesions were the most common alteration found in BE, even in patients who had not developed dysplasia, being present in more than 85% of patients

with BE at all histological grades (BE; BE+LGD; BE+HGD; BE+LGD+HGD) before EA [201]. These studies also demonstrated that clones with p16 changes were frequently selected, often expanding to the entire BE segment through a selective sweep in the process of clonal evolution.[142, 199] Loss of p53 was found later in the progression, almost exclusively in a genetic background of a prior p16 inactivation, coinciding often with the appearance of LGD. In addition, p53 loss of function was considered to be a decisive mechanism in the BE malignant pathway not only because p53 LOH was strongly associated with the development of 4N cell populations that arise before aneuploidy, but also because patients with p53 LOH had a much higher risk of progression to EA.[122, 142, 184]

Besides p16 and p53, other studies also identified sporadic and less prevalent genetic alterations along BE malignant pathway. Mutations in KRAS, and amplifications of genes as HER-2, EGFR and TGFα were detected in EA and appear to be late events in cancer progression, whereas others were found to be already detectable in BE, such as APC inactivation, and Rb LOH, and cyclin D1, Bcl-2 and Src kinase overexpression. Nevertheless, evidence points that these alterations contribute to BE progression instead of having a direct role on BE pathogenesis.[149, 202]

Together, these studies led the proposal of a general model where loss of p16 is the main initiating event in BE malignant pathway that provides a selective advantage to the mutant clones. Consequently, clonal expansion occurs by a selective sweep through the neoplasm. In parallel, cells with neutral mutations could also arise but since they normally do not disturb cell fitness, they most likely only spread when coupled to a driver mutation. The emergence and expansion of clones with loss of p53 seems to require a previous inactivation of p16. Inactivation of p53 is also associated with genomic instability, which is permissive for the following development of tetraploid and aneuploid clones resulting in neoplastic progression. Cancer progression would most likely follow a branched non-linear evolution, with neoplastic clones diverging, maintaining the same p16 and p53 abnormalities but with different ploidies and additional somatic genetic alterations. [183, 199, 200, 203, 204] Subsequently, new data came out challenging this theory. In a study evaluating p16, p53 and point mutations in squamous surrounding tissue, neo-squamous islands and individualized crypts from BE and dysplasia areas, no fixed founder mutation was found throughout progression. Instead, there was evident clonal heterogeneity, with multiple p16 independent clones.[205] Thus, a much more heterogeneous scenario than what was advocated by the previous theory was found. Based on these findings, a different model was proposed: BE heterogeneity could develop from multiple independent clones that evolve separately, where some clones could go extinct while others maintained. So, genetic abnormalities existing in these clones would not necessarily spread through BE segment, depending on the particular competitive advantage of each clone. The cancer evolution envisaged by this proposal gives rise to a much more heterogeneous BE and subsequent malignant stages. Hypothetically, both theories could coexist in BE malignant pathway but the technology at the time did not allow an extensive analysis of the molecular

profile of BE and EA samples and the information retrieved from a small number of selected genes has made this issue difficult to clarify.[187, 205, 206]

The recent and fast evolution of molecular techniques brought important insight into the complex mutational landscape of BE and EA and the main molecular events involved in BE malignant progression to cancer. [207]. Technologies such as SNP (single nucleotide polymorphism) arrays, WGS (whole genome sequencing), WES (whole exome sequencing), and NGS (next generation sequencing) have a higher sensitivity and allow a deeper coverage of the genome. As a result, they allow the identification of somatic mutations at lower allelic fraction than what was achievable by traditional molecular techniques, and enable the simultaneous detection of mutations and somatic copy number alterations.[208] Notably, however, the fundamental concepts associated to the previous cancer models before their advent, appear to remain unaltered: the heterogeneous nature and the high complexity associated with BE and EA was reinforced; the touchstone that EA evolve from BE holds true, with several sequencing studies demonstrating that many coding mutations in EA are present as early as in BE; and lastly, the concepts of branched evolution and non-linearity associated with BE malignant progression have also not changed.[184, 204, 207]

By unraveling the prominent genomic alterations at the invasive cancer stage, these studies showed that EA is highly heterogeneous with only a restricted number of genes recurrently mutated across numerous cases. In agreement with earlier studies, the most prevalent gene mutations were found in p53, followed by p16. In fact, p53 was the only gene frequently mutated in EA, throughout several studies. [184-186] Nevertheless, other genes were also found to be significantly mutated but in a smaller percentage of cases. While some had been previously implicated in EA, such as SMAD4 [209] and PIK3CA [210], new recurrent mutations were identified in chromatin remodeling factors such as TLR4, ELMO1, DOCK2 and SMARCA4, and in novel tumor suppressor genes such as ARID1A.[211-213] Analysis of SNP variations allowed the assessment of mutational patterns or signatures in EA and to infer about the causative mutagens. This revealed a tendency for A to C transversions at AA sites resulting in an enrichment of CTT trinucleotides, which has been proposed to be associated with oxidative DNA damage caused by GERD since in a subsequent study this same pattern was found in BE.[211, 214] In addition to being highly mutated, mostly resulting in widespread loss of function of several tumor suppressors, EA is characterized by having a wide range of copy number alterations in genes with recognized involvement in carcinogenesis. Recent studies found recurrent genomic amplifications in loci of oncogenes (e.g. EGFR, HERBB2, KRAS), cell cycle regulators (e.g. CCND1), and transcription factors (e.g. MYC, GATA4, GATA6) [183, 215], and uncovered novel potential mechanisms underlying those rearranged genomes. Amplification of several oncogenes in this cancer is frequently caused by major chromosome catastrophes such as chromothripsis. This is a process where several genes could be affected resultant from a massive chromosomal shattering due to mitotic chromosomal segregation anomalies, and breakage-fusion-bridge events in which telomeres are lost after breaking, followed by

chromosomal fusion and anomalous separation in anaphase.[185, 216] Moreover, a study measuring the absolute amount of somatic DNA alterations in various types of neoplasias found that whole–genome doubling is a common event in cancer, including EA, that has been associated with CIN and a faster route in the oncogenic process. It also provided additional evidence that tetraploidy, detected in the earlier studies using flow cytometry, and subsequent aneuploidy are cell cycle events involved in BE malignant progression to EA.[186, 217]

Sequencing studies evaluating the genome and epigenome of EA and co-existing BE found that the mutational context at both stages is very similar and that abnormalities in DNA methylation are frequent not only in EA but also in BE.[183] In agreement, another study sequencing the exome of EA and matched BE found that 80% of the mutations present in EA were already detected in paired BE.[218] In a study assessing the mutational spectra in three different groups of patient samples (never-dysplastic BE, BE with HGD and EA), BE from patients with no signs of progression harbored frequent mutations in genes previously identified as drivers in EA, including ARID1 and SMARCA4.[213] Furthermore, the most prevalent mutations in EA were also detected at equivalent mutational rates in BE and HGD samples. The only exceptions were p53 and SMAD4 mutations, which were found to be stage specific and clearly defined the boundaries between BE with no dysplasia to HGD and EA, respectively. In contrast, other studies detected p53 mutations in BE adjacent to EA and in non-dysplastic BE years before progression to HGD or EA.[208, 212, 214] P53 aberrant expression was also observed in non-dysplastic BE samples from a small proportion of patients that were prospectively followed, specifically, in 7% from the group of non-progressors and 18% of progressors.[219] Moreover, despite early studies implicating p16 loss of function in BE malignant pathway to cancer, recent studies showed no significant differences in the frequency of homozygous deletions in fragile sites of some tumor suppressors, including chromosome 9p loss or p16 LOH, in BE samples from patients that developed EA and non-progressors.[186] Thus, the data emerged by these newer sequencing technologies further reinforced the complexity associated with BE disease and the difficulty to integrate all these molecular changes in assays that could be used to predict the risk of cancer progression associated to each particular alteration. These studies clearly demonstrated that despite being a benign epithelium, BE could develop several types of molecular abnormalities in a diversity of genes. Considering that the vast majority of BE patients will not develop cancer, the contribution of each player to BE oncogenesis, from the plethora of molecular events occurring during progression, is unclear. [183, 184]

In order to understand the dynamics of somatic genomic evolution leading to cancer and get further insight into the roots of neoplastic progression in BE, a prospective study addressed the genomic profile over space and time in BE patients with or without later progression. While the genome of non-progressors displayed low levels of copy number anomalies and remained relatively stable with low CIN over time, in BE from progressors, as approaching the time of cancer diagnosis they developed CIN, with a striking increase in gains or losses of whole chromosomes or chromosomes arms, followed by an increase in genetic diversity and selection

of clones over space in BE segments. In a subset of these progressors, catastrophic genome-doubling events with widespread aneuploidy were detected.[220] These findings were concordant with the concept that aneuploidy is a driver of neoplastic progression, but were novel in respect to the demonstration that aneuploidy occurs just before the development of cancer.[183] Furthermore, these results suggest that in some patients there appears to exist a restricted time window of opportunity for early detection of cancer. This was also favored by a recent study reporting that in 25% of BE patients in follow up, the progression to EA is missed by current surveillance programs. Importantly, these data also suggest that acquisition of the sequence alterations is not uniform between all cases that progress to EA and the possibility of existing multiple evolutionary pathways driving the molecular evolution to cancer.[184, 207, 220] Indeed, the findings of two subsequent studies performing WGS and SNP in EA and WES

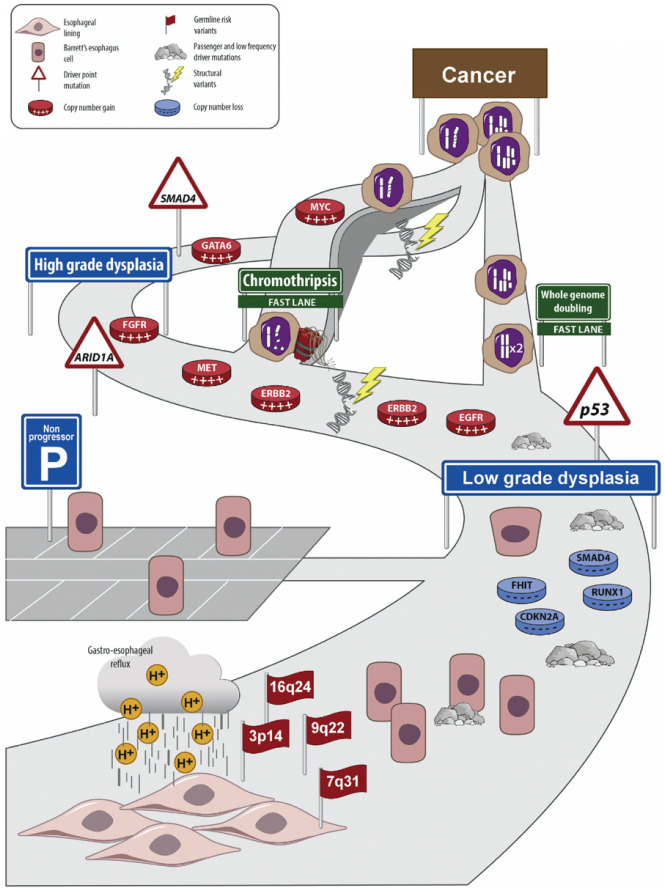

Figure 4. Pathways of BE progression to EA. BE can progress to EA along the traditional pathway following the multistep sequence metaplasia, LGD, HGD and EA, or by faster roots of genome doubling or genome catastrophes after p53 inactivation. (Retrieved from [204])

on paired samples of BE and EA corroborate this novel concept[214, 216], suggesting that BE progression to malignancy can occur by faster roots than the traditional pathway of tumorigenesis, where p53 mutations are followed by genomic catastrophe (chromothripsis) or genome doubling events. EA arising in these contexts are enriched in oncogenic amplification anomalies and presented a decreased frequency of tumor gene inactivation. Based on these

findings, two distinct pathways for cancer progression in BE arose as alternatives to the first established model (Fig. 4). [204]

While the traditional model is characterized by gradual loss of tumor p16 and p53 suppressor genes, followed by oncogene activation and then genomic instability development, in the novel pathways of cancer development, p53 inactivation is an early event and BE can accelerate via whole-genome doubling or genome catastrophes that are followed by genomic instability, aneuploidy and oncogene activation. These faster routes for cancer development might explain the failure of current surveillance and management standards to mitigate the increasing incidence of EA.[146, 204, 221]

All in all, despite the tremendous advances made towards understanding BE pathogenesis and carcinogenesis, and in particular the recent exciting era of discovery associated with massive scale data accomplished by NGS, many molecular events remain poorly understand. Most significantly, we are still far from being able to translate this knowledge into a molecular profile able to predict cancer risk in BE disease. This is even more important now considering that some patients can progress to malignancy by more rapid pathways, as previously discussed, that shorten the window of opportunity to detect progression to cancer at an early stage. So, future research must take advantage of these new technologies to further clarify the mechanisms associated with BE malignant progression and to identify biomarkers that could predict which BE patients have a higher risk of developing cancer, or in other words, which BEs are "born to be bad". Hopefully this knowledge will help create the tools that would allow managing BE patients according to their cancer risk, improving surveillance programs' efficiency and, above all, increasing the chances of treating them before EA development.[3, 91, 163]

1.3 Diagnosis and management of Barrett's esophagus patients

In the western world, BE diagnosis requires the presence of two criteria: (i) an endoscopically recognized segment of red velvet mucosa of any length extending above the gastro-esophageal junction (GEJ) (Fig. 5A), and (ii) a histological evaluation confirming the presence of IM (Fig. 5B). As discussed above, the identification of goblet cells in the metaplastic epithelium in order to establish a definite BE diagnosis is not required by all gastroenterology societies, such as BSG that only requires the presence of metaplastic columnar epithelium (Fig. 5C).[64, 222] Despite this major disagreement, once BE diagnosis is confirmed, all guidelines recommend the surveillance of these patients aiming to diagnose HGD or EA at an early stage.[9, 91, 223]

The standard of care for endoscopic surveillance is to use high-definition and high-resolution white light endoscopy (WD-WLE) for a detailed and accurate inspection of the surface of the columnar mucosa.[221, 223] The extent of BE segment should be recorded using the Prague C&M criteria [77] (Fig. 5D), a reliable and validated endoscopic reporting system developed to standardize BE endoscopic classification and to reduce inter and intra-observer variability. BE is

traditionally classified as long or short segment according to its length, ≥3cm or <3 cm respectively. This is relevant since there is scientific evidence demonstrating that longer BE segments have a higher risk of cancer development.[10, 116] Recent guidelines from the British Society of Gastroenterology (BSG), Cancer Council Australia and French Society of Digestive Endoscopy (SFED) already take this into account when they advocate the interval between endoscopic surveillance for non-dysplastic BE patients. Furthermore, all visible lesions should be described using the Paris classification.[10, 37, 95, 224]

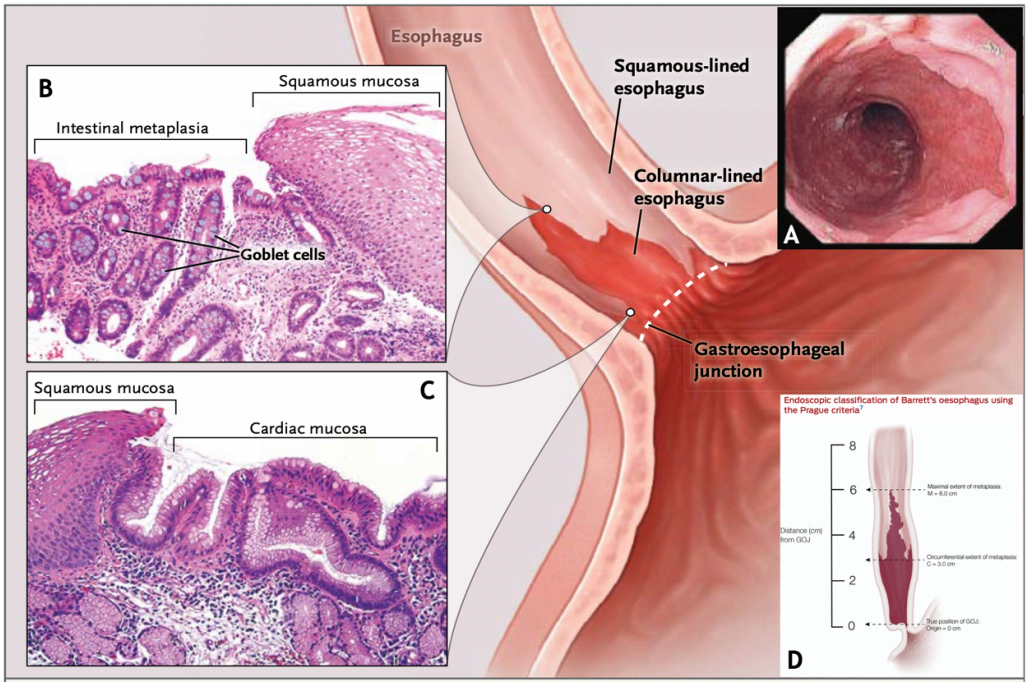

Figure 5. Diagnostic criteria of Barrett's esophagus. (A-C) The diagnosis of BE requires the endoscopic evidence of red velvet mucosa extending upwards GEJ (**A**) and the histological confirmation of the presence of IM in the biopsy specimens **(B)**. Some gastroenterology societies, such as BSG, only require the presence of columnar metaplasia (cardiac mucosa) to establish the diagnosis of BE **(C)**. **(D)** Prague criteria of BE. (adapted from [77, 81, 140])

An adequate and systematic biopsy sampling is also extremely important in order to maximize the sensitivity for IM, dysplasia and/or adenocarcinoma detection. Biopsies should be collected according to the Seattle protocol: random 4 quadrant biopsies should be obtained, every 2 cm over the entire extension of the columnar mucosa. Targeted biopsies of any visible lesion should be sampled separately. [222, 225, 226]

The histologic report should specify the presence of squamous epithelium, inflammation, columnar lined esophagus (CLE), native esophageal elements, intestinal metaplasia (IM), dysplasia and or EA. Dysplasia should be classified according to the Vienna classification: negative for dysplasia; indefinite for dysplasia; low-grade dysplasia (LGD); high-grade dysplasia (HGD); invasive epithelial neoplasia.[116, 160, 227] There are also studies suggesting that

dysplasia extent correlates with an increased cancer risk, so it is clinically relevant that pathologists describe dysplasia as focal or diffuse.[64]

Dysplasia remains the gold standard criterion for cancer risk stratification in BE patients and the basis to define guidelines for surveillance and management of those patients (Table 1).[160, 221, 224]

Table 1. Guidelines for Surveillance of Barrett's esophagus by different gastroenterology societies. (Retrieved from [81])

Disease stage	British Society of Gastroenterology (2013, 2015)[8]	American College of Gastroenterology (2015)[11]	American Society of Gastrointestinal Endoscopy (2012)[15]	American Gastroenterology Association (2011)[10]
Non-dysplastic Barrett's oesophagus	- Barrett's oesophagus <3 cm with intestinal metaplasia: surveillance endoscopy every 3-5 years - Barrett's oesophagus ≥3 cm: surveillance every 2-3 years	Surveillance endoscopy every 3-5 years	- No surveillance can be considered - If surveillance is elected: surveillance endoscopy every 3-5 years with 4-quadrant biopsies every 2 cm	Surveillance endoscopy every 3-5 years
Barrett's oesophagus indeterminate for dysplasia	- Review by second GI pathologist - p53 immunostain in addition to histopathological assessment - Optimisation of antireflux medication, repeat endoscopy in 6 months. - If no definite dysplasia found, surveillance as for non-dysplastic Barrett's oesophagus	- Review by second pathologist preferably GI pathologist - Repeat endoscopy after optimisation of acid suppression for 3-6 months - If Barrett's oesophagus indeterminate for dysplasia is found again, repeat exam-surveillance after 12 months	- Review by second pathologist - Increase antisecretory therapy - Repeat endoscopy and biopsy to clarify dysplasia status - Consider endoscopic ablation in select cases	—
Low grade dysplasia	- p53 immunostain - Repeat endoscopy in 6 months - If low grade dysplasia is found again and confirmed by expert GI pathologist, offer endoscopic therapy - If endoscopy therapy declined, surveillance every 6 months	- Review by second pathologist preferably GI pathologist - Endoscopic therapy preferred or surveillance every 12 months - Follow-up every year until no dysplasia seen on two consecutive endoscopies	- Confirm with expert GI pathologist. - Repeat endoscopy in 6 months to confirm low grade dysplasia - Surveillance endoscopy every year with 4-quadrant biopsies every 1-2 cm Consider endoscopic resection or ablation	- Confirm with expert pathologist - Surveillance endoscopy every 6-12 months - Consider endoscopic eradication therapy
High grade dysplasia or intramucosal carcinoma	- Endoscopic therapy preferred over oesophagectomy or endoscopic surveillance - Endoscopic mucosal resection recommended as most accurate staging intervention - EMR is therapy of choice if visible mucosal irregularities - If oesophagectomy elected, post-surgery surveillance on a symptomatic basis	- Review by second pathologist preferably GI pathologist - If mucosal irregularity present, do EMR - Endoscopic therapy recommended	- Confirm with expert GI pathologist - Consider endoscopic resection or RFA - EUS for local staging and lymphadenopathy - Consider surgical consultation - Surveillance endoscopy every 3 months in select patients, 4-quadrant biopsies every 1 cm	- Confirm with expert pathologist - If mucosal irregularity present, do EMR - Endoscopic eradication preferred over surveillance or surgery - If treatment not elected, surveillance every 3 months

GI = gastrointestinal. EMR = endoscopic mucosal resection. RFA = radiofrequency ablation. EUS = endoscopic ultrasound

In the past, the first line of treatment for Barrett's neoplasia was esophagectomy.[86] In the last decades, endoscopic therapies such as radiofrequency ablation (RFA), endoscopical mucosal or submucosal resection (EMR or ESMR, respectively) were developed to treat superficial neoplastic lesions that are associated with very good oncological outcomes and low morbidity/mortality rates.[9, 223] Esophagectomy is only indicated when endoscopic therapy is considered as non-curative, such as for advanced EA that presents invasion of deeper layers and a significant risk of lymph node metastasis.[226]

1.3.1 Current paradigm in screening and surveillance of Barrett's esophagus and future perspectives

Despite widespread screening and surveillance of BE with an effort to prevent a progression to cancer this practice has been revealed unsuccessful as rates of EA still continue to rise.[87] EA

continue to be a highly deadly cancer. Patients with advanced cancer have a poor prognosis with a low overall 5-year survival rate of less than 15% and for distant staged disease this value decrease to only 2.8%. However, when diagnosed at early stages, namely T1, the survival rate increases to more than 90%. So the best chance to improve survival is to detect EA at an early and potentially curable stage. [9, 91, 228]

The value and efficacy of this practice has been a controversial issue since it has several limitations.[140, 224] The selection of patients for screening is based on the presence of symptomatic GERD. However, there is a significant proportion of BE patients without reflux symptoms, mainly those with shorts segments. In fact, 40% of patients with EA did not describe any chronic manifestations of reflux and more than 90% do not have a prior BE diagnosis. This suggests that GERD is ineffective as a marker to target BE patients in the general population since it misses the cases without symptoms leading to a limited impact of surveillance on EA incidence and survival.[81, 140, 229]

Moreover, endoscopy as a screening tool is an invasive procedure and not without risks.[222] Screening programs with periodic endoscopies and biopsies are also expensive and time consuming for endoscopists and pathologists. The Seattle protocol is so laborious and demanding that there is poor adherence to this extensive biopsy sampling by endoscopists, particularly in long BE segments. This is important since inadequate sampling decreases the sensibility for dysplasia and extensive biopsy is even more important in long BE segments which have a higher risk of progression. Even when the Seattle protocol is strictly followed there is a chance of sampling error considering the small area of abnormal lining collected. In fact, dysplasia is not always associated with nodular areas or mucosal irregularities being sometimes flat, without apparent endoscopic alterations and focally distributed. Therefore, recognition of dysplasia can be difficult and easily missed despite meticulous endoscopic examination. [64, 95, 224] Furthermore, the diagnosis of dysplasia is highly complex mainly in the context of inflammation and regeneration making it difficult for pathologist to agree. Indeed, several studies demonstrated a significant inter- and intra-observer variability on dysplasia graduation even among experts. This is worrisome since surveillance intervals and management decisions are based on the histological assessment of dysplasia.[9, 95, 221]

With recent epidemiologic data showing that risk of cancer in BE patients is much lower than previously calculated and with the absence of randomized trials demonstrating a survival benefit, the cost-effectiveness of the current surveillance programs has been questioned.[77, 95, 230] Nevertheless and despite all these shortcomings, as pointed by Spechler and Souza, “to date, medical societies have taken the position that, in the absence of definitive data, it is better to error by performing unnecessary screening and surveillance than by forgoing the opportunity to identify curable esophageal neoplasms”.[140]

To overcome all these limitations, it is crucial in the near future to focus research on strategies to improve endoscopic surveillance and management of BE patients. The rationale is to develop

less invasive and more cost-effective screening tools as reliable biomarkers that could improve BE diagnosis and stratification. The ideal scenario would be to diagnose BE with no invasive methods and to be able to identify those that will progress stratifying BE population into low- and high-risk groups of malignant progression and defining surveillance intervals and therapy accordingly to cancer risk. As a result, the surveillance programs would be more cost-effective, being possible to (i) either exclude patients or to extend surveillance intervals for low-risk groups, and (ii) to intensify surveillance for high-risk cases or to anticipate treatment.[91, 231]

Intense clinical, endoscopic and fundamental research is actively ongoing to reach this goal. As examples, advanced endoscopic imaging systems allowing the endoscopist to distinguish areas of dysplasia/early EA in BE mucosa and new methods of collecting BE samples (Cytosponge) are being explored.[232, 233] In parallel, panels incorporating clinical, demographic and molecular parameters have been proposed to predict cancer progression in BE patients. Unfortunately, up to now, none of these strategies has been validated and reached the clinical setting.[9, 140, 234]

1.4 Biomarkers

By definition, a biomarker is a natural occurring molecule, gene or characteristic, which can be accurately measured or calculated as an indication of physiological processes, pathological conditions or a response to therapeutic intervention. [235, 236] In that sense, they constitute biological variables that should detect a stage already established, predict a future stage or both, correlating with a biological outcome.[237] Biomarkers could be found in tissues, blood or body fluids and its quantitative measure should influence medical decisions by aiding, improving or even changing patient's management.[236, 238] Ultimately, a biomarker should be useful and constitute a benefit for the patient.[239] An ideal biomarker should be as sensitive and specific as possible for the state or episode it purports to identify, easily measurable, consistent or stable over time, reproducible, cost-effective and accurate, which means that it must provide a reliable indication of the burden of the disease. It should also be applicable to the clinical or primary care setting and if possible, its evaluation should involve minimally invasive procedures.[141, 237, 240]

The quest for a reliable biomarker is an arduous, demanding, and overly long process. Not only is it challenging in time, but also involves the organization of large-scale studies and therefore requires substantial scientific, clinical and financial resources.[221, 239] Cancer biomarkers research has been expanding, specially fuelled in the recent years by advances in technology that allowed to set a goal towards a new era of precise medicine in which prevention and treatment decisions would take in consideration individual variability. With this in mind, extensive molecular profiles from several types of cancer have been determined in order to deepen the understanding of oncogenic mechanisms and to find the driving factors in cancer formation and progression. High-throughput "omics" technologies have allowed to measure thousands of different proteins, DNA, RNA, cell metabolites, microbial and host cell products, delivering data

that can be used to discover viable biomarkers. Consequently, a vast array of new biomarker candidates has been described in the literature every year.[221, 241] Nevertheless, despite very promising at the research stage, very few reach the clinical setting. The reasons for this shortcoming include methodological flaws, such as suboptimal biomarker discovery and validation, and poor clinical performance. Even when biomarkers pass with success the validation phase, they must prove their potential and clinical utility and the great majority fail to improve patient care over current clinical standards revealing to be clinically useless. As a result, only a scarce number of cancer biomarkers have been effectively implemented in daily medical practice to this day.[242, 243] In order to narrow the gap between biomarkers discovery and approval for clinical use, a five-phase model was defined to guide biomarker development and validation (Fig.6). In phase 1, or exploratory phase, potential biomarkers are identified. Phase 2 involves the development of an assay in which the sensitivity and specificity of the biomarkers are evaluated in individuals with the disease in relation to the control subjects. Subsequently, biomarkers need to be submitted to a validation process through retrospective and prospective longitudinal studies. In the first, the capacity of the selected biomarkers to detect the disease before its clinical diagnosis is evaluated (phase 3). In the second it is investigated the effective number and characteristics of the cases identified by using the biomarkers (phase 4). Finally, phase 5 consists in developing a large randomized population trial to assess the impact of the biomarker's detection on the reduction of the population disease burden. [240, 244]

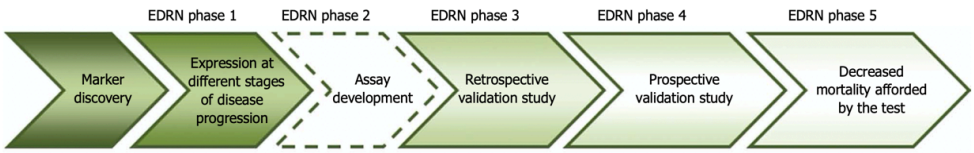

Figure 6. Biomarkers development. Phases of biomarkers development advocated by the Early Detection Research Network before clinical implementation. (Adapted from [236])

In the context of BE disease, it would be extremely valuable to develop biomarkers to inform clinical practice at multiple stages of the cancer pathway. Diagnostic biomarkers would be useful to detect the presence of BE in the general population, helping to diagnose cases without GERD symptoms.[236, 240] Biomarkers of BE progression will be extremely important to estimate the risk of cancer development and thus distinguish the patients with a higher risk of malignant progression from those who will remain with stable and non-dysplastic BE. This would transform the management of BE patients. Surveillance programs would be optimized and become cost-effective by the adjustment of endoscopic intervals to individual cancer risk: focusing surveillance on high-risk patients or even submit patients to early and preventive endoscopic therapeutic intervention, whereas low-risk patients could benefit from longer intervals between endoscopies or even be discharged from surveillance programs, not being subjected to unnecessary invasive procedures such as periodic endoscopies or endoscopic treatment.[146, 235] Biomarkers aiding the diagnosis of dysplasia and making the differential diagnosis between dysplastic and reactive and regenerative changes would also be of clinical

value.[141] For patients diagnosed at baseline with advanced EA, biomarkers to predict the response to neoadjuvant treatment or to guide the best therapeutic approach, including serving as biomarkers for molecular targeted therapies, could be extremely helpful. Finally, prognostic biomarkers can be useful as an indication of overall survival in EA patients.[236, 238, 240]

Despite the clinical need for all these different types of biomarkers, most research in the field has focused in finding biomarkers able to stratify the risk of progression among BE patients.[141, 245] Along with the known risk factors associated with BE pathogenesis and carcinogenesis, namely demographic, environmental and clinical factors, several molecular biomarkers have been under intensive investigation to evaluate its predictive power for malignant progression in BE patients.[84] It was envisioned that genetic and epigenetic alterations driving the BE progression to EA have the potential to be used as biomarkers able to distinguish in advance progressors from non-progressors.[240] In that sense, several types of molecular markers have been investigated: DNA content abnormalities (aneuploidy/ tetraploidy), chromosomal instability (CIN), tumor suppressor anomalies either by mutations, LOH or promoter methylation, epigenetic changes, altered gene expression, proliferation and cell cycle abnormalities, among others.[3, 246] In 2000, one of such seminal studies in a longitudinal cohort showed that patients with baseline biopsies with tetraploid or aneuploid cell fractions have an increased risk of progression to cancer, compared to patients with diploid biopsies.[3, 247, 248] Several other studies have followed demonstrating combinations of different molecular markers to be associated with a higher risk of developing malignancy. For example, one study showed that inactivation through methylation of p16, RUNX3 and HPP1 occurs early in the BE neoplastic sequence and predicts the risk of malignant progression.[249] Another study using a risk-prediction model of 29 different somatic chromosomal alterations, representative of CIN, demonstrated a better performance in predicting EA than p53 mutations, histopathology or flow cytometry DNA content.[250] In fact, over the years, it became evident that panels with combination of different molecular markers, or even in addition with clinical factors would be more sensitive and specific for progression than using one biomarker alone or only assess cancer risk based on the presence of risk factors.[251, 252] Furthermore, evolution of the “omics” techniques have provided novel insights about the underlying molecular mechanisms involved in BE malignant progression and in parallel revealed new potential biomarkers such as clonal diversity and mutational load [141, 185] Importantly, the increased sensibility of these novel techniques opened the field to novel avenues as the search for serum, cytology and breath-based biomarkers.[146]

Nevertheless, despite the tremendous efforts in finding a reliable biomarker or a panel of biomarkers for BE, this goal has not yet been achieved.[141] In fact, to date, the diagnosis of dysplasia continues to be the gold standard to assess the risk of EA development. Currently, North American guidelines continue not to recommend the use of biomarkers in clinical decisions regarding BE management.[146, 253] In contrast, BSG guidelines argue that evaluation of nuclear p53 expression by immunohistochemistry (IHC) already reach the level of

evidence necessary to be used in clinical practice to aid the histological evaluation of dysplasia.[10] Given that p53 was one of the first and most extensively studied biomarkers, there is already a vast amount of studies demonstrating that abnormal p53 IHC is a good predictor of progression and improves dysplasia diagnosis reproducibility.[235, 254] The validation and implementation of biomarkers to the clinical setting has been hindered by the conjugation of several factors.

Low rates of progression among BE patients limits the number of progressors to a few individuals in the studied cohorts and reinforces the need for large prospective population studies in the process of biomarkers validation.[251] Other causes related with methodological flaws have also been reported including absence of good follow-up, poor reproducibility of results between studies and problems with the development of accurate assays. Also, most biomarkers lacked sufficient sensitivity and specificity when tested in larger population trials. Finally, analysis and evaluation of some biomarkers need specialized equipment and appropriate laboratory expertise.[141, 240, 246] One way to overcome part of these limitations would be to organize multicenter collaborations in order to achieve larger samples sizes. Furthermore, now that high-throughput technology reached the accuracy and sensitivity needed to study the complex BE cancerigenesis process, this is the prime time to look for novel potential biomarkers. A solution to accomplish this challenging goal would be to gather a multidisciplinary group from the basic to clinical science that would propose innovative ways of unlocking some of the remaining mysteries associated to the pathways underlying BE malignant progression and then translate these findings into useful tools to be used in the clinical setting.[141] The increasing awareness that not all BE patients have the same risk of progression and that the majority of BE patients will never develop cancer [245, 254], together with recent data suggesting that some BE patients may develop rapidly progressing cancer in which the "window of opportunity" for endoscopic treatment is short [141], makes the discovery of these molecular markers even more important now than ever before.[245] Unfortunately, a missed progressive case continues to have profound consequences because there are no efficient therapeutic options for patients with advanced disease. However, much success have been achieved by advancements in endoscopic therapies in which curable treatment, without the need of major surgery or chemotherapy, is offered to patients with early cancer.[252, 254] It is therefore imperative to develop risk stratification tools to turn BE surveillance more effective. Finding a marker able to stratify BE patients according to cancer risk would be the "holy grail" of biomarkers because it would allow focusing surveillance to those high-risk patients that most likely will require early therapeutic intervention.[245, 255]

1.5 The centrosome in health and cancer

Looking for hallmarks in cancer could provide the unique opportunity to translate this knowledge into benefits to clinical practice, namely by developing tools that would help diagnosis, prognosis and guide cancer treatment. Considering that number and structure of centrosomes are tightly controlled in normal cells but are frequently found to be altered in

cancer cells, centrosomes abnormalities are then appealing features for the development of new strategies to apply in cancer medicine.

The centrosome is a small organelle with an important responsibility in cell homeostasis. It is a central player in cell organization and division [256], being increasingly acknowledged as the main center for microtubule organization, having also an important role in signal transduction paths and proteolytic activities[257]. The centrosome has therefore a preponderant role in several cellular processes known to be deregulated in cancer, namely cell division, cell differentiation, cell polarity, genomic composition and signaling pathways.[258-260] It is therefore conceivable that centrosome deregulation could contribute to cancer and in fact, centrosome amplification is currently recognized as a hallmark of cancer cells [261] and an attractive target for cancer therapies [262].

A growing body of evidence has been demonstrated that centrosome defects are pervasive in all major classes of human cancer and suggested they could be more than merely bystanders and play a role in tumorigenesis [263]. Furthermore, several molecular mechanisms linking centrosome alterations with cancer phenotypes have been established in animal and *in vitro* models bringing some understanding to the nature of this relation [264-266]. However, and despite the increasing knowledge in the field, the origin and impact of centrosome abnormalities in human cancer remain elusive and we are still far from getting the complete picture of this relationship [266]. One of the critical questions that remains unanswered is: are centrosome abnormalities simple passengers resulting from deregulation of other cellular processes in human cancer, or can they initiate cancer and promote tumorigenesis giving selective advantages to cancer cells? [267, 268] Further investigation will be crucial to give insight into the importance of centrosome abnormalities in cancer development and to exploit this knowledge to provide new tools to support cancer diagnosis, prognosis and therapeutics [263, 268].

1.5.1 The centrosome structure and function

The centrosome is a small cytoplasmic organelle well known as the major microtubule-organizing center (MTOC) in animal cells. The centrosome is comprised by a pair of orthogonally oriented centrioles embedded in an organized matrix of proteins, designated as pericentriolar material (PCM) (Fig. 7) [269, 270]. Centrioles are small cylindrical structures, with approximately 500 nm in length and 250 nm in diameter (in human somatic culture cells). Each centriole is made of nine sets of microtubules (MTs) organized in a radially symmetrical manner and a proximal-distal polarity. Centriolar MTs are highly acetylated and glutamylated and such post-translational modifications are thought to contribute to centriole stability [271, 272]. Within a centrosome the two centrioles differ in that the older mother centriole has subdistal and distal appendages, whereas the daughter centriole does not (Fig. 7). The subdistal appendages provide the place for cytoplasmic microtubule (MT) anchoring at the centrosome and the distal appendages are necessary for cilia/flagella formation [271, 273].

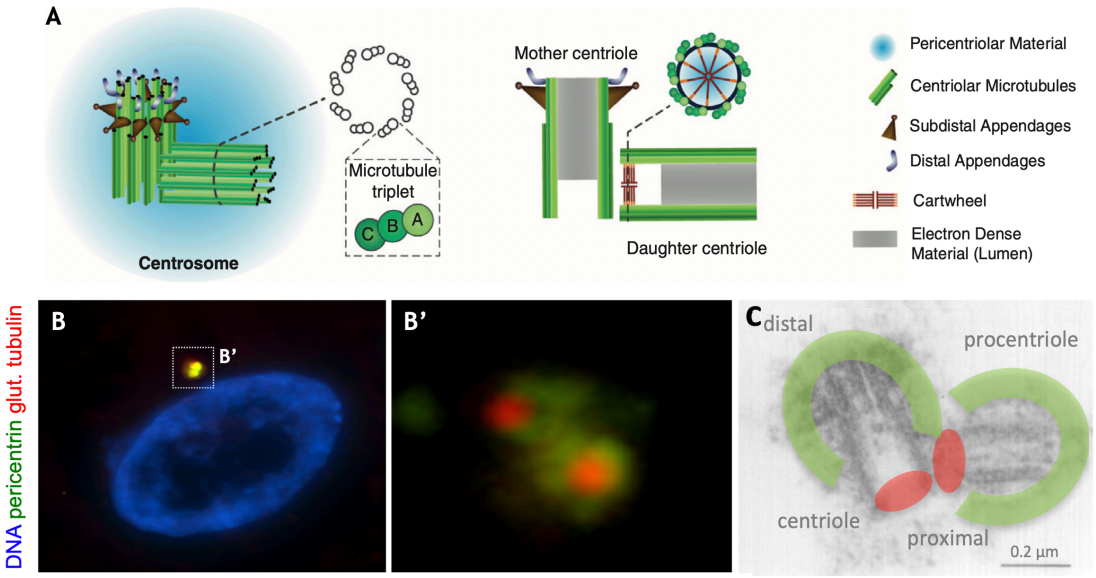

Figure 7. The Centrosome. A) Schematic representation of the centrosome showing the structural components of mother and daughter centrioles (retrieved from [274]). **B)** Esophageal squamous cell stained for PCM (pericentrin), centrioles (GT335–glutamylated tubulin) and DNA. **B')** Enlargement of centrosome shown in B. **C)** Electron micrograph of a longitudinal section through the centriole and procentriole overlaid with the approximate position of the PCM marker pericentrin (green) and the centriole marker GT335 (red). (A was retrieved from [274] and C was adapted [275]).

The PCM assembles around the centrioles and plays a role in cytoplasmic MT anchoring and nucleation [276]. The PCM size and composition changes throughout the cell cycle and in cell differentiation, with a rapidly turnover of some of the proteins through trafficking on microtubules [269, 277]. So, the PCM is a dynamic structure composed of a lattice of permanent and transient proteins that assemble around the centrioles in an ordered fashion [278]. Over 200 different proteins have been identified in PCM and while the function of some of these is still unknown, several have been found to play different roles including in MT nucleation, spindle organization and centrosome biogenesis [276, 277].

As a MTOC, the centrosome controls several interphase and mitotic MT related processes in the cell. In interphase, centrosome regulates the MT network required for intracellular traffic and positioning of several molecules and organelles; is involved in the stability of cell junctions and adhesions, contributing to the definition and maintenance of cell shape and cell polarity, important features for cell organization and for the development and maintenance of tissue architecture [278, 279] [258, 278]; and it also mediates cellular locomotion, and the organization of immune synapses [278]. Nevertheless, it is in mitosis that centrosome have its most notorious role ensuring the fidelity of cell division. During mitosis two centrosomes organize the MT array that forms the bipolar spindle, crucial for the accurate segregation of chromosomes to each daughter cell. They also determine the cell division plane, by controlling the positioning and orientation of the mitotic simple in the cell through the interaction of the astral MTs with the cellular cortex. The centrosome also has several non-MT related roles being the most relevant its cell cycle regulatory activity. [278, 279]

1.5.2 Centrosome regulation

The number of centrosomes is tightly regulated in a healthy cycling cell. In fact, the centrosome duplication cycle is coordinated with cell cycle progression through parallel regulatory mechanisms, being strictly coupled with DNA replication. Like DNA replication, centriole duplication occurs an in a semi-conservative manner, where "one and only one" new centriole forms orthogonally to an already existing centriole. Hence, at mitotic onset, the cell presents the correct number of two centrosomes (4 centrioles) that organize a bipolar spindle allowing the accurate segregation of chromosomes during cell division. Upon mitosis each daughter cell inherits the accurate complement of DNA (2n) and one centrosome (2 centrioles).[269, 270, 273] Centrosome duplication has been extensively studied and has been divided in four steps: centriole disengagement, procentriole formation, procentriole elongation, and centrosome separation (Fig. 8).

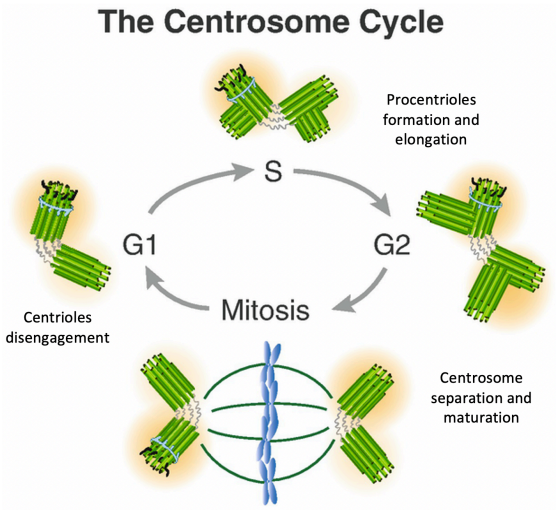

Figure 8. Schematic representation of the canonical centrosome cycle. During mitosis there are two centrosomes, one at each pole of the mitotic spindle, both composed of mother and daughter centrioles. Centrioles disengagement occurs in late mitosis to early G1 phase and orthogonal configuration is lost. During this stage the daughter centriole acquires its own PCM becoming the new mother centriole able to duplicate. During phase S, the procentrioles form on each mother centriole and elongate. By late G2 the new daughter centrioles reach their full length and from G2 to mitosis the two centrosomes separate and migrate to opposite poles of the cell to form the mitotic spindle. (Adapted from [280])

Centriole disengagement occurs in late mitosis to early G1 phase, wherein the mother and daughter centriole within a centrosome disengage, losing their orthogonal configuration but remaining connected through their proximal ends by a proteinaceous linker. This process is mediated by separase and PLK1. Centriole disengagement is considered an important licensing factor for centriole biogenesis. [258, 271, 281] During G1, the daughter centriole gains its own PCM becoming able to duplicate. Towards the G1/S transition, procentriole formation begins. PLK4, the master regulator of centriole duplication is recruited to each parental centriole with the assistance of CEP63, CEP152 and CEP192 and together they are distributed in rings around the centriolar wall. At this stage PLK4 accumulates at one specific location from the side at the proximal end of the parental centrioles. PLK4 then binds to and phosphorylates STIL, which

facilitates its association with SAS-6 and triggers its recruitment. SAS-6 in conjunction with CEP135 is needed to form the cartwheel, the structure that will dictate the nine-fold symmetry of the procentriole and holding it engaged to the parental centriole.[279, 282] CPAP stabilizes the cartwheel and is crucial for the recruitment of cytoplasmic MTs that connect to each cartwheel spoke and then the procentriole starts to assemble and begins to grow orthogonally from the parental centrioles. During S and G2 the procentrioles elongate and by late G2, the procentrioles reach their full length. This process is controlled by the capping proteins CP110 and CEP97, which associate to the distal ends of the centrioles to stop further growth and thus determining the final length of the newly formed centrioles. [258, 264, 283] Research over the past years has revealed several other proteins playing important roles in these processes. From G2 to mitosis, the flexible link that maintained the two parental centrioles connected is disrupted and the two centrosomes separate and migrate to opposite poles of the cell to form a bipolar spindle [271]. During this transition, centrosomes undergo a process known as centrosome maturation characterized by the increase recruitment and accumulation of PCM components, and in which the kinases Aurora-A, PLK1 and CDK1 play an important role [284]. Several proteins were already identified as being involved in PCM recruitment, anchoring and organization. An historical example is the role of pericentrin, which is directly connected with the periphery of the centrioles, and is responsible for the recruitment and organization of other PCM proteins, such as, gamma-tubulin [285]. During mitosis the daughter centriole loses the cartwheel, which is targeted for degradation. By the end of mitosis, each daughter cell inherits exactly one centrosome with a pair of centrioles, and by the beginning of G1 the daughter centriole fully matures into a mother centriole by acquiring both distal and subdistal appendages. At this point cells can reenter a new cell cycle, or either enter in G0 or become terminally differentiated. In these stages the mother centriole could be recruited for ciliogenesis or the centrosome may be inactivated and no longer function as the main MTOC of the cell. [284]

1.5.3 Centrosome deregulation

The link between centrosome aberrations and cancer was postulated long ago and impressively, several decades before the identification of tumor suppressor genes and oncogenes. The first descriptions recognizing that aberrant mitotic figures are common in cancer cells date back to the end of 19th century and were made by two pathologists, Gino Galeotti and David von Hansemann resulting from the observation of histological tumor tissues [264]. But it was only in 1914, in a landmark publication, that the biologist Theodor Boveri proposed for the first time that centrosome amplification could cause cancer [286]. By observing that sea urchin embryos with multiple centrosomes undergo abnormal mitosis and generate highly aneuploid daughter cells, he conceived a theory where extra centrosomes would lead to multipolar spindles and incorrect chromosome segregation during mitosis, hence promoting aneuploidy and tumorigenesis. [258, 264, 287] Nevertheless, his postulate implicating centrosome aberrations in the etiology of cancer was left unnoticed for almost 100 years. It was only by the end of 20th century, with the increasing knowledge about centrosome biology and their key roles in cellular

homeostasis together with the observation that loss of the tumor suppressor p53 in mouse fibroblasts leads to centrosome amplification, that centrosomes returned to the focus of research associated with a variety of human diseases, including cancer.[264, 288, 289]

Several studies have already shown that centrosome aberrations are present in a broad spectrum of human malignancies [263]. These studies identified several types of alterations, including the presence of extra centrioles/centrosomes, longer and aberrant centriole structures, and changes in PCM composition, shape and size. However, the mechanistic insights linking centrosomes abnormalities with human tumors are still poorly understood. Decoding the underlying mechanisms originating the broad range of these centrosomal aberrations in cancer as well as their physiological consequences in tumor formation and progression has been challenging.[278, 290] Nevertheless, numerous studies in cultured cells and model organisms have begun to elucidate the underlying mechanisms regarding the origin and impact of centrosome abnormalities in cancer [272, 291].

1.5.3.1 Types of centrosome abnormalities

Centrosome anomalies in cancer have been largely subdivided into two main categories: numerical and structural aberrations. Despite conceptually different, they often occur together in tumors [258, 277].

Numerical defects correspond to an abnormal centrosome copy number. While centrosome loss has not been documented in human tumors, the presence of extra centrioles, also know as centrosome amplification, has been widely described and is probably the best characterized centrosome abnormality phenotype in cancer cells. Structural aberrations comprehend anomalies on centriole structure and/or on the amount, composition, or even phosphorylation status of PCM components [264, 267, 270, 277]. Contrary to numerical defects, structural aberrations have been much less explored in human cancer, mainly due to technical limitations. An accurate evaluation of structural anomalies implies the use of electron microscopy and so far the vast majority of studies only used immunostaining techniques labeling centrosomes with one PCM marker, which gave only an indication of alterations in volume and shape of that particular PCM component [272, 292-297]. Moreover, using solely a single PCM marker is insufficient to distinguish from an increased amount of PCM or an increased number of centrosomes that could be localized close to each other reflecting instead a numerical aberration. Notwithstanding these technical restrains, currently, there are no doubts that centrosome abnormalities are a prominent feature in human neoplasias and are thus considered a hallmark of cancer [264, 287].

1.5.3.2 Centrosome abnormalities in human cancer

A growing body of evidence has established that most malignancies display centrosome aberrations and these are currently acknowledged as a hallmark of cancer [287]. Centrosomes have been evaluated in a broad range of different types of human cancer: not only in tumors

from diverse organs (brain, head and neck, breast, lung, stomach, pancreas, liver, gallbladder, colon, prostate, uterus) but also in tumors derived from different cell types, such as epithelial, mesenchymal and blood cell lineages. This extensive analysis has demonstrated that centrosome aberrations, and particularly centrosome amplification, are a prevalent finding in nearly all solid and hematological malignancies surveyed [263, 272, 298].

Remarkably, centrosome abnormalities have been observed in the earliest pre-invasive stages of cancer progression supporting a role in cancer initiation. In a study characterizing centrosome changes along the adenoma-carcinoma sequence of colorectal carcinoma, namely in low-grade intraepithelial neoplasia (LGIN), high-grade intraepithelial neoplasia (HGIN) and invasive carcinoma, numerical and structural centrosome defects were detected as early as in LGIN of the cancer pathway [299]. In accordance, previous work had also demonstrated that intraepithelial neoplasias of prostate and the uterine cervix and female breast in situ carcinomas already present centrosome defects [300, 301]. Likewise, in organotypic cultures and animal models, centrosomes defects are an early event in the progression of malignant phenotypes.[266]

In addition, centrosome abnormalities have been shown to increase along the carcinogenic pathway, being more pronounced in late stage disease suggesting they may also be involved in cancer progression [257, 263]. In cervical cancer numerical centrosome aberrations positively correlate with progression from cervical intraepithelial neoplasia CIN I, CIN II, CIN III and, ultimately, invasive carcinoma [301]. Furthermore, other studies in invasive cancers have shown that the frequency of centrosome abnormalities increases with tumor stage (from stage I to IV), namely in head and neck squamous cell carcinoma, in ovarian cancer, and in biliary tract malignancies including gallbladder cancers, intrahepatic collangiocellular carcinoma and bile duct carcinomas [302-304]. In contrast, in non-small cell lung cancer and hepatocellular carcinoma there was no significant relation between centrosome aberrations and tumor stage [292, 293, 305]. Concerning the degree of differentiation, in the vast majority of human cancers, centrosome aberrations tended to be more pronounced in high-grade neoplasias, which are poorly differentiated tumors that normally have a worst prognostic than low-grade neoplasias, which are well differentiated and less aggressive tumors. This trend was shown in diversified types of cancers, including oral squamous cell carcinomas, gliomas, breast, ovarian, prostate and bladder neoplasias, among others [294, 303, 306-310]. Nevertheless, just as it was found for tumor stage, there are some cases where centrosome aberrations were not found to be associated with tumor grade, namely in breast and lung cancer [305, 311-313].

Centrosome defects have also been correlated with several other clinical criteria for aggressive disease and consequently poor prognosis, such as, lymph node and/or distant metastasis, early tumor recurrence and poor survival. For example, studies on breast cancer showed a highly significant correlation between centrosome aberrations and lymph node metastasis [311, 314]. Likewise, centrosome amplification in head and neck squamous cell carcinomas represent a

phenotypic marker of cancer aggressiveness, being frequently associated with tumor recurrence, and are significantly correlated with the presence of distant metastasis, poorer disease free survival and worse overall survival [304, 315]. In ovarian cancer, patients with a higher incidence of extra centrosomes have a significant poor survival outcome [316]. In giant cell tumor of bone, a benign tumor but with a potential aggressive outcome, centrosome amplification was significantly increased in recurrent and malignant tumors when compared to non-recurrent cases [317]. In gallbladder cancer, patients with centrosome amplification developed tumor recurrence whereas patients without extra centrosomes did not, and centrosome amplification proved to be an independent prognostic factor for tumor recurrence [306]. Notably, in squamous cell carcinoma of the larynx, centrosome amplification was not only a better predictor of tumor recurrence than tumor stage but it was also able to predict recurrence even in tumors without lymph node metastasis [318].

Similarly to solid tumors, several studies have demonstrated a correlation between centrosome aberrations and clinical aggressiveness in many hematological neoplasias such as myeloid malignancies, chronic lymphocytic leukemias and in several types of lymphomas. More aggressive types of lymphomas, such as mantle cell lymphoma, Burkitt's lymphoma and diffuse large B-cell lymphoma, display more centrosome abnormalities than more indolent types such as follicular and marginal B-cell lymphomas [263, 319]. Furthermore, regardless of lymphoma subtype, centrosome amplification positively correlates with the mitotic index, and particularly in follicular lymphomas the population of cells with supernumerary centrosomes significantly increases with tumor grading [320]. Notably, in a study on multiple myeloma where the authors generated a gene-expression-derived index strictly related to centrosome amplification, which they called centrosome index (CI), they found that CI is a powerful and independent prognostic factor meaning that a high CI discriminates the patients with poor prognosis irrespective of disease phase or treatment option [321].

Several molecular alterations have also been associated with centrosome aberrations depending on the type of cancer studied. In hepatocellular carcinoma the population of cells with centrosome aberrations tends to be significantly higher in tumors with p53 loss (a frequent genetic event associated with advanced stage disease and poorly differentiated tumors), than those with wild-type p53 [292]. In contrast, studies in non-small lung cancer showed that centrosome aberrations were significantly correlated with loss of pRb, p16 and cyclin E overexpression, but not with p53 mutation and expression [293, 305]. In ovarian and squamous head and neck carcinomas, centrosome anomalies were positively associated with overexpression of Aurora-A, a serine-threonine kinase that is crucial for regular centrosome function [316, 322]. On the other hand, in breast cancer, centrosome amplification significantly correlated with loss of expression of the tumor suppressor BRCA1, but not with Aurora-A or p53 expression [313]. In cervical cancer, high-risk HPV infection was suggested to be associated with the progressive numerical centrosome defects observed during cancer progression [301].

Numerous studies have also found a correlation between centrosome abnormalities and chromosomal instability (CIN) and aneuploidy, two recognized hallmarks of cancer, in several types of solid and hematological malignancies [278], including hepatocellular and urothelial carcinomas, osteosarcomas, chronic myeloid leukemia and non-Hodgkin's lymphomas [292, 297, 320, 323, 324]. For example, centrosome aberrations were found to co-occur with mitotic spindle abnormalities, CIN and aneuploidy in pre-invasive stages of cervix, prostate and breast cancers [300, 301]. Remarkably, lesions with centrosome defects lacking CIN were more common than lesions presenting CIN without centrosome aberrations, suggesting that, at least in these models, centrosome abnormalities precede CIN and may have a functional impact in the malignant progression of these pre-invasive lesions [300]. In invasive cancers, like breast and prostate cancer, centrosome defects showed a significant positive correlation with CIN, aneuploidy, and worst malignant features such as loss of tissue differentiation, metastasis and poor prognosis, suggesting their potential involvement in malignant progression as well [266, 294, 307, 309]. Furthermore, a study where numerical and structural centrosome defects where detected in tumor cell lines from Hodgkin lymphomas, colorectal, prostate and breast carcinomas, it was confirmed that these aberrations contributed to the formation of aberrant mitotic spindles and chromosome missegregation. In fact, these cell lines showed high variability in chromosome number and centrosome defects strongly correlated with CIN reinforcing their potential role in genetic instability in human cancer [295].

1.5.3.3 Causes of centrosome abnormalities

Several pathways by which cells could acquire supernumerary centrosomes have already been described. One major mechanism generating extra centrosomes is centriole overduplication. This can be driven either by deregulation of the cell cycle, culminating in consecutive rounds of duplication during the same S-phase, or by deregulation of centrosome biogenesis by alterations on the levels, timing and localization of proteins involved in the centriole duplication process.[291, 325] For example, overexpression of key centriole biogenesis molecules such as PLK4, STIL or SAS6 promotes the formation of several procentrioles around each mother centriole in cultured cells [326]. Centriole overduplication can also be triggered by overexpression of PCM proteins, such as pericentrin [327], or even as a consequence of mutations in tumor suppressor genes or oncogenes [328]. For example, BRCA1 tumor suppressor loss of function leads to an increase of gamma-tubulin levels, promoting centrosome amplification [329]. Premature centriole disengagement as a result of mitotic delay could also result in supernumerary centrosomes, by licensing an anticipated procentriole formation.[330] Furthermore if premature centriole disengagement is followed by complete separation of the paired centrioles, and each one continues to be surrounded by PCM they could function as individual centrosomes since maintain capacity to recruit microtubules, which could result in multipolar spindle formation [331]. Despite *de novo* centriole assembly could be a normal occurring event in specific contexts[332], *de novo* assembly could also result from deregulation of centrosome biogenesis, wherein extra centrioles arise dispersed in the cytoplasm not

connected to the pre-existent centrioles during S-phase. For instance, abnormal increased levels of pericentrin could result in de novo centriole formation [287, 327].

Extra centrosomes could also accumulate due to polyploidization events, namely through cell fusion, mitotic slippage and cytokinesis failure, which generate tetraploid cells with the double of DNA content and number of centrosomes [264]. Cell fusion could be induced by virus [333]. The latter two mechanisms could result either from alterations affecting the molecules responsible for the regulation of mitotic progression or cytokinesis phase. It is known, for example, that malfunctions of spindle assembly checkpoint (SAC) allow cells to progress to a new G1 phase without mitosis or cytokinesis completion [278, 287]. These mechanisms of centrosome amplification, occurring in parallel with the doubling of the genome, could provide a benefit against detrimental mutations and errors on chromosome segregation on the cancerigenesis pathway and furthermore have the potential to create tetraploid cells with a genomic combination that provides a growth advantage. In line with a pro-tumorigenic role of tetraploid cells, an increasing amount of data has been providing evidence that an intermediate stage of tetraploidization is a common event in malignant pathways of several tumors, including in BE cancerigenesis [334], which normally precedes aneuploidy [277, 298].

Structural centrosome defects have been far less studied than numerical alterations. To date, the prevailing thinking is that they probably arise from gene expression alterations or altered posttranslational modifications that drive changes in the levels and or activity of centrosome proteins, affecting the structure of the centrioles and/or inducing abnormal PCM amounts [264, 277, 290]. In accordance, several studies have shown that CPAP controls centriole length [335] and its overexpression leads to overly long centrioles in different human cancer and non-cancer cell lines [335-337]. Importantly, it was demonstrated that centriole over-elongation could generate centriole amplification by ectopic procentriole assembly and centriole fragmentation with the potential detrimental effects previously described [337]. Moreover, studies in cell lines reported that overexpression of some PCM proteins (e.g. pericentrin, CEP135) also gives rise to structural abnormalities [298]. Excess PCM proteins could accumulate in the centrosome originating enlarged centrosomes or additionally could dissociate from the centrosome forming acentriolar bodies by a process called PCM fragmentation [290], which could have the capacity to nucleate microtubules and give rise to multipolar spindles during mitosis [331].

Determining if centrosome abnormalities result from intrinsic dysfunctions in centrosome biogenesis process, or if instead they arise secondary to deregulation of other cellular processes, has been challenging. Moreover, given that structural abnormalities could lead to numerical changes and that both numerical and structural centrosome aberrations can co-occur in most cancer types, it is difficult to determine which driving mechanisms are more prominent in cancer and what is the relevance of each one in the development of individual human tumors. It is possible that a particular mechanism may be exclusive of specific types of cancer but it is also conceivable that more than one mechanism could cooperate in a particular cancer pathway. For

example, in cervical cancer it was demonstrated that human papilloma virus (HPV)-16 oncoproteins E6 e E7 promote centrosome amplification by different mechanisms: through cytokinesis failure resulting in increased ploidy and centrosome number, and through abnormal centrosome duplication, respectively [338]. In the future, it will be important to develop new methods that would allow a better characterization of centrosome aberrations in human cancer and to disentangle the broad spectrum of these alterations among different neoplasias.

1.5.3.4 Consequences of centrosome abnormalities

Concerning the impact of centrosome amplification in tumorigenesis, a causal link between an increased number of centrosomes and the formation of aberrant multipolar mitotic spindles during cell division driving chromosomal instability (CIN) and aneuploidy, was proposed long ago by Theodor Boveri [270, 278]. As the centrosome plays an important role in the organization of a bipolar mitotic spindle that ensures the equal division of genomic material to the daughter cells, centrosome amplification could lead to aberrant mitotic spindles and chromosome missegregation, promoting CIN and aneuploidy, two recognized hallmarks of cancer [278, 298]. In accordance, several clinical studies in a broad range of solid and hematological tumors showed that centrosome aberrations have a positive correlation with multipolar mitoses, CIN and aneuploidy supporting its clinical relevance in human cancer.[263, 339] However, multipolar cell division is intrinsically inefficient, most frequently culminating in cell death, mitotic catastrophe or cellular senescence, which would lead to tumor growth impairment [278]. Indeed, live imaging of cancer cells has demonstrated that multipolar spindles mostly originate unviable highly aneuploid daughter cells, due to massive loss of genetic material, resulting in death of cell progeny [325, 340, 341]. So this constitutes an apparent paradox since multipolar cell divisions resulting from extra centrosomes can be detrimental for cell survival and act as tumor suppressors instead of promoting tumorigenesis.[278]. In the attempt to solve this mystery, several studies performed long-term live cell imaging and found that many cancer cell lines from different origins have developed survival mechanisms to cope with centrosome amplification during mitosis, either by inactivation of their supernumerary centrosomes through detachment from the spindle structure, and/or by clustering them into two dominant spindle poles forming a pseudo-bipolar spindle array that originates two viable daughter cells [270, 342-345]. Nevertheless, before the centrosome clustering process is complete, these cancer cells pass through a transient multipolar spindle in which the occurrence of incorrect merotelic attachments and lagging chromosomes drives low levels of chromosome missegregation and resulting in progeny with low levels of aneuploidy that is compatible with cell survival [267, 277, 340, 341]. So, these studies provide a mechanistic link by which centrosome amplification could promote CIN and aneuploidy in cancer, and a possible explanation for the strong correlation between them in human tumors [270, 291]. Furthermore, structural abnormalities could also have profound impact on fidelity of chromosome segregation, by also promoting CIN and aneuploidy [265]. Some alterations such as premature centriole disengagement or PCM fragmentation, could give rise to extra MTOC, despite resulting mostly in structurally compromised centrosomes, causing

loss of spindle pole integrity and generating multipolar spindles. In fact, some studies already demonstrated that depletion of ninein as well as other centriolar satellite proteins drives PCM fragmentation resulting in multipolar spindle formations [331]. Additionally, it was shown that overly long centrioles nucleate more PCM and consequently have an increased MT nucleation capability, promoting errors in chromosome segregation and consequently enhancing CIN [337]. Importantly, a recent study addressing the fundamental question of centrosome amplification being sufficient to drive tumorigenesis, by using PLK4 overexpression to generate prevalent supernumerary centrosomes in mice, was able to demonstrate that continuous increased centrosome numbers are sufficient to initiate spontaneous tumors in several tissues, establishing a causal link between them [346].

Extra centrosomes could also play a role in tumorigenesis by interfering with asymmetric division of stem cells. Studies in Drosophila have shown that transplantation of neuroblasts (neural stem cells) with supernumerary centrosomes into the abdomen of adult flies generated highly proliferative and lethal tumors. Intriguingly, these tumors were only slightly aneuploidy, suggesting a different mechanism may be driving the development of this aggressive phenotype. Amplified centrosomes in neuroblasts generate abnormal spindle orientation, resulting in an increase of symmetric over asymmetric cell division and consequently in an expansion of the neuroblast population which could promote overproliferation and a tumor initiation event. Hypothetically, this mechanism could also be present in human tumors, particularly in those cancers derived from stem cells that undergo asymmetric cell division. [264, 277] However, it is important to note that supernumerary centrosomes in developing mouse brains do not induce spindle alignment defects during division of neuronal stem cells. In contrast, these cells, through inefficient centrosome clustering, originate highly aneuploid progeny that undergo apoptosis leading to tissue degeneration and culminating in microcephaly.[347] These findings suggest that the consequences of centrosome amplification in the context of asymmetric cell division seem to vary depending on cell type and host organism.[270]

As the centrosome plays a crucial role on the organization and maintenance of MT network in interphase cells, centrosome abnormalities could also promote changes in cell shape, adhesion, polarity, and motility with impact on tissues architecture.[291] So, potentially these structural defects could influence cancer cell properties, namely, enhancing their propensity to invade and metastasize.[290, 291] In fact, supernumerary centrosomes in interphase cells normally cluster and recruit more PCM, thus increasing their MT nucleation activity. [264] Through increased MT nucleation, extra centrosomes can affect focal adhesion between cancer cells and led to the formation of protrusions, promoting cell migration and invasion of the surrounding extracellular matrix in 3D culture models of a non-tumorigenic breast cell line. [348] Consonantly, recent studies also using 3D spheroid cultures of a normal mammary epithelial cell line have shown that overexpressing ninein-like protein, to the levels found in human tumors, gave rise to the formation of aggregates, which they called centrosome related bodies (CRBs), that cause reorganization of the MT cytoskeleton, disrupting cell polarity, cell-cell

adhesion and epithelial architecture and by an increased response to growth factors, they also boost overproliferation [349]. In consequence, those epithelial cells acquire an invasive phenotype, namely through three different mechanisms: invadopodia formation, non-cell-autonomous budding of mitotic cells and basal extrusion.[265, 350] Indeed, another study using 3D breast organoids but also a zebrafish model demonstrated that supernumerary centrosomes trigger a secretory response of pro-invasive factors that leads to the induction of an invasive phenotype by a non-cell autonomous mechanism, namely through a paracrine effect on surrounding cancer cells with no amplified centrosomes [351]. So, centrosome abnormalities could be crucial in human tumors, not only in the promotion of CIN and aneuploidy but also in actively contributing to tumor invasion and metastatic spreading [258, 265].

An important but much less investigated matter is the association of ciliogenesis defects and cancer. Since centrioles are also required for cilia formation, alterations in centriole numbers may affect ciliary signaling pathways [290] which were already found deregulated in tumors. In accordance, ciliogenesis is disrupted in different cancers, as breast [352], pancreatic [353] and renal cell carcinomas [354]. Notably, ciliogenesis defects have been associated with inhibition or enhancement of tumor growth depending on the perturbed signaling pathway.[355, 356] Nevertheless, this relation remains elusive and future research on this area will be important to clarify how ciliogenesis deregulation could contribute to cancer [357].

Despite the tempting perspective that accurate characterization of centrosome abnormalities in human cancer has potential to impact diagnosis, prognosis and cancer treatment, further work is still needed before the exciting data obtained in model systems can be extrapolated to the clinical setting.[265] Evidences so far are very promising, and considering that centrosome amplification is an appealing feature for targeted therapies, several drugs are being developed and tested. For example, PLK4 inhibitors were developed considering their crucial role in centriole duplication and the promising results obtained with these inhibitors in different tumors cell lines and patient-derived xenograft models has already resulted in one of them (CFI-400945) entering in phase I and II clinical trials (reviewed in [358]). Also, since it was already shown that inhibition of centrosome clustering selectively promotes cells death in cancer cells having supernumerary centrosomes [343, 359], inhibitors against proteins involved in this process, such as HSET are being developed [360]. Nevertheless, the success of using these drugs alone or as combined therapies depends how patients respond to these treatments and if they are able to increase overall survival. So, in the near future it is crucial to understand if centrosome anomalies are truly prevalent and relevant for human cancer. Definite proof of the underlying mechanisms of origin and impact of centrosome abnormalities in human tumors needs to be further investigated. Studying centrosome abnormalities along the cancer pathways and combine model systems with patient samples will probably increase the odds of success of accomplishing this demanding task.

1.6 Framework of the thesis: research problem, aims, objectives and approaches

The major concern in Barrett's esophagus disease relies on the fact that is the precursor lesion of EA.[141] Actually, BE patients have an increased and persistent risk of developing this neoplasia over time.[361] Despite the low rate of BE neoplastic progression the risk is not neglectable and, importantly, the incidence of both disorders has been climbing in parallel. [91, 237] Furthermore, EA is a cancer with high morbidity and mortality unless diagnosed at early stages.[9, 91] These evidences constitute the rationale for gastrointestinal (GI) societies worldwide recommending endoscopic screening and surveillance for BE patients with the goal to detect an aggressive and lethal tumor at a curable stage and therefore improve EA survival rates.[253, 254] Up to now, pathological assessment of dysplasia is the basilar stone for clinical decision making, regarding BE management. Evaluation of p53 through immunohistochemistry was proposed by BSG to aid the diagnosis of dysplasia but the poor reproducibility of this technique, associated with methodological flaws and inter-observer variation, has been a major hurdle against its widespread clinical use and in fact the other GI societies do not recommend the use of any biomarkers for evaluation of cancer risk besides dysplasia.[9, 10, 34, 35]

Nevertheless, the success of this practice has been hampered by several limitations: a significant proportion of BE patients remain undiscovered due to lack of reflux symptoms, and therefore they are not under surveillance[140]; most of EA cases do not have a previous diagnosis of BE[103]; endoscopic surveillance with biopsies is costly, time-consuming and too invasive for being applied to the overall population [91, 222]; there are poor adherence to guidelines regarding surveillance intervals, use of the Seattle protocol to collect biopsies and a confirmatory opinion for dysplasia diagnosis by a second pathologist [224]; the endoscopic recognition of dysplasia can be very difficult and easily missed despite careful evaluation, which leads to sampling error [224]; the grading of dysplasia is challenging, subjective, and not reproducible [221]. Above all, current clinical strategies cannot anticipate cancer development. Until now, none of the existing clinical and histological criteria allow to stratify BE patients according to cancer risk, this is, to discriminate the ones that will remain with stable BE from those with a higher risk of malignant progression [362]. Consequently, all BE patients have to be submitted to periodic invasive procedures despite the great majority will never progress to cancer.[160] Considering the low progression rates of malignant progression, surveillance implies a labor- intensive practice and is not cost-effective for most of BE patients.[363]

All in all, despite all the efforts made thus far, conventional surveillance strategies are increasingly recognized as being unsuccessful, not only because EA incidence rates still continue to increase but also because they have failed to reduce mortality from this malignancy.[228, 253] By shedding light into the fragilities of current practice, this scenario provided several opportunities for improvement, highlighting the urgent need for the development of better strategies to improve BE screening, surveillance and management.[251] Indeed, despite all the

progress made in the understanding of BE disease, the pathways underlying BE malignant progression remain ill-defined and, until now, none of this knowledge has been translated in tools to be used in the clinical setting. Thus, it is imperative to find more targeted strategies, namely, to identify predictors of disease behavior that could aid patient management.[91] Moreover, it is crucial to find biomarkers able to trace a risk profile of BE patients so that surveillance intervals and therapy could be defined according to cancer risk. These clinical tools would be of great value since the efficient prediction of cancer progression would allow improvement of the cost-effectiveness of surveillance programs by focusing surveillance on high-risk patients, but even more important by the improvement of patient care. So, while in high-risk cases the intensification of surveillance would be advised or eventually prophylactic treatment could be pondered to prevent malignant progression, in low-risk cases the intervals between endoscopies could be extended or patients could even be excluded from surveillance.[231, 364] The enduring hope is that molecular markers could be integrated in the clinical setting and the joint use of these markers with clinical, endoscopic and histologic factors would allow a transition from a curative to a preventive cancer model where a risk profile for each BE patient could be traced, founding the base for subsequent clinical decisions and allowing to intervene at the BE stage, this is, before the appearance of dysplasia.

The present work was designed to tackle this important clinical oncologic problem and so the global aim of this thesis was to better understand the pathways underlying BE malignant progression and thereby identify reliable biomarkers relevant for the diagnosis, prognosis and management of BE patients, thus ultimately contributing to an improved understanding of BE biology and an optimized support for clinical decisions.

To ensure the success of this project and being part of a multidisciplinary team with expertise in molecular genetics, cell biology, computational biology, and patient-oriented translational research, we took a multifaceted approach to accomplish our aim using both (i) an unbiased approach, exploring transcriptome datasets from clinical samples to define a gene set associated with cancer development and, thus, identify early molecular biomarkers predictive of BE progression to malignancy, and (ii) an hypothesis-driven approach, exploring when and how centrosome abnormalities arise in BE, from the early premalignant stages to metastatic disease.

Through the unbiased approach we aimed to answer the following questions:

Objective 1 – Is there a gene expression profile associated with BE malignant transformation?

Objective 2 – Are there molecular biomarkers of BE able to predict progression to malignancy?

Objective 3 – Could these molecular biomarkers of BE to be evaluated by techniques readily available in all pathology laboratories?

Objective 4 – What is the functional context of the candidate markers in BE malignant progression?

This approach was developed based on the premise that multiple molecular abnormalities, including genetic, epigenetic and proteomic changes, are drivers of BE cancer progression, operating together to influence the process of cancerigenesis along the BE malignant pathway.[236] Since BE evolves to EA through a sequence of metaplasia, dysplasia (low/high grade) and finally invasive carcinoma, that is characterized by progressive accumulation of genetic changes related to processes of clonal evolution, it is envisioned that these molecular changes could be used as markers to predict cancer progression.[3, 362] Furthermore, it was recently demonstrated that even BE without dysplasia already presents several genetic abnormalities, which could be involved in the initial steps of cancer progression.[213] Since these changes occur before the appearance of histologic features of dysplasia, this raises an important possibility of using these events as potential and valuable biomarkers to identify BE patients with higher risk of progression.[363] The implementation of markers uncovered by previous studies has been hampered by diverse limitations: their assessment involves technical expertise and the use of complex and expensive technology that is not broadly available in the clinical setting; most of them also require the collection of fresh material that is not a standard practice outside of research centers; and the use of biomarkers panels, despite its advantages, is even more expensive to be used in daily practice. The reliability of these markers has been questioned by several drawbacks and convincing evidence that its use is beneficial in relation to standard of care in order to change this clinical practice is still lacking. Given de low rates of cancer development the big challenge will be to distinguish the molecular events that are drivers of cancer progression from the ones involved in BE pathogenesis or from the process of injury and regeneration triggered by GERD and consequently are present even in those BE patients that have not progressed to cancer.[213] Under this context, it is difficult to find reliable biomarkers of cancer prediction and this has been a real challenge for BE researchers.

With all these limitations in mind we devised a strategy combining a bioinformatics analysis pipeline for biomarkers discovery and a validation set of FFPE samples from BE patients to verify and validate the results of the candidate genes. Bioinformatics constitute a versatile approach to overcome the problem of small sample sizes because allows to maximize the discovery of novel predictive biomarkers of progression by using and combining publicly available data into larger meta-cohorts reaching to more meaningful results. It also provides the possibility to compare accurately and efficiently the exponential amounts of biological data obtained in each study, otherwise very hard, or even impossible, to analyze by manual means. So, we used an innovative bioinformatics framework applied to 3 publicly available microarray datasets on BE transcriptomes (objectives 1 and 2). Considering that we aimed to develop inexpensive and practical biomarkers in order to be suited for clinical implementation, we envisioned that the ideal scenario would be to find biomarkers able to be evaluated by a method already available in all pathology labs (objective 3).

The final phase of this part of the project consisted in understanding the functional context our two candidate biomarkers in BE carcinogenesis (objective 4).

Following a hypothesis-driven approach we wanted to know:

Objective 5 - Are there centrosome/centriole number abnormalities along the BE-dysplasia-adenocarcinoma sequence?

Objective 6 – When do arise these centrosome/centriole abnormalities along the BE-dysplasia-adenocarcinoma sequence?

Objective 7 – How do the centrosome abnormalities observed correlate with the characterized genetic lesions and ploidy changes occurring in BE malignant progression?

The rationale beyond this approach was based on the fact that centrosome defects, in particular supernumerary centrosomes are widespread in human tumors and are therefore recognized as a hallmark of cancer.[263, 270] Studies have already demonstrated that centrosome anomalies can occur as early as pre-invasive stages of tumor development [299, 300], favoring the possibility that centrosome dysfunction could have a role in the initiation of the cancerigenesis process rather than being a byproduct of oncogenic deregulation. [264, 278] Furthermore, in a broad range of different cancer types, the presence of extra centrosomes correlated with advanced stage disease and clinical aggressiveness features such as tumor recurrence, metastasis and resistance to therapy. [263, 264, 272] These findings highlight the possibility of using it together with other clinical parameters as a prognostic factor or as a potential advanced disease biomarker meaning that could be useful to predict clinical outcome and survival in oncological disease. [263, 270] The that extra centrosomes are a specific phenotype of cancer cells that is prevalent in human cancer, makes them appealing targets in cancer therapy.[269] However, despite the exciting prospects of using centrosome abnormalities as a valid tool for clinical assistance, they have not reached the clinical setting. For that, first it is vital to understand the overall picture concerning the relation of centrosomes with cancer and focus research on fundamental questions that remain intangible. Indeed, the timing, mechanisms and contribution of centrosome dysfunction in human tumors must be clarified. [264] Moreover, it is not known how the centrosome amplification incidence varies along cancer progression. These caveats could be partly explained by the complexity that it is to study human cancer considering that there is a plethora of different cancer types, with distinct cellular origins, affected by different micro and macro-environmental factors, and so it is conceivable that incidence of centrosome defects and its causes and consequences could be cancer specific and context dependent.[289] Also several methodological issues have been restraining data interpretation and generalization of the results. Most studies in which centrosome profile was assessed in human neoplasias did not do a single-cell analysis trough tumorigenesis and only use score PCM components, which may not contain centrioles, and thus not constitute bona-fide centrosomes.[263]

Taking into consideration all these evidences and being BE carcinogenesis characterized by deregulation in cellular processes partly controlled by the centrosome, including polarity and cell division, we decided to explore these features anticipating that centrosome number defects could also be present along BE malignant pathway. Although several studies have described centrosome dysfunction in association with cancer initiation and progression, its contribution to BE tumorigenesis remains unknown. Ultimately, he envisioned that the findings of this study could be extended to other tumor models and would help to decipher the role of centrosome amplification in human cancer. In fact, BE tumorigenesis constitutes an excellent human cancer model to study centrosome abnormalities as: (i) it has a clinically well-established, and genetically well-defined, multistep pathway of progression, (ii) it allows the sampling of all stages of disease within the same patient, (iii) its malignant transformation is accompanied by a progressive accumulation of well-characterized genetic lesions that are observed in many other solid tumors [63, 142], and (iv) it is the only cancer model that has representative cell lines from all the steps of progression, that contain the genomic alterations found in vivo, and that can be manipulated to further test mechanistic hypothesis. Furthermore, considering that the first stage of BE malignant pathway is the pre-malignant condition, it is possible to study the centrosome profile in the stage preceding noninvasive precursor lesions, before the onset of the neoplastic transformation, which is fundamental to elucidate and provide evidence about the potential involvement of centrosome abnormalities in the beginning of the tumorigenic process in BE cancerigenesis, and extrapolate to other human cancers. Regardless of the fact that only a small percentage of patients with BE will progress to cancer, implicating that samples from all stages of the pathway are rare, and cohorts with these characteristics are always small without cooperation of other international centers to gather more samples, the presence of different stages of disease in neoplasia resections allows the unique study of its sequential pathway of progression in each individual patient, and thus overcoming in part the need to have a large sample size normally imposed to reduce the effects of inter-patient variability.

So, considering our goals and in order to overcome the limitations pointed to previous studies, we established a method to identify and score bona fined centrosomes on a cell-by-cell basis in paraffin-embedded patient tissue samples by immunofluorescence microscopy. To harness the advantages of this model of human cancerigenesis, we selected three cohorts of patients that allowed us to examine all stages of BE malignant progression, this is, along metaplasia-dysplasia-adenocarcinoma-metastasis sequence (objectives 5 and 6). We also validated a panel of cell lines that represent all these stages of disease as a model to test the origin of centriole amplification and to understand if there is a mechanistic link between centrosome amplification dynamics and the well-known genetic and ploidy alterations along BE tumorigenesis (objective 7). By investigating centrosome abnormalities in BE tumorigenesis we aimed to improved our understanding of BE biology and that this knowledge could be used as a tool to improve its diagnosis, prognosis and treatment in the future.

CHAPTER 2:

CYR61 and TAZ Upregulation and Focal Epithelial to Mesenchymal Transition May Be Early Predictors of Barrett's Esophagus Malignant Progression

PLOS ONE

RESEARCH ARTICLE

CYR61 and *TAZ* Upregulation and Focal Epithelial to Mesenchymal Transition May Be Early Predictors of Barrett's Esophagus Malignant Progression

Joana Cardoso[1,2]*, Marta Mesquita[3,4], António Dias Pereira[4,5], Mónica Bettencourt-Dias[1], Paula Chaves[3,4], José B. Pereira-Leal[1,2]

1 Instituto Gulbenkian de Ciência, Oeiras, Portugal, **2** Ophiomics—Precision Medicine, Lisboa, Portugal, **3** Serviço de Anatomia Patológica, Instituto Português de Oncologia de Lisboa Francisco Gentil, E.P.E., Lisboa, Portugal, **4** Faculdade de Ciências da Saúde–Universidade da Beira Interior, Covilhã, Portugal, **5** Serviço de Gastrenterologia, Instituto Português de Oncologia de Lisboa Francisco Gentil, E.P.E., Lisboa, Portugal

* jvaz@ophiomics.com

Citation: Cardoso J, Mesquita M, Dias Pereira A, Bettencourt-Dias M, Chaves P, Pereira-Leal JB (2016) *CYR61* and *TAZ* Upregulation and Focal Epithelial to Mesenchymal Transition May Be Early Predictors of Barrett's Esophagus Malignant Progression. PLoS ONE 11(9): e0161967. doi:10.1371/journal.pone.0161967

Editor: John P. Lynch, University of Pennsylvania, UNITED STATES

Received: March 15, 2016

Accepted: August 15, 2016

Published: September 1, 2016

Data Availability Statement: All relevant data are within the paper and its Supporting Information files.

Funding: This work was supported by funding from FCT grants HMSP-CTSAU-ICT-0075-2009 and SFRH-BPD-26487-2006. Ophiomics Precision Medicine provided support in the form of salaries for authors JC and JPL but these funders did not have any additional role in the study design, data collection and analysis, decision to publish, or preparation of the manuscript. The specific roles of these authors are articulated in the 'author contributions' section.

Abstract

Barrett's esophagus is the major risk factor for esophageal adenocarcinoma. It has a low but non-neglectable risk, high surveillance costs and no reliable risk stratification markers. We sought to identify early biomarkers, predictive of Barrett's malignant progression, using a meta-analysis approach on gene expression data. This *in silico* strategy was followed by experimental validation in a cohort of patients with extended follow up from the Instituto Português de Oncologia de Lisboa de Francisco Gentil EPE (Portugal). Bioinformatics and systems biology approaches singled out two candidate predictive markers for Barrett's progression, *CYR61* and *TAZ*. Although previously implicated in other malignancies and in epithelial-to-mesenchymal transition phenotypes, our experimental validation shows for the first time that *CYR61* and *TAZ* have the potential to be predictive biomarkers for cancer progression. Experimental validation by reverse transcriptase quantitative PCR and immunohistochemistry confirmed the up-regulation of both genes in Barrett's samples associated with high-grade dysplasia/adenocarcinoma. In our cohort *CYR61* and *TAZ* up-regulation ranged from one to ten years prior to progression to adenocarcinoma in Barrett's esophagus index samples. Finally, we found that *CYR61* and *TAZ* over-expression is correlated with early focal signs of epithelial to mesenchymal transition. Our results highlight both *CYR61* and *TAZ* genes as potential predictive biomarkers for stratification of the risk for development of adenocarcinoma and suggest a potential mechanistic route for Barrett's esophagus neoplastic progression.

Competing Interests: Authors JC and JPL received funding from commercial company Ophiomics Precision Medicine, for this study. There are no patents, products in development or marketed products to declare. This does not alter our adherence to all the PLOS ONE policies on sharing data and materials.

Introduction

Barrett's esophagus (BE) is a premalignant metaplastic condition originated by the replacement of the normal squamous epithelium (NE) of the esophagus with a specialized columnar epithelial type that displays mixed gastric and intestinal characteristics [1]. BE is the major risk factor for the development of esophageal adenocarcinoma (EA) [2] and may progress to EA, through a low-grade to high-grade dysplasia (HGD) sequence. EA is the cancer with the fastest rising incidence in high-income countries [3] and has poor prognosis, with a high-related mortality and morbidity. Based on an estimated annual cancer risk of 0.5%, international guidelines universally recommend periodic endoscopic surveillance with a systematized biopsy protocol [4]. However, data reviewed on recent international guidelines estimates that BE risk of progression is very low (0.12%-0.33% patients/year [5, 6]. This fueled a running controversy on the costs/benefits of routine surveillance [7]. Apart from this debate, biopsy-based identification and grading of dysplasia in BE specimens is still the gold standard method to identify BE patients at risk of neoplastic progression [4], despite all the problems associated with such practice: costly, invasive, subjective dysplasia grading, biopsy sampling errors, unnecessary biopsying of low risk BE patients. Thus, a major current need in BE clinical management is of better methods and predictive biomarkers to stratify patients with an increased risk of disease progression [8], ideally early and/or biopsy-independent.

Recent high-throughput molecular studies have been instrumental for the enhanced understanding of many molecular events driving the BE "metaplasia-dysplasia-carcinoma" sequence [9, 10]. Despite all the resulting knowledge prompting the evaluation of >200 novel candidate biomarkers as predictors of progression (reviewed in [11]), none has yet reached routine clinical practice [12]. Molecular biomarkers of BE that predict progression to malignancy are still needed because their usage, alone or in combination with other biomarkers can facilitate more cost-effective surveillance. However due to the low progression rate of non-dysplastic BE few patients are available per discovery study. High-throughput molecular studies using robust sample sizes are scarce and thus published biomarker studies typically include very small patient cohorts. To maximize the discovery of new progression biomarkers, publicly available data needs to be used and combined into larger meta-cohorts. In particular the mining and re-analysis of existent gene expression data can be of great value, even if merging of distinct datasets may produce noisy predictions because such predictions can then be validated in patient cohorts.

In the present study, we set to define early molecular biomarkers predictive of BE progression to malignancy, through the usage of an innovative bioinformatics framework applied to publicly available global transcriptome data associated with BE to EA progression. *In-silico* generated prediction were validated in a cohort of patients under surveillance for more than ten years. We shown that *CYR61* and *TAZ* are up-regulated in BE index biopsies (negative for dysplasia) from patients that progress to cancer (P-BE), years before the development of EA as compared to index biopsies from BE patients that did not progress (non P-BE). To our knowledge, this is the first study to show that molecular changes associated with features of the epithelial to mesenchymal transition (EMT) invasive phenotype, usually detectable in late EA progression, can occur remarkably early in at risk BE mucosa. These changes are observable also at the protein level and show promise of clinical utility.

Materials and Methods

Public data collection, pre-processing and graphical display

We mined Gene Expression Omnibus (GEO) repository (http://www.ncbi.nlm.nih.gov/geo) [13, 14] or directly asked the authors for public microarray datasets on BE transcriptomes

according to the criteria: 1) existence of clinical information on EA presence/absence at BE sample collection and 2) microarray experiments performed in the Affymetrix® Human Genome U133A microarray platform (HGU133a). Three datasets on HGU133a were retrieved: Kimchi *et al.* [15], Stairs *et al.* [16] and Watts *et al.* [17]. Kimchi *et al.* [15] study contained 8 BE samples adjacent to EA and thus these were classified as progressed BE (P-BE) plus 8 paired EA samples. Both Stairs *et al.* [16] and Watts *et al.* [17] series contained BE samples (n = 7 and n = 18, respectively) that were negative for dysplasia/EA at the time of collection and thus were classified as non-progressed (nonP-BE). In addition, the Watts *et al.* [17] dataset also contained EA samples but from distinct individuals of the nonP-BE samples.

Data analysis was performed with R Statistical Computing software [14] complemented with Bioconductor [18] packages. Heatmaps and Venn-diagrams were plotted using gplots (http://CRAN.R-project.org/package=gplots) and VennDiagram (http://CRAN.R-project.org/package=VennDiagram) packages, respectively. Affy [19] and frma [20] packages were respectively used for raw data uploading and pre-processing and for frozen robust multi-array (fRMA) normalization. The R script used is available upon request.

Differential expression analysis

We have used a Bayesian differential expression analysis (DEA) approach implemented in the R package limma [21] to define differentially expressed genes. Threshold for selection of differentially expressed probe sets was set to a B-statistic parameter Lods (already adjusted for multiple testing) $\geq$5 and a log2 ratio $\geq$ +0.58 or $\leq$- 0.58. The very conservative Lods>5 was based on DEA results between EA samples from Kimchi *et al.* [15] and Watts *et al.* [17] datasets, where no significant DE probe sets are expected, to control for inter-dataset variability noise.

Barcode analysis

Probe set barcode values were calculated with the frma [20] and frma-associated hgu133abarcodevecs package, using the method described by McCall *et al.* [22, 23] (http://rafalab.jhsph.edu/barcode/). A probe set was defined as expressed (= 1) or non-expressed (= 0) in a given sample according to fRMA cutoffs. BE barcodes were filtered per dataset using very stringent criteria. A probe set was integrated in the dataset barcode if expressed in 100% or $\geq$ 75% in P-BE or nonP-BE samples, respectively. Group-specific barcodes were calculated by intersecting probe set IDs expressed in each dataset. EA-specific dataset barcodes were estimated as for nonP-BE i.e. probe sets were expressed in $\geq$ 75% samples to be integrated in the EA barcode.

Gene set enrichment analysis

To find over-represented gene ontology biological processes (GO-BP) among specific sets of genes we used the gene set enrichment analysis (GSEA) tool from InnateDB (http://www.innatedb.ca/) using Entrez ID as gene identifier.

GeneMANIA network analysis

The guilt-by-association GeneMANIA Cytoscape plugin algorithm [24] (http://genemania.org/) was used to identify genes functionally-related to our query genes, with gene symbols as identifiers.

Samples and clinical data

For validation we used 19 formalin fixed paraffin-embedded (FFPE) BE samples from P-BE and nonP-BE (clinical data in S1 Table) of a cohort of 331 non-dysplastic Barrett's esophagus

enrolled in an endoscopic surveillance program (mean surveillance of 6.2 years ranging from 1 to 25) at the Instituto Português de Oncologia de Lisboa Francisco Gentil (IPOLFG), with an observed incidence of high-grade dysplasia or adenocarcinoma of 3,4/1000 patient-years during about the 30 years of existence of the surveillance program. All cases, at diagnosis, were analysed as per normal routine by two experienced GI pathologists. Patients select for this study were part of a cohort of patients diagnosed with Barrett's Esophagus under surveillance at the IPO. This included a group of nine patients that progressed to high grade dysplasia or adenocarcinoma during surveillance (Progressed, P-BE), being the diagnostic confirmed by two independent pathologists, as standard practice and international recommendations. It included another group, as control, of 10 patients that did not display any dysplasia or carcinoma at any time during surveillance (termed non-Progressed, nonP-BE). In our cohort, progressor patients were defined as those with no dysplastic Barrett´s esophagus in the index endoscopy who progress during follow up to HGD or ADC. Non-progressors were defined as patients with no dysplastic Barret's esophagus in the index endoscopy who remind free of dysplasia or ADC during a mean follow-up similar to that of progressors. The non-Progressed patients were randomly selected from our database. In the P-BE patients we analyzed samples from two time points, before and after malignant progression, named as t0 and t1. In the first time point (t0) we studied the initial biopsy diagnosed BE negative for dysplasia. In the second time point (t1) we examined two areas, the BE and the adjacent HGD/EA on mucosectomies or surgical pieces from these same patients. In the control group of nonP-BE patients we also studied two time points: t0 and t1 for the index and for most recent follow-up biopsies, respectively. In this set of patients all samples from t0, t1 or in any other follow-up archived sample (between t0 and t1) displayed any signs of malignancy. We chose to use a balanced number of non-progressors to avoid artificially inflating p-values in the comparisons. Histopathological characterization and area selection was carried out on hematoxylin- and eosin-stained sections under the supervision of an experienced pathologist. The study was approved by the institutional review board and a waiver of consent was obtained prior to initiating this retrospective study (project GIC/721 IPOLFG, EPE).

RNA extraction and cDNA synthesis

Archived BE FFPE tissue sections (5 μm) were deparaffinized and counterstained with Mayer's hematoxylin and eosin. BE-enriched areas were needle microdissected under the pathologist guidance. Total RNA was extracted with the RNeasy FFPE kit (Qiagen), according to manufacturer's instructions with a slight modification: proteinase K cell-lysis at 56°C was performed overnight. The RNase-Free DNase Set (Qiagen) "on column" DNA digestion procedure was included. Each extracted RNA was reverse-transcribed with the First-Strand cDNA Synthesis kit (GE Healthcare), using a 1:1 mixture of random primers ($pd(N)_6$) and oligo-dT primers ($NotI\text{-}d(T)_{18}$. High quality total RNA (3 μg) from two control cell lines (HCT116 and a primary skin fibroblasts) was used to synthesize cDNA to be used as dilution standards in qRT-PCR.

Quantitative real-time PCR

RNA concentration and integrity could not be assessed using standard methods due to known FFPE degradation issues and to the small amounts of extracted samples. Thus, to indirectly check the amount of each isolated total RNA FFPE sample and its quantitative real-time PCR (qRT-PCR) downstream performance, we prepared two standards dilution series using cDNA from the two control cell lines, corresponding to 100, 10 1, 0.1, 0.01, 0.001 and 0.0001 ng of the original total RNA. These series were subsequently used to calculate a qRT-PCR standard

curve for the non-differentially expressed gene *MAPKAPK2* (Lods = -2.7). Primer sets were designed with the NCBI Primer-BLAST tool [25], to work at 59°C and with an amplicon length of 70–100bp (S2 Table). Duplicates of each BE sample were analyzed by qRT-PCR using SsoFast™ EvaGreen® Supermix (Bio-Rad, Hercules CA, USA) reagent in 10μL of reaction mixture containing template (2μL, ~200pg/μL) and primers (0.5μM each). Samples were processed in a CFX96 Touch™ Real-Time PCR Detection System (Bio-Rad, Hercules CA, USA) according to the cycling program: 95°C for 60 s, 50 cycles of 95°C for 10s and 59°C for 15s. Fluorescence data collection occurred at 59°C. Relative differential expression analysis of target genes by qRT-PCR was based on the $2^{-\Delta\Delta Ct}$ methodology from Livak *et al.* [26] using mean quantification cycle of duplicates as cycle threshold (Ct) compared to the Ct of the calibrator gene GAPDH.

Immunohistochemistry

Immunohistochemistry (IHC) of BE samples (3 μm thick tissue sections) was performed according to standard protocols. Primary antibodies were diluted in Bond Primary Antibody Diluent (Leica Microsystems) plus background-reducing components at the dilutions: *CYR61* (1:600, mouse monoclonal [3H3], Abcam, ab80112), *TAZ* (1:300, mouse monoclonal, Abcam, ab118373), *E-Cadherin* (1:80, mouse monoclonal 4A2C7, Invitrogen, 33-4000). Antigen retrieval consisted of pressure-cooking for 6 minutes in pH6 sodium citrate 0.01M buffered solution for *CYR61*, of 20 minutes of microwave exposure at 750W in pH6 sodium citrate 0.01M buffer and of 25 minutes in Epitope Retrieval Solution 2 (ER2) Leica Bond III system for E-Cadherin. Signal detection of *CYR61* and *TAZ* was obtained using the Rabbit/Mouse Peroxidase/DAB+ Dako REAL Envision Detection System while *E-Cadherin* visualization was performed in the Leica Bond III system with the detection system Bond Polymer Refine Detection plus Bond DAB Enhancer. Nuclei were counterstained with Mayer's hematoxylin. Images were acquired on a Leica DM5500 microscope.

IHC staining specificity was evaluated with a three level score. IHC scores for CYR61 antibody (ab80112) were defined as "Low" when a weakly positive diffuse protein staining was observed (+), "Intermediate" when scored areas included few areas of weakly positive and most areas with positive diffuse staining (++) and "High" when no negative areas were observed and the majority of evaluated areas presented a strongly positive diffuse staining (+++). IHC scores for TAZ antibody (ab118373) were defined as "Low" when protein staining was negative to weakly positive cytoplasmatic diffuse staining in the majority of visualized areas (-), "Intermediate" when weakly positive cytplasmatic and low to strong nuclear staining was observed in some areas (+) and "High" when low to strong cytoplasmatic staining and very strong nuclear staining was observed in the majority of evaluated areas (++).

Western-blotting

The western-blotting procedure was performed according to standard protocols. Total protein extracts (20μg) from the two breast cancer cell lines MDA231 and MCF7 were resolved by SDS-PAGE on a 12% acrylamide gel (BIO-RAD) and transferred to a PVDF membrane (GE Healthcare) on a Mini-Protean system (BIO-RAD). The molecular weight marker used for electrophoresis was the Kaleidoscope (∫BIO-RAD) and transfer conditions were 250 mA, 100 min. CYR61 (ab80112) and TAZ (ab118373) antibodies were both diluted 1:200 in 0.2% fish skin gelatin, 1x TBST and the loading control β-Actin antibody (Sigma) was diluted 1:2000 in 1% milk, 1x PBS. All primary antibodies were incubated overnight at 4°C. Detection for all antibodies was performed by incubation with mouse Horseradish Peroxidase antibody (Jackson Immunoresearch) at 1:10.000 dilution and the western-blot signal developed with and ECL system (BIO-RAD) and detected on an x-ray Amersham Hyperfilm ECL (GE Healthcare).

Statistical analysis

Data analysis was performed with R language for Statistical Computing [14]. Expression differences between P-BE and nonP-BE microarray data was determined with a Bayesian T-test implemented in the R package limma [21]. We used hypergeometric testing to assess gene set enrichment. Statistical significance of qRT-PCR data was calculated with Wilcoxon Rank Sum test (confidence level = 0.95). IHC categorical data was analyzed with Pearson's Chi-squared test.

Results

Hypotheses generation: mining public gene transcriptomics data

We implemented a bioinformatics pipeline for data mining that takes as input the small number of expression profiling data sets available for nonP-BE, P-BE and EA (Fig 1A), insures that data is comparable using fRMA normalization (Fig 1B) and identifies genes differentially expressed between P-BE and nonP-BE (Fig 1C). Subsequently cross checks these against a database of human gene expression patterns to binarize the genes with bimodal gene expression (Fig 1D) and implements a network analysis to cross check the selected list of candidate genes against other data types (such as protein interactions, gene co-expression, etc) for plausibility (Fig 1E). Finally, the output of this pipeline is submitted to one additional filtering step, based on manual literature curation of selected genes (Fig 1F, Table 1). From a list of 12749 unique starting genes, our approach predicts the two genes *CYR61* and *WWTR1* (alias *TAZ*) that *in silico* can distinguish P-BE from nonP-BE samples. Details of the methods are given in methods section, and a detailed step-by-step description of each step and resulting lists of genes is given as supplementary material (S1 Fig and S1 Results).

mRNA levels of *CYR61* and *TAZ* distinguish nonP-BE from P-BE in paraffin-embedded samples

Given the existing variability associated with microarray technology results (lab-, user- platform-associated, etc) and the technology limitations (probe sensitivity and specificity) it is essential to use an independent mean to verify and reproduce the results of candidate genes.

We evaluated *CYR61* and *TAZ* as early biomarkers of BE progression in a validation set of FFPE samples from 19 BE patients (detailed characteristics of the patients used in the

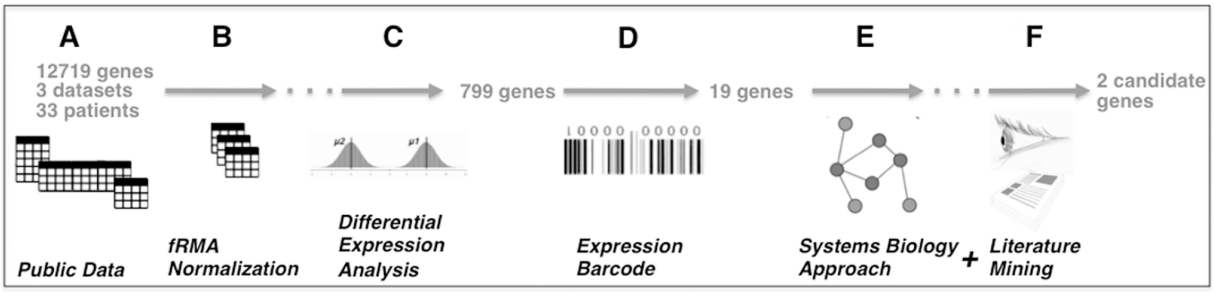

Fig 1. Bioinformatics analysis workflow of BE datasets for biomarker discovery. A. Three publicly available microarray datasets of BE data containing 33 BE samples with progression information were used to interrogate the expression levels of 12719 unique genes. **B.** After data normalization with frozen robust multi-array (fRMA) we first performed **C.** differential gene expression analysis, which allowed the identification of 799 differentially expressed genes. Normalized fRMA data was subsequently submitted to **D.** gene expression barcode which further restricted the number of selected candidates to 19. The combined usage of a **E.** systems biology approach plus **F.** manual literature curation selected the two most promising candidates.

doi:10.1371/journal.pone.0161967.g001

validation set of the present study is available in S1 Table). In total, 9 P-BE patients (t0, n = 9 and t1, n = 9 samples) and 10 nonP-BE patients (t0, n = 10 and t1, n = 10 samples) were included (see Materials and Methods)

Using qRT-PCR we compared *CYR61* and *TAZ* mRNA levels from t1 P-BE tissue co-occurring with HGD/EA with nonP-BE samples without any histological signs of malignancy. The analysis revealed that the transcriptional levels of both genes were significantly increased (*P* value<0.005) in P-BE samples (Fig 2A) as predicted *in silico*. We have also detected a significant up-regulation (average fold change >2, *P* value <0.01) in the index samples (t0) of P-BE patients, years before the development of HGD/EA as compared to nonP-BE index samples (t0) from patients that never developed HGD/EA (Fig 2A, Table 2). This early up-regulation could be detected as early as 13 years (average: 4.6 years; range: 1-13 years) in the P-BE group. In the nonP-BE group, the maximum follow-up interval was of 17 years (average: 9.4 years; range: 3-17 years). In addition, using the microarray and qRT-PCR data we verified that *CYR61* and *TAZ* expression levels are not correlated and thus P-BE and nonP-BE samples could be better segregated when using independent information from both markers (S4 Fig). Their combined usage may enhance sensitivity for the early detection of patients at risk of BE malignant progression in BE index samples.

Protein levels of *CYR61* and *TAZ* distinguish P-BE from nonP-BE in paraffin embedded samples

Validation of the *in silico* predictions by qRT-PCR is encouraging, but clinical use could be simpler if routine techniques such as immunohistochemistry were to be used. We have thus implemented an IHC assay. We have started by evaluating the specificity of both antibodies by Western-blot analysis (S5A Fig). IHC results of *CYR61* and *TAZ* proteins were categorized into three different groups according to staining intensities (Fig 2B, Table 2): low, intermediate and high. CYR61 antibody presented a diffuse cytoplasmatic and/or nuclear staining as shown in the positive control (S5B Fig) and TAZ antibody mostly stained nuclei although it is also

Table 1. Cancers where *CYR61* and *TAZ* over-expression has been previously correlated with poor outcome.

Cancer Type	*CYR61 (references)*	*TAZ (references)*
Breast	[27]	[28, 29]
Prostate	[30–32]	---
Colorectal	[33]	[34]
Gastric	[35, 36]	---
Esophageal Squamous Cell	[37, 38]	---
Esophageal Adenocarcinoma	[39]	---
Pancreas	[40, 41]	---
Hepatocellular	[42]	---
Non-Small Cell Lung	[43]---	[43],[44]
Thyroid Carcinoma	[45]	[46][a]
Renal cell carcinoma	[47]	---
Ovary	[48]	---
Glioma	[49]	[50]
Osteosarcoma	[51]	---
Epithelioid Hemangioendothelioma	---	[52]
Oral (squamous cell)	[53, 54]	---

[a]Papillary

doi:10.1371/journal.pone.0161967.t001

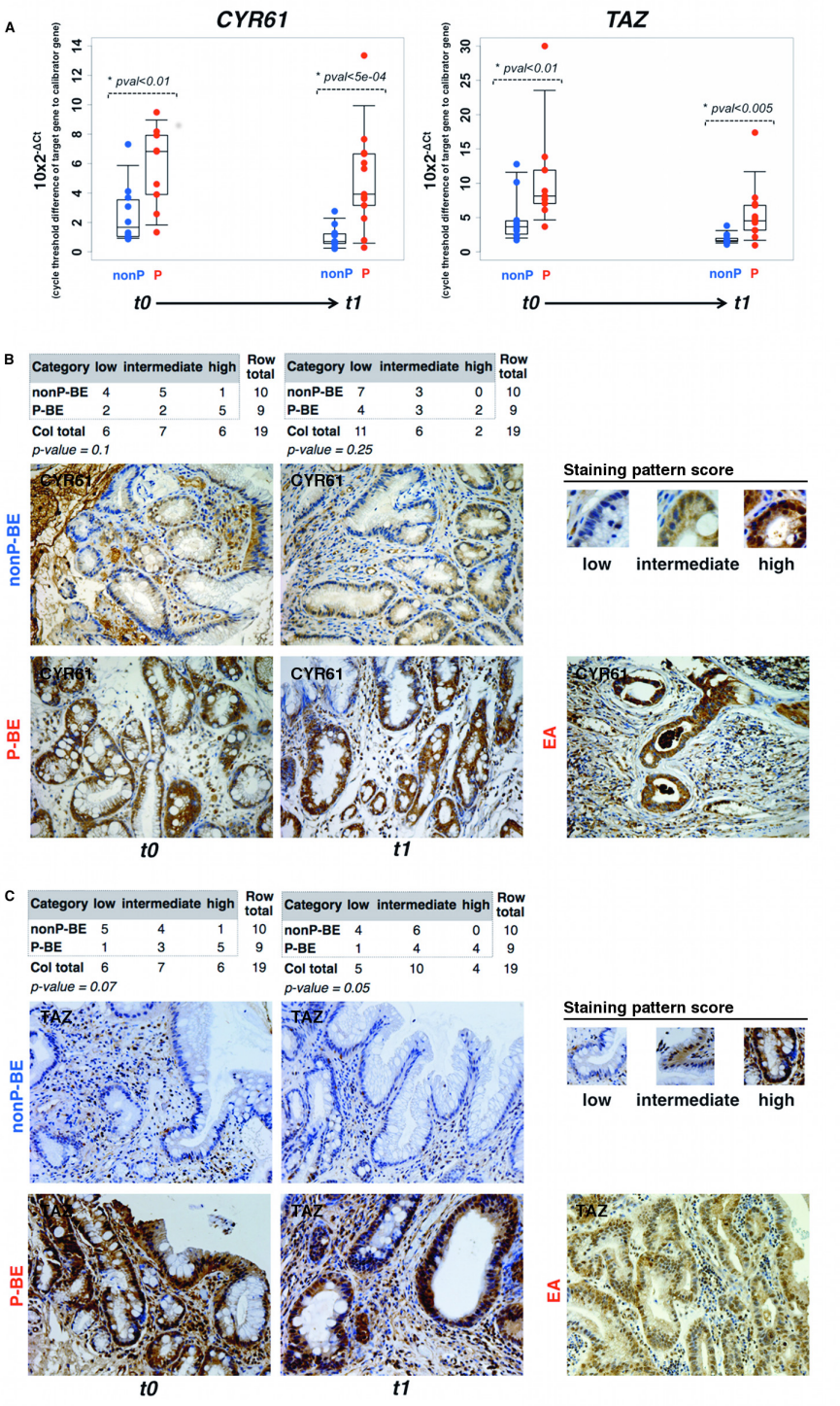

Fig 2. *CYR61* and *TAZ* mRNA and protein levels are significantly increased in early and late at risk BE biopsies. A. Timeline analysis of *CYR61* (left panel) and *TAZ* (right panel) expression levels by qRT-PCR of P-BE associated with EA (t1) and in the patient-matched BE index biopsies, free of dysplasia/EA (t0). Index BE biopsies were collected at t0 while, after several years of follow-up, EA-associated BE biopsies in the

P-BE group and EA-free BE biopsies in the nonP-BE group were designated as collected at t1. The average years of follow-up between t0 and t1 was 4.6 and 9.4 years for P-BE and nonP-BE samples. **B.** and **C.** panels display respectively representative samples of *CYR61* and *TAZ* protein levels in BE (t0 and t1) and in EA, evaluated by immunohistochemistry. Staining patterns used to score the protein levels (low, intermediate and high) are represented on the top right of each panel. The counts and statistical test (Pearson's Chi-squared test) results are represented in the top left of the panels. (Magnification ×200).

doi:10.1371/journal.pone.0161967.g002

presented a diffuse pattern in the cytoplasm (S5C Fig). Blinded analysis showed that despite the somewhat heterogeneous cytoplasmatic staining of *CYR61* protein, its levels were mainly intermediate to high in the P-BE group and mostly varied from low to intermediate in the non-P-BE group (Fig 2B). *CYR61* protein over-expression differences were more pronounced in the early time point t0. Interestingly, samples displaying the highest amounts of *CYR61* often exhibited strong nuclear accumulation. As for *CYR61*, despite some heterogeneity of *TAZ* IHC pattern (Fig 2C, Table 2), *TAZ* protein levels were increased in the P-BE as compared to non-P-BE group, with P-BE samples from t0 displaying a more distinct *TAZ* over-expression. Overall, protein levels validated the *in silico* transcriptional changes and correlated with qRT-PCR results (Table 2). Further, they highlighted once more the very early (at t0) differences of *CYR61* and *TAZ* expression between progressors and non-progressors.

CYR61 and *TAZ* up-regulation is correlated to an epithelial-to-mesenchymal transition phenotype

In our network analysis for prioritizing genes (Fig 1E), we found that EMT and stemness-related genes are significantly over-represented in the *in silico* P-BE samples ($p = 5.5\times10^{-8}$).

Table 2. Per patient quantitative assessment of *CYR61* and *TAZ* expression levels by qRT-PCR and IHC.

		Age at			t0				t1			
		(biopsy order)		YearsFUp	qRT-PCR		IHC		qRT-PCR		IHC	
Group	ID	1st	last		CYR61	TAZ	CYR61	TAZ	CYR61	TAZ	CYR61	TAZ
nonP-BE	11	64	81	17	Low	Low	++	+	Low	Low	+	+
nonP-BE	13	62	65	3	Low	Low	++	+	Low	Low	+	+
nonP-BE	14	65	75	10	Low	Low	++	++	Low	Low	+	+
nonP-BE	21	66	77	11	Low	Low	+	-	Low	Low	++	-
nonP-BE	22	67	74	7	Low	Low	+	+	Low	Low	+	+
nonP-BE	25	32	42	10	High	High	++	-	Low	Low	+	-
nonP-BE	26	64	76	12	Low	High	+	-	Low	Low	++	+
nonP-BE	27	42	52	10	Low	Low	++	-	Low	Low	++	+
nonP-BE	28	52	63	11	Low	Low	+++	-	Low	Low	+	-
nonP-BE	29	51	54	3	Low	Low	+	+	Low	Low	+	-
P-BE	2	71	72	1	Low	High	+++	+	Low	High	+++	+
P-BE	3	46	59	13	High	High	++	++	Low	High	+	++
P-BE	4	50	54	4	Low	High	+++	+	Low	Low	++	+
P-BE	5	51	53	2	Low	High	++	++	Low	Low	+	++
P-BE	6	45	48	3	High	High	+++	+	High	High	++	-
P-BE	17	62	67	5	High	High	+++	++	High	High	+	+
P-BE	18	48	54	6	High	High	+	-	High	High	+++	+
P-BE	19	68	69	1	Low	Low	+++	++	High	Low	+	++
P-BE	20	51	57	6	High	High	+	++	Low	Low	++	++

Degree of immunostaining is indicated by the "+" and "-"signs: "+++" = very strong staining; "++" = strong staining; "+" = weak staining; "-"= absence of positive staining. YearsFUp = Years of follow-up; qRT-PCR = quantitative real time PCR; IHC = immunohistochemistry.

doi:10.1371/journal.pone.0161967.t002

Out of the 19 barcoded genes, 52% (*SPARC*, *CYR61*, *JUN*, *ACTN1*, *COL4A1*, *PPAP2B*, *DUSP1*, *CTSB* and *TAZ*) have been previously detected in molecular signatures of EMT/stemness phenotypes [55–57]. Such phenotypes are clearly associated with an aggressive clinical behavior, poor outcome and resistance to treatment (reviewed in [58]). Given the involvement of *CYR61*, *TAZ* and other P-BE up-regulated genes in stemness/EMT-related cellular functions (e.g. cell adhesion/motility, inflammation, differentiation/wounding, extracellular matrix) (reviewed in [58]) we checked if core EMT markers such as *TWIST1*, *ZEB1*, *SNAI1*, *SNAI2* and *CDH1* (alias *E-cadherin*) (reviewed by [59]) were also differentially expressed. *TWIST1* was the only significantly over-expressed gene (Lods = 5.84, fold change>2) in P-BE samples. As shown in Fig 3A, we validated *TWIST1* up-regulation by qRT-PCR analysis in early P-BE samples (t0) before the emergence of any microscopic signs of malignancy. Furthermore, using routine pathology IHC for *E-cadherin* we also detected foci of lower *E-cadherin* expression in P-BE samples both in early (t0) and late (t1) P-BE samples (Fig 3B), an observation usually associated with invasive EA cells. The appearance of such foci is indicative of very early P-BE cellular adhesion and/or extracellular matrix changes absent in nonP-BE samples. This observation suggests that an aggressive mechanism, typical of advanced metastatic lesions, is active in non-malignant BE cells of at risk patients. These features of neoplastic progression occur in P-BE in a time point far earlier than we anticipated. The presence in P-BE samples of alterations typical of aggressive behavior in the context of cancer, suggest that at very early stages in BE there is already a proneness for later development of dysplasia and EA.

Discussion

In the present work, we aimed at maximizing the identification of potentially translatable biomarkers of early BE progression to EA using an original bioinformatics pipeline applied to public BE expression profiling data. This discovery framework allowed the straightforward comparison of BE samples from distinct datasets and the trimming of promising over-expressed biomarkers to *CYR61* and *TAZ* genes. Validation with qRT-PCR and IHC emphasized *CYR61* and *TAZ* over-expression as early markers of at risk BE index samples, years before HGD/EA emergence. The access to Barrett's patients that progressed during the surveillance program allowed the unique opportunity to validate biomarkers in Barrett's samples from the same group of patients before and after malignant progression. This allowed us to overcome the limitations derived from inter-patient variability in studies where different sets of patients were used in each step of Barrett's malignant progression. To our knowledge, this is the first time that risk stratification biomarkers were validated in BE samples coming from the same set of patients. Finally, changes in EMT biomarkers were detected in index samples of at risk BE. This observation fits into *CYR61* and *TAZ* functional context and further suggests that in at risk BE, proteins associated with EMT can be operational from very early, before any visible signs of malignancy.

CYR61 and *TAZ* emerged from our pipeline as the most promising biomarkers of at risk BE and we experimentally validated their up-regulation in a different cohort. Several studies have implicated *CYR61* and *TAZ* in the biology of major cancers (Table 1). BE is a metaplastic response of the esophageal surface to chronic injury caused by gastric reflux, possibly amplified by an inflammatory response [60]. BE progression to EA could plausibly be mediated by the known functions of these two genes in extracellular matrix, cell migration, angiogenesis and stemness/EMT. *CYR61* is an important factor in acid-induced esophageal epithelial transformation [61] and its up-regulation is an early response of esophageal cells exposed to low pH [62]. In a non-esophageal context, *CYR61* plays a role in inflammation, it is notably expressed at wounded tissues [63] and also up regulated upon mechanical stress (reviewed in [64]).

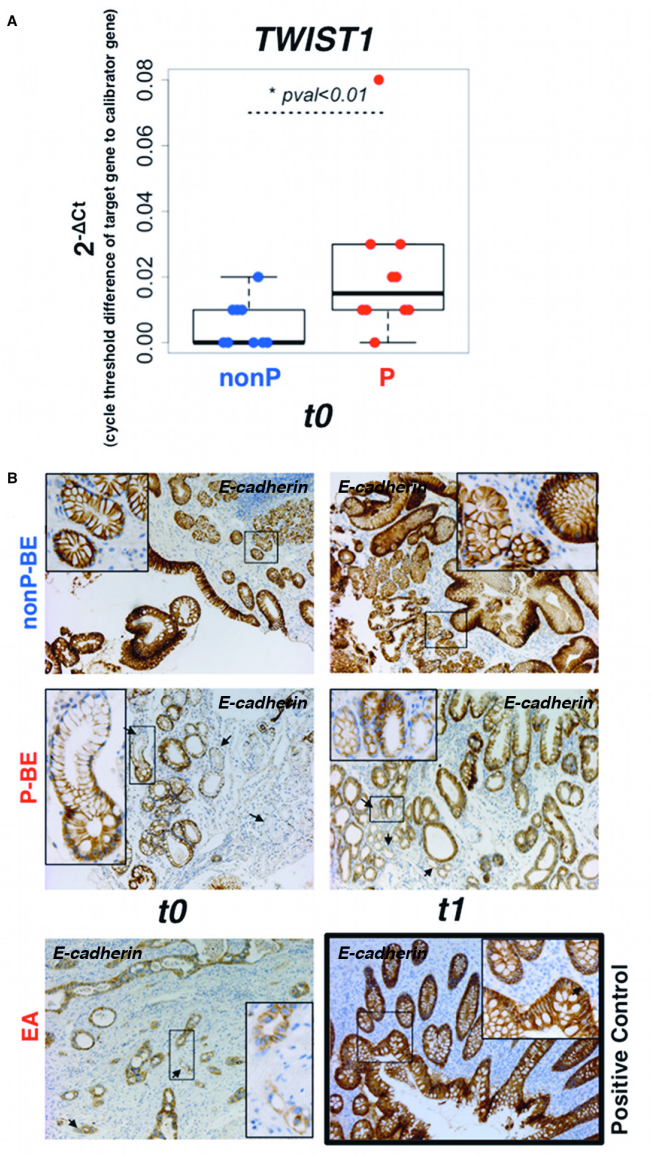

Fig 3. Changes in epithelial-to-mensenchymal biomarkers are visible in early and late BE backgrounds. A. qRT-PCR validation of *TWIST1* transcription factor in the patient-matched BE index biopsies, free of dysplasia/EA (t0). **B.** *E-cadherin* protein levels were evaluated by immunohistochemistry staining in P-BE associated with EA (t1) and in the patient-matched BE index biopsies, free of dysplasia/EA (t0). Arrows denote foci of lower *E-cadherin* expression. Normal appendix was used as *E-cadherin* immunostaining positive control. (Magnification: picture ×100, detail ×200).

doi:10.1371/journal.pone.0161967.g003

CYR61 has also an independent prognostic value in esophageal squamous cell carcinoma [37, 38] and is a negative predictor in early onset sporadic colorectal [65, 66] and ovarian [48] cancers. Functionally, *CYR61* is a ligand for several integrins which in turn can trigger cancer cells motility (reviewed in [67]) as it was recently demonstrated in pancreatic cancer [41]. *TAZ* is a key mediator of mechanotransduction, also implicated in human tumorigenesis: *TAZ*

transducer activities are required to sustain self-renewal and tumor-initiation capacities [29], cell proliferation and EMT in breast cancer stem cells [28, 68] and to regulate mesenchymal differentiation in malignant gliomas [50].

Many putative biomarkers of BE malignant progression resulted from previous studies (reviewed in [11]) but no biomarker has been used in routine clinical practice [12]. Typically, most biomarkers were discovered in a context of a detectable high-grade dysplasia/EA, a time point where the neoplasia is already established and therefore where markers of tumor development are of little use and only cancer progression is at stake. This type of cancer-associated molecular alterations in non-cancer tissues (e.g. BE and NE) but adjacent to a tumor are often referred to as a cancer field effect and have already been described in BE [69]. We analyzed *CYR61* and *TAZ* levels in non-dysplastic/EA-free BE index biopsies of P-BE and nonP-BE patients by qRT-PCR to distinguish whether *CYR61* and *TAZ* up-regulation were a cancer field effect or an early property of P-BE samples. We found that, in fact, the up-regulation of these genes in BE years before the appearance of dysplasia (t0), reveals the establishment of a signaling pathway prone for progression to dysplasia/EA at very early stages through an intrinsic alteration of cell properties that directly, or by interaction with stromal tissue will facilitate tumor initiating features. Interestingly, we observed that *CYR61* and to a lesser degree also *TAZ* expression levels, slightly decreased when progressing from index (t0) to advanced (t1) BE. Differences between P-BE and nonP-BE are thus more significant at t0. This phenomenon of increased expression on localized benign disease and a decreased expression upon progression to metastasis is known to occur in several contexts such as for *CYR61* in prostate cancer (reviewed in [70]). While no mechanistic explanation justifies yet this observation in BE, it is possible that, as in prostate, *CYR61* and *TAZ* are more important in the neoplastic initiation than progression.

Although *CYR61* up-regulation was previously described in BE samples where dysplasia/EA is already present [39], our work is the first to describe that such up-regulation is in fact a very early event in Barrett's tumorigenic process, being an indicator for a later establishment of dysplasia/EA, since it is detected in BE index biopsies. *CYR61* belongs to the CCN family of six structurally related proteins, a multi-tasking group of secreted proteins which primarily function in adhesion, migration, proliferation, ECM synthesis, inflammation and mechanical stress regulation (reviewed in [67]). Furthermore, *CYR61* has an already established role in cancer malignant progression and prognosis in major and diverse tumors (Table 1) and is a downstream target of *TAZ* [71]. *TAZ* is a major downstream effector and is regulated by the Hippo tumor suppressor pathway, a pathway relevant in organ size control, tissue regeneration, stem cell self-renewal (reviewed by [72]), cell polarity and cancer (reviewed by [73]). *TAZ* has also been implicated in the malignant phenotype of several tumors (Table 1) but differently from *CYR61*, *TAZ* over-expression has never been under scrutiny in human BE or EA. We anticipate that the biological functions of both genes, *TAZ* as a major regulator of the hippo pathway and its downstream effector *CYR61*, may contribute to BE progression to EA and we demonstrate for the fist time that they have predictive value.

The functional context of our validated targets and of other genes detected in our analysis suggested the early occurrence of mechanisms known to operate in EMT. As additional examples of such, we detected early *TWIST1* up-regulation and lower *E-cadherin* expression foci very early in BE (i.e. in BE index samples) from patients that progressed later on to cancer. These are classical biomarkers associated to aggressive features of malignant progression such as EMT. The early occurrence of *in vivo* EMT in the absence of any histological signs of cancer was recently demonstrated in pancreatic cancer and can be partially facilitated by inflammation [74]. EMT occurs both in wound healing and tumors (reviewed in [75]) a scenario that fits into *CYR61* and *TAZ* functional context. How EMT could contribute to early stages of BE

malignant progression and/or if only some EMT-related pathways are activated is currently unknown. However, EMT occurrence was described in EA [76] and in an immortalized normal epithelial cell line. In the latter *CYR61* up-regulation was critical and exacerbated acid-induced EMT phenotypes such as triggering *E-cadherin* loss [61]. Moreover, it was recently reported that *TAZ* and *CYR61* were implicated in lung cancer progression and EMT via angiomotin [43].

Our observations indicate that in particular, being *CYR61* an extracellular matrix secreted protein it harbors the potential to become a serum biomarker to stratify the risk of progression to malignancy in BE [32, 36] allowing for less invasive follow-up exams. This could supply an extra tool to define the risk of malignant progression and the possibility of reducing the number of biopsies needed, in particular for low risk patients.

Despite the very low BE progression frequency, we had access to a small, yet precious and very rare, cohort of FFPE follow-up samples for validation and more importantly to implement *CYR61* and *TAZ* detection by IHC, a method directly translatable to all pathology labs. Although FFPE-based qRT-PCR *CYR61* and *TAZ* measurements are a valid profiling option, already validated in oncologic diagnosis (reviewed in [77, 78]), assaying mRNA in the clinical routine may not be the most desirable because of technical and cost constrains. Since IHC is a method not limited by the quantity of material and can assess protein presence at single cell level, we tested commercially available antibodies against our two gene candidates and found two that, after optimization, the expected immunostains were obtained and the results could be easily translated to a routine diagnostic lab. Though the qRT-PCR and IHC data showed independently a significant difference between P-BE and nonP-BE samples in both timepoints, we have not observed clear correlation between the results of both methodologies within the same patient. The discrepant results observed in Table 2 may be justified do to inherent differences between qPCR and IHC, two techniques that are very different in nature. qPCR is quantitative, whether IHC is qualitative; furthermore, for the qPCR analysis we enriched the sample by microdissection, whereas no equivalent procedure was possible for IHC. In addition, IHC is prone to variation-dependent biases while qPCR is not observer dependent.

Given the very low BE progression frequency we will always be limited by the number of available archived collections of P-BE index samples (t0) and its follow-up samples until histological signs of malignancy are displayed (t1), which spans periods of many years. Additionally, our country has lower BE incidence rates when compared to other developed countries and we do not have a national BE register. Despite all this, our small cohort of patients that progressed during surveillance reproduces the actual expected risk progression in Barrett's patients. Indeed, compared with the several international cohorts reviewed by the British Society of Gastroenterology guidelines [79] our cohort is quite representative. We are aware that larger numbers are needed in future tests with these two markers, which will certainly implicate several international multi-institutional collaborations.

Conclusions

Given the running debate on the costs/benefits of BE surveillance programs [80–82] and despite the diminished risk of progression [83] biomarkers to better stratify the patients who have real increased risk of neoplastic progression are required. Furthermore, it is important to stress that the risk may be low but still, BE is the precursor lesion of one of the fastest growing cancer types in developed countries over the past decades. Our results support the use of *CYR61* and *TAZ* as early biomarkers to discriminate which BE patients have an increased risk to progress to dysplasia and cancer and further suggest that proteins/genes involved in EMT are critical to trigger the BE lesions that evolve to more aggressive lesions. Our findings also

highlighted that these and other yet unknown markers should be supervised right from the non-dysplastic BE index biopsy. Such procedure has the potential to greatly improve BE management by sparing low risk patients from unnecessary invasive exams and to impact the overall costs (ethical and economical) of surveillance programs.

Supporting Information

S1 Fig. An original bioinformatics prioritization framework allowed the identification of at risk BE biomarkers.
(PDF)

S2 Fig. Microarray data of BE samples from distinct datasets is highly correlated.
(PDF)

S3 Fig. Differential expression analysis of P-BE and nonP-BE microarray data highlighted more than 700 genes potentially involved in BE malignant progression.
(PDF)

S4 Fig. CYR61 and TAZ expression levels are not correlated.
(PDF)

S5 Fig. Validation of CYR61 and TAZ antibodies specificity.
(PDF)

S6 Fig. GeneMania network of the 19 selected candidate biomarkers, network neighbors and associated function showed an enrichment of genes related with cell adhesion, motility and response to stimuli.
(PDF)

S7 Fig. CYR61 and TAZ are biological linked and share important cellular functions.
(PDF)

S1 Results. Systems biology approach for biomarker prioritization.
(PDF)

S1 Table. Clinical data of patients used for the validation set.
(XLSX)

S2 Table. Primer sequences for target and reference genes.
(XLSX)

S3 Table. Differentially expression analysis filtered genes (Lods $>$ 5).
(XLSX)

S4 Table. Barcode genes exclusively associated with P-BE.
(XLSX)

S5 Table. GSEA results for GO-BP significant categories (corrected p-value$<$0.05) obtained with the 19 selected genes and 100 GeneMania network neighbors.
(XLSX)

S6 Table. GSEA results for GO-BP categories (corrected p-value$<$0.05) obtained with CYR61, TAZ and 100 GeneMania network neighbors.
(XLSX)

Acknowledgments

We are grateful to Leonor David from the Institute of Molecular Pathology and Immunology of the University of Porto (Portugal) for her helpful comments on our manuscript.

Author Contributions

Conceived and designed the experiments: JC.

Performed the experiments: JC MM.

Analyzed the data: JC MM PC.

Contributed reagents/materials/analysis tools: JC MM ADP PC MBD JPL.

Wrote the paper: JC MM ADP PC MBD JPL.

Conceived and designed the study, performed all data analysis, experiments and wrote the paper: JC. Performed the immunohistochemical experiments: MM. Contributed to patient selection and clinical data: ADP. The pathologist of the study: PC. Provided funding and contributed to paper editing and review: MBD. Study supervisor, provided funding, contributed to paper editing and review: JPL.

References

1. Chandrasoma PT, Der R, Dalton P, Kobayashi G, Ma Y, Peters J, et al. Distribution and significance of epithelial types in columnar-lined esophagus. Am J Surg Pathol. 2001; 25(9):1188–93. Epub 2001/11/02. PMID: 11688579.
2. Cook MB, Wild CP, Everett SM, Hardie LJ, Bani-Hani KE, Martin IG, et al. Risk of mortality and cancer incidence in Barrett's esophagus. Cancer Epidemiol Biomarkers Prev. 2007; 16(10):2090–6. Epub 2007/09/25. 1055-9965.EPI-07-0432 [pii] doi: 10.1158/1055-9965.EPI-07-0432 PMID: 17890521.
3. Edgren G, Adami HO, Weiderpass Vainio E, Nyren O. A global assessment of the oesophageal adenocarcinoma epidemic. Gut. 2012. Epub 2012/08/25. gutjnl-2012-302412 [pii] doi: 10.1136/gutjnl-2012-302412 PMID: 22917659.
4. Wang KK, Sampliner RE. Updated guidelines 2008 for the diagnosis, surveillance and therapy of Barrett's esophagus. Am J Gastroenterol. 2008; 103(3):788–97. Epub 2008/03/18. AJG1835 [pii] doi: 10.1111/j.1572-0241.2008.01835.x PMID: 18341497.
5. Shaheen NJ, Falk GW, Iyer PG, Gerson LB. ACG Clinical Guideline: Diagnosis and Management of Barrett's Esophagus. Am J Gastroenterol. 2015; 111(1):30–50. Epub 2015/11/04. ajg2015322 [pii] doi: 10.1038/ajg.2015.322 PMID: 26526079.
6. Whiteman DC, Appleyard M, Bahin FF, Bobryshev YV, Bourke MJ, Brown I, et al. Australian clinical practice guidelines for the diagnosis and management of Barrett's esophagus and early esophageal adenocarcinoma. J Gastroenterol Hepatol. 2015; 30(5):804–20. Epub 2015/01/23. doi: 10.1111/jgh.12913 PMID: 25612140.
7. Spechler SJ, Fitzgerald RC, Prasad GA, Wang KK. History, molecular mechanisms, and endoscopic treatment of Barrett's esophagus. Gastroenterology. 2010; 138(3):854–69. Epub 2010/01/19. S0016-5085(10)00018-1 [pii] doi: 10.1053/j.gastro.2010.01.002 PMID: 20080098.
8. Varghese S, Lao-Sirieix P, Fitzgerald RC. Identification and clinical implementation of biomarkers for Barrett's esophagus. Gastroenterology. 2012; 142(3):435–41 e2. Epub 2012/01/24. S0016-5085(12)00081-9 [pii] doi: 10.1053/j.gastro.2012.01.013 PMID: 22266150.
9. Nancarrow DJ, Clouston AD, Smithers BM, Gotley DC, Drew PA, Watson DI, et al. Whole genome expression array profiling highlights differences in mucosal defense genes in Barrett's esophagus and esophageal adenocarcinoma. PLoS One. 2011; 6(7):e22513. Epub 2011/08/11. doi: 10.1371/journal.pone.0022513 PONE-D-11-05378 [pii]. PMID: 21829465.
10. Wang J, Qin R, Ma Y, Wu H, Peters H, Tyska M, et al. Differential gene expression in normal esophagus and Barrett's esophagus. J Gastroenterol. 2009; 44(9):897–911. Epub 2009/05/27. doi: 10.1007/s00535-009-0082-2 PMID: 19468668.

11. Ong CA, Lao-Sirieix P, Fitzgerald RC. Biomarkers in Barrett's esophagus and esophageal adenocarcinoma: predictors of progression and prognosis. World J Gastroenterol. 2010; 16(45):5669–81. Epub 2010/12/04. PMID: 21128316.
12. Moyes LH, Going JJ. Still waiting for predictive biomarkers in Barrett's oesophagus. J Clin Pathol. 2011; 64(9):742–50. Epub 2011/05/25. jclinpath-2011-200084 [pii] doi: 10.1136/jclinpath-2011-200084 PMID: 21606229.
13. Barrett T, Troup DB, Wilhite SE, Ledoux P, Rudnev D, Evangelista C, et al. NCBI GEO: archive for high-throughput functional genomic data. Nucleic Acids Res. 2009; 37(Database issue):D885–90. Epub 2008/10/23. gkn764 [pii] doi: 10.1093/nar/gkn764 PMID: 18940857; PubMed Central PMCID: PMC2686538
14. R Development Core Team. R: A Language and Environment for Statistical Computing. Vienna, Austria: R Foundation for Statistical Computing; 2009.
15. Kimchi ET, Posner MC, Park JO, Darga TE, Kocherginsky M, Karrison T, et al. Progression of Barrett's metaplasia to adenocarcinoma is associated with the suppression of the transcriptional programs of epidermal differentiation. Cancer Res. 2005; 65(8):3146–54. Epub 2005/04/19. 65/8/3146 [pii] doi: 10.1158/0008-5472.CAN-04-2490 PMID: 15833844.
16. Stairs DB, Nakagawa H, Klein-Szanto A, Mitchell SD, Silberg DG, Tobias JW, et al. Cdx1 and c-Myc foster the initiation of transdifferentiation of the normal esophageal squamous epithelium toward Barrett's esophagus. PLoS One. 2008; 3(10):e3534. Epub 2008/10/28. doi: 10.1371/journal.pone.0003534 PMID: 18953412.
17. Watts GS, Tran NL, Berens ME, Bhattacharyya AK, Nelson MA, Montgomery EA, et al. Identification of Fn14/TWEAK receptor as a potential therapeutic target in esophageal adenocarcinoma. Int J Cancer. 2007; 121(10):2132–9. Epub 2007/06/28. doi: 10.1002/ijc.22898 PMID: 17594693.
18. Gentleman RC, Carey VJ, Bates DM, Bolstad B, Dettling M, Dudoit S, et al. Bioconductor: open software development for computational biology and bioinformatics. Genome Biol. 2004; 5(10):R80. Epub 2004/10/06. gb-2004-5-10-r80 [pii] doi: 10.1186/gb-2004-5-10-r80 PMID: 15461798; PubMed Central PMCID: PMC545600.
19. Gautier L, Cope L, Bolstad BM, Irizarry RA. affy—analysis of Affymetrix GeneChip data at the probe level. Bioinformatics. 2004; 20(3):307–15. Epub 2004/02/13. doi: 10.1093/bioinformatics/btg405 20/3/307 [pii]. PMID: 14960456.
20. McCall MN, Bolstad BM, Irizarry RA. Frozen robust multiarray analysis (fRMA). Biostatistics. 2010; 11 (2):242–53. Epub 2010/01/26. kxp059 [pii] doi: 10.1093/biostatistics/kxp059 PMID: 20097884.
21. Smyth GK. Linear models and empirical bayes methods for assessing differential expression in microarray experiments. Stat Appl Genet Mol Biol. 2004; 3:Article3. Epub 2006/05/02. doi: 10.2202/1544-6115.1027 PMID: 16646809.
22. McCall MN, Uppal K, Jaffee HA, Zilliox MJ, Irizarry RA. The Gene Expression Barcode: leveraging public data repositories to begin cataloging the human and murine transcriptomes. Nucleic Acids Res. 2011; 39(Database issue):D1011–5. Epub 2011/01/05. gkq1259 [pii] doi: 10.1093/nar/gkq1259 PMID: 21177656
23. Zilliox MJ, Irizarry RA. A gene expression bar code for microarray data. Nat Methods. 2007; 4(11):911–3. Epub 2007/10/02. nmeth1102 [pii] doi: 10.1038/nmeth1102 PMID: 17906632.
24. Montojo J, Zuberi K, Rodriguez H, Kazi F, Wright G, Donaldson SL, et al. GeneMANIA Cytoscape plugin: fast gene function predictions on the desktop. Bioinformatics. 2010; 26(22):2927–8. Epub 2010/10/12. btq562 [pii] doi: 10.1093/bioinformatics/btq562 PMID: 20926419.
25. Ye J, Coulouris G, Zaretskaya I, Cutcutache I, Rozen S, Madden TL. Primer-BLAST: a tool to design target-specific primers for polymerase chain reaction. BMC Bioinformatics. 2012; 13:134. Epub 2012/06/20. 1471-2105-13-134 [pii] doi: 10.1186/1471-2105-13-134 PMID: 22708584.
26. Livak KJ, Schmittgen TD. Analysis of relative gene expression data using real-time quantitative PCR and the 2(-Delta Delta C(T)) Method. Methods. 2001; 25(4):402–8. Epub 2002/02/16. doi: 10.1006/meth.2001.1262 S1046-2023(01)91262-9 [pii]. PMID: 11846609.
27. Tsai MS, Bogart DF, Castaneda JM, Li P, Lupu R. Cyr61 promotes breast tumorigenesis and cancer progression. Oncogene. 2002; 21(53):8178–85. Epub 2002/11/22. doi: 10.1038/sj.onc.1205682 PMID: 12444554.
28. Chan SW, Lim CJ, Guo K, Ng CP, Lee I, Hunziker W, et al. A role for TAZ in migration, invasion, and tumorigenesis of breast cancer cells. Cancer Res. 2008; 68(8):2592–8. Epub 2008/04/17. 68/8/2592 [pii] doi: 10.1158/0008-5472.CAN-07-2696 PMID: 18413727.
29. Cordenonsi M, Zanconato F, Azzolin L, Forcato M, Rosato A, Frasson C, et al. The Hippo transducer TAZ confers cancer stem cell-related traits on breast cancer cells. Cell. 2011; 147(4):759–72. Epub 2011/11/15. S0092-8674(11)01218-9 [pii] doi: 10.1016/j.cell.2011.09.048 PMID: 22078877.

30. D'Antonio KB, Toubaji A, Albadine R, Mondul AM, Platz EA, Netto GJ, et al. Extracellular matrix associated protein CYR61 is linked to prostate cancer development. J Urol. 2010; 183(4):1604–10. Epub 2010/02/23. S0022-5347(09)03150-4 [pii] doi: 10.1016/j.juro.2009.12.006 PMID: 20172544.

31. Franzen CA, Chen CC, Todorovic V, Juric V, Monzon RI, Lau LF. Matrix protein CCN1 is critical for prostate carcinoma cell proliferation and TRAIL-induced apoptosis. Mol Cancer Res. 2009; 7(7):1045–55. Epub 2009/07/09. 1541-7786.MCR-09-0017 [pii] doi: 10.1158/1541-7786.MCR-09-0017 PMID: 19584265.

32. Terada N, Shiraishi T, Zeng Y, Mooney SM, Yeater DB, Mangold LA, et al. Cyr61 is regulated by cAMP-dependent protein kinase with serum levels correlating with prostate cancer aggressiveness. Prostate. 2011; 72(9):966–76. Epub 2011/10/26. doi: 10.1002/pros.21501 PMID: 22025384.

33. Ladwa R, Pringle H, Kumar R, West K. Expression of CTGF and Cyr61 in colorectal cancer. J Clin Pathol. 2011; 64(1):58–64. Epub 2010/11/18. jcp.2010.082768 [pii] doi: 10.1136/jcp.2010.082768 PMID: 21081514.

34. Pan J, Li S, Chi P, Xu Z, Lu X, Huang Y. Lentivirus-mediated RNA interference targeting WWTR1 in human colorectal cancer cells inhibits cell proliferation in vitro and tumor growth in vivo. Oncol Rep. 2012; 28(1):179–85. Epub 2012/04/04. doi: 10.3892/or.2012.1751 PMID: 22470139.

35. Lin MT, Chang CC, Lin BR, Yang HY, Chu CY, Wu MH, et al. Elevated expression of Cyr61 enhances peritoneal dissemination of gastric cancer cells through integrin alpha2beta1. J Biol Chem. 2007; 282 (47):34594–604. Epub 2007/10/02. M706600200 [pii] doi: 10.1074/jbc.M706600200 PMID: 17905740.

36. Zhao ZS, Li L, Wang HJ, Wang YY. Expression and prognostic significance of CEACAM6, ITGB1, and CYR61 in peripheral blood of patients with gastric cancer. J Surg Oncol. 2011; 104(5):525–9. Epub 2011/05/28. doi: 10.1002/jso.21984 PMID: 21618249.

37. Xie JJ, Xu LY, Xie YM, Du ZP, Feng CH, Dong H, et al. Involvement of Cyr61 in the growth, invasiveness and adhesion of esophageal squamous cell carcinoma cells. Int J Mol Med. 2011; 27(3):429–34. Epub 2011/01/21. PMID: 21249313. doi: 10.3892/ijmm.2011.603

38. Zhou ZQ, Cao WH, Xie JJ, Lin J, Shen ZY, Zhang QY, et al. Expression and prognostic significance of THBS1, Cyr61 and CTGF in esophageal squamous cell carcinoma. BMC Cancer. 2009; 9:291. Epub 2009/08/25. 1471-2407-9-291 [pii] PMID: 19698122. doi: 10.1186/1471-2407-9-291

39. Di Martino E, Wild CP, Rotimi O, Darnton JS, Olliver RJ, Hardie LJ. IGFBP-3 and IGFBP-10 (CYR61) up-regulation during the development of Barrett's oesophagus and associated oesophageal adenocarcinoma: potential biomarkers of disease risk. Biomarkers. 2006; 11(6):547–61. Epub 2006/10/24. K16Q733086XL4HM8 [pii] doi: 10.1080/13547500600896791 PMID: 17056474.

40. Haque I, Mehta S, Majumder M, Dhar K, De A, McGregor D, et al. Cyr61/CCN1 signaling is critical for epithelial-mesenchymal transition and stemness and promotes pancreatic carcinogenesis. Mol Cancer. 2011; 10:8. Epub 2011/01/15. 1476-4598-10-8 [pii] PMID: 21232118. doi: 10.1186/1476-4598-10-8

41. Maity G, Mehta S, Haque I, Dhar K, Sarkar S, Banerjee SK, et al. Pancreatic tumor cell secreted CCN1/Cyr61 promotes endothelial cell migration and aberrant neovascularization. Sci Rep. 2014; 4:4995. Epub 2014/05/17. srep04995 [pii] PMID: 24833309. doi: 10.1038/srep04995

42. Li ZQ, Ding W, Sun SJ, Li J, Pan J, Zhao C, et al. Cyr61/CCN1 is regulated by Wnt/beta-catenin signaling and plays an important role in the progression of hepatocellular carcinoma. PLoS One. 2012; 7(4): e35754. Epub 2012/04/28. [pii]. PMID: 22540002. doi: 10.1371/journal.pone.0035754

43. Hsu YL, Hung JY, Chou SH, Huang MS, Tsai MJ, Lin YS, et al. Angiomotin decreases lung cancer progression by sequestering oncogenic YAP/TAZ and decreasing Cyr61 expression. Oncogene. 2015; 34 (31):4056–68. Epub 2014/11/11. onc2014333 [pii] PMID: 25381822. doi: 10.1038/onc.2014.333

44. Zhou Z, Hao Y, Liu N, Raptis L, Tsao MS, Yang X. TAZ is a novel oncogene in non-small cell lung cancer. Oncogene. 2011; 30(18):2181–6. Epub 2011/01/25. onc2010606 [pii] PMID: 21258416. doi: 10.1038/onc.2010.606

45. Chen G, Jin M, Lin S, Wang P, Liu J, Li W, et al. Increased expression cysteine-rich61 (Cyr61) in patients with thyroid carcinomas. African Journal of Pharmacy and Pharmacology. 2011; 5(22):2517–21. Epub 15 December, 2011. doi: 10.5897/AJPP11.708

46. de Cristofaro T, Di Palma T, Ferraro A, Corrado A, Lucci V, Franco R, et al. TAZ/WWTR1 is overexpressed in papillary thyroid carcinoma. Eur J Cancer. 2010; 47(6):926–33. Epub 2010/12/07. S0959-8049(10)01076-2 [pii] PMID: 21131195. doi: 10.1016/j.ejca.2010.11.008

47. Chintalapudi MR, Markiewicz M, Kose N, Dammai V, Champion KJ, Hoda RS, et al. Cyr61/CCN1 and CTGF/CCN2 mediate the proangiogenic activity of VHL-mutant renal carcinoma cells. Carcinogenesis. 2008; 29(4):696–703. Epub 2008/01/24. bgn019 [pii] PMID: 18212329. doi: 10.1093/carcin/bgn019

48. Shen H, Cai M, Zhao S, Wang H, Li M, Yao S, et al. CYR61 overexpression associated with the development and poor prognosis of ovarian carcinoma. Med Oncol. 2014; 31(8):117. Epub 2014/07/23. PMID: 25048722. doi: 10.1007/s12032-014-0117-2

49. Xie D, Yin D, Wang HJ, Liu GT, Elashoff R, Black K, et al. Levels of expression of CYR61 and CTGF are prognostic for tumor progression and survival of individuals with gliomas. Clin Cancer Res. 2004; 10(6):2072–81. Epub 2004/03/26. PMID: 15041728.

50. Bhat KP, Salazar KL, Balasubramaniyan V, Wani K, Heathcock L, Hollingsworth F, et al. The transcriptional coactivator TAZ regulates mesenchymal differentiation in malignant glioma. Genes Dev. 2011; 25(24):2594–609. Epub 2011/12/23. 25/24/2594 [pii] PMID: 22190458. doi: 10.1101/gad.176800.111

51. Sabile AA, Arlt MJ, Muff R, Bode B, Langsam B, Bertz J, et al. Cyr61 expression in Osteosarcoma indicates poor prognosis and promotes intratibial growth and lung metastasis in mice. J Bone Miner Res. 2012. Epub 2011/10/07. doi: 10.1002/jbmr.535 PMID: 21976359.

52. Errani C, Zhang L, Sung YS, Hajdu M, Singer S, Maki RG, et al. A novel WWTR1-CAMTA1 gene fusion is a consistent abnormality in epithelioid hemangioendothelioma of different anatomic sites. Genes Chromosomes Cancer. 2011; 50(8):644–53. Epub 2011/05/18. PMID: 21584898. doi: 10.1002/gcc.20886

53. Kok SH, Chang HH, Tsai JY, Hung HC, Lin CY, Chiang CP, et al. Expression of Cyr61 (CCN1) in human oral squamous cell carcinoma: An independent marker for poor prognosis. Head Neck. 2010; 32(12):1665–73. Epub 2010/09/18. PMID: 20848406. doi: 10.1002/hed.21381

54. Tang QL, Fan S, Li HG, Chen WL, Shen XM, Yuan XP, et al. Expression of Cyr61 in primary salivary adenoid cystic carcinoma and its relation to Ki-67 and prognosis. Oral Oncol. 2011; 47(5):365–70. Epub 2011/03/29. S1368-8375(11)00081-9 [pii] doi: 10.1016/j.oraloncology.2011.02.022 PMID: 21439895.

55. Jechlinger M, Grunert S, Tamir IH, Janda E, Ludemann S, Waerner T, et al. Expression profiling of epithelial plasticity in tumor progression. Oncogene. 2003; 22(46):7155–69. Epub 2003/10/17. 1206887 [pii]. doi: 10.1038/sj.onc.1206887 PMID: 14562044.

56. Kim H, Watkinson J, Varadan V, Anastassiou D. Multi-cancer computational analysis reveals invasion-associated variant of desmoplastic reaction involving INHBA, THBS2 and COL11A1. BMC Med Genomics. 2010; 3:51. Epub 2010/11/05. 1755-8794-3-51 [pii] PMID: 21047417. doi: 10.1186/1755-8794-3-51

57. Taube JH, Herschkowitz JI, Komurov K, Zhou AY, Gupta S, Yang J, et al. Core epithelial-to-mesenchymal transition interactome gene-expression signature is associated with claudin-low and metaplastic breast cancer subtypes. Proc Natl Acad Sci U S A. 2010; 107(35):15449–54. Epub 2010/08/18. 1004900107 [pii] PMID: 20713713. doi: 10.1073/pnas.1004900107

58. Thiery JP, Acloque H, Huang RY, Nieto MA. Epithelial-mesenchymal transitions in development and disease. Cell. 2009; 139(5):871–90. Epub 2009/12/01. S0092-8674(09)01419-6 [pii] PMID: 19945376. doi: 10.1016/j.cell.2009.11.007

59. Zeisberg M, Neilson EG. Biomarkers for epithelial-mesenchymal transitions. J Clin Invest. 2009; 119 (6):1429–37. Epub 2009/06/03. 36183 [pii] PMID: 19487819. doi: 10.1172/JCI36183

60. Fitzgerald RC. Pre-Invasive Disease: Pathogenesis and Clinical Management. In: Fitzgerald RC, editor. Pre-Invasive Disease: Pathogenesis and Clinical Management. New York: Springer Science +Business Media; 2011. p. 315–40.

61. Modak C, Mouazzen W, Narvaez R, Reavis KM, Chai J. CCN1 is critical for acid-induced esophageal epithelial cell transformation. Biochem Biophys Res Commun. 2010; 392(4):533–7. Epub 2010/01/26. S0006-291X(10)00106-3 [pii] PMID: 20097175. doi: 10.1016/j.bbrc.2010.01.057

62. Duggan SP, Gallagher WM, Fox EJ, Abdel-Latif MM, Reynolds JV, Kelleher D. Low pH induces co-ordinate regulation of gene expression in oesophageal cells. Carcinogenesis. 2006; 27(2):319–27. Epub 2005/08/23. bgi211 [pii] doi: 10.1093/carcin/bgi211 PMID: 16113055.

63. Chen CC, Mo FE, Lau LF. The angiogenic factor Cyr61 activates a genetic program for wound healing in human skin fibroblasts. J Biol Chem. 2001; 276(50):47329–37. Epub 2001/10/05. M107666200 [pii]. doi: 10.1074/jbc.M107666200 PMID: 11584015.

64. Chaqour B, Goppelt-Struebe M. Mechanical regulation of the Cyr61/CCN1 and CTGF/CCN2 proteins. FEBS J. 2006; 273(16):3639–49. Epub 2006/07/22. EJB5360 [pii] doi: 10.1111/j.1742-4658.2006.05360.x PMID: 16856934.

65. Hong Y, Ho KS, Eu KW, Cheah PY. A susceptibility gene set for early onset colorectal cancer that integrates diverse signaling pathways: implication for tumorigenesis. Clin Cancer Res. 2007; 13(4):1107–14. Epub 2007/02/24. 13/4/1107 [pii] doi: 10.1158/1078-0432.CCR-06-1633 PMID: 17317818.

66. Ladwa R, Pringle H, Kumar R, West K. Expression of CTGF and Cyr61 in colorectal cancer. J Clin Pathol. 2010; 64(1):58–64. Epub 2010/11/18. jcp.2010.082768 [pii] PMID: 21081514. doi: 10.1136/jcp.2010.082768

67. Chen CC, Lau LF. Functions and mechanisms of action of CCN matricellular proteins. Int J Biochem Cell Biol. 2009; 41(4):771–83. Epub 2008/09/09. S1357-2725(08)00318-X [pii] PMID: 18775791. doi: 10.1016/j.biocel.2008.07.025

68. Lei QY, Zhang H, Zhao B, Zha ZY, Bai F, Pei XH, et al. TAZ promotes cell proliferation and epithelial-mesenchymal transition and is inhibited by the hippo pathway. Mol Cell Biol. 2008; 28(7):2426–36. Epub 2008/01/30. MCB.01874-07 [pii] PMID: 18227151. doi: 10.1128/MCB.01874-07

69. Selaru FM, Wang S, Yin J, Schulmann K, Xu Y, Mori Y, et al. Beyond Field Effect: Analysis of Shrunken Centroids in Normal Esophageal Epithelia Detects Concomitant Esophageal Adenocarcinoma. Bioinform Biol Insights. 2007; 1:127–36. Epub 2008/04/22. PMID: 18425214.

70. Terada N, Kulkarni P, Getzenberg RH. Cyr61 is a potential prognostic marker for prostate cancer. Asian J Androl. 2012; 14(3):405–8. Epub 2012/02/22. aja2011149 [pii] PMID: 22343491. doi: 10.1038/aja.2011.149

71. Zhang H, Liu CY, Zha ZY, Zhao B, Yao J, Zhao S, et al. TEAD transcription factors mediate the function of TAZ in cell growth and epithelial-mesenchymal transition. J Biol Chem. 2009; 284(20):13355–62. Epub 2009/03/28. M900843200 [pii] PMID: 19324877. doi: 10.1074/jbc.M900843200

72. Zhao B, Tumaneng K, Guan KL. The Hippo pathway in organ size control, tissue regeneration and stem cell self-renewal. Nat Cell Biol. 2011; 13(8):877–83. Epub 2011/08/03. ncb2303 [pii] PMID: 21808241. doi: 10.1038/ncb2303

73. Martin-Belmonte F, Perez-Moreno M. Epithelial cell polarity, stem cells and cancer. Nat Rev Cancer. 2011; 12(1):23–38. Epub 2011/12/16. nrc3169 [pii] PMID: 22169974. doi: 10.1038/nrc3169

74. Rhim AD, Mirek ET, Aiello NM, Maitra A, Bailey JM, McAllister F, et al. EMT and dissemination precede pancreatic tumor formation. Cell. 2012; 148(1–2):349–61. Epub 2012/01/24. S0092-8674(11)01369-9 [pii] PMID: 22265420. doi: 10.1016/j.cell.2011.11.025

75. Leopold PL, Vincent J, Wang H. A comparison of epithelial-to-mesenchymal transition and re-epithelialization. Semin Cancer Biol. 2012; 22(5–6):471–83. Epub 2012/08/07. S1044-579X(12)00104-6 [pii] PMID: 22863788. doi: 10.1016/j.semcancer.2012.07.003

76. Tomizawa Y, Wu TT, Wang KK. Epithelial mesenchymal transition and cancer stem cells in esophageal adenocarcinoma originating from Barrett's esophagus. Oncol Lett. 2012; 3(5):1059–63. Epub 2012/07/12. [pii]. doi: 10.3892/ol.2012.632ol-03-05-1059 PMID: 22783391.

77. Farragher SM, Tanney A, Kennedy RD, Paul Harkin D. RNA expression analysis from formalin fixed paraffin embedded tissues. Histochem Cell Biol. 2008; 130(3):435–45. Epub 2008/08/06. PMID: 18679706. doi: 10.1007/s00418-008-0479-7

78. Paik S, Kim CY, Song YK, Kim WS. Technology insight: Application of molecular techniques to formalin-fixed paraffin-embedded tissues from breast cancer. Nat Clin Pract Oncol. 2005; 2(5):246–54. Epub 2005/11/03. ncponc0171 [pii] doi: 10.1038/ncponc0171 PMID: 16264960.

79. Fitzgerald RC, di Pietro M, Ragunath K, Ang Y, Kang JY, Watson P, et al. British Society of Gastroenterology guidelines on the diagnosis and management of Barrett's oesophagus. Gut. 2013; 63(1):7–42. Epub 2013/10/30. gutjnl-2013-305372 [pii] PMID: 24165758. doi: 10.1136/gutjnl-2013-305372

80. Aldulaimi DM, Cox M, Nwokolo CU, Loft DE. Barrett's surveillance is worthwhile and detects curable cancers. A prospective cohort study addressing cancer incidence, treatment outcome and survival. Eur J Gastroenterol Hepatol. 2005; 17(9):943–50. Epub 2005/08/12. doi: 00042737-200509000-00010 [pii]. PMID: 16093872.

81. Hirst NG, Gordon LG, Whiteman DC, Watson DI, Barendregt JJ. Is endoscopic surveillance for non-dysplastic Barrett's esophagus cost-effective? Review of economic evaluations. J Gastroenterol Hepatol. 2011; 26(2):247–54. Epub 2011/01/26. PMID: 21261712. doi: 10.1111/j.1440-1746.2010.06506.x

82. Somerville M, Garside R, Pitt M, Stein K. Surveillance of Barrett's oesophagus: is it worthwhile? Eur J Cancer. 2008; 44(4):588–99. Epub 2008/02/15. S0959-8049(08)00007-5 [pii] PMID: 18272361. doi: 10.1016/j.ejca.2008.01.015

83. Hvid-Jensen F, Pedersen L, Drewes AM, Sorensen HT, Funch-Jensen P. Incidence of adenocarcinoma among patients with Barrett's esophagus. N Engl J Med. 2011; 365(15):1375–83. Epub 2011/10/15. PMID: 21995385. doi: 10.1056/NEJMoa1103042

CHAPTER 3:

Centrosome amplification arises before neoplasia and increases upon p53 loss in tumorigenesis

Published Online: 8 May, 2018 | Supp Info: http://doi.org/10.1083/jcb.201711191

JCB Journal of Cell Biology

REPORT

Centrosome amplification arises before neoplasia and increases upon p53 loss in tumorigenesis

Carla A.M. Lopes[1,2*], Marta Mesquita[1,3*], Ana Isabel Cunha[1], Joana Cardoso[4], Sara Carapeta[4], Cátia Laranjeira[1], António E. Pinto[1], José B. Pereira-Leal[4], António Dias-Pereira[1,3], Mónica Bettencourt-Dias[2**], and Paula Chaves[1,3**]

Centrosome abnormalities are a typical hallmark of human cancers. However, the origin and dynamics of such abnormalities in human cancer are not known. In this study, we examined centrosomes in Barrett's esophagus tumorigenesis, a well-characterized multistep pathway of progression, from the premalignant condition to the metastatic disease. This human cancer model allows the study of sequential steps of progression within the same patient and has representative cell lines from all stages of disease. Remarkably, centrosome amplification was detected as early as the premalignant condition and was significantly expanded in dysplasia. It was then present throughout malignant transformation both in adenocarcinoma and metastasis. The early expansion of centrosome amplification correlated with and was dependent on loss of function of the tumor suppressor p53 both through loss of wild-type expression and hotspot mutations. Our work shows that centrosome amplification in human tumorigenesis can occur before transformation, being repressed by p53. These findings suggest centrosome amplification in humans can contribute to tumor initiation and progression.

Introduction

The centrosome has key roles in microtubule organization, signaling, polarity, and cell division—all processes deregulated in tumorigenesis. Each centrosome, composed of two centrioles and a pericentriolar protein matrix (PCM), duplicates once per cell cycle to ensure bipolar spindle assembly during cell division (Bornens, 2012; Godinho and Pellman, 2014). Centrosome number amplification can lead to aberrant mitotic spindles and associated cell death (Holland et al., 2012; Marthiens et al., 2013). However, cancer cells with centrosome amplification can often survive cell division while generating genomic instability (Ganem et al., 2009; Silkworth et al., 2009). Moreover, centrosome amplification can promote aneuploidy and invasiveness in cultured cells as well as promote and enhance tumorigenesis in mice (Godinho et al., 2014; Coelho et al., 2015; Serçin et al., 2016; Levine et al., 2017). As centrosome amplification is found in human tumors (Chan, 2011) but not in normal cells, it is an appealing feature to explore for diagnosis, prognosis, and therapy.

Despite being a cancer hallmark, the timing, mechanisms, and impact of centrosome deregulation in human cancer are poorly understood (Godinho and Pellman, 2014). Moreover, whether the incidence of centrosome amplification changes through progression is not known. This partly stems from lack of studies surveying centrosomes at the single-cell level through tumorigenesis. Moreover, most studies score only PCM components, which may not harbor centrioles and thus not represent bona-fide centrosomes (Chan, 2011; Godinho and Pellman, 2014). Understanding the dynamics of centrosome amplification is essential to decipher its role in cancer.

It is critical to examine centrosomes along cancer progression. Barrett's esophagus (BE) is a premalignant condition in which the normal esophageal epithelium is replaced by a stomach/intestine-like metaplastic lining as a result of chronic reflux (Spechler et al., 2011). Its malignant transformation is a multistep process from metaplasia (premalignant condition) to dysplasia (intraepithelial neoplasia), adenocarcinoma (invasive neoplasia), and metastasis (Fig. 1 A; Haggitt, 1994). Given the risk of developing cancer, BE patients are included in a surveillance program (Spechler et al., 2011; Fitzgerald et al., 2014), which allows the study of the intermediate step between normal tissue and tumor initiation. Despite the increasing incidence of esophageal adenocarcinoma, only some BE patients will progress (0.1–0.3%/yr; Hvid-Jensen et al., 2011; Schouten et al., 2011). However, neoplasia resections allow the unique study of sequential stages of progression in each individual patient and thus the more specific

[1]Instituto Português de Oncologia de Lisboa Francisco Gentil, Lisbon, Portugal; [2]Instituto Gulbenkian de Ciência, Oeiras, Portugal; [3]Faculdade de Ciências da Saúde, Universidade da Beira Interior, Covilhã, Portugal; [4]Ophiomics-Precision Medicine, Lisbon, Portugal.

*C.A.M. Lopes and M. Mesquita contributed equally to this paper; **M. Bettencourt-Dias and P. Chaves contributed equally to this paper; Correspondence to Carla A.M. Lopes: lopes.carla.am@gmail.com; Paula Chaves: pchaves@ipolisboa.min-saude.pt; Mónica Bettencourt-Dias: mdias@igc.gulbenkian.pt; C. Laranjeira's present address is Foundation for National Scientific Computing, Fundação para a Ciência e Tecnologia, Lisbon, Portugal.

detection of consistent differences through progression (Ross-Innes et al., 2015; Stachler et al., 2015).

In this study, we used BE to uncover when and how centrosome amplification arises. We established a method to identify centrosomes at the single-cell level in clinical samples and found that centriole number abnormalities arise early in BE progression both in clinical samples and cell lines. Moreover, we found an increase in abnormalities in dysplasia, which were dependent on p53 loss of function. Our findings suggest centrosome amplification can arise early in human tumorigenesis, being normally repressed by p53.

Results and discussion

Centrosome amplification arises as early as the premalignant condition and increases in dysplasia

To determine when centrosome number abnormalities arise, we selected cohorts of patients that allowed us to examine all stages of disease. We therefore included metaplasia samples from biopsies of patients that did not progress (cohort 1) as well as samples from patients subjected to resection upon progression to dysplasia (cohort 2) or adenocarcinoma (cohort 3; Fig. 1 A and Table S1). In these, we analyzed in each patient areas of metaplasia, dysplasia, and adenocarcinoma (cohort 2) along with areas of metaplasia, adenocarcinoma, and lymph node metastasis (cohort 3). As comparison standards for normal epithelial tissue, we examined samples of native esophagus (normal lining; Fig. 1 A) and ileum (Fig. S1 B).

We established a method to identify centrosomes at the single-cell level in tissue samples by immunofluorescence (IF). To ensure centrosome scoring, we labeled its structural components: the centrioles (with glutamylated tubulin) and the PCM (with pericentrin; Fig. 1 B). Thus, only centrioles surrounded by the PCM were scored. Moreover, the background of glutamylated tubulin staining was sufficient to define cell boundaries (Fig. S1 A), thus allowing centriole number scoring cell by cell.

Centriole amplification was never observed in the normal lining of the esophagus (Fig. 1, B and C) or the ileum (Fig. S1, C and D). Although centriole amplification was also not detected in metaplasia from biopsies that had not progressed, cells with supernumerary centrioles were detected early in metaplasia adjacent to dysplasia or adenocarcinoma as well as in all subsequent steps of progression (Fig. 1, B and C; and Fig. S1, C–E). Moreover, the number of centrioles found per cell increased upon progression (Fig. S1 D). Centriole amplification increased significantly from metaplasia to dysplasia (Figs. 1 C and S1 C). Our data also indicate a decrease in adenocarcinoma followed by an increase in metastasis (Figs. 1 C and S1 C). This change in incidence along progression suggests that the percentage of cells with centrosome amplification is dynamic. Our observations suggest that the impact of these abnormalities is likely context dependent, being differently tolerated and having different consequences along progression.

Loss of p53 function correlates with the increase in centrosome amplification

Mutations in p53, the most mutated gene in human cancers (Petitjean et al., 2007), define the boundary from metaplasia to dysplasia in BE progression (Weaver et al., 2014). As p53 loss is associated with centrosome amplification in many human tumors (Chan, 2011; Godinho and Pellman, 2014), we hypothesized that p53 inactivation is responsible for the increased centrosome amplification observed in dysplasia.

To test this, we sequenced p53 in metaplasia and dysplasia samples from the same patient (cohort 2). In agreement with previous studies (Hamelin et al., 1994; Gleeson et al., 1995, 1998; Del Portillo et al., 2015), we found that p53 was mutated in dysplasia: all samples contained multiple mutations in high frequency, with some individual mutations being detected in 97% of the reads, whereas metaplasia samples either retained WT p53 or had fewer mutations in lower frequency (Fig. 2 and Table S2). In the BE clinical setting, p53 status is assessed by immunohistochemistry (IHC), a reliable method recommended to aid the dysplasia diagnosis as it detects mutational and nonmutational changes leading to p53 inactivation (Bian et al., 2001; Kaye et al., 2010; Fitzgerald et al., 2014). Using this approach, we confirmed that all dysplasia samples had abnormal p53 expression, indicative of p53 mutations or loss, whereas most metaplasia samples retained WT p53 expression (Fig. S2 and Table S2). Collectively, these results confirm that p53 is first altered in dysplasia and suggest that this change underlies the increased penetrance of centrosome amplification detected at this stage.

Profile of centrosome amplification in cell lines is similar to patient samples

To test the consequences of p53 loss in centrosome amplification, we took advantage of a well-characterized cell line panel established from all stages of BE progression and containing genomic alterations found in vivo: metaplasia cells are diploid and have WT p53, whereas dysplasia cells are aneuploid and have distinct p53 mutations (Fig. S3 A and Table S3; Palanca-Wessels et al., 2003; Jaiswal et al., 2007). We therefore first asked whether this panel showed a similar trend in centriole amplification along progression to that observed in patient samples. As comparison standards for normal cells, we used native epithelia-derived cells (Table S3; Harada et al., 2003). To assess centrioles, we used two markers (glutamylated tubulin and centrin) in mitotic cells, which normally have four centrioles.

As in tissue samples, centriole amplification was not found in normal lining cells, but it was detected in metaplasia cells and in all cell lines from the subsequent stages (Fig. 3). Moreover, the number of centrioles found per cell increased upon progression (Fig. S3 B). Importantly, the incidence of centriole amplification increased from metaplasia to dysplasia (Fig. 3). This was validated with an additional centriolar marker and confirmed in interphase cells (Fig. S3, C and D). The higher percentage of cells with amplification observed in cell lines compared with tissue samples was likely caused by undercounting in tissue samples, which resulted from technical limitations (see Materials and methods). Interestingly, we had in our collection both an adenocarcinoma cell line (ESO51) and the tumor it was derived from (case 8 in cohort 3), and both had a lower degree of amplification (10% cell line and 2.5% tissue) as compared with the other lines and tumors (up to 31.8% cell lines and 6.5% tissues).

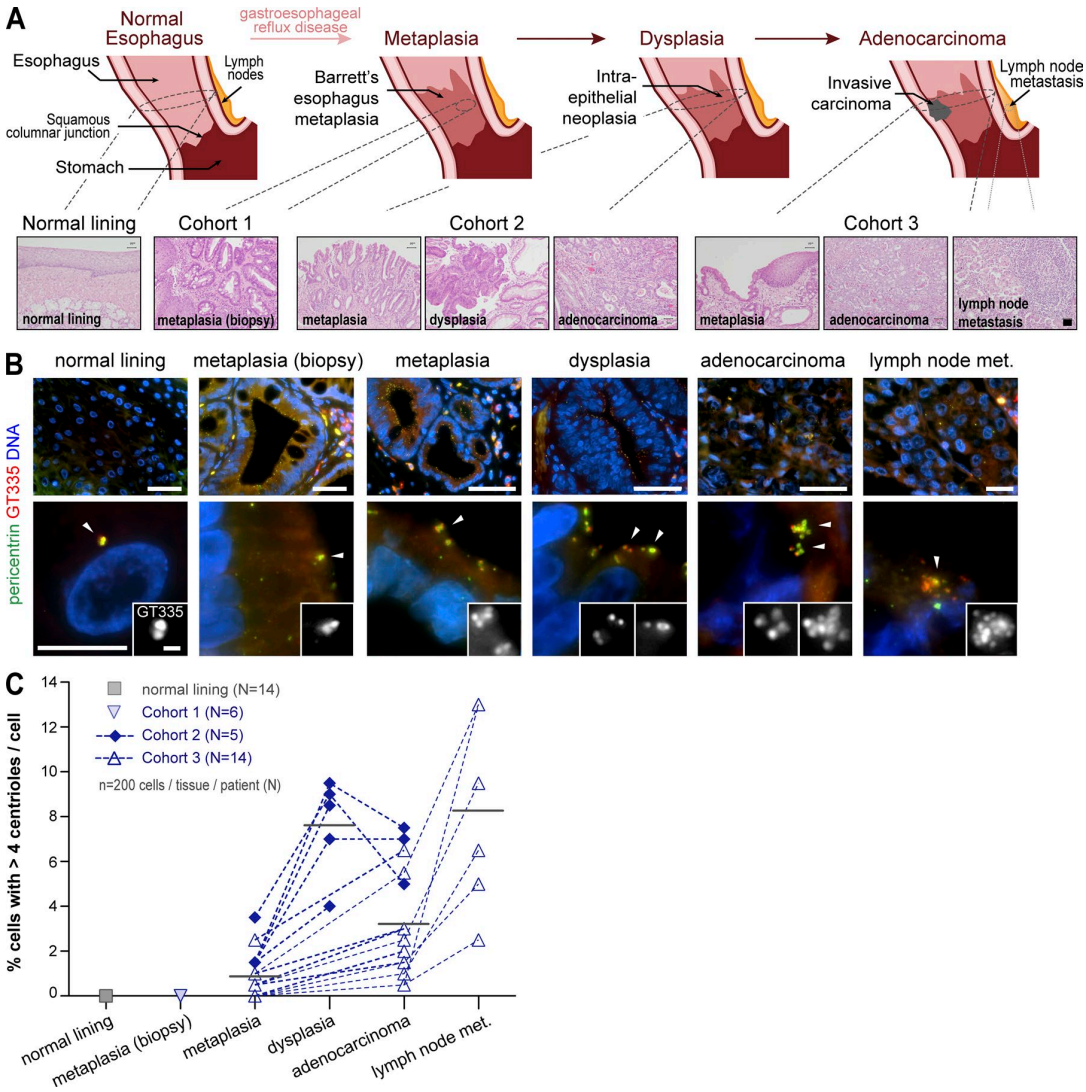

Figure 1. **Centriole amplification arises early and is associated with tumor initiation in patient samples. (A)** BE multistep pathway of progression. Tissue samples' origins are highlighted. Normal lining: native esophageal epithelium. Cohort 1: metaplasia from biopsies of patients that have not progressed. Cohort 2: dysplasia and adjacent metaplasia as well as foci of adenocarcinoma when present in each patient. Cohort 3: adenocarcinoma and adjacent metaplasia as well as lymph node metastasis (met.) when present in each patient. Representative histopathologic features (H&E) of the samples are shown. Bar, 50 mm. **(B and C)** Samples were stained for PCM (pericentrin), centrioles (GT335), and DNA. **(B)** Representative images with enlargements of cells and centrioles in a single cell (arrowheads). Bars: (top) 50 µm; (bottom, main images) 10 µm; (bottom, insets) 1 µm. **(C)** Quantification of cells with centriole amplification for the tissue samples present in each case analyzed. *n* = 200/tissue/patient. N, number of cases analyzed. Gray lines indicate means of all samples analyzed for each tissue of origin.

Collectively, these observations suggest cell lines keep the centrosome characteristics of their tissue of origin and are thus a good model to test the molecular changes underlying centrosome amplification.

WT p53 controls centriole amplification in metaplasia

Previous work showed that p53 loss alone in normal human cells does not lead to centrosome number defects. However, loss of p53 is required for the survival of cells experimentally perturbed to gain or lose centrosomes (Cuomo et al., 2008; Holland et al., 2012; Lambrus et al., 2015; Wong et al., 2015). Given the small population of cells with supernumerary centrioles in metaplasia, we hypothesized that there is underlying centrosome amplification in metaplasia that is normally suppressed by p53. Cellular stress normally induces p53, leading to its nuclear accumulation and activation of downstream effectors to prevent the expansion of those cells (Rivlin et al., 2011). We found that all interphase metaplasia cells with centriole amplification showed p53 nuclear accumulation, whereas the majority (70%) of cells with normal centriole number had undetectable p53 (Fig. 4 A). To test whether p53 was preventing the expansion of cells with amplification, we depleted p53 by siRNA (Fig. S3 E). Indeed, p53 depletion in metaplasia resulted in an increase in centriole amplification to similar levels detected in dysplasia (Fig. 4, B–D). This result was

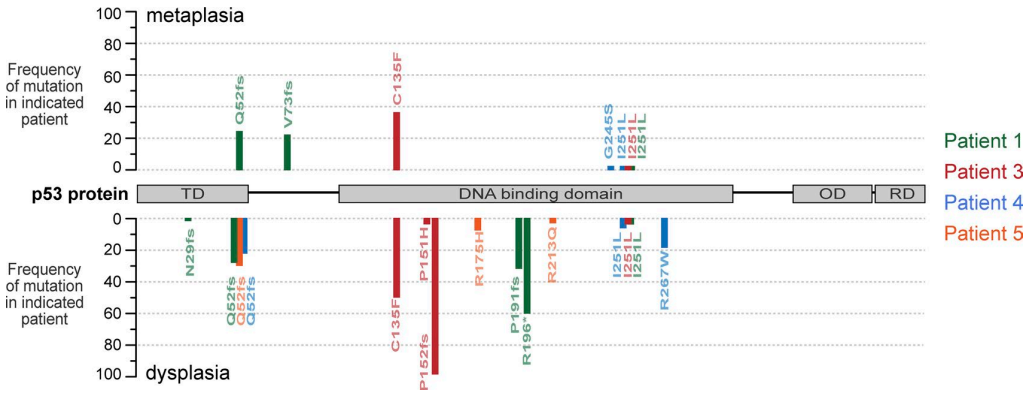

Figure 2. **p53 is deregulated in dysplasia patient samples.** The mutational status of p53 in dysplasia and adjacent metaplasia samples (cohort 2) was determined by NGS. The positions and frequency of the mutations identified in each patient in metaplasia and dysplasia areas are shown above and below the protein schematic, respectively. fs, frameshift mutation; OD, oligomerization domain; RD, regulatory domain; TD, transactivation domain. The asterisk indicates a nonsense mutation.

confirmed using different p53 siRNAs or shRNA (Fig. S3, F–I). Significantly, p53 depletion alone was not sufficient to generate centriole amplification in normal lining cells (Fig. S3, J and K). It is therefore likely that yet-unidentified molecular changes occurring in metaplasia (Weaver et al., 2014) promote centriole amplification at this stage.

Importantly, supernumerary centrioles in metaplasia both before and after p53 loss were active, as they were able to recruit γ-tubulin and nucleate microtubules (Figs. 4 C and S3, L and M), thus potentially contributing to genomic instability (Ganem et al., 2009; Silkworth et al., 2009). Future studies are needed to elucidate the fate of metaplasia cells dividing with supernumerary centrioles. In the absence of p53, an increase in centrosome amplification may play a role in tumor initiation by conferring the genomic instability required for the acquisition of malignant properties. In agreement with this, chromosomal instability was detected in metaplasia adjacent to neoplasia and was progressively more frequent in dysplasia and adenocarcinoma (Chaves et al., 2007; Paulson et al., 2009).

Centrosome number deregulation can occur by several mechanisms including centrosome biogenesis deregulation and cytokinesis failure (Godinho and Pellman, 2014). In the latter, centrosome numbers increase in concert with ploidy (Davoli and de Lange, 2011). Ploidy is known to be deregulated in BE tumorigenesis: tetraploidy was detected in BE and predicts progression to aneuploidy, which is preceded by p53 changes (Reid et al., 2010). Moreover, ploidy deregulation is likely also surveyed by p53 (Thompson and Compton, 2010; Ganem et al., 2014). To test the association between deregulation of ploidy and centriole numbers, we investigated both features in metaplasia cells with or without p53. We detected ploidy deregulation in mitotic metaplasia cells (Fig. 4 E) and binucleated cells in metaplasia that elicited a p53 response (Fig. S3 N). Ploidy deregulation was aggravated upon p53 silencing (Fig. S3, O–Q). Moreover, both centriole number and ploidy increased upon p53 loss (Fig. 4 E), suggesting a common origin such as cell division failure. If centriole amplification detected upon p53 loss in metaplasia results exclusively from cell division failure, then blocking metaplasia cells in S phase and thus

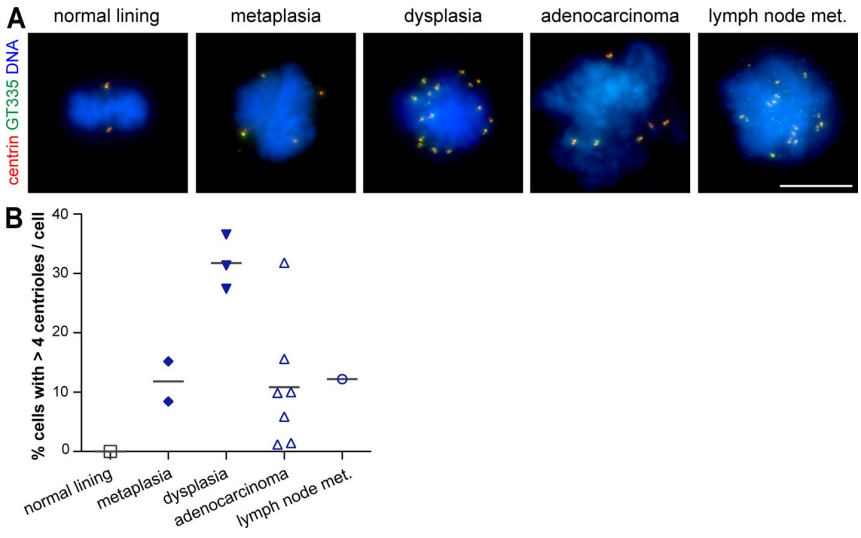

Figure 3. **Profile of centriole amplification in representative cell lines is similar to that in patient samples. (A and B)** Cells derived from the normal lining and from all stages of BE progression were stained for centrioles (centrin and GT335) and DNA. **(A)** Representative images. Bar, 10 µm. **(B)** Quantification of mitotic cells with centriole amplification in each cell line ($n \geq 60$/cell line) of the indicated tissue of origin. Gray lines indicate means of all cell lines for each tissue of origin. Met., metastasis.

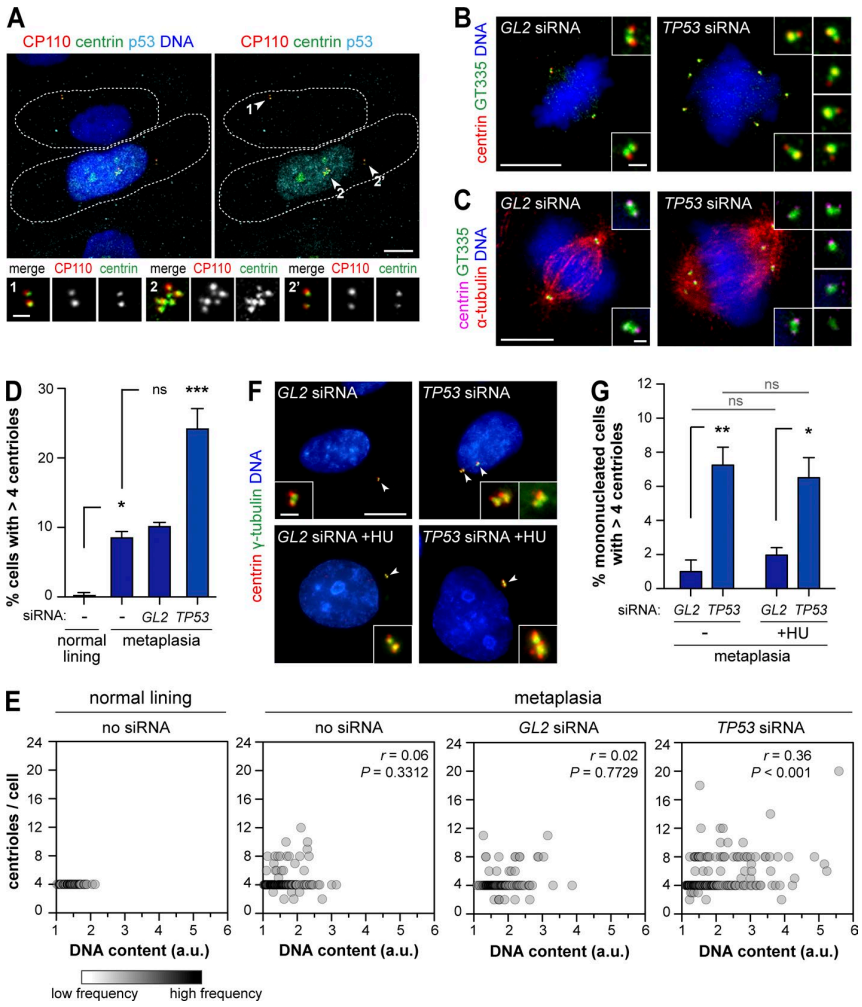

Figure 4. **p53 represses centriole amplification in metaplasia. (A)** Metaplasia cells were stained for p53, centrioles (centrin and CP110), and DNA. Dashed lines denote individual cell outlines given by the CP110/centrin background signal. Insets show centrioles (arrowheads) in p53-negative (1) and p53-positive (2 and 2′) cells. **(B–E)** Metaplasia cells transfected with control (*GL2*) or p53 (*TP53*) siRNA were stained for centrioles (centrin and GT335) and DNA (B) or centrioles, microtubules (α-tubulin), and DNA (C). Untreated metaplasia and normal lining cells were also analyzed. **(B and C)** Representative images with enlargements of centrioles. Bars: (main images) 10 µm; (insets) 1 µm. **(D)** Quantification of mitotic cells with centriole amplification. $n \geq 100$/condition/experiment. **(E)** Correlation between centriole number and DNA content in each mitotic cell (individual circles). Data are from two independent experiments. $n \geq 100$/condition/experiment; Spearman test. **(F and G)** Asynchronous (-) or S phase–arrested (hydroxyurea [+HU]) metaplasia cells transfected with control (*GL2*) or p53 (*TP53*) siRNA were stained for centrioles (centrin) and γ-tubulin. **(F)** Representative images with enlargements of centrioles (arrowheads). Bars: (main images) 10 µm; (insets) 1 µm. **(G)** Quantification of cells with centriole amplification. $n \geq 60$/condition/experiment. Error bars show means ± SEM of three independent experiments. *, $P < 0.05$; **, $P < 0.01$; ***, $P < 0.001$ (ANOVA).

not allowing them to divide should abrogate the increase in amplification. We found that p53 loss was still able to promote centriole amplification in S phase–arrested metaplasia cells (hydroxyurea treatment; Fig. 4, F and G; and Fig. S3, R and S), suggesting that at least part of the amplification observed does not result from failed cell division. Previous work showed that S phase arrest was sufficient to generate centrosome amplification in p16-deficient human mammary cells (McDermott et al., 2006). However, this was not the case in control metaplasia cells (Fig. 4, F and G), which also lack the tumor suppressor p16, one of the earliest changes in BE (Table S3; Reid et al., 2010). The contribution of this and other early events to centrosome amplification deserves further study. Collectively, these results suggest centriole amplification can arise independently of cell division failure in BE metaplasia and demonstrate a key role for p53 in preventing the expansion of those cells.

p53 hotspot mutations R175H and R248W deregulate centriole number control

As most tumor suppressors, p53 inactivation can be caused by nonsense or frameshift mutations that lead to a truncated nonfunctional protein. In most cases, however, including BE tumorigenesis, p53 contains a missense mutation resulting in the expression of a full-length protein that loses the WT function and may gain oncogenic function (Fig. 2; Rivlin et al., 2011; Weaver et al., 2014). Hence, it is relevant to study the effect of p53 missense mutations on centrosome number as it could be different from loss of WT function. Notably, all three dysplasia cell lines, which have either a frameshift mutation or the missense mutations R175H or R248W, exhibited similar levels of centriole amplification (Fig. 3 B and Table S3). R175H and R248W are known hotspot mutations in BE neoplasia and other tumors (Fig. 2; Petitjean et al., 2007; Weaver et al., 2014). Expression of these mutants in $p53^{-/-}$ MEFs and in a lung metastasis cell line led to centrosome amplification (Tarapore et al., 2001; Noll et al., 2012). In this study, we tested whether expression of R175H or R248W mutants prevents the amplification elicited by p53 loss in metaplasia (Fig. 5 A). In contrast with expression of WT p53, neither mutant prevented the accumulation of cells with amplification (Fig. 5, B–D). Moreover, amplified centrioles were active as they nucleated microtubules (Fig. 5 C). These results show both residues are essential for p53 to control centriole number in metaplasia and that loss of WT p53 function leads to increase in centriole amplification upon progression from metaplasia to dysplasia. Moreover, previous findings that R175H and R248W

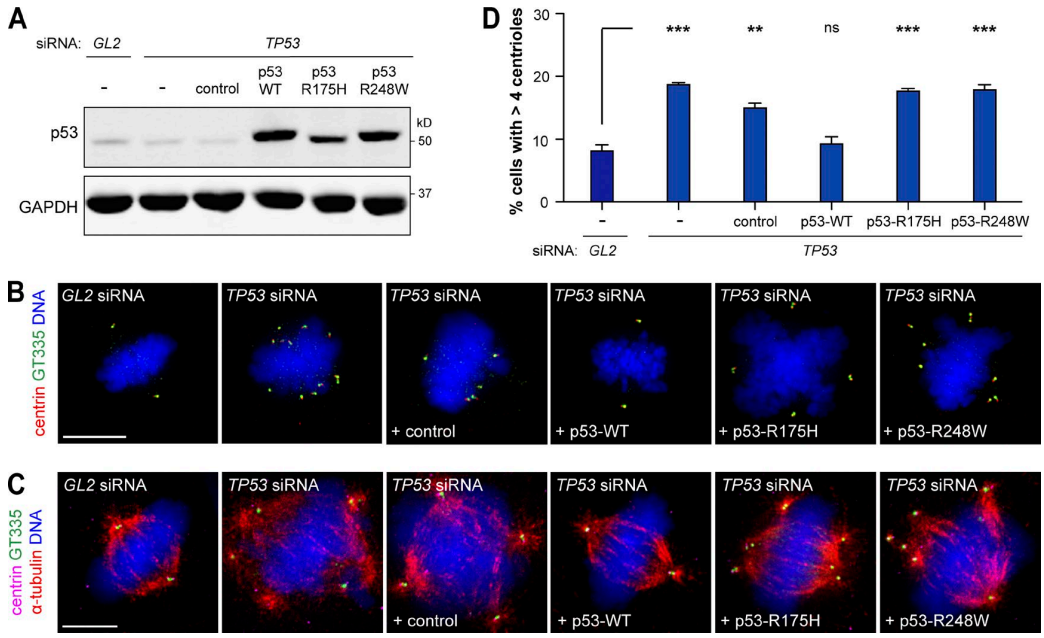

Figure 5. **The p53 hotspot mutations R175H and R248W deregulate centriole numbers in metaplasia. (A–D)** Metaplasia cells depleted of endogenous p53 (*TP53*) were transfected with WT p53, p53-R175H, p53-R248W, or the empty plasmid (control). Metaplasia cells transfected with control siRNA (*GL2*) or siRNA against endogenous p53 (*TP53*) alone were also analyzed. **(A)** Protein levels were assessed by WB. GAPDH was used as a loading control. **(B–D)** Cells were stained for centrioles (centrin and GT335) and DNA (B) or centrioles, microtubules (α-tubulin), and DNA (C). **(B and C)** Representative images are shown. Bars, 10 µm. **(D)** Quantification of mitotic cells with centriole amplification. $n \geq 100$/condition/experiment. Error bars show means ± SEM of two independent experiments. **, $P < 0.01$; ***, $P < 0.001$ (ANOVA).

mutations can promote genomic instability and invasion (Rivlin et al., 2011; Muller and Vousden, 2014) further support a role for centrosome amplification in those processes. Further studies are needed to determine how distinct p53 mutations affect tumorigenesis and whether that is related to centrosome amplification.

In summary, we showed that centrosome amplification (A) is never observed in native epithelia, suggesting centriole number control is robust in the normal population; (B) it arises as early as the premalignant condition and is present in all stages in all patients; (C) its incidence is dynamic during progression; (D) it significantly increases from metaplasia to dysplasia; and (E) this increase correlates with and is dependent on loss of p53 function. These findings have important implications in our understanding of centrosome amplification in cancer progression.

An association between p53 loss and centrosome amplification is found in several cancers (Chan, 2011). Our findings clarify this relationship in human cancer: centrosome amplification, though low in incidence, arises in the context of functional WT p53 that plays a crucial role in preventing widespread centrosome amplification. Our study thus supports the existence of a p53-dependent pathway preventing proliferation upon centrosome number deregulation (Ganem et al., 2014; Lambrus et al., 2015; Fava et al., 2017). Future work will be important to elucidate the mechanisms activating p53 upon centrosome amplification.

Our analysis at the single-cell level also revealed that despite the dynamic clonal evolution in BE progression (Reid et al., 2010; Weaver et al., 2014), centrosome amplification is never eliminated nor close to 100%. As centrosome amplification leads to genomic instability (Ganem et al., 2009; Silkworth et al., 2009), ability to invade (Godinho et al., 2014; Kushner et al., 2014), and non–cell-autonomous effects (Marusyk et al., 2014; Ganier et al., 2018), it does not have to be present in a high fraction of cells to impact tumor progression. This suggests cells with centrosome deregulation may be advantageous at the population level by promoting the fitness of the other cells.

Given widespread occurrence of p53 mutations and centrosome amplification in human tumors, our findings on the timing and ordering of these events and aneuploidy in BE tumorigenesis are likely to be extended to other cancers. Moreover, the clarification of the relationship between centrosome amplification and loss of p53 function suggests that this can be part of a wanting gene signature that predicts significant centrosome amplification in tumor samples. This could be useful to identify patients that will respond to centrosome-related inhibitors currently in clinical trials (Godinho and Pellman, 2014; Mason et al., 2014). Finally, the cell lines used in this study will be an excellent tool to get further insight into how supernumerary centrosomes arise and how they contribute to tumor progression, invasiveness, and metastasis.

Materials and methods

Patient selection and clinical samples

For the purpose of this study, three cohorts of patients were selected from the Pathology Department database of Instituto Português de Oncologia de Lisboa Francisco Gentil (IPOLFG). Cohort 1: biopsies from six BE patients included in the surveillance program, with metaplasia negative for dysplasia until the

moment of this study (in a followup from 1998–2012). An additional set of similar biopsies from another 22 BE patients was evaluated separately (Fig. S1 E). Cohort 2: five patients included in the surveillance program that were submitted to endoscopic resection or esophagectomy upon progression to high-grade dysplasia or adenocarcinoma. Cohort 3: 14 patients that when first examined already had adenocarcinoma and were submitted to esophagectomy (without neoadjuvant therapy). All formalin-fixed paraffin-embedded (FFPE) samples were selected not compromising future diagnostic studies. Areas of metaplasia, dysplasia, adenocarcinoma, and/or lymph node metastasis were selected. All cases were anonymized after a clinical record review for demographic data. Staging and grading were performed according to the American Joint Committee on Cancer staging system and the World Health Organization criteria, respectively (Amin et al., 2010; Bosman et al., 2010). As standards of comparison for normal squamous- and columnar-lined mucosa, respectively, the squamous-lined mucosa from the proximal margin of 14 total gastrectomies for gastric adenocarcinoma and the ileal mucosa from the proximal margin of 14 right-hemicolectomies for intestinal adenocarcinoma were used. Material from BE patients was obtained in the context of IPOLFG surveillance program and was used without compromising future patient management. All samples were routinely anonymized upon collection for the archival file, thus guaranteeing the privacy, confidentiality, and protection of patients and their personal data. This study was approved by the IPOLFG Research Council and Ethics committee.

Cell culture

Human telomerase-immortalized (hTERT) BAR-T and BAR-T10 cell lines derived from biopsies of patients with nondysplastic BE as well as BAR-T cell lines expressing the pSUPER-p53RNAi or the control empty vector pSUPER-retro.neo (all from R. Souza, Baylor University Medical Center, Dallas, TX; Jaiswal et al., 2007; Zhang et al., 2010) were cocultured with a fibroblast feeder layer (Swiss 3T3 cells [85022108; European Collection of Authenticated Cell Cultures] treated with 10 µg/ml mitomycin C [Sigma-Aldrich] for 2 h) and maintained in KBM2 medium (Lonza) supplemented with 5% FBS, 0.1 nM cholera toxin (Sigma-Aldrich), 70 µg/ml bovine pituitary extract (BPE; Sigma-Aldrich), 400 ng/ml hydrocortisone (Sigma-Aldrich), 20 ng/ml EGF, 20 µg/ml adenine (Sigma-Aldrich), 5 µg/ml insulin (Sigma-Aldrich), 5 µg/ml transferrin (Gibco), and 100 U/ml penicillin-streptomycin (Gibco). Cells were seeded in wells precoated with collagen IV (1 µg/cm^2; Sigma-Aldrich) for individual experiments. hTERT CP-B, CP-C, and CP-D cell lines derived from biopsies of patients with high-grade dysplasia (from P. Rabinovitch, University of Washington, Seattle, WA; Palanca-Wessels et al., 2003) were maintained in MCDB 153 medium (Sigma-Aldrich) supplemented with 5% FBS, 0.4 µg/ml hydrocortisone, 20 ng/ml EGF, 1 nM cholera toxin, 140 µg/ml BPE, 20 µg/ml adenine, 4 mM glutamine (Gibco), 0.1% insulin-transferrin-sodium selenite (Sigma-Aldrich), and 100 U/ml penicillin-streptomycin. Adenocarcinoma-derived cell lines ESO26, ESO51 (both established previously; Boonstra et al., 2010), OE19, OE33, FLO-1, SK-GT-4, OACP4, KYAE-1, and lymph node metastasis-derived cell line OACM5.1 (from W. Dinjens, Erasmus Medical Center Cancer Institute, Rotterdam, Netherlands) were grown in RPMI 1640 or in RPMI 1640–Ham's F12 (Kyae-1 cell line) supplemented with 10% FBS and 100 U/ml penicillin-streptomycin. The ESO51 cell line was derived from the tumor in case 8 from cohort 3 (Table S1). All cell lines have been recently validated (Boonstra et al., 2010). As standards of comparison for normal cells, we used hTERT normal esophageal epithelial cells (EPC2; from S. Godinho, Barts Cancer Institute, London, England, UK) as well as a common experimentally used nontransformed hTERT cell line derived from normal human RPE1. hTERT-ECP2 was grown in keratinocyte-serum-free medium with glutamine supplemented with EGF, BPE (Gibco), and 100 U/ml penicillin-streptomycin (Harada et al., 2003), and hTERT-RPE1 cells were grown in DMEM-F12 (Gibco) supplemented with sodium bicarbonate, 10% FBS, and 100 U/ml penicillin-streptomycin. All cells were grown at 37°C in a 5% CO_2 atmosphere and tested for the presence of mycoplasma.

IF microscopy

Tissue samples

From each FFPE block, 3-µm-thick tissue sections were transferred to positively charged glass slides and oven dried (70°C) for at least 1 h. Sections were then deparaffinized in xylene, placed in 100% ethanol, treated with 2% hydrogen peroxide in methanol solution for 10 min to block the endogenous peroxidase, and then washed in distilled water. Antigen retrieval was done in a pressure cooker in a 0.01-M sodium citrate–buffered solution, pH 6, for 6 min followed by incubation with a blocking buffer (TBS with 5% BSA) for 10 min at RT. Slides were then incubated with primary antibodies diluted in Bond primary antibody diluent (Leica Microsystems) with background-reducing components for 1 h at RT followed by washes in TBS before incubation with secondary antibodies for 30 min at 37°C. Slides were then washed extensively with TBS, dehydrated through gradient alcohols, and mounted in Vectashield with DAPI for DNA staining (Vector Laboratories).

Cell lines

Cells were grown on coverslips and were fixed with ice-cold methanol at −20°C for 10 min. Standard IF procedures involved blocking (30 min) and antibody incubations (overnight at 4°C for 1 h at RT) in PBS with 10% FBS, and washes were performed in PBS. Coverslips were mounted on glass slides in Vectashield with DAPI (Vector Laboratories). For DNA content analysis by IF, coverslips were incubated for 10 min in PBS with 1 µg/ml Hoechst 33342 (Invitrogen) before being mounted in Vectashield (Vector Laboratories).

Image acquisition

Images were obtained at RT using a T*i*-E inverted microscope (Nikon) with a Plan Apochromat VC 100× 1.40 NA oil objective, an ORCA ER2 charge-coupled device camera (Hamamatsu Photonics), and Nikon software or with an Eclipse T*i*-E (Nikon) microscope with a Plan Apochromat 100× 1.49 NA oil objective, an Evolve electron-multiplying charge-coupled device camera (Photometrics), and MetaMorph software (Molecular Devices). Images were acquired as a z series (0.2-µm z interval) and are

presented as maximum-intensity projections. Images were prepared using Photoshop (Adobe) and ImageJ (National Institutes of Health).

Antibodies

Primary antibodies used were against glutamylated tubulin (1:800 [tissue sections] and 1:500 [cell lines]; mouse; GT335; AdipoGen), pericentrin (1:250; rabbit; ab4448; Abcam), centrin (1:500; rabbit; N-17; Santa Cruz Biotechnology, Inc.), centrin (1:500; mouse; 20H5; EMD Millipore), A647-conjugated centrin (1:500; mouse; 20H5; EMD Millipore), γ-tubulin (1:500; mouse; GTU88; Sigma-Aldrich), α-tubulin (1:50; rat; YL1/2; AbD Serotec), p53 (1:100; mouse; DO-1; EMD Millipore), E-cadherin (1:30; rabbit; Cell Signaling Technology), and CP110 (1:250; rabbit; Jiang et al., 2012). The secondary antibodies FITC, Cy5, and rhodamine red (1:50 [tissue sections] and 1:200 [cell lines]; Jackson ImmunoResearch Laboratories, Inc.) as well as Alexa Fluor 488 and 647 (1:500 [cell lines]; Thermo Fisher Scientific) were also used.

Centrosome/centriole number and DNA content analysis by IF

Tissue samples

We used two markers that have robust staining in paraffin-embedded samples and that label the two structural components of the centrosome: the centrioles (marked by glutamylated tubulin [GT335]) and the PCM (marked by pericentrin). Centriole number was assessed by GT335 when it colocalized with pericentrin, thus identifying centrosomes. To achieve good staining and resolution at the cellular level, we used thin tissue samples (3 µm thick, as normally used in the clinic). Immunostaining of centrosomes was judged satisfactory when it was detected in the adjacent epithelium. The analysis was done taking into consideration the limitations derived from the specificities of working in FFPE samples: cellular truncation and cell overlapping. We first tested our accuracy of counting centrioles using GT335 marker with or without a costaining with a membrane marker (E-cadherin) and found that the background of GT335 staining was sufficient to distinguish cell limits and that the results obtained were similar. The counts were performed by going through all the z series acquired (see IF microscopy section) covering the whole depth of the section to assess the transversal and sagittal plans of each cell, thus identifying the transition to adjacent cells. Cells whose limits could not be clearly distinguished as well as cells overlapping with neighboring cells were not considered. To test for the occurrence of undercounting and overcounting related to the usage of histological sections, we did an extensive analysis in our standards of comparison for normal cells (14 ileum and 14 squamous) that were cut at the same thickness as all the other samples. Given that this analysis was performed in typically well-differentiated areas (i.e., not proliferative), the number of centrosomes expected per cell was one (with two centrioles). Whereas we detected an expected undercounting (cells with 0 centrioles), we never detected an overcounting (cells with more than two centrioles), suggesting that the method used to distinguish cell limits was robust. In each case, at least 200 countable cells with centrosomes were examined. Depending on the cell cycle stage, a cell either has one centrosome with two centrioles (G1) or two centrosomes with two centrioles each (S, G2, and M; Bettencourt-Dias et al., 2011). Because we did not use a cell cycle stage marker, only cells with more than four centrioles were considered to contain an abnormal centriole number content (centriole amplification).

Cell lines

Centrioles were considered when paired signals of two centriole markers (GT335, centrin, or CP110) were observed or when a centriole marker (centrin) colocalized with a PCM marker (γ-tubulin). For cell-by-cell centriole number and DNA content analysis in mitotic cells, sum projections of DNA staining (Hoechst) were used to determine total intensity of signal as measured by ImageJ software (National Institutes of Health). Total intensity was corrected according to the background intensity signal: corrected total cell fluorescence = integrated density – (area of selected cell × mean fluorescence of background readings). The number of cells and samples analyzed, number of experiments performed, and statistical analyses are detailed in the figure legends.

DNA extraction and p53 next-generation sequencing (NGS)

FFPE tissue sections (5 µm) were deparaffinized and counterstained with H&E. Metaplasia- and dysplasia-enriched areas were microdissected with a needle under pathologist's guidance. Total DNA was extracted with GeneRead DNA FFPE kit (QIAGEN) according to the manufacturer's instructions with a slight modification: proteinase K cell lysis at 56°C was performed overnight. DNA was eluted in 20 µl of elution buffer. To evaluate DNA concentration and integrity, DNA isolated from each sample was quantified in TapeStation 2200 using the Genomic DNA ScreenTape (Agilent Technologies). Because of the small amounts of extracted DNA from each sample area, DNA was precipitated according to the sodium acetate precipitation of small nuclei acids protocol (Thermo Fisher Scientific). Genomic DNA libraries were prepared using the Ion Ampliseq Library kit (2.0) as well as the community panel Ion Ampliseq TP53 and quantified by quantitative PCR with the Ion Library Quantification kit (Thermo Fisher Scientific). The emulsion PCR of amplified libraries was performed using Ion Chef (Thermo Fisher Scientific). Sequencing runs were performed with Ion personal machine using 316 Chips (Thermo Fisher Scientific) aiming for a mean sequencing depth coverage of 500×. With the exception of one sample where the amount of DNA was too low for robust analysis, we were able to sequence all coding exons of p53 by NGS in all paired samples.

Analysis of p53 by IHC

Analysis was performed as currently used to assess p53 in morphological lesions using tissue samples. Staining of p53 (1:150; mouse; DO-7; Cell Marque) was performed on either a fully automated IHC BOND III system (Leica Biosystems) using ER1 solution (15 min) for antigen retrieval and Novocastra bond polymer refine detection or on a Ventana Benchmark Ultra (Roche) using the CC1 solution (24 min) for antigen retrieval and an OptiView DAB IHC detection kit (Ventana). An expert pathologist qualitatively evaluated p53 immunostaining as WT, positive, or negative. WT expression: weak positivity similar to the observed in the normal native epithelium (internal control). Positive expression: the intensity of staining was graded as weak, moderate, or

intense compared with the native epithelium and as focal or diffuse according to the amount of positive cells (<10% vs. >10%). Negative expression: complete absence or only occasional scattered positive cells within a context of WT staining (metaplasia or native epithelium).

RNAi, transfection, and drug treatment

Endogenous *TP53* was depleted using siRNA oligonucleotides (5′-GGGAGTTGTCAAGTCTCTG-3′; Sigma-Aldrich) targeting the 3′ UTR region. The *TP53* gene was alternatively depleted using other siRNA oligonucleotides: *TP53*[1] (sc-29435; Santa Cruz Biotechnology, Inc.) or *TP53*[2] (5′-GACTCCAGTGGTAATCTAC-3′; Sigma-Aldrich; same sequence as in BAR-T–pSUPER-p53RNAi cell line [Brummelkamp et al., 2002]). Luciferase (*GL2*) siRNA (5′-CGTACGCGGAATACTTCGA-3′; Takara Bio Inc.) was used as a control. Cells were transfected with 50 nM siRNA for 72 h using Lipofectamine RNAiMAX (Thermo Fisher Scientific). For S phase arrest, 16 h after siRNA treatment, cells were treated with 4 mM hydroxyurea (Sigma-Aldrich) for 48 h. Transient plasmid transfections were performed with Lipofectamine LTX (Invitrogen) according to the manufacturer's instructions 16 h after siRNA transfection and were analyzed after 48 h. p53 constructs were obtained from Addgene (Baker et al., 1990).

Cell lysis, SDS-PAGE, and Western blotting (WB)

Cells were harvested and pelleted before snap freezing in liquid nitrogen. Cell lysates were prepared by resuspending pellets in lysis buffer (50 mM Hepes, pH 7.4, 100 mM KCl, 1 mM EGTA, 1 mM $MgCl_2$, 10% glycerol, 0.05% NP-40, 1× protease inhibitor cocktail, and 1× phosphatase inhibitor cocktail) for 10 min on ice. Lysates were then centrifuged for 10 min at 14,000 rpm at 4°C, and protein concentration of the cleared supernatant was determined by Bradford assay. Laemmli buffer was added to the samples to 1× and then boiled at 99°C for 5 min before analysis on polyacrylamide gels. Standard WB procedures involved blocking in TBS supplemented with 5% milk powder and 1% milk powder in TBS-T (0.1% Tween-20 in TBS) for antibody incubations, and washes were performed in TBS-T. Primary antibodies were against p53 (1:1,000; mouse) and GAPDH (1:1,000; rabbit; 14C10; Cell Signaling Technology). IRDye secondary antibodies were used at 1:10,000 and were purchased from Odyssey and LI-COR Biosciences.

Cell cycle phase distribution and DNA content analysis by flow cytometry

Cells were harvested, pelleted, and washed in 1× PBS before being fixed in 70% ice-cold ethanol and kept on ice for 30 min. After washes with 1× PBS, cells were resuspended in 1× PBS with 100 µg/ml RNase A (QIAGEN) and 100 µg/ml propidium iodide (Sigma-Aldrich) and incubated at 37°C for 30 min in the dark. Cells were then analyzed with FACScan (BD).

Online supplemental material

Fig. S1 shows analysis of centriole numbers in patient samples. Fig. S2 shows analysis of p53 status in patient samples by IHC. Fig. S3 shows centriole number and ploidy in cell lines. Table S1 shows centriole number analysis in paraffin-embedded tissue. Table S2 shows analysis of p53 status. Table S3 shows cell line information and centriole analysis.

Acknowledgments

We thank S. Esteves (IPOLFG) for statistical analysis and the M. Bettencourt-Dias laboratory members A. Fry, S. Godinho, R. Souza, S. Spechler, F. Janody, L. David, A. Holland, and C. Martins for useful discussion. We are grateful to W. Dinjens, R. Souza, S. Godinho, and P. Rabinovitch for cell lines.

This work was funded by Fundação para a Ciência e a Tecnologia–Harvard Medical School Program Portugal (HMSP-CT/SAU-ICT/0075/2009), Liga Portuguesa Contra o Cancro, European Molecular Biology Organization Installation, and Sociedade Portuguesa de Gastroenterologia.

The authors declare no competing financial interests.

Authors contributions: C.A.M. Lopes and M. Mesquita designed and performed experiments, analyzed and interpreted data, and wrote the manuscript. A.I. Cunha, S. Carapeta, C. Laranjeira, and A.E. Pinto performed experiments. J. Cardoso designed and performed experiments and analyzed and interpreted data. J.B. Pereira-Leal discussed experimental design. A. Dias-Pereira discussed experimental design and edited the manuscript. M. Bettencourt-Dias and P. Chaves discussed experimental design, interpreted and discussed the data, and edited the manuscript.

Submitted: 1 December 2017
Revised: 7 April 2018
Accepted: 17 April 2018

References

Amin, M.B., S. Edge, F. Greene, D.R. Byrd, R.K. Brookland, M.K. Washington, J.E. Gershenwald, C.C. Compton, K.R. Hess, D.C. Sullivan, et al. 2010. AJCC Cancer Staging Manual. Sixth edition. Springer, New York. 1032 pp.

Baker, S.J., S. Markowitz, E.R. Fearon, J.K.V. Willson, and B. Vogelstein. 1990. Suppression of human colorectal carcinoma cell growth by wild-type p53. *Science.* 249:912–915. https://doi.org/10.1126/science.2144057

Bettencourt-Dias, M., F. Hildebrandt, D. Pellman, G. Woods, and S.A. Godinho. 2011. Centrosomes and cilia in human disease. *Trends Genet.* 27:307–315. https://doi.org/10.1016/j.tig.2011.05.004

Bian, Y.S., M.C. Osterheld, F.T. Bosman, J. Benhattar, and C. Fontolliet. 2001. p53 gene mutation and protein accumulation during neoplastic progression in Barrett's esophagus. *Mod. Pathol.* 14:397–403. https://doi.org/10.1038/modpathol.3880324

Boonstra, J.J., R. van Marion, D.G. Beer, L. Lin, P. Chaves, C. Ribeiro, A.D. Pereira, L. Roque, S.J. Darnton, N.K. Altorki, et al. 2010. Verification and unmasking of widely used human esophageal adenocarcinoma cell lines. *J. Natl. Cancer Inst.* 102:271–274. https://doi.org/10.1093/jnci/djp499

Bornens, M. 2012. The centrosome in cells and organisms. *Science.* 335:422–426. https://doi.org/10.1126/science.1209037

Bosman, F.T., F. Carneiro, R.H. Hruban, and N.D. Theise. 2010. WHO Classification of Tumours of the Digestive System. Fourth edition. WHO press, Geneva, Switzerland. 417 pp.

Brummelkamp, T.R., R. Bernards, and R. Agami. 2002. A system for stable expression of short interfering RNAs in mammalian cells. *Science.* 296:550–553. https://doi.org/10.1126/science.1068999

Chan, J.Y. 2011. A clinical overview of centrosome amplification in human cancers. *Int. J. Biol. Sci.* 7:1122–1144. https://doi.org/10.7150/ijbs.7.1122

Chaves, P., M. Crespo, C. Ribeiro, C. Laranjeira, A.D. Pereira, A. Suspiro, P. Cardoso, C.N. Leitão, and J. Soares. 2007. Chromosomal analysis of Barrett's cells: demonstration of instability and detection of the metaplastic lineage involved. *Mod. Pathol.* 20:788–796. https://doi.org/10.1038/modpathol.3800787

Coelho, P.A., L. Bury, M.N. Shahbazi, K. Liakath-Ali, P.H. Tate, S. Wormald, C.J. Hindley, M. Huch, J. Archer, W.C. Skarnes, et al. 2015. Over-expression of Plk4 induces centrosome amplification, loss of primary cilia and associated tissue hyperplasia in the mouse. *Open Biol.* 5:150209. https://doi.org/10.1098/rsob.150209

Cuomo, M.E., A. Knebel, N. Morrice, H. Paterson, P. Cohen, and S. Mittnacht. 2008. p53-Driven apoptosis limits centrosome amplification and genomic instability downstream of NPM1 phosphorylation. *Nat. Cell Biol.* 10:723–730. https://doi.org/10.1038/ncb1735

Davoli, T., and T. de Lange. 2011. The causes and consequences of polyploidy in normal development and cancer. *Annu. Rev. Cell Dev. Biol.* 27:585–610. https://doi.org/10.1146/annurev-cellbio-092910-154234

Del Portillo, A., S.M. Lagana, Y. Yao, T. Uehara, N. Jhala, T. Ganguly, P. Nagy, J. Gutierrez, A. Luna, J. Abrams, et al. 2015. Evaluation of mutational testing of preneoplastic Barrett's mucosa by next-generation sequencing of formalin-fixed, paraffin-embedded endoscopic samples for detection of concurrent dysplasia and adenocarcinoma in Barrett's esophagus. *J. Mol. Diagn.* 17:412–419. https://doi.org/10.1016/j.jmoldx.2015.02.006

Fava, L.L., F. Schuler, V. Sladky, M.D. Haschka, C. Soratroi, L. Eiterer, E. Demetz, G. Weiss, S. Geley, E.A. Nigg, and A. Villunger. 2017. The PIDDosome activates p53 in response to supernumerary centrosomes. *Genes Dev.* 31:34–45. https://doi.org/10.1101/gad.289728.116

Fitzgerald, R.C., M. di Pietro, K. Ragunath, Y. Ang, J.-Y. Kang, P. Watson, N. Trudgill, P. Patel, P.V. Kaye, S. Sanders, et al. British Society of Gastroenterology. 2014. British Society of Gastroenterology guidelines on the diagnosis and management of Barrett's oesophagus. *Gut.* 63:7–42. https://doi.org/10.1136/gutjnl-2013-305372

Ganem, N.J., S.A. Godinho, and D. Pellman. 2009. A mechanism linking extra centrosomes to chromosomal instability. *Nature.* 460:278–282. https://doi.org/10.1038/nature08136

Ganem, N.J., H. Cornils, S.Y. Chiu, K.P. O'Rourke, J. Arnaud, D. Yimlamai, M. Théry, F.D. Camargo, and D. Pellman. 2014. Cytokinesis failure triggers hippo tumor suppressor pathway activation. *Cell.* 158:833–848. https://doi.org/10.1016/j.cell.2014.06.029

Ganier, O., D. Schnerch, P. Oertle, R.Y.H. Lim, M. Plodinec, and E.A. Nigg. 2018. Structural centrosome aberrations promote non-cell-autonomous invasiveness. *EMBO J.* 37:e98576. https://doi.org/10.15252/embj.201798576

Gleeson, C.M., J.M. Sloan, J.A. McGuigan, A.J. Ritchie, and S.E.H. Russell. 1995. Base transitions at CpG dinucleotides in the p53 gene are common in esophageal adenocarcinoma. *Cancer Res.* 55:3406–3411.

Gleeson, C.M., J.M. Sloan, D.T. McManus, P. Maxwell, K. Arthur, J.A. McGuigan, A.J. Ritchie, and S.E.H. Russell. 1998. Comparison of p53 and DNA content abnormalities in adenocarcinoma of the oesophagus and gastric cardia. *Br. J. Cancer.* 77:277–286. https://doi.org/10.1038/bjc.1998.44

Godinho, S.A., and D. Pellman. 2014. Causes and consequences of centrosome abnormalities in cancer. *Philos. Trans. R. Soc. Lond. B Biol. Sci.* 369:20130467. https://doi.org/10.1098/rstb.2013.0467

Godinho, S.A., R. Picone, M. Burute, R. Dagher, Y. Su, C.T. Leung, K. Polyak, J.S. Brugge, M. Théry, and D. Pellman. 2014. Oncogene-like induction of cellular invasion from centrosome amplification. *Nature.* 510:167–171. https://doi.org/10.1038/nature13277

Haggitt, R.C. 1994. Barrett's esophagus, dysplasia, and adenocarcinoma. *Hum. Pathol.* 25:982–993. https://doi.org/10.1016/0046-8177(94)90057-4

Hamelin, R., J.-F. Fléjou, F. Muzeau, F. Potet, P. Laurent-Puig, F. Fékété, and G. Thomas. 1994. TP53 gene mutations and p53 protein immunoreactivity in malignant and premalignant Barrett's esophagus. *Gastroenterology.* 107:1012–1018. https://doi.org/10.1016/0016-5085(94)90225-9

Harada, H., H. Nakagawa, K. Oyama, M. Takaoka, C.D. Andl, B. Jacobmeier, A. von Werder, G.H. Enders, O.G. Opitz, and A.K. Rustgi. 2003. Telomerase induces immortalization of human esophageal keratinocytes without p16INK4a inactivation. *Mol. Cancer Res.* 1:729–738.

Holland, A.J., D. Fachinetti, Q. Zhu, M. Bauer, I.M. Verma, E.A. Nigg, and D.W. Cleveland. 2012. The autoregulated instability of Polo-like kinase 4 limits centrosome duplication to once per cell cycle. *Genes Dev.* 26:2684–2689. https://doi.org/10.1101/gad.207027.112

Hvid-Jensen, F., L. Pedersen, A.M. Drewes, H.T. Sørensen, and P. Funch-Jensen. 2011. Incidence of adenocarcinoma among patients with Barrett's esophagus. *N. Engl. J. Med.* 365:1375–1383. https://doi.org/10.1056/NEJMoa1103042

Jaiswal, K.R., C.P. Morales, L.A. Feagins, K.G. Gandia, X. Zhang, H.Y. Zhang, K. Hormi-Carver, Y. Shen, F. Elder, R.D. Ramirez, et al. 2007. Characterization of telomerase-immortalized, non-neoplastic, human Barrett's cell line (BAR-T). *Dis. Esophagus.* 20:256–264. https://doi.org/10.1111/j.1442-2050.2007.00683.x

Jiang, K., G. Toedt, S. Montenegro Gouveia, N.E. Davey, S. Hua, B. van der Vaart, I. Grigoriev, J. Larsen, L.B. Pedersen, K. Bezstarosti, et al. 2012. A Proteome-wide screen for mammalian SxIP motif-containing microtubule plus-end tracking proteins. *Curr. Biol.* 22:1800–1807. https://doi.org/10.1016/j.cub.2012.07.047

Kaye, P.V., S.A. Haider, P.D. James, I. Soomro, J. Catton, S.L. Parsons, K. Ragunath, and M. Ilyas. 2010. Novel staining pattern of p53 in Barrett's dysplasia--the absent pattern. *Histopathology.* 57:933–935. https://doi.org/10.1111/j.1365-2559.2010.03715.x

Kushner, E.J., L.S. Ferro, J.Y. Liu, J.R. Durrant, S.L. Rogers, A.C. Dudley, and V.L. Bautch. 2014. Excess centrosomes disrupt endothelial cell migration via centrosome scattering. *J. Cell Biol.* 206:257–272. https://doi.org/10.1083/jcb.201311013

Lambrus, B.G., Y. Uetake, K.M. Clutario, V. Daggubati, M. Snyder, G. Sluder, and A.J. Holland. 2015. p53 protects against genome instability following centriole duplication failure. *J. Cell Biol.* 210:63–77. https://doi.org/10.1083/jcb.201502089

Levine, M.S., B. Bakker, B. Boeckx, J. Moyett, J. Lu, B. Vitre, D.C. Spierings, P.M. Lansdorp, D.W. Cleveland, D. Lambrechts, et al. 2017. Centrosome Amplification Is Sufficient to Promote Spontaneous Tumorigenesis in Mammals. *Dev. Cell.* 40:313–322.e5. https://doi.org/10.1016/j.devcel.2016.12.022

Marthiens, V., M.A. Rujano, C. Pennetier, S. Tessier, P. Paul-Gilloteaux, and R. Basto. 2013. Centrosome amplification causes microcephaly. *Nat. Cell Biol.* 15:731–740. https://doi.org/10.1038/ncb2746

Marusyk, A., D.P. Tabassum, P.M. Altrock, V. Almendro, F. Michor, and K. Polyak. 2014. Non-cell-autonomous driving of tumour growth supports sub-clonal heterogeneity. *Nature.* 514:54–58. https://doi.org/10.1038/nature13556

Mason, J.M., D.C. Lin, X. Wei, Y. Che, Y. Yao, R. Kiarash, D.W. Cescon, G.C. Fletcher, D.E. Awrey, M.R. Bray, et al. 2014. Functional characterization of CFI-400945, a Polo-like kinase 4 inhibitor, as a potential anticancer agent. *Cancer Cell.* 26:163–176. https://doi.org/10.1016/j.ccr.2014.05.006

McDermott, K.M., J. Zhang, C.R. Holst, B.K. Kozakiewicz, V. Singla, and T.D. Tlsty. 2006. p16INK4a prevents centrosome dysfunction and genomic instability in primary cells. *PLoS Biol.* 4:350–365. https://doi.org/10.1371/journal.pbio.0040051

Muller, P.A.J., and K.H. Vousden. 2014. Mutant p53 in cancer: new functions and therapeutic opportunities. *Cancer Cell.* 25:304–317. https://doi.org/10.1016/j.ccr.2014.01.021

Noll, J.E., J. Jeffery, F. Al-Ejeh, R. Kumar, K.K. Khanna, D.F. Callen, and P.M. Neilsen. 2012. Mutant p53 drives multinucleation and invasion through a process that is suppressed by ANKRD11. *Oncogene.* 31:2836–2848. https://doi.org/10.1038/onc.2011.456

Palanca-Wessels, M.C.A., A. Klingelhutz, B.J. Reid, T.H. Norwood, K.E. Opheim, T.G. Paulson, Z. Feng, and P.S. Rabinovitch. 2003. Extended lifespan of Barrett's esophagus epithelium transduced with the human telomerase catalytic subunit: a useful in vitro model. *Carcinogenesis.* 24:1183–1190. https://doi.org/10.1093/carcin/bgg076

Paulson, T.G., C.C. Maley, X. Li, H. Li, C.A. Sanchez, D.L. Chao, R.D. Odze, T.L. Vaughan, P.L. Blount, and B.J. Reid. 2009. Chromosomal instability and copy number alterations in Barrett's esophagus and esophageal adenocarcinoma. *Clin. Cancer Res.* 15:3305–3314. https://doi.org/10.1158/1078-0432.CCR-08-2494

Petitjean, A., E. Mathe, S. Kato, C. Ishioka, S.V. Tavtigian, P. Hainaut, and M. Olivier. 2007. Impact of mutant p53 functional properties on TP53 mutation patterns and tumor phenotype: lessons from recent developments in the IARC TP53 database. *Hum. Mutat.* 28:622–629. https://doi.org/10.1002/humu.20495

Reid, B.J., X. Li, P.C. Galipeau, and T.L. Vaughan. 2010. Barrett's oesophagus and oesophageal adenocarcinoma: time for a new synthesis. *Nat. Rev. Cancer.* 10:87–101. https://doi.org/10.1038/nrc2773

Rivlin, N., R. Brosh, M. Oren, and V. Rotter. 2011. Mutations in the p53 Tumor Suppressor Gene: Important Milestones at the Various Steps of Tumorigenesis. *Genes Cancer.* 2:466–474. https://doi.org/10.1177/1947601911408889

Ross-Innes, C.S., J. Becq, A. Warren, R.K. Cheetham, H. Northen, M. O'Donovan, S. Malhotra, M. di Pietro, S. Ivakhno, M. He, et al. 2015. Whole-genome sequencing provides new insights into the clonal architecture of Barrett's esophagus and esophageal adenocarcinoma. *Nat. Genet.* 47:1038–1046. https://doi.org/10.1038/ng.3357

Schouten, L.J., J. Steevens, C.J.R. Huysentruyt, C.E. Coffeng, Y.C.A. Keulemans, F.E. van Leeuwen, A.L.C. Driessen, and P.A. van den Brandt. 2011. Total cancer incidence and overall mortality are not increased among

patients with Barrett's esophagus. *Clin. Gastroenterol. Hepatol.* 9:754–761. https://doi.org/10.1016/j.cgh.2011.04.008

Serçin, Ö., J.-C. Larsimont, A.E. Karambelas, V. Marthiens, V. Moers, B. Boeckx, M. Le Mercier, D. Lambrechts, R. Basto, and C. Blanpain. 2016. Transient PLK4 overexpression accelerates tumorigenesis in p53-deficient epidermis. *Nat. Cell Biol.* 18:100–110. https://doi.org/10.1038/ncb3270

Silkworth, W.T., I.K. Nardi, L.M. Scholl, and D. Cimini. 2009. Multipolar spindle pole coalescence is a major source of kinetochore mis-attachment and chromosome mis-segregation in cancer cells. *PLoS One.* 4:e6564. https://doi.org/10.1371/journal.pone.0006564

Spechler, S.J., P. Sharma, R.F. Souza, J.M. Inadomi, and N.J. Shaheen. American Gastroenterological Association. 2011. American Gastroenterological Association Technical Review on the Management of Barrett's Esophagus. *Gastroenterology.* 140:1084–1091. https://doi.org/10.1053/j.gastro.2011.01.031

Stachler, M.D., A. Taylor-Weiner, S. Peng, A. McKenna, A.T. Agoston, R.D. Odze, J.M. Davison, K.S. Nason, M. Loda, I. Leshchiner, et al. 2015. Paired exome analysis of Barrett's esophagus and adenocarcinoma. *Nat. Genet.* 47:1047–1055. https://doi.org/10.1038/ng.3343

Tarapore, P., Y. Tokuyama, H.F. Horn, and K. Fukasawa. 2001. Difference in the centrosome duplication regulatory activity among p53 'hot spot' mutants: potential role of Ser 315 phosphorylation-dependent centrosome binding of p53. *Oncogene.* 20:6851–6863. https://doi.org/10.1038/sj.onc.1204848

Thompson, S.L., and D.A. Compton. 2010. Proliferation of aneuploid human cells is limited by a p53-dependent mechanism. *J. Cell Biol.* 188:369–381. https://doi.org/10.1083/jcb.200905057

Weaver, J.M.J., C.S. Ross-Innes, N. Shannon, A.G. Lynch, T. Forshew, M. Barbera, M. Murtaza, C.-A.J. Ong, P. Lao-Sirieix, M.J. Dunning, et al. OCCAMS consortium. 2014. Ordering of mutations in preinvasive disease stages of esophageal carcinogenesis. *Nat. Genet.* 46:837–843. https://doi.org/10.1038/ng.3013

Wong, Y.L., J.V. Anzola, R.L. Davis, M. Yoon, A. Motamedi, A. Kroll, C.P. Seo, J.E. Hsia, S.K. Kim, J.W. Mitchell, et al. 2015. Reversible centriole depletion with an inhibitor of Polo-like kinase 4. *Science.* 348:1155–1160. https://doi.org/10.1126/science.aaa5111

Zhang, X., C. Yu, K. Wilson, H.Y. Zhang, S.D. Melton, X. Huo, D.H. Wang, R.M. Genta, S.J. Spechler, and R.F. Souza. 2010. Malignant transformation of non-neoplastic Barrett's epithelial cells through well-defined genetic manipulations. *PLoS One.* 5:1–11. https://doi.org/10.1371/journal.pone.0013093

CHAPTER 4:
General Discussion

As of today, management of Barrett's esophagus disease continues to be a real challenge for medical societies.[251] Despite the tremendous advances towards the understanding of BE pathogenesis and carcinogenesis, the mechanisms underlying BE malignant progression remain ill-defined and somewhat puzzling. This translates into the lack of biomarkers guiding clinical decisions regarding BE diagnosis, prognosis and treatment.

4.1 Cyr61 and TAZ are early predictors of BE progression: "a light at the end of the tunnel"

The paradigm in BE surveillance is that the vast majority of the patients will not develop cancer. Nevertheless, for those that will progress the consequences could be fatal if not detected at an early stage. As a result, all patients undergo periodic endoscopies with biopsies, even if to most of these patients this will prove to be an excessive procedure. The surveillance of these patients is therefore not only problematic but also highly questionable, and so the assessment of the magnitude of cancer risk in BE patients has important clinical and economic impact. Notwithstanding all the efforts in biomarkers discovery, current practice has been hampered by the lack of tools able to predict which BE patients are at increased risk of progression. Identification of early and objective biomarkers that enable BE risk stratification would direct endoscopy surveillance to high-risk patients to prevent EA, would reduce health care costs, and ultimately improve BE patient's quality of life.

In this part of the project, we set out to identify early molecular biomarkers predictive of BE progression to malignancy that could be easily translated to the clinical setting to identify the BE patients with a higher risk of cancer development. By doing this, I also aimed to contribute to a better understanding of BE disease through the investigation of novel pathways that could be involved in BE neoplastic transformation.

4.1.1 "Hit the mark" in biomarkers discovery: old data, new look, and stringent criteria

We anticipated that based on gene expression levels, BE patients could be stratified as having a high or low risk of progression to cancer. We applied an innovative bioinformatics framework to public gene transcriptomics datasets to directly compare never-dysplastic BE to BE adjacent to EA (see page 60, Fig1). Merging distinct and heterogeneous datasets could originate noisy predictions. So, *in silico* strategy consisted in using a differential expression analysis approach to search for genes that are differently expressed between the two groups. The list of candidate genes obtained was further submitted to a barcode analysis against a database of human gene expression patterns to binarize the expression of each gene (expressed vs. not expressed), which further restricted the selected candidate genes. The expression barcodes obtained are very

robust against random sources of noise because the cutoffs values are calculated using as reference large amounts of annotated public data. As a final step to select the candidate genes, the output of this pipeline was submitted to a manual literature curation in which we use knowledge-driven biomarker prioritization criteria considering that filtered genes must have biological functions linked to functions potentially relevant for BE malignant progression and have previously been associated with cancer progression to other tumors. This approach allowed trimming de candidates to the two most significant ones. This discovery pipeline allowed us to identify: i) genes that are differentially expressed in BE between progressors and non-progressors; ii) an expression profile associated with BE malignant transformation; and iii) the most significant genes among the over-expressed candidates, the CYR61 and TAZ genes (see page 141, Fig S1).

We then designed a retrospective case-control study using a stringent set of criteria (discussed below) to select a strong validation cohort of patients and the two candidates were validated using to complementary approaches: qRT-PCR and IHC. Although qRT-PCR is a highly sensitive and specific method already validated for diagnostic purposes in FFPE samples, it involves the use of specific equipment and technical expertise that is not widely available in all pathology laboratories. Another restraining factor is the amount of sample needed to do this technique considering that biopsies have a limited quantity of material available. Furthermore, BE areas are often intermingled with squamous epithelium being necessary to needle micro dissect BE for RNA extraction, which is technical demanding and not practical in a daily basis. On the other hand, IHC is a method not limited by the quantity of material and allows the evaluation of protein expression derived from molecular abnormalities in intact histological morphology. It is already used for decades as an adjunct for diagnosis, prognosis, and therapeutics, involving mastery in histopathology coupled with pathobiology that constitutes the expertise of anatomic pathology practice. Given the low costs, low turnaround time and easily applicability of this technique, IHC could be considered ideal as a tool to work in FFPE samples that are the base for morphologic diagnosis and surveillance of BE disease. For these reasons, IHC biomarkers have advantages and are more easily applicable when compared to molecular biomarkers. All in all, the strategy followed in this study can be considered unique and the first, to our knowledge, to overcome several limitations of previous studies and meet several requirements acknowledged as imperative for early predictive biomarkers discovery.

Validation with qPCR and IHC not only confirmed the in-silico predictions, but it also revealed that CYR61 and TAZ are upregulated and overexpressed in non-dysplastic BE index biopsies from progressors years before the development of HGD/EA (see page 62, Fig2). Although both qPCR and IHC data independently showed a significant difference between progressors and non-progressors from the index biopsies to the second timepoint, we did not observe a clear correlation between the results of both methodologies within the same patient. This could be explained by inherent differences between qPCR and IHC. While qPCR quantifies mRNA levels and is not observer dependent, IHC evaluates protein expression levels qualitatively, which

could introduce some inter-observer bias. Moreover, whereas for the qPCR analysis the sample was enriched by microdissection, the assessment of IHC staining was done by visual selection of BE areas. Nevertheless, and despite these differences, both CYR61 and TAZ were validated as risk stratification biomarkers in FFPE samples using IHC, a practical methodology with low costs. Indeed, the specific and interpretable CYR61 and TAZ immunostaining obtained allowed us to establish a qualitative scoring system. Moreover, given that both CYR61 and TAZ overexpression levels appeared to be dispersed and not focal, we found that their analysis was not dependent on biopsy sampling. This makes this interpretation easier in the clinical setting since at non-dysplastic BE stage all the available samples are biopsies. The possibility of assessing these markers using such practical methodology makes CYR61 and TAZ two biomarkers with great promise of clinical utility. This constitutes a great advantage in comparison to the great majority of previous studies in which biomarkers research was done in fresh frozen biopsies specimens that are not normally collected for diagnostic purposes, and are therefore not a practical and readily available option outside the academic and research centers.[206, 249, 365-368].

The selection criteria used to identify BE patients for inclusion in validation cohorts is a key factor in biomarkers research and it has been recognized as suboptimal and with several flaws in the majority of studies centered in finding markers of neoplastic progression in BE.[364] The rigorous and strict selection criteria used in our study allowed us to overcome several limitations identified in previous studies. First, and despite the small number of cases derived from the recognized low rates of cancer progression among BE patients, the use of index biopsy samples that tell the story about the molecular events occurring in BE years before the appearance of dysplasia makes this a rare and precious cohort that can be considered determinant in finding early predictive biomarkers. This contrasts with some of the first published biomarkers associated with a higher risk of progression that were discovered in BE from patients with dysplasia or EA and therefore in a time point where neoplasia is already established, which is not ideal if the goal is to identify early biomarkers able to predict cancer development.[369-372] In that context it is difficult, or even impossible, to demonstrate that these molecular alterations in BE really precede tumor initiation and are not the result of a cancer field effect, a phenomena already identified in non-cancer tissues that are adjacent to neoplasias and also have already been described in BE.[373]

Trough the evaluation of CYR61 and TAZ levels in non-dysplastic BE-index biopsies from progressors and non-progressors by qPCR we could determine that upregulation of these proteins is an early molecular alteration in patients that latter on will progress to cancer and are not a cancer field effect. Furthermore, and despite the small number of progressors, this cohort provided reproducibility and accuracy while excluding the inter-patient variability obtained when different sets of patients are used in each stage of BE malignant pathway. Second, we ensured that biopsy sampling was done strictly according to Seattle protocol. Not only was the quality of baseline sampling and non-dysplastic BE diagnosis ensured for all patients, but also

the diagnosis of HGD/EA in the progressors group was evaluated by two independent pathologists and confirmed in mucosectomies or esophagectomy specimens. This is in striking contrast with several studies that included in the progressors group patients with a diagnosis of HGD/EA accessed by a single pathologist in a single biopsy collected from only one endoscopy.[206, 365, 366] Considering the challenges and consequent inter-observer variability associated with this diagnosis, it is possible that some of these patients could have been over-diagnosed and thus potentially not real progressors. Third, it was also important to consider a minimum surveillance interval between index BE and HGD/EA diagnosis to exclude or minimize the odds of including patients with prevalent HGD/EA at baseline. When patients that are in follow up are diagnosed with EA at an advanced stage at the time of progression, it is not possible to exclude the existence of prevalent cancer in previous biopsies that was not detected due to sampling errors, and in that sense these cases should not be considered for inclusion in progressors cohorts. In our cohort, all patients included in this cohort had an index biopsy negative for dysplasia and a second biopsy also negative for dysplasia performed at least one year after the index biopsy. So, the surveillance period between BE diagnosis and malignant progression was more than two years for all those patients, with one exception that was 1.5 year and which was not excluded since the stage at diagnosis of progression was the earliest in TNM classification.

To ensure the quality of baseline sampling and diagnosis, our progressors group did not include patients with advanced cancer and for all the TNM grading was T1N0Mx. Our cohort was thus designed using more stringent criteria than previous studies that either did not considered a minimum surveillance interval between the index biopsy and time of progression[249], or only excluded patients with a period inferior to 6 months between these two time points [374, 375]. Additionally, most studies did not exclude patients with advanced EA at the time of progression[206, 365, 366, 374, 375] and none, to this date, have used as a selection criterion the quality of biopsy baseline sampling [206, 249, 365-368, 374, 375]. Finally, another point that we considered relevant, and that was not taken in account in some prior studies, was to differentiate BE from LGD in both progressors and non-progressors groups.[367, 368] Here, we excluded patients with LGD at baseline biopsy from the study. BE and LGD are different biological entities and constitute two different steps in BE malignant pathway. In fact, patients with LGD have a significantly higher risk of progression than patients with non-dysplastic BE, and therefore should not be included together since this will change the outcomes in biomarkers validation.[364]

In the end, and as in the majority of previous BE biomarker studies, we were not able to overcome the challenge of having a large amount of progressors. Despite the 30 years of existence of the Instituto Português de Oncologia Francisco Gentil (IPOFG) surveillance program with a cohort of 331 non-dysplastic BE patients, we were only able to select 9 patients with index samples negative for dysplasia and with follow-up samples of progression to HGD/EA during surveillance. We were not able to obtain samples from other national and

international hospitals that strictly accomplish our inclusion criteria. Indeed, considering the above limitations and compared with the several international cohorts reviewed by the British Society of Gastroenterology guidelines our cohort is quite representative.[10] Still, we recognized that greater sample numbers are needed in future studies to further validate CYR61 and TAZ as predictive biomarkers. Moreover, since upregulation of these markers was only determined by assessing its levels in progressors versus non-progressors, it will also be important in the future to establish a cutoff value for their expression levels that can clearly detect the patients with an increased risk of malignant progression. Recently, a large community-based case-control, the Amsterdam ReBus progressor cohort, was designed to overcome the challenge of inadequate sample sizes and to constitute the starting point for future biomarker validation studies[364], thus opening the opportunity for future collaborations. The ultimate goal would be to organize a prospective study in which these two markers could be integrated in a larger panel (with other molecular biomarkers and/or clinical risk factors) to assess cancer risk in BE patients.

Taken together, our results support that CYR61 and TAZ are promising early biomarkers with predictive value that could be supervised right from the beginning, in non-dysplastic BE index biopsies, to distinguish which BE patients have a higher risk of progression to dysplasia/cancer. Importantly, our work emphasizes that these molecular alterations can be identified using current methodology that is accessible in the clinical setting. This provides the ideal scenario to revolutionize the paradigm in BE surveillance and management towards a swift from curative to preventive medicine, opening the opportunity to objectively assess the individual cancer risk in each BE patient and to act before malignant progression. With the aid of early biomarkers such as the ones identified in this study it will be possible to decide between early ablation for high-risk patients (non-dysplastic BE with an abnormal molecular profile) and extended surveillance intervals or even exclusion from surveillance for those with low risk BE.

4.1.2 Cyr61 and TAZ as clues to unravel novel mechanisms operating in BE progression: “one more piece of the puzzle”

By highlighting that CYR61 and TAZ overexpression are very early events in patients progressing to cancer, our study opened new perspectives about the comprehension of BE disease, revealing that molecular alterations prone for malignant progression can occur at very early stages in the metaplastic process. We therefore investigated the functional context of these markers in BE carcinogenesis.

Both CYR61 and TAZ were already associated with tumorigenesis and cancer progression in several other neoplasias.[376, 377] Cysteine-rich angiogenic inducer 61 (CYR61) is an extracellular matrix protein that belongs to the CCN (CYR61, CGTF and NOV) family, a group of secreted proteins that function as a central hub for stromal-epithelial communication[378], thereby modulating a multitude of biological processes such as cellular adhesion, migration, differentiation, proliferation, survival, extracellular matrix synthesis and angiogenesis.[379-381]

Accordingly, CYR61 emerged as a multifunctional protein that plays crucial roles in skeletal and cardiovascular development during embryonic stage, being also essential in the regulation of several processes in adulthood such as wound healing, tissue repair, inflammation, fibrogenesis and mechanical stress response.[376, 378, 382] CYR61 overexpression was already identified in a broad range of cancers and clinical analysis revealed that CYR61 levels significantly correlate with tumor size, stage and grade, recurrence, lymph node involvement and distant metastasis, as it was shown for gliomas [383], osteosarcoma [384, 385], breast [386, 387], gastric [388], ovarian [389, 390] and squamous cell carcinomas[391], among others.[376] Importantly, CYR61 was proven to have predictive power being associated with worst prognosis and poor overall survival in these tumors.[383, 385, 387-389, 391] Considering the molecular mechanism by which CYR61 enhances the cancerigenesis process, several studies have proposed that CYR61 plays a key role in the induction of genes that promote mesenchymal transformation of epithelial cells, a process called epithelial-to mesenchymal transition (EMT) and thereby promoting cell migration and invasion abilities, and tumor metastasis.[392-394] Together, these works provided evidences that favor CYR61 as an important tumor-promoting factor with a key role in cancer progression. In accordance, experimental data has shown that CYR61 overexpression enhances tumor growth and progression in breast cancer [395] and osteosarcoma tumors [396] by promoting invasiveness *in vitro* and inducing tumorigenesis *in vivo*. In osteosarcomas, it was already demonstrated that CYR61 silencing reduces in vitro osteosarcoma cell invasion and migration and decreases tumor vascular density, hampering the dissemination process and strongly reducing *in vivo* lung metastasis.[396, 397] In ovarian carcinomas, CYR61 stimulates cell proliferation and could be involved in ovarian carcinogenesis by promoting survival and resistance to apoptosis.[398]

Similar to CYR61, elevated TAZ expression has also been implicated in the malignant phenotype of a broad range of neoplasias, such as melanoma, glioblastoma, squamous cell carcinomas, breast, lung and colon cancers.[399, 400] TAZ, also known by its gene name WWTR1, is a transcriptional coactivator protein with a PDZ-binding motif that functions as a major downstream effector of the Hippo tumor suppressor pathway, a signaling cascade with key regulatory functions in tissue growth and organ size control during development and in tissue homeostasis, repair and regeneration during postnatal life. [399, 401] TAZ activity is also essential for self-renewal and growth of stem cells and tissue-specific progenitor cells.[402, 403] TAZ functions as an oncogenic protein during tumorigenesis regulating several cellular processes that are relevant for cancer initiation, progression and metastasis. In glioblastoma TAZ overexpression drives mesenchymal differentiation, which correlates with poor overall survival and treatment resistance.[404] In breast cancer, TAZ overexpression and increased activity: correlates with high grade and metastatic breast cancer, promoting proliferation, migration, invasion and EMT in cancer cells [399, 405]; is required to sustain self-renewal and tumor-initiating abilities in breast cancer stem cell population; and confers stem cell features to non-cancer stem cells.[406] Furthermore, overexpression of TAZ correlates with a higher proliferation status, invasion and metastatic capacity of colon cancer cells [407] and associates

with more frequent metastasis and therapeutic resistance in lung cancer.[408, 409] In the clinical setting, just like CYR61, TAZ overexpression proved to be useful as an independent predictor of poor prognosis being also associated with worse overall survival and poor patient outcome in breast [410], colorectal [407] and lung [411] cancers.

Collectively, this large body of work demonstrates that CYR61 and TAZ are important players in multiple biologic processes, at both cellular and tissue level, that are crucial for cancer development. So, considering the known functions of CYR61 and TAZ in physiologic processes as well as its involvement in tumorigenesis, deregulation of these two genes could plausibly contribute to the malignant phenotype of BE cells. Although the BE metaplastic process in the esophageal mucosa is considered an adaptive response to chronic gastro-esophageal reflux (and, in that sense, more resistant to that insult), it is known that in this context of chronic injury due to recurrent reflux/healing of BE mucosa episodes, and enhanced by an inflammatory response, some BE cells acquire abnormal physiologic capacities and transform into cancer cells. [2, 3, 114] Furthermore, within this continuous process of regeneration, BE malignant progression to EA is characterized the occurrence of several molecular and cellular events, including increased proliferation, altered cell adhesion, inhibition of apoptosis, enhanced angiogenesis, invasion and metastatic capacities[2, 143], all processes that were already described to be altered in consequence of CYR61 and TAZ overexpression in other models of cancer.

Notably, previous evidences already demonstrated the involvement of CYR61 in the very beginning of the BE metaplastic process. Indeed, it was shown that CYR61 up-regulation occurs as an early response of esophageal epithelial cells to low pH conditions, functioning as a key player in acid-driven esophageal epithelial transformation in BE pathogenesis.[412, 413] Moreover, in the esophageal context, previous work indicates that CYR61 may act as an inducer of tumorigenesis. While CYR61 was found overexpressed in esophageal squamous cell carcinomas (ESCC) enhancing proliferation, migration and invasiveness capacities in ESCC cell lines[414, 415]; in BE tumorigenesis CYR61 up-regulation was present in BE samples adjacent to dysplasia and EA compared to adjacent squamous epithelium and to BE from patients with no signs of malignant progression.[416] This was the first study suggesting that CYR61 overexpression could be an early event in BE cancer pathway. However, the fact that CYR61 up-regulation was described in BE samples from a time point where dysplasia/EA was already developed did not allow the evaluation of CYR61 as a predictive marker to assess cancer risk in BE patients before malignant progression. In contrast to CYR61, TAZ overexpression has never been linked before with BE pathogenesis and cancerigenesis.

Here, we demonstrate for the first time that both CYR61 and TAZ are upregulated in BE years before malignant progression to dysplasia/EA. This reveals that at very early stages in BE, specific signaling pathways, where these and likely other functionally related genes operate, could be deregulated and promoting alterations in cell properties that, either directly or by interaction with stromal tissue, will facilitate tumor initiating features, priming BE for

cancerigenesis. Surprisingly, we noted that transcriptional levels of CYR61 and of TAZ (though to a lesser degree in the latter) slightly decreased from BE in the index biopsies to BE adjacent to dysplasia/EA. While we do not have a mechanistic explanation for this observation, we conceive that CYR61 and TAZ could be more relevant in neoplastic initiation than in progression. In fact, this trend does not seem to be exclusive of BE malignant pathway. High CYR61 expression in localized disease and early neoplastic stages and decreasing in advanced and metastatic cancer was already previously described in prostate [380] and colorectal [417] cancers. Also in hepatocellular carcinoma, a higher expression of CYR61 was documented in hepatic cirrhosis tissue adjacent to cancer, considered a precancerous lesion, than in neoplastic tissue.[418] Interestingly, a clinical study also demonstrated that CYR61 overexpression was significantly related with reduced overall survival for patients in early ESCC cancer stages functioning as an independent prognostic factor for those patients. In contrast, it did not affect the overall survival in patients with late stage cancer, suggesting that CYR61 could be more relevant at the early stages of ESCC cancer development and could potentially be used as an early tumor biomarker able to identify high-risk patients.[419]

Together these evidences support that CYR61 deregulation may be more relevant at early stages of tumor development, at least in these cancer models, and reinforce that CYR61 could function as an early biomarker to risk stratify patients. Furthermore, given that CYR61 is a secreted extracellular matrix protein, this study opens the perspective of using CYR61 as a potential serum biomarker to stratify cancer risk in BE patients with the simple collection of blood samples, allowing for less invasive follow-up exams, as it was already demonstrated for colorectal cancer[420].

4.1.3 Epithelial-to-mesenchymal transition (EMT): "a new rising path in BE cancerigenesis"

Notably, not only have both CYR61 and TAZ been found to play key roles in epithelial-to mesenchymal transition (EMT) and stemness, but they are also mechanistically linked: CYR61 is a downstream transcriptional target of TAZ.[421] Moreover, besides CYR61 and TAZ, our *in silico* analysis also uncovered that EMT and stemness-related genes were also significantly over-represented in BE associated with progression. EMT is a natural occurring developmental program in embryogenesis that is also relevant for adult tissue homeostasis, as a physiologic response in tissue regeneration and wound healing, and pathological conditions such as fibrosis and cancer. [422] In the context of neoplasias, cancer cells undergoing EMT suppress their epithelial features and acquire a mesenchymal-like phenotype that allows them to adopt a migratory and invasive behavior during cancer progression.[423, 424] These findings prompted us to hypothesize that mechanisms operating in EMT could be activated early in BE malignant pathway. We therefore assessed if core EMT markers were also differentially expressed early in BE progression.

As cancer cells undergo EMT, they suffer profound phenotypic changes characterized by the progressive loss of cell-to-cell junctions, apical-basal polarity and acquisition of front to back polarity and enhanced cell-matrix interactions.[425] This shift in differentiation is mediated by the activation of several transcription factors (e.g. Slug, Snail, Twist, ZEB1) that trigger the concomitant downregulation and loss of epithelial markers, including the cell adhesion protein E-cadherin, considered a hallmark of EMT, followed by upregulation and gain of expression of mesenchymal markers, like N-cadherin and vimentin.[422, 426] In agreement with the activation of an EMT program early in BE, our in silico analysis showed that TWIST1 was significantly overexpressed in BE associated with progression and, notably, we were able to validate its up-regulation as early as in the BE index biopsies from patients that progressed later on (see page 65, Fig 3A). Furthermore, we also detected focal loss of E-cadherin protein expression in the same samples (see page 65, Fig 3B), an event usually observed later on in malignant progression, being normally associated with invasive cancer cells.[427] These findings suggest that, in striking contrast with BE of patients that did not progress, changes in cellular adhesion and/or extracellular matrix are occurring very early in high-risk BE, and that aggressive mechanisms, typical of advanced metastatic cancer stages, are activated early in non-malignant BE cells of at risk patients. Strikingly, these typical features of aggressive behavior in the context of cancer occur in BE progressors in a time point far earlier than we anticipated, reinforcing once more the concept that it is possible at very early stages to distinguish BE that is prone for later development of dysplasia/EA from low risk BE by the identification of the cellular events that are triggering BE malignant transformation.

The contribution of EMT in cancer has long been the focus of intense research and it was already associated with tumor initiation, progression, invasion and metastasis.[423, 428] Accumulating evidence has revealed that EMT confers cancer cells with stem-like properties, enabling them to have tumor-initiating and self-renew potential, thus enhancing tumorigenesis.[429] Indeed, the early occurrence of in vivo EMT in the absence of any histological signs of invasive cancer was previously demonstrated in a mouse model of pancreatic cancer. In that study, EMT was identified in pre-invasive pancreatic lesions and areas of acinar-to-ductal metaplasia, and these cells presenting a mesenchymal phenotype and stem cell features were able to invade, enter in the bloodstream and seed in the liver before the establishment of pancreatic cancer, a process that was enhanced in the background of inflammation.[430]

Although the EMT program could be activated in both wound healing and cancer, at present, it is currently unknown how EMT could contribute to early stages of BE malignant transformation and progression and if only some EMT-related pathways are activated. Still, EMT occurrence was already described in early stages of EA [431] and in an esophageal squamous epithelial cell line [413] in which acid-induced CYR61 up-regulation mediates E-cadherin loss and promotes expression of the N-cadherin mesenchymal protein, typical of an EMT phenotype. In addition, a

link between CYR61, TAZ, EMT and cancer progression was already established in lung cancer via the tumor suppressor angiomotin.[432]

Future studies are needed to further clarify the CYR61, TAZ and EMT participation in BE pathogenesis and tumorigenesis in order to understand the extent to which these players are contributing to BE malignant progression and why progression only takes place several years after these alterations appearing. An interesting hypothesis that must be considered is that these molecular changes could occur very early but are kept in check by controlling/surveillance mechanisms. Then, later on, upon a "second hit" change, these alterations can now effectively constitute a fitness advantage and contribute to transformation. So, in the end, these cells are the "fuel" that needs the "lighter" to be dangerous. While the involvement of these players needs to be further explored to decipher how they can be exploited to improve BE diagnosis, prognosis and treatment, our study unraveled a novel and potential mechanistic route for BE cancer progression.

4.2 Centrosome amplification in BE tumorigenesis: "a clue in the chicken or egg conundrum"

Centrosome abnormalities and particularly extra centrosomes are common features across different types of solid and hematological tumors, being now recognized as a hallmark of human cancers.[263, 264] Indeed, centrosome defects have already been observed in early pre-invasive stages of some types of neoplasias raising the possibility of their involvement in tumor initiation. [264, 299, 300] Moreover, in most malignancies, centrosome amplification has been correlated with advanced tumor stage, tumor recurrence, metastasis, chemoresistance and poor patient prognosis suggesting a role in cancer progression and aggressiveness as well. [258, 263, 264] Collectively, these findings strongly support the hypothesis that centrosome aberrations are more than simple bystanders and likely contribute to tumorigenesis and highlight the great potential of using centrosome anomalies, together with other clinical parameters, as a prognostic/advanced disease biomarker and thus predict clinical outcome and survival in oncological disease.[263, 264, 270] Importantly, given that centrosomal abnormalities are unique of cancer cells, they constitute an appealing feature for developing targeted therapeutic strategies, that potentially are only harmful for neoplastic cells.[269]

In this part of the project we followed a hypothesis driven approach: in light of these evidences we anticipated that centrosome number defects plausibly constitute an early hit in BE tumorigenesis that could also be present along BE malignant pathway and in that sense may contribute for cancer initiation and progression. This question is clinically relevant because deciphering the incidence of centrosome abnormalities, as well as when and how they arise in BE tumorigenesis, will allow a better understanding of BE biology and may improve its diagnosis, prognosis and treatment. Ultimately, the findings of this study could be extended to other tumor models and help decipher the role of centrosome amplification in human cancer.

4.2.1 A bona-fide method to score centrosomes in human samples: "looking for a needle in a haystack"

Despite the enormous amount of previous clinical studies already demonstrating that centrosome defects are pervasive in human neoplasias, the timing and mechanisms of centrosome deregulation in human tumorigenesis are still poorly understood and its contribution to cancer remains controversial.[263, 264] Furthermore, whether the incidence of cells with centrosome amplification changes during malignant progression is not known. This limitation stems in part from two main methodological issues that constrain data interpretation. [263]

The first limitation stems from the fact that the majority of studies done in tumor histological specimens scored centrosomes using only antibodies recognizing PCM proteins, such us pericentrin or gamma-tubulin, which give only an indication of alterations in volume, number and shape of those particular PCM components, that do not necessarily reflect a true alteration in centrosomes.[266] PCM proteins could dissociate from the centrioles or could accumulate in microtubules minus end autonomously from the centrioles and form extra acentriolar foci structures.[272] As a result, staining for PCM markers alone, without a co-staining with a centriole marker, makes it impossible to distinguish an increased amount of PCM that could result from assemblies without centrioles from a true increase in centrosome numbers revealed by the presence of extra centrioles. Although aggregates of acentriolar PCM may have a microtubule-nucleating capacity, and function as if they were extra centrosomes, the underlying causal mechanisms for such defects are different and thus it is crucial to be able to discriminate both types of abnormalities. Actually, in the single previous work investigating the presence of centrosome abnormalities during BE carcinogenesis, where the authors used PCM markers alone to do the analysis, they recognized that without doing a double staining with a PCM and centriolar marker they were not able to do an accurate counting of bonafide centrosomes.[433]

The second limitation has to do with the method used to count centrosomes. Previous studies did not do a cell-by-cell analysis throughout tumorigenesis. Instead, they report a continuous distribution of centrosome numbers by counting the number of PCM signals versus nuclei per area in image projections, giving an average of signals per nuclei.[299, 304] Furthermore, several studies established cut-offs to consider a case positive or negative for centrosome defects.[300, 317, 323] However, understanding the incidence of centrosome amplification at the single cell level and the dynamics of this population of cells throughout progression is crucial for deciphering its role in human cancer and, ultimately, impact its use in the clinical setting.

While the use of electron microscopy (EM) would allow overcoming these drawbacks by providing an accurate method to evaluate the ultrastructural details and quantifying centrosome anomalies, it would be very demanding and practically unfeasible for a large number of cells, since it would require thousands of serial sections to score centrosomes and their structural

anomalies in a tumor sample.[272, 289] In fact, the very few studies using electron microscopy to identify the ultrastructural centrosome abnormalities in human tumor samples (e.g. extra centrioles, disrupted centriole structure, overly long centrioles, and excess PCM), do not provide quantitative analyses of the incidence of such defects. [434, 435] Furthermore, to use this methodology it is necessary to have a tumor bank of samples specifically processed to be visualized by EM, which in the particular case of BE disease would take many decades to collect.

Taking into account all these limitations, there is a clear need for better-quality, accurate and feasible methods that would allow the correct evaluation of centrosome number anomalies in human tissue samples, and thus provide a huge improvement to the field. Here, to assess the incidence of centrosome number abnormalities along the sequential stages of BE malignant pathway we first established an accurate and reliable immunofluorescence microscopy-based method to identify bona-fide centrosomes at the single cell level in formalin-fixed paraffin-embedded (FFPE) tissue samples.

For that, we took into consideration the technical demands derived from the specificities of working in FFPE samples. First, it is important to note that, given the cross-linkage of proteins and consequent antigen masking given by the formalin fixation process, not all antibodies are suitable to use in FFPE samples.[436] Despite de use of antigen retrieval to unmask the antigens, not all antibodies achieve a good quality immunolabeling. We therefore first tested several anti-centrosomal antibodies and chose the two markers that have robust staining (i.e. good sensitivity and reproducibility with minimal cross-reactivity and background) in FFPE samples, and that would allow us to identify true centrosomes by labeling the two structural components of the centrosome: the centrioles (marked by glutamylated tubulin, GT335) and the PCM (marked by pericentrin). Centriole number was assessed by GT335 when it colocalized with pericentrin, thus ensuring the scoring of true centrosomes. Immunostaining of centrosomes was judged satisfactory when it was detected in normal cells localized in the adjacent epithelium, like fibroblasts and lymphocytes that function as an internal control.

The centrosome is a tiny cytoplasmic organelle whose centrioles have a size that is close to the limit of resolution of an optical microscope, which makes their scoring an arduous task. Here, we chose immunofluorescence microscopy (IF) as a visualization method. In contrast to brightfield immunohistochemistry (IHC), IF has higher resolution and better performance in multiple labeling since the fluorochrome is directly conjugated with the secondary antibody thus minimizing cross-reactivity. Although IHC could be used to visualize multiple antigens, the overlapping colors of signals that colocalize in the same cellular compartment is not as clear as in IF and may obscure the results. Furthermore, the chromogenic precipitate formed in IHC easily saturates, giving rise to gross signals with limited resolution that restricts quantitative analysis.[437] Here, we used 3-micra-thick tissue sections, as normally used in the clinic, to achieve good staining and resolution at cellular level.

The task of scoring centrosomes/centrioles in a cell-by-cell basis is even more challenging in histological sections due to caveats such as cellular truncation, overlapping of neighboring cells, and the difficulty in identifying the limits of the cells composing the tissues samples. To test the accuracy of counting centrioles on a cell-by-cell basis, we co-stained normal ileum samples for centrioles (GT335) and the membrane marker e-cadherin (see page 167, Fig S1A). With this, we found that the background of GT335 staining, which is visible in the cytoplasm but absent in the cell membrane where e-cadherin was present, was sufficient to define cell boundaries. This allowed us to validate the fidelity of our method of scoring centriole numbers cell by cell without the presence of a membrane marker. Nevertheless, cells whose limits could not be clearly distinguished, as well as cells overlapping with neighboring cells, were excluded from the analysis. To clearly identify the transition between adjacent cells and ensure that all the centrioles present in each cell per section were quantified, the counts were not performed directly down the eyepiece of the microscope, but rather going through the Z series of acquired images, covering the whole depth of the section to perceive the transversal and sagittal plans of each cell. It is important to note that the use of thin 3-µm-thick tissue sections will likely results in an undercounting of the full extent of centrosome amplification due to the cell truncation artifact. However, an increase in thickness would result in worst quality staining (i.e. loss of antibody sensitivity and specificity and higher background) and an increase in cell overlap, which would make the quantification of centrosome numbers even more difficult. A good compromise between advantages (e.g. good resolution and staining) and disadvantages (e.g. cell truncation and resulting undercounting) had to be met taking in account these limitations. To assess the occurrence of undercounting and/or overcounting of centrosome numbers as a result of using thin histological sections, we did an extensive analysis using our standards of comparison for normal cells (see description of controls used in section 4.2.2 below). Given that centrosome counting was performed in well-differentiated areas that are not normally proliferative, the expected number of centrosomes per normal cell is one (with two centrioles). As predicted, the presence of some cells with 0 or only 1 centriole confirmed the undercounting of centrosome numbers. In contrast, we never detected an overcounting in any of the controls since we did not find more than 2 centrioles per cell, supporting that the method used to differentiate cell limits was robust and reliable.

In the end, at least 200 cells with centrosomes were scored per sample. However, to obtain this number of countable cells, tissue sections with thousands of cells were analyzed. In biopsies, where the areas are smaller, more than one section was used to ensure enough and different cells were analyzed. While diagnosis guidelines for FISH interpretation in histologic sections recommend counting at least 100 cells, we decided to count twice that amount to increase our method's fidelity.[438] Considering that a healthy cycling cell either has one centrosome with two centrioles (G1) or two centrosomes with two centrioles each (S, G2, and M), depending on the cell cycle stage [289], a cell was considered to have centriole number amplification only when it contained more than four centrioles. Although it is plausible that some cells with three and four centrioles could already represent centrosome amplification if those cells were in G1

stage, the absence of a cell cycle stage marker did not allow us to make any corroborated conclusion about these numbers being normal or an abnormal centriole content in cells, and these were therefore considered as normal. Given this limitation and the necessary use of thin tissue samples as explained before, we are likely underscoring the full extent of centrosome amplification. Nevertheless, and despite all the restraints, we established a meticulous and reliable method for quantifying bona fide centrosomes in human FFPE samples. In fact, the trend in the centrosome amplification profile obtained in a panel of cell lines representing all sequential steps of disease progression (see section 4.2.3) was similar to the one obtained with the tissue samples along the different stages of BE progression, reinforcing and validating the accuracy of the method used in tissue samples. Furthermore, we believe that future studies on centrosome amplification during cancer progression using histological samples will benefit of using a similar methodology.

4.2.2 Centrosome amplification arises before cancer development and is present along BE malignant pathway

Having established a reliable method to score the incidence of centrosome number abnormalities, we set out to determine when and how centrosome number abnormalities arise in the multistep BE cancerigenesis. As previously highlighted in the framework, BE malignant pathway constitutes an excellent cancer model not only because it allows the analysis of the premalignant condition, the intermediate step between normal tissue and tumor initiation, but also because it provides the unique opportunity to study all sequential stages of the disease within each individual patient, thus reducing the effects of inter-patient variability. By taking into account the advantages of the model, we first selected cohorts of patient samples that would allow us to analyze all stages of BE progression. So, we analyzed metaplasia from patients that did not progressed and metaplasia adjacent to neoplasia, dysplasia (LGD and HGD whenever they were both present, but for simplicity we only refer to it as dysplasia), EA and lymph node metastasis (when present) from the patients with malignant progression. As the cellular origin of BE metaplastic condition remains unknown [162], there is currently a lack of a suitable control for BE studies. The solution we encountered to overcome this gap in knowledge, was to examine both the native squamous epithelium of the esophagus and ileum epithelium as standards of comparison for normal epithelial tissue. The rationale for choosing these two types of tissues as standards of normality was, on one hand, to use the native tissue where BE metaplasia arises – squamous epithelium of the esophagus, and, on the other hand, the tissue that is morphologically similar to BE metaplasia – the ileum epithelium, a simple columnar epithelium composed mainly of columnar (enterocytes) and goblet cells.

Centrosome number analysis through BE progression revealed that: i) centrosome amplification is never detected in both normal linings and metaplasia from patients that had not progressed; ii) centriole amplification arises very early, in metaplasia adjacent to either dysplasia or EA, being present in all subsequent stages of malignant transformation; iii) centriole amplification is present in all tumors of all patients; iv) centriole number per cell is deregulated from early

stages and increased upon progression; v) the small fraction of cells with centrosome amplification significantly expands from metaplasia to dysplasia; and vi) the incidence of centriole amplification is dynamic during progression (see page 79, Fig1C and page 167, FigS1D).

As expected, centrosome number abnormalities were never observed in cells of normal epithelial tissue (native esophagus and ileum) (see page 79, Fig1C), which reinforces that number of centrosomes is tightly regulated in healthy normal cells. Our study also showed that while centrosome amplification was never found in metaplasia cells from biopsies of patients that had not progressed, this was significantly different in patients that evolved to malignancy.

Centrosome amplification was detected very early in the premalignant condition, the stage prior tumor initiation, and it significantly increased from metaplasia to dysplasia, the step before the onset of invasion. Surprisingly, this increase did not consistently accumulate through progression (see page 79, Fig 1C). In fact, our data indicate a tendency of centrosome amplification incidence to decrease in EA, after invasion has taken place, and rising again in lymph node metastasis, which is normally the initial step in cancer spreading. This variable incidence along the progressive stages of BE cancerigenesis suggests that the proportion of cells with centrosome amplification is dynamic. In fact, it was already demonstrated that cancer cell lines have an intrinsic set point for the penetrance of cells with amplified centrosome, reflecting the dynamic nature of those cells.[439]

This variable incidence of centrosome amplification, together with the observation that it is more prominent at specific stages, dysplasia and lymph node metastasis, also suggests that centrosome abnormalities may be differently tolerated and may have different roles throughout tumor progression. Plausibly, the impact of these alterations is context dependent, meaning that tumors could regulate the proportion of cells with extra centrosomes through a dynamic equilibrium between being detrimental or conferring a selective advantage for BE progression at specific stages. Considering that dysplasia precedes the establishment of invasive neoplasia, perhaps centrosome amplification could contribute to the development of invasiveness in this phase of BE progression pathway. In accordance with this, experiments in 3D cultured cells revealed that centrosome amplification leads to an increased migratory and invasive capacity of those cells.[264, 348] Following the same line of thought, the increased incidence of cells with centrosome amplification in lymph node metastasis we detected in vivo could be viewed as an indication that centrosome abnormalities could be important for the process of metastasis. Indeed, the perspective that centrosome defects could contribute to the first steps of metastasis by promoting invasive behaviors has recently emerged. [440] Experimental approaches in 3D culture models demonstrated that cells harboring centrosome aberrations could contribute to metastasis by promoting the invasion and dissemination of cells with oncogenic mutations and metastatic potential through cell-autonomous and non-cell autonomous mechanisms.[348, 350, 351] Importantly, the observation that the non-cell autonomous process triggered by cells with

centrosome defects could enhance an invasive phenotype and dissemination of surrounding cancer cells carrying normal centrosomes, supports the perception that centrosome abnormalities could be advantageous and contribute for cancer development even when they are only present in a subset of cancer cells in the tumor population.[350, 440] Interestingly, our centrosome analysis at the single cell level throughout BE malignant pathway revealed that the population of cells with centrosome amplification was never eliminated or close to 100%. While the fact that this subpopulation of cells is not the most abundant could indicate they represent a less important clone and just a byproduct of BE cancer progression that do not confer a fitness advantage for tumor evolution, the observations that cells with centrosome amplification arise as early as in the premalignant condition, do not disappear along BE malignant pathway, and are more prominent in specific stages suggest that centrosome amplification is not a random consequence and rather a relevant event for BE tumorigenesis. Given its non-cell autonomous effects, centrosome deregulation does not have to be present in a high fraction of cells to have an important impact in tumor progression and may constitute an advantage at the population level by enhancing the fitness of other cancer cell sub-clones. Furthermore, there is growing evidence showing that in addition to genetic heterogeneity, clonal diversity may also dictate the potential of a cancer to adapt and overcome different selective pressures and thus determine the course of malignant progression, drug resistance and recurrence.[441] Indeed, it was already demonstrated that intra-tumor heterogeneity in BE disease has predictive value and positively correlates with a higher risk of BE progression to EA.[442]

Collectively, the observations that centrosome amplification arises before neoplastic transformation, is kept throughout the multistep pathway of cancerigenesis, and that its incidence varies along progression, strongly support our hypothesis that centrosome amplification could be relevant for BE cancer initiation and progression. Future work will be crucial to understand the nature of this relation and how centrosome amplification contributes for BE tumorigenesis. For example, studies with 3D culture cells would provide important clues to clarify why cells with centrosome amplification are selected at dysplasia stage, namely to test if and how they contribute for invasiveness in this cancer model. Furthermore, despite centrosome deregulation being present in only a cell subpopulation, it has potential to be biologically and clinically important given that these cells could establish a positive interaction with other clones and increase the fitness of multiple tumor cell populations [443], influencing BE disease progression and making them appealing therapeutic targets. Future studies will be important to clarify the causes and consequences of this non-genetic heterogeneity and to understand if patients could potentially benefit from including centrosome-related inhibitors to current therapeutic strategies to treat BE cancer.

Importantly, and in addition to contributing to the understanding of BE disease progression, we consider that our work also provided answers that have an important impact on deciphering the role of centrosome deregulation in human tumorigenesis. The analysis of centrosome amplification at the single cell level in this unique human cancer model, with a well-defined

cancer pathway that allows the study of all steps of malignant transformation within the same patient as well as the study of the premalignant condition, the biological stage that precedes tumor initiation, contributed to get further insights about the timing and dynamics of centrosome deregulation along cancer progression. Indeed, our observations suggest that centrosome amplification in humans can contribute to tumor initiation and progression and support the concept that centrosome defects are more than merely passengers in cancer evolution being active players in cancer progression.

4.2.3 Centrosome amplification increases in dysplasia upon loss of p53: "guilty until proven innocent"

The discovery of the timing and dynamics of centrosome amplification along BE progression prompted us to search for the molecular causes that could underlie these changes. To do this, we first tried to correlate those findings with the well characterized genetic and ploidy changes of BE progression.

Considering the striking expansion of cells with centrosome amplification from metaplasia to dysplasia, we conceived that an important genetic alteration permissive for centrosome numbers alterations possibly occurred at this point. A previous large-scale study reported that p53 mutations are stage specific, being recurrently found in HDG and EA, but rarely in metaplasia, and clearly define the boundaries between metaplasia and dysplasia.[213] Moreover, given that p53 loss was associated with centrosome amplification in several other human cancers [263, 264], we hypothesized that p53 inactivation could be responsible for the increase of cells with extra centrosomes observed in the transition of metaplasia to dysplasia in BE.

To corroborate our hypotheses, we evaluated p53 status in our cohort with metaplasia and dysplasia samples within the same patients (cohort 2), which allowed us to confirm that p53 is indeed first altered in dysplasia, while most metaplasia samples retained WT p53 expression (see page 80, Fig2), favoring our hypothesis that p53 loss may underlie the increased penetrance of centrosome amplification at this stage. To test the consequences of p53 loss in centrosome amplification, we took advantage of a panel of established and validated cell lines representing all sequential steps of BE progression (normal esophageal lining, metaplasia, dysplasia, adenocarcinoma and lymph node metastasis) and whose genomic alterations are well characterized and similar with those found *in vivo* [444, 445]. For example, metaplastic cell lines are diploid and retain WT p53 while dysplastic and cancer cell lines are aneuploid and have lost WT p53 function due to different p53 mutations. Importantly, our study of centrosome amplification profile in these cell lines also revealed a similar trend to the one obtained in patient tissue samples along BE progression namely the absence of centrosome amplification in normal lining cells, the presence of centrosome amplification in cell lines representative of metaplasia and all other subsequent stages, and the increase in the incidence of cells with supernumerary centrioles from metaplasia to dysplasia (see page 80, Fig3B). These findings

support the concept that cell lines maintain the centrosome profile from their tissues of origin and thus validated this panel as a good model to test the molecular alterations underlying the increase in centrosome amplification. So, in cell lines, and consistent with what we observed in vivo, centrosome amplification arises in metaplasia in the background of WT p53, and its incidence significantly increases in dysplasia, where p53 WT function is lost.

Previous studies already demonstrated that while p53 loss *per se* is not sufficient to trigger centrosome number defects in normal human cells, it is required for their survival when they are experimentally induced to gain or lose centrosomes [439, 446-448]. We therefore hypothesized that the underlying small population of cell with extra centrioles present in metaplasia could be normally repressed by WT and functional p53, and so p53 loss at that stage would result in an increase in the incidence of supernumerary centrioles. Indeed, we found that metaplasia cells with centriole amplification, but not the ones with normal centriole numbers, exhibited the typical p53 accumulation in the nucleus that is induced in response to cellular stress and leads to activation of downstream effectors to prevent the expansion of those cells (see page 81, Fig4A) [449]. To test if p53 was indeed preventing the expansion of those cells with extra centrioles we depleted p53 in metaplasia cells and as expected, loss of WT p53 expression resulted in the increase of centriole amplification penetrance to similar levels encountered in dysplasia cell lines (see page 80, Fig4B-D). In addition to study loss of WT function by removing p53 protein (siRNA) we also investigated the effect of p53 missense mutations as they lead to the expression of a full-length protein that not only lose their WT function as may gain an oncogenic function [449] and considering that p53 sequencing of our patient samples revealed not only nonsense and frameshift mutations but also missense mutations. In particular, we studied the role of R175H and R248W as they are among the most frequent hotspot mutation detected in EA as well as in other cancers [213, 450] and since previous evidences already showed that expression of those specific mutants in p53 negative MEFs and in a lung metastasis cell line originate centrosome amplification [451, 452]. Moreover, all three dysplasia cell lines either have a frameshift mutation or the missense mutations R175H and R248W [453] displaying similar levels of centrosome amplification. We found that both residues are essential for p53 keep its WT function and that these mutations exhibit loss-of-function effects in respect to p53 centriole number control in metaplasia since neither of the two mutants was able to hamper the accumulation of cells with centriole amplification in striking contrast with expression of WT p53 protein that rescue the levels of centrosome amplification to the ones observed in metaplasia with intact p53 WT function (see page 82, Fig5B-D).

Furthermore, we also tested if p53 depletion alone would be sufficient to generate centrosome amplification in normal lining cells and this was not verified (see page 169, FigS3 J and K), suggesting that probably are other molecular changes present in metaplasia [213] that are promoting centriole amplification at this stage. The precise role of these mutations at such early stage remains elusive, but possibly could provide a fitness advantage for a clone without leading to malignancy. For example, inactivation of p16 tumor suppressor is highly prevalent in BE,

even in patients that have not developed cancer, and normally precedes p53 loss [142, 185, 200]. Correspondingly, metaplasia and dysplasia cell lines used in this study all present p16 inactivation [444, 445, 454]. So, centriole amplification in BE arises in the genetic background of p16 loss and functional WT p53. Nevertheless, while previous work demonstrating that S phase arrest in p16-deficient human mammary cells was enough to generate multiple centrosomes due to premature centriole splitting [455], prolonged S phase arrest in our metaplasia cells in the background of WT p53 did not lead to an increase in centrosome amplification (see page 81, Fig4 F and G). Future studies addressing the contribution of this and other early events for centrosome deregulation and their relation with p53 loss will be crucial to get further insights regarding the causes of centrosome amplification in BE malignant progression.

Together, our results corroborate that centrosome amplification arises in the premalignant condition in the background of WT p53 that plays a crucial role in preventing widespread centrosome amplification. This supports the existence of a p53-dependent pathway that prevents cellular proliferation of cells with extra centrosomes and plausibly is responsible for the maintenance of the low levels of centrosome amplification observed at metaplasia stage. In accordance with this, it was already shown in model organisms and cell cultures where centrosome amplification or loss activate a p53-dependent pathway that conducts to cell cycle arrest or even cell death and in turn p53 loss is necessary for the survival of those cells [347, 448, 456]. In turn, WT p53 loss results in the increase of cells with centrosome amplification, in accordance with the trend observed in the transition of metaplasia to dysplasia in patient samples. Future work investigating by which mechanisms p53 response is activated upon centrosome number deregulation are still needed.

Besides significant and specific genetic changes such as loss of p53 function, BE progression is also characterized by ploidy changes. Many tumors arise from a transient tetraploid event [277], and in BE tumorigenesis tetraploidy is a common and early event that dictates an increased risk of developing aneuploidy and both are highly predictive of malignant progression [334, 457], being normally preceded by p53 changes [142]. Moreover, ploidy changes are normally policed by p53. [456, 458] Therefore, we surveyed whether there was a correlation between ploidy deregulation and centriole amplification by examining both features in metaplasia cells with and without p53. This analysis will inform us regarding the ordering of these events throughout progression, and possibly indicate the possible mechanisms underlying centrosome number deregulation. Indeed, while there are several mechanisms that could promote centrosome number deregulation in cells, including centrosome biogenesis deregulation and cytokinesis failure [264], the latter generates both supernumerary centrosomes and tetraploid cells.[459] Although metaplasia cells already presented an abnormal ploidy profile and binucleated cells that elicited a p53 response, p53 silencing resulted in aggravated ploidy deregulation that positively correlated with the increase in centriole amplification, suggesting a plausibly common origin such as cell division failure. To verify if centriole amplification in metaplasia results

exclusively from tetraploidy derived from cell division failure upon p53 loss, we blocked cells in S phase considering this would stop cell division and consequently abrogate the increase in amplification (see page 81, Fig4 F and G and page 169, FigS3 R and S). Surprisingly, we found that p53 loss still leads to centrosome amplification in metaplasia cells under those conditions, suggesting that at least part of these cells with extra centrioles are not resulting from cell division failure and that p53 could also be crucial in preventing centriole biogenesis deregulation.

Regarding the possible consequences of metaplasia cells having low levels of centrosome amplification, and considering the observed correlation between centrosome amplification and ploidy changes, we conceive that this subset of cells with multiple centrosomes arising early in metaplasia could be contributing to promote the genomic instability that is known to be present in metaplasia adjacent to EA [32, 460]. In agreement, previous evidence already showed that extra centrosomes correlates with CIN in several other tumors and cancer cell lines and experimental data demonstrated that extra centrosomes alone are sufficient to enhance segregation errors due to occurrence of lagging chromosomes during cell division in non-transformed immortalized cell lines [340, 341]. Future studies elucidating the fate of this cellular population in the context of BE tumorigenesis will be crucial to clarify if centrosome amplification mediates CIN in BE and in consequence if they could be potentially involved in tumor initiating features. It is plausibly that in the absence of p53 the consequent increase in centrosome amplification observed in the transition of metaplasia to dysplasia could be generating genetically unstable and potentially harmful cells, this is, harboring driver mutations that without p53 control could survive and promote BE malignant transformation and progression. In line with this hypothesis, recent studies showed that transient centrosome amplification enhances tumorigenesis in aged mice [346] and significantly decreases the latency of tumor development in p53-deficient mice [461, 462].

Furthermore, considering that p53 mutations R175H and R248W studied by us were previously found to promote genomic instability and invasion [449, 463], this further supports that centrosome amplification may also have a role and contribute to those malignant features in BE progression. Consistently, our results demonstrate that centrosome amplification has a higher penetrance in dysplasia, the stage before invasion takes place. Still, future studies are needed to investigate the role of distinctive p53 mutations in BE tumorigenesis and whether they could be related to centrosome number deregulation.

Considering that centrosome amplification is a prevalent feature in human tumors and that p53 mutations occur in almost every type of cancer [464] our findings on the timing and ordering of supernumerary centrosomes, the demonstration that exists a p53 dependent pathway that controls cell populations with centrosome number deregulation and their relation with aneuploidy in BE tumorigenesis are likely to be extrapolated to other cancers.

CHAPTER 5:
Conclusions and Future Perspectives

The starting point of this project was the clinical need to find reliable biomarkers to guide medical decisions, allowing for the improvement of cost-effectiveness of BE clinical management, and, specially, the standard of care for BE patients [9, 235, 253]. Although biomarkers are required to inform clinical practice at multiple stages of the BE pathway [240], identifying markers able to stratify non dysplastic BE patients according to cancer risk would be the "holy grail" of biomarkers search since it would allow to focus attention and resources on those patients that most likely will benefit from it [245] and to intervene at metaplasia stage, before BE progression. Based on this motivation we traced two different strategies to increase the odds of achieving success.

By trailing a meta-analysis approach on gene expression data followed by experimental validation in a cohort of BE patients, our work provided evidence that there is a gene expression profile associated with BE malignant transformation. Importantly, we identified two genes that were significantly up regulated years before neoplastic progression and our results support that CYR61 and TAZ are potential early predictive biomarkers of BE malignant progression and could be used to discriminate among BE patients the ones with an increased risk of malignant progression. Regardless the need of confirming these results in larger cohort of patients and in prospective trials, these biomarkers hold promise to be assessed by available techniques in the clinical setting and applied to standard histological samples. Furthermore, by investigating the functional context of these two genes we have unraveled EMT as potential mechanistic route for BE malignant progression. Future studies investigating the extent to which CYR61, TAZ and EMT markers are priming BE towards malignant transformation will be fundamental to deep our knowledge of BE carcinogenesis.

Through the study of centrosome profile along BE malignant progression, using a robust and accurate method to identify and score bona-fide centrosomes in a cell by cell basis we have demonstrated that centrosome amplification arises as early as in the premalignant condition, before the onset of neoplasia, and significantly expands at dysplasia stage, which correlates and is dependent of loss of function of the tumor suppressor p53. Our results support that cells with supernumerary centrosomes could be important for the beginning of the tumorigenic process. Furthermore, our findings *in vivo* corroborate that centrosome amplification is an important feature of BE malignant progression given that centrosome dysfunction is specific of BE patients that progress to malignancy. For this reason, further exploring on how centrosome amplification contributes for BE cancerigenesis could unravel novel pathways and relevant drivers that could be translated into useful tools to be used in the clinical setting. Indeed, future investigation of the relationship between centrosome amplification and p53 loss of function could allow to discover a wanting gene signature able to predict the presence of significant centrosome amplification at specific stages of BE progression and impact clinical decisions regarding BE

management. For instance, if this wanting gene signature was able to identify the presence of centrosome amplification in BE samples and dictate an increased risk of progression this could help to decide for a stricter surveillance or even an early BE ablation. In turn, when identified later on in cancer progression could help identify the patients that would respond to the newly developed centrosome inhibitors currently being tested in clinical trials [264, 465], making these patients electable for targeted therapies. Importantly, our study also puts in evidence the importance of having a cell line panel that mirrors the biological events regarding centrosome dynamics along BE malignant pathway as it can be used to get further mechanistic insight into how centrosome amplification arises and their contribution for BE progression, invasiveness and metastasis. The nature of this relation could be further explored to potentially identify new biomarkers or develop new therapies.

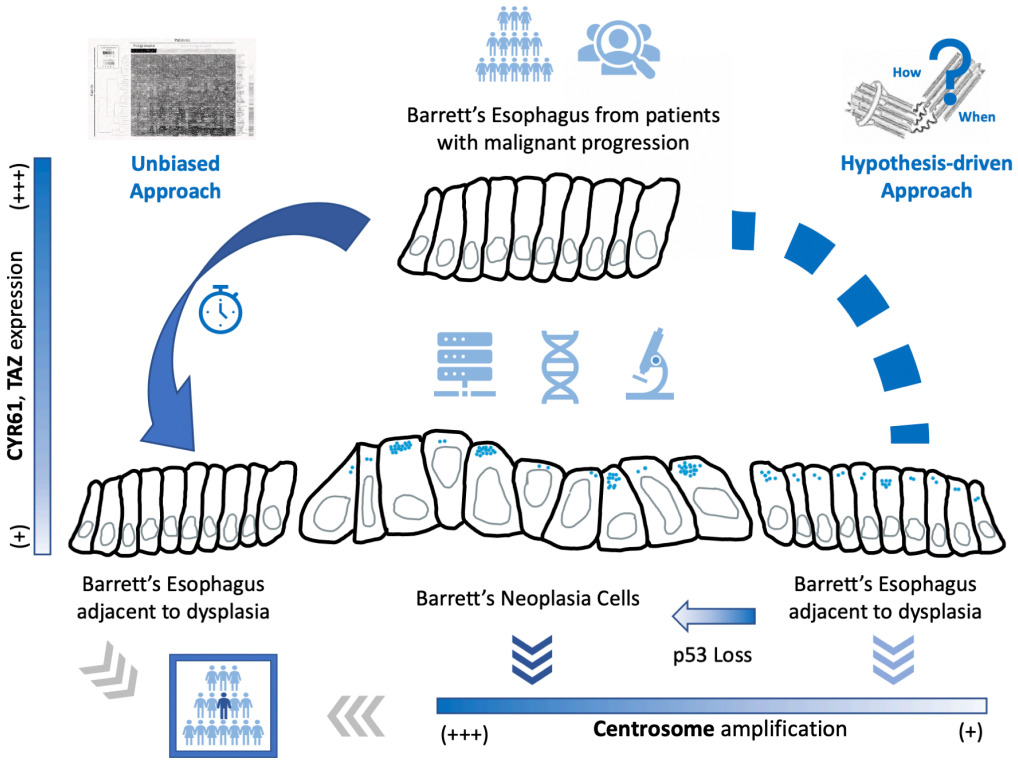

Figure 9. CYR61, TAZ and centrosomes as novel players in BE malignant development: "the hat-trick of the match".

As a final remark, in both research avenues, we demonstrated that oppositely to BE with no signs of progression to dysplasia, in BE prone for malignant progression there are deregulation of signaling pathways and the occurrence of anomalies in cell features as centrosome amplification, that directly or indirectly create a permissive background that enhances tumor initiating capacities in BE cells. So, not only is the cancer risk in BE different from patient to patient but there also seems to exist different pathological states in BE right from the beginning. We therefore conceive the possibility that some BE are "born to be bad". By further exploring this perspective in order to identify these silent but potential aggressive phenotypes we envision

that it is possible to change the paradigm in BE clinical management towards a precision and personalized medicine in which a risk profile is traced for every patient to guide medical decisions and improve patient care.

CHAPTER 6:
References

1. Estores, D. and V. Velanovich, *Barrett esophagus: epidemiology, pathogenesis, diagnosis, and management*. Curr Probl Surg, 2013. **50**(5): p. 192-226.
2. Wang, D.H. and R.F. Souza, *Biology of Barrett's esophagus and esophageal adenocarcinoma*. Gastrointest Endosc Clin N Am, 2011. **21**(1): p. 25-38.
3. Naini, B.V., R.F. Souza, and R.D. Odze, *Barrett's Esophagus: A Comprehensive and Contemporary Review for Pathologists*. Am J Surg Pathol, 2016. **40**(5): p. e45-66.
4. Ghaus, S., et al., *Diagnosis and Surveillance of Barrett's Esophagus: Addressing the Transatlantic Divide*. Dig Dis Sci, 2016. **61**(8): p. 2185-93.
5. Playford, R.J., *New British Society of Gastroenterology (BSG) guidelines for the diagnosis and management of Barrett's oesophagus*. Gut, 2006. **55**(4): p. 442.
6. Riddell RH, O.R., *Definition of Barrett's Esophagus: Time for a Rethink—Is Intestinal Metaplasia Dead?* Am J Gastroenterol., 2009. **104(10)**: p. 2588-94.
7. Spechler, S.J., et al., *American Gastroenterological Association medical position statement on the management of Barrett's esophagus*. Gastroenterology, 2011. **140**(3): p. 1084-91.
8. Hagen, C.E., G.Y. Lauwers, and M. Mino-Kenudson, *Barrett esophagus: diagnostic challenges*. Semin Diagn Pathol, 2014. **31**(2): p. 100-13.
9. Golger, D., A. Probst, and H. Messmann, *Barrett's esophagus: lessons from recent clinical trials*. Ann Gastroenterol, 2016. **29**(4): p. 417-423.
10. Fitzgerald, R.C., et al., *British Society of Gastroenterology guidelines on the diagnosis and management of Barrett's oesophagus*. Gut, 2014. **63**(1): p. 7-42.
11. Haggitt, R.C., et al., *Adenocarcinoma complicating columnar epithelium-lined (Barrett's) esophagus*. Am J Clin Pathol, 1978. **70**(1): p. 1-5.
12. Skinner, D.B., et al., *Barrett's esophagus. Comparison of benign and malignant cases*. Ann Surg, 1983. **198**(4): p. 554-65.
13. Smith, R.R., et al., *The spectrum of carcinoma arising in Barrett's esophagus. A clinicopathologic study of 26 patients*. Am J Surg Pathol, 1984. **8**(8): p. 563-73.
14. Rosenberg, J.C., et al., *Analysis of adenocarcinoma in Barrett's esophagus utilizing a staging system*. Cancer, 1985. **55**(6): p. 1353-60.
15. Paraf, F., et al., *Surgical pathology of adenocarcinoma arising in Barrett's esophagus. Analysis of 67 cases*. Am J Surg Pathol, 1995. **19**(2): p. 183-91.
16. Murray, L., et al., *Risk of adenocarcinoma in Barrett's oesophagus: population based study*. BMJ, 2003. **327**(7414): p. 534-5.
17. Bhat, S., et al., *Risk of malignant progression in Barrett's esophagus patients: results from a large population-based study*. J Natl Cancer Inst, 2011. **103**(13): p. 1049-57.
18. Wang, K.K., R.E. Sampliner, and G. Practice Parameters Committee of the American College of, *Updated guidelines 2008 for the diagnosis, surveillance and therapy of Barrett's esophagus*. Am J Gastroenterol, 2008. **103**(3): p. 788-97.
19. Gatenby, P.A., et al., *Relevance of the detection of intestinal metaplasia in non-dysplastic columnar-lined oesophagus*. Scand J Gastroenterol, 2008. **43**(5): p. 524-30.
20. Kelty C, G.M., Van Wyk Q, *Barrett's oesophagus: intestinal metaplasia is not essential for cancer risk*. Scand J Gastroenterol 2007. **42**: p. 1271–4.
21. Dias Pereira, A. and P. Chaves, *Columnar-lined oesophagus without intestinal metaplasia: results from a cohort with a mean follow-up of 7 years*. Aliment Pharmacol Ther, 2012. **36**(3): p. 282-9.
22. Chandrasoma, P., et al., *Columnar-lined esophagus without intestinal metaplasia has no proven risk of adenocarcinoma*. Am J Surg Pathol, 2012. **36**(1): p. 1-7.
23. Booth, C.L. and K.S. Thompson, *Barrett's esophagus: A review of diagnostic criteria, clinical surveillance practices and new developments*. J Gastrointest Oncol, 2012. **3**(3): p. 232-42.
24. Hahn, H.P., et al., *Intestinal differentiation in metaplastic, nongoblet columnar epithelium in the esophagus*. Am J Surg Pathol, 2009. **33**(7): p. 1006-15.
25. Phillips, R.W., H.F. Frierson, Jr., and C.A. Moskaluk, *Cdx2 as a marker of epithelial intestinal differentiation in the esophagus*. Am J Surg Pathol, 2003. **27**(11): p. 1442-7.
26. Steininger, H., et al., *Expression of CDX2 and MUC2 in Barrett's mucosa*. Pathol Res Pract, 2005. **201**(8-9): p. 573-7.

27. DeMeester, S.R., et al., *Cytokeratin and DAS-1 immunostaining reveal similarities among cardiac mucosa, CIM, and Barrett's esophagus.* Am J Gastroenterol, 2002. **97**(10): p. 2514-23.
28. Rogge-Wolf, C., et al., *Prevalence of mabDAS-1 positivity in biopsy specimens from the esophagogastric junction.* Am J Gastroenterol, 2002. **97**(12): p. 2979-85.
29. Chu, P.G., Z. Jiang, and L.M. Weiss, *Hepatocyte antigen as a marker of intestinal metaplasia.* Am J Surg Pathol, 2003. **27**(7): p. 952-9.
30. Glickman, J.N., et al., *Phenotypic characteristics of a distinctive multilayered epithelium suggests that it is a precursor in the development of Barrett's esophagus.* Am J Surg Pathol, 2001. **25**(5): p. 569-78.
31. Romagnoli, S., et al., *Molecular alterations of Barrett's esophagus on microdissected endoscopic biopsies.* Lab Invest, 2001. **81**(2): p. 241-7.
32. Chaves, P., et al., *Chromosomal analysis of Barrett's cells: demonstration of instability and detection of the metaplastic lineage involved.* Mod Pathol, 2007. **20**(7): p. 788-96.
33. Liu, W., et al., *Metaplastic esophageal columnar epithelium without goblet cells shows DNA content abnormalities similar to goblet cell-containing epithelium.* Am J Gastroenterol, 2009. **104**(4): p. 816-24.
34. Spechler, S.J., et al., *American Gastroenterological Association technical review on the management of Barrett's esophagus.* Gastroenterology, 2011. **140**(3): p. e18-52; quiz e13.
35. Shaheen, N.J., et al., *ACG Clinical Guideline: Diagnosis and Management of Barrett's Esophagus.* Am J Gastroenterol, 2015.
36. Takubo, K., et al., *Histopathological diagnosis of adenocarcinoma in Barrett's esophagus.* Dig Endosc, 2013.
37. Whiteman, D.C., et al., *Australian clinical practice guidelines for the diagnosis and management of Barrett's esophagus and early esophageal adenocarcinoma.* J Gastroenterol Hepatol, 2015. **30**(5): p. 804-20.
38. Bhardwaj, A., et al., *Barrett's Esophagus: Emerging Knowledge and Management Strategies.* Patholog Res Int, 2012. **2012**: p. 814146.
39. Oryu, M., et al., *Differences in the Characteristics of Barrett's Esophagus and Barrett's Adenocarcinoma between the United States and Japan.* ISRN Gastroenterol, 2013. **2013**: p. 840690.
40. Barrett, N.R., *Chronic peptic ulcer of the oesophagus and 'oesophagitis'.* Br J Surg, 1950. **38**(150): p. 175-82.
41. Tileston, W., *Peptic ulcer of the oesophagus.* Am J Med Sci 1906. **132**: p. 240-265.
42. Lyall, A., *Chronic peptic ulcer of the oesophagus: a report of eight cases.* Br J Surg, 1937. **24**: p. 534-47.
43. Lortat-Jacob, J.L., *Les maladies peptiques de l'oesophage.* J Int Chir, 1951. **11**: p. 152-75.
44. Lortat-Jacob, J.L., *Sept cas d'ulcere de l'oesophage.* Mem Acad Chir (Paris), 1951. **77**: p. 829- 37.
45. Giuli, R., *[Endo-brachyesophagus, Jean-Louis Lortat-Jacob and the Barrett esophagus. The history of a modern disease].* Ann Gastroenterol Hepatol (Paris), 1993. **29**(2): p. 87-91.
46. Bosher, L.H. and F.H. Taylor, *Heterotopic gastric mucosa in the esophagus with ulceration and stricture formation.* J Thorac Surg, 1951. **21**(3): p. 306-12.
47. Morson, B.C. and J.R. Belcher, *Adenocarcinoma of the oesophagus and ectopic gastric mucosa.* Br J Cancer, 1952. **6**(2): p. 127-30.
48. Moersch, R.N., F.H. Ellis, Jr., and D.J. Mc, *Pathologic changes occurring in severe reflux esophagitis.* Surg Gynecol Obstet, 1959. **108**(4): p. 476-84.
49. Bremner, C.G., V.P. Lynch, and F.H. Ellis, Jr., *Barrett's esophagus: congenital or acquired? An experimental study of esophageal mucosal regeneration in the dog.* Surgery, 1970. **68**(1): p. 209-16.
50. Hayward, J., *The lower end of the oesophagus.* Thorax, 1961. **16**: p. 36-41.
51. Abrams, L. and D. Heath, *Lower Oesophagus Lined with Intestinal and Gastric Epithelia.* Thorax, 1965. **20**: p. 66-72.
52. Hershfield, N.B., et al., *Secretory function of Barrett's epithelium.* Gut, 1965. **6**(6): p. 535-9.
53. Trier, J.S., *Morphology of the epithelium of the distal esophagus in patients with midesophageal peptic strictures.* Gastroenterology, 1970. **58**(4): p. 444-61.

54. Hage, E. and S.A. Pedersen, *Morphological characteristics of the columnar epithelium lining the lower oesophagus in patients with Barrett's syndrome*. Virchows Arch A Pathol Pathol Anat, 1972. **357**(3): p. 219-29.
55. Borrie, J. and L. Goldwater, *Columnar cell-lined esophagus: assessment of etiology and treatment. A 22 year experience*. J Thorac Cardiovasc Surg, 1976. **71**(6): p. 825-34.
56. Paull, A., et al., *The histologic spectrum of Barrett's esophagus*. N Engl J Med, 1976. **295**(9): p. 476-80.
57. Adler, R.H., *The lower esophagus lined by columnar epithelium. Its association with hiatal hernia, ulcer, stricture, and tumor*. J Thorac Cardiovasc Surg, 1963. **45**: p. 13-34.
58. Hawe, A., et al., *Adenocarcinima in the columnar epithelial lined lower (Barret) oesophagus*. Thorax, 1973. **28**(4): p. 511-4.
59. Sampliner, R.E., *Practice guidelines on the diagnosis, surveillance, and therapy of Barrett's esophagus. The Practice Parameters Committee of the American College of Gastroenterology*. Am J Gastroenterol, 1998. **93**(7): p. 1028-32.
60. DeMeester, S.R. and T.R. DeMeester, *Columnar mucosa and intestinal metaplasia of the esophagus: fifty years of controversy*. Ann Surg, 2000. **231**(3): p. 303-21.
61. Wiseman, E.F. and Y.S. Ang, *Risk factors for neoplastic progression in Barrett's esophagus*. World J Gastroenterol, 2011. **17**(32): p. 3672-83.
62. Prasad, G.A., et al., *Predictors of progression in Barrett's esophagus: current knowledge and future directions*. Am J Gastroenterol, 2010. **105**(7): p. 1490-1502.
63. Reid, B.J., et al., *Barrett's oesophagus and oesophageal adenocarcinoma: time for a new synthesis*. Nat Rev Cancer, 2010. **10**(2): p. 87-101.
64. Khieu, M. and S.S. Bhimji, *Barrett Esophagus*, in *StatPearls*. 2018: Treasure Island (FL).
65. Schlottmann, F., M.G. Patti, and N.J. Shaheen, *From Heartburn to Barrett's Esophagus, and Beyond*. World J Surg, 2017. **41**(7): p. 1698-1704.
66. Shaheen, N.J., et al., *ACG Clinical Guideline: Diagnosis and Management of Barrett's Esophagus*. Am J Gastroenterol, 2016. **111**(1): p. 30-50; quiz 51.
67. Runge, T.M., J.A. Abrams, and N.J. Shaheen, *Epidemiology of Barrett's Esophagus and Esophageal Adenocarcinoma*. Gastroenterol Clin North Am, 2015. **44**(2): p. 203-31.
68. Rubenstein, J.H., *Clinical prediction and screening for barrett esophagus*. Gastroenterol Hepatol (N Y), 2014. **10**(3): p. 187-9.
69. Modiano, N. and L.B. Gerson, *Barrett's esophagus: Incidence, etiology, pathophysiology, prevention and treatment*. Ther Clin Risk Manag, 2007. **3**(6): p. 1035-145.
70. Splittgerber, M. and V. Velanovich, *Barrett esophagus*. Surg Clin North Am, 2015. **95**(3): p. 593-604.
71. Basu, K.K. and J.S. de Caestecker, *Surveillance in Barrett's oesophagus: a personal view*. Postgrad Med J, 2002. **78**(919): p. 263-8.
72. Schoofs, N., R. Bisschops, and H. Prenen, *Progression of Barrett's esophagus toward esophageal adenocarcinoma: an overview*. Ann Gastroenterol, 2017. **30**(1): p. 1-6.
73. Cameron, A.J., et al., *Prevalence of columnar-lined (Barrett's) esophagus. Comparison of population-based clinical and autopsy findings*. Gastroenterology, 1990. **99**(4): p. 918-22.
74. Rex, D.K., et al., *Screening for Barrett's esophagus in colonoscopy patients with and without heartburn*. Gastroenterology, 2003. **125**(6): p. 1670-7.
75. Ward, E.M., et al., *Barrett's esophagus is common in older men and women undergoing screening colonoscopy regardless of reflux symptoms*. Am J Gastroenterol, 2006. **101**(1): p. 12-7.
76. Fock, K.M. and T.L. Ang, *Global epidemiology of Barrett's esophagus*. Expert Rev Gastroenterol Hepatol, 2011. **5**(1): p. 123-30.
77. Whiteman, D.C. and B.J. Kendall, *Barrett's oesophagus: epidemiology, diagnosis and clinical management*. Med J Aust, 2016. **205**(7): p. 317-24.
78. Ronkainen, J., et al., *Prevalence of Barrett's esophagus in the general population: an endoscopic study*. Gastroenterology, 2005. **129**(6): p. 1825-31.
79. Zagari, R.M., et al., *Gastro-oesophageal reflux symptoms, oesophagitis and Barrett's oesophagus in the general population: the Loiano-Monghidoro study*. Gut, 2008. **57**(10): p. 1354-9.
80. Zou, D., et al., *Epidemiology of symptom-defined gastroesophageal reflux disease and reflux esophagitis: the systematic investigation of gastrointestinal diseases in China (SILC)*. Scand J Gastroenterol, 2011. **46**(2): p. 133-41.

81. Pophali, P. and M. Halland, *Barrett's oesophagus: diagnosis and management*. BMJ, 2016. **353**: p. i2373.
82. Dent, J., *Barrett's esophagus: A historical perspective, an update on core practicalities and predictions on future evolutions of management*. J Gastroenterol Hepatol, 2011. **26 Suppl 1**: p. 11-30.
83. Thrift, A.P., N. Pandeya, and D.C. Whiteman, *Current status and future perspectives on the etiology of esophageal adenocarcinoma*. Front Oncol, 2012. **2**: p. 11.
84. Brandtner, A.K. and M. Quante, *Risk prediction in Barrett's esophagus - aspects of a combination of molecular and epidemiologic biomarkers reflecting alterations of the microenvironment*. Scand J Clin Lab Invest Suppl, 2016. **245**: p. S63-9.
85. Thrift, A.P., *Determination of risk for Barrett's esophagus and esophageal adenocarcinoma*. Curr Opin Gastroenterol, 2016. **32**(4): p. 319-24.
86. Macias-Garcia, F. and J.E. Dominguez-Munoz, *Update on management of Barrett's esophagus*. World J Gastrointest Pharmacol Ther, 2016. **7**(2): p. 227-34.
87. Pohl, H., B. Sirovich, and H.G. Welch, *Esophageal adenocarcinoma incidence: are we reaching the peak?* Cancer Epidemiol Biomarkers Prev, 2010. **19**(6): p. 1468-70.
88. Wani, S., et al., *Diagnosis and Management of Low-Grade Dysplasia in Barrett's Esophagus: Expert Review From the Clinical Practice Updates Committee of the American Gastroenterological Association*. Gastroenterology, 2016. **151**(5): p. 822-835.
89. Masclee, G.M., et al., *The incidence of Barrett's oesophagus and oesophageal adenocarcinoma in the United Kingdom and The Netherlands is levelling off*. Aliment Pharmacol Ther, 2014. **39**(11): p. 1321-30.
90. Lagergren, J. and F. Mattsson, *No further increase in the incidence of esophageal adenocarcinoma in Sweden*. Int J Cancer, 2011. **129**(2): p. 513-6.
91. di Pietro, M., D. Alzoubaidi, and R.C. Fitzgerald, *Barrett's esophagus and cancer risk: how research advances can impact clinical practice*. Gut Liver, 2014. **8**(4): p. 356-70.
92. Bennett, C., et al., *Consensus statements for management of Barrett's dysplasia and early-stage esophageal adenocarcinoma, based on a Delphi process*. Gastroenterology, 2012. **143**(2): p. 336-46.
93. Coleman, H.G., et al., *Increasing incidence of Barrett's oesophagus: a population-based study*. Eur J Epidemiol, 2011. **26**(9): p. 739-45.
94. van Soest, E.M., et al., *Increasing incidence of Barrett's oesophagus in the general population*. Gut, 2005. **54**(8): p. 1062-6.
95. de Jonge, P.J., et al., *Barrett's oesophagus: epidemiology, cancer risk and implications for management*. Gut, 2013.
96. Schneider, J.L. and D.A. Corley, *The Troublesome Epidemiology of Barrett's Esophagus and Esophageal Adenocarcinoma*. Gastrointest Endosc Clin N Am, 2017. **27**(3): p. 353-364.
97. Cook, M.B., et al., *Risk of mortality and cancer incidence in Barrett's esophagus*. Cancer Epidemiol Biomarkers Prev, 2007. **16**(10): p. 2090-6.
98. Cameron, A.J., B.J. Ott, and W.S. Payne, *The incidence of adenocarcinoma in columnar-lined (Barrett's) esophagus*. N Engl J Med, 1985. **313**(14): p. 857-9.
99. Rana, P.S. and D.A. Johnston, *Incidence of adenocarcinoma and mortality in patients with Barrett's oesophagus diagnosed between 1976 and 1986: implications for endoscopic surveillance*. Dis Esophagus, 2000. **13**(1): p. 28-31.
100. Solaymani-Dodaran, M., et al., *Risk of oesophageal cancer in Barrett's oesophagus and gastro-oesophageal reflux*. Gut, 2004. **53**(8): p. 1070-4.
101. Falk, G.W., *Barrett's oesophagus: frequency and prediction of dysplasia and cancer*. Best Pract Res Clin Gastroenterol, 2015. **29**(1): p. 125-38.
102. de Jonge, P.J., et al., *Risk of malignant progression in patients with Barrett's oesophagus: a Dutch nationwide cohort study*. Gut, 2010. **59**(8): p. 1030-6.
103. Hvid-Jensen, F., et al., *Incidence of adenocarcinoma among patients with Barrett's esophagus*. N Engl J Med, 2011. **365**(15): p. 1375-83.
104. Desai, T.K., et al., *The incidence of oesophageal adenocarcinoma in non-dysplastic Barrett's oesophagus: a meta-analysis*. Gut, 2012. **61**(7): p. 970-6.
105. Singh, S., et al., *Incidence of esophageal adenocarcinoma in Barrett's esophagus with low-grade dysplasia: a systematic review and meta-analysis*. Gastrointest Endosc, 2014. **79**(6): p. 897-909 e4; quiz 983 e1, 983 e3.
106. Phoa, K.N., et al., *Radiofrequency ablation vs endoscopic surveillance for patients with Barrett esophagus and low-grade dysplasia: a randomized clinical trial*. JAMA, 2014. **311**(12): p. 1209-17.

107. Rastogi, A., et al., *Incidence of esophageal adenocarcinoma in patients with Barrett's esophagus and high-grade dysplasia: a meta-analysis.* Gastrointest Endosc, 2008. **67**(3): p. 394-8.
108. Shaheen, N.J., et al., *Radiofrequency ablation in Barrett's esophagus with dysplasia.* N Engl J Med, 2009. **360**(22): p. 2277-88.
109. Duits, L.C., et al., *Barrett's oesophagus patients with low-grade dysplasia can be accurately risk-stratified after histological review by an expert pathology panel.* Gut, 2015. **64**(5): p. 700-6.
110. Weusten, B., et al., *Endoscopic management of Barrett's esophagus: European Society of Gastrointestinal Endoscopy (ESGE) Position Statement.* Endoscopy, 2017. **49**(2): p. 191-198.
111. Winberg, H., et al., *Risk factors and chemoprevention in Barrett's esophagus--an update.* Scand J Gastroenterol, 2012. **47**(4): p. 397-406.
112. Wong, A. and R.C. Fitzgerald, *Epidemiologic risk factors for Barrett's esophagus and associated adenocarcinoma.* Clin Gastroenterol Hepatol, 2005. **3**(1): p. 1-10.
113. di Pietro, M. and R.C. Fitzgerald, *Barrett's oesophagus: an ideal model to study cancer genetics.* Hum Genet, 2009. **126**(2): p. 233-46.
114. Clemons, N.J., S.Y. Koh, and W.A. Phillips, *Advances in understanding the pathogenesis of Barrett's esophagus.* Discov Med, 2014. **17**(91): p. 7-14.
115. Spechler, S.J., *Barrett esophagus and risk of esophageal cancer: a clinical review.* JAMA, 2013. **310**(6): p. 627-36.
116. Evans, R.P., et al., *Evolving management of metaplasia and dysplasia in Barrett's epithelium.* World J Gastroenterol, 2016. **22**(47): p. 10316-10324.
117. Vakil, N., et al., *The Montreal definition and classification of gastroesophageal reflux disease: a global evidence-based consensus.* Am J Gastroenterol, 2006. **101**(8): p. 1900-20; quiz 1943.
118. Gordon, C., et al., *The role of the hiatus hernia in gastro-oesophageal reflux disease.* Aliment Pharmacol Ther, 2004. **20**(7): p. 719-32.
119. Hardikar, S., et al., *The role of tobacco, alcohol, and obesity in neoplastic progression to esophageal adenocarcinoma: a prospective study of Barrett's esophagus.* PLoS One, 2013. **8**(1): p. e52192.
120. Avidan, B., et al., *Hiatal hernia size, Barrett's length, and severity of acid reflux are all risk factors for esophageal adenocarcinoma.* Am J Gastroenterol, 2002. **97**(8): p. 1930-6.
121. Weston, A.P., A.S. Badr, and R.S. Hassanein, *Prospective multivariate analysis of clinical, endoscopic, and histological factors predictive of the development of Barrett's multifocal high-grade dysplasia or adenocarcinoma.* Am J Gastroenterol, 1999. **94**(12): p. 3413-9.
122. Spechler, S.J., et al., *History, molecular mechanisms, and endoscopic treatment of Barrett's esophagus.* Gastroenterology, 2010. **138**(3): p. 854-69.
123. Friedrich, M.J., *Global Obesity Epidemic Worsening.* JAMA, 2017. **318**(7): p. 603.
124. Long, E. and I.L. Beales, *The role of obesity in oesophageal cancer development.* Therap Adv Gastroenterol, 2014. **7**(6): p. 247-68.
125. Lynch, K.L., *Is Obesity Associated with Barrett's Esophagus and Esophageal Adenocarcinoma?* Gastroenterol Clin North Am, 2016. **45**(4): p. 615-624.
126. Watanabe, S., M. Hojo, and A. Nagahara, *Metabolic syndrome and gastrointestinal diseases.* J Gastroenterol, 2007. **42**(4): p. 267-74.
127. Ireland, C.J., et al., *Risk factors for Barrett's esophagus: a scoping review.* Cancer Causes Control, 2016. **27**(3): p. 301-23.
128. Falk, G.W., et al., *Barrett's esophagus: prevalence-incidence and etiology-origins.* Ann N Y Acad Sci, 2011. **1232**: p. 1-17.
129. Kubo, A., et al., *Cigarette smoking and the risk of Barrett's esophagus.* Cancer Causes Control, 2009. **20**(3): p. 303-11.
130. Wroblewski, L.E., R.M. Peek, Jr., and K.T. Wilson, *Helicobacter pylori and gastric cancer: factors that modulate disease risk.* Clin Microbiol Rev, 2010. **23**(4): p. 713-39.
131. Polk, D.B. and R.M. Peek, Jr., *Helicobacter pylori: gastric cancer and beyond.* Nat Rev Cancer, 2010. **10**(6): p. 403-14.
132. Appelman, H.D., et al., *Progression of esophageal dysplasia to cancer.* Ann N Y Acad Sci, 2014. **1325**: p. 96-107.
133. Halland, M., D. Katzka, and P.G. Iyer, *Recent developments in pathogenesis, diagnosis and therapy of Barrett's esophagus.* World J Gastroenterol, 2015. **21**(21): p. 6479-90.

134. Labenz, J., et al., *The epidemiology, diagnosis, and treatment of Barrett's carcinoma*. Dtsch Arztebl Int, 2015. **112**(13): p. 224-33; quiz 234.
135. Schneider, J.L. and D.A. Corley, *A review of the epidemiology of Barrett's oesophagus and oesophageal adenocarcinoma*. Best Pract Res Clin Gastroenterol, 2015. **29**(1): p. 29-39.
136. Shaheen, N.J. and J.E. Richter, *Barrett's oesophagus*. Lancet, 2009. **373**(9666): p. 850-61.
137. Brown, C.S. and M.B. Ujiki, *Risk factors affecting the Barrett's metaplasia-dysplasia-neoplasia sequence*. World J Gastrointest Endosc, 2015. **7**(5): p. 438-45.
138. Rubenstein, J.H. and N.J. Shaheen, *Epidemiology, Diagnosis, and Management of Esophageal Adenocarcinoma*. Gastroenterology, 2015. **149**(2): p. 302-17 e1.
139. Falk, G.W., *Updated Guidelines for Diagnosing and Managing Barrett Esophagus*. Gastroenterol Hepatol (N Y), 2016. **12**(7): p. 449-51.
140. Spechler, S.J. and R.F. Souza, *Barrett's esophagus*. N Engl J Med, 2014. **371**(9): p. 836-45.
141. Qureshi, A.P., et al., *Biomarkers for Barrett's esophagus - a contemporary review*. Expert Rev Mol Diagn, 2018. **18**(11): p. 939-946.
142. Maley, C.C., *Multistage carcinogenesis in Barrett's esophagus*. Cancer Lett, 2007. **245**(1-2): p. 22-32.
143. Zibadi, S. and D. Coppola, *Surgical and Molecular Pathology of Barrett Esophagus*. Cancer Control, 2015. **22**(2): p. 177-85.
144. Hanahan, D. and R.A. Weinberg, *The hallmarks of cancer*. Cell, 2000. **100**(1): p. 57-70.
145. Hanahan, D. and R.A. Weinberg, *Hallmarks of cancer: the next generation*. Cell, 2011. **144**(5): p. 646-74.
146. Konda, V.J.A. and R.F. Souza, *Biomarkers of Barrett's Esophagus: From the Laboratory to Clinical Practice*. Dig Dis Sci, 2018. **63**(8): p. 2070-2080.
147. Morales, C.P., R.F. Souza, and S.J. Spechler, *Hallmarks of cancer progression in Barrett's oesophagus*. Lancet, 2002. **360**(9345): p. 1587-9.
148. Appelman, H.D., et al., *The esophageal mucosa and submucosa: immunohistology in GERD and Barrett's esophagus*. Ann N Y Acad Sci, 2013. **1300**: p. 144-165.
149. Phillips, W.A., et al., *Barrett's esophagus*. J Gastroenterol Hepatol, 2011. **26**(4): p. 639-48.
150. Krishnadath, K.K. and K.K. Wang, *Molecular pathogenesis of Barrett esophagus: current evidence*. Gastroenterol Clin North Am, 2015. **44**(2): p. 233-47.
151. Langner, C., et al., *Multilayered epithelium at the gastroesophageal junction is a marker of gastroesophageal reflux disease: data from a prospective Central European multicenter study (histoGERD trial)*. Virchows Arch, 2014. **464**(4): p. 409-17.
152. Flejou, J.F., *Barrett's oesophagus: from metaplasia to dysplasia and cancer*. Gut, 2005. **54 Suppl 1**: p. i6-12.
153. Goldblum, J.R., *Barrett's esophagus and Barrett's-related dysplasia*. Mod Pathol, 2003. **16**(4): p. 316-24.
154. Odze, R.D., *What the gastroenterologist needs to know about the histology of Barrett's esophagus*. Curr Opin Gastroenterol, 2011. **27**(4): p. 389-96.
155. Odze, R.D., *Barrett esophagus: histology and pathology for the clinician*. Nat Rev Gastroenterol Hepatol, 2009. **6**(8): p. 478-90.
156. Naini, B.V., et al., *Barrett's oesophagus diagnostic criteria: endoscopy and histology*. Best Pract Res Clin Gastroenterol, 2015. **29**(1): p. 77-96.
157. Goldblum, J.R., *Current issues in Barrett's esophagus and Barrett's-related dysplasia*. Mod Pathol, 2015. **28 Suppl 1**: p. S1-6.
158. Waters, K.M., et al., *Refined Criteria for Separating Low-grade Dysplasia and Nondysplastic Barrett Esophagus Reduce Equivocal Diagnoses and Improve Prediction of Patient Outcome: A 10-Year Review*. Am J Surg Pathol, 2018. **42**(12): p. 1723-1729.
159. Montgomery, E., et al., *Some observations on Barrett esophagus and associated dysplasia*. Ann Diagn Pathol, 2018. **37**: p. 75-82.
160. Zeki, S. and R.C. Fitzgerald, *Targeting care in Barrett's oesophagus*. Clin Med (Lond), 2014. **14 Suppl 6**: p. s78-83.
161. Gindea, C., et al., *Barrett esophagus: history, definition and etiopathogeny*. J Med Life, 2014. **7 Spec No. 3**: p. 23-30.
162. Rhee, H. and D.H. Wang, *Cellular Origins of Barrett's Esophagus: the Search Continues*. Curr Gastroenterol Rep, 2018. **20**(11): p. 51.

163. Clemons, N.J., W.A. Phillips, and R.V. Lord, *Signaling pathways in the molecular pathogenesis of adenocarcinomas of the esophagus and gastroesophageal junction.* Cancer Biol Ther, 2013. **14**(9): p. 782-95.
164. Wang, D.H., et al., *Aberrant epithelial-mesenchymal Hedgehog signaling characterizes Barrett's metaplasia.* Gastroenterology, 2010. **138**(5): p. 1810-22.
165. Liu, T., et al., *Regulation of Cdx2 expression by promoter methylation, and effects of Cdx2 transfection on morphology and gene expression of human esophageal epithelial cells.* Carcinogenesis, 2007. **28**(2): p. 488-96.
166. Milano, F., et al., *Bone morphogenetic protein 4 expressed in esophagitis induces a columnar phenotype in esophageal squamous cells.* Gastroenterology, 2007. **132**(7): p. 2412-21.
167. Menke, V., et al., *Conversion of metaplastic Barrett's epithelium into post-mitotic goblet cells by gamma-secretase inhibition.* Dis Model Mech, 2010. **3**(1-2): p. 104-10.
168. Pavlov, K., et al., *Embryological signaling pathways in Barrett's metaplasia development and malignant transformation; mechanisms and therapeutic opportunities.* Crit Rev Oncol Hematol, 2014. **92**(1): p. 25-37.
169. Bian, Y.S., et al., *Nuclear accumulation of beta-catenin is a common and early event during neoplastic progression of Barrett esophagus.* Am J Clin Pathol, 2000. **114**(4): p. 583-90.
170. Moyes, L.H., et al., *Activation of Wnt signalling promotes development of dysplasia in Barrett's oesophagus.* J Pathol, 2012. **228**(1): p. 99-112.
171. Cooke, G., A. Blanco-Fernandez, and J.P. Seery, *The effect of retinoic acid and deoxycholic acid on the differentiation of primary human esophageal keratinocytes.* Dig Dis Sci, 2008. **53**(11): p. 2851-7.
172. Chang, C.L., et al., *Retinoic acid-induced glandular differentiation of the oesophagus.* Gut, 2007. **56**(7): p. 906-17.
173. Colleypriest, B.J., S.G. Ward, and D. Tosh, *How does inflammation cause Barrett's metaplasia?* Curr Opin Pharmacol, 2009. **9**(6): p. 721-6.
174. Picardo, S.L., et al., *Barrett's to oesophageal cancer sequence: a model of inflammatory-driven upper gastrointestinal cancer.* Dig Surg, 2012. **29**(3): p. 251-60.
175. Dvorak, K., et al., *Bile acids in combination with low pH induce oxidative stress and oxidative DNA damage: relevance to the pathogenesis of Barrett's oesophagus.* Gut, 2007. **56**(6): p. 763-71.
176. Clemons, N.J., K.E. McColl, and R.C. Fitzgerald, *Nitric oxide and acid induce double-strand DNA breaks in Barrett's esophagus carcinogenesis via distinct mechanisms.* Gastroenterology, 2007. **133**(4): p. 1198-209.
177. Cardin, R., et al., *Oxidative DNA damage in Barrett mucosa: correlation with telomeric dysfunction and p53 mutation.* Ann Surg Oncol, 2013. **20 Suppl 3**: p. S583-9.
178. Clark, R.J., et al., *microRNA involvement in the onset and progression of Barrett's esophagus: a systematic review.* Oncotarget, 2018. **9**(8): p. 8179-8196.
179. Garman, K.S., et al., *MicroRNA expression differentiates squamous epithelium from Barrett's esophagus and esophageal cancer.* Dig Dis Sci, 2013. **58**(11): p. 3178-88.
180. Revilla-Nuin, B., et al., *Predictive value of MicroRNAs in the progression of barrett esophagus to adenocarcinoma in a long-term follow-up study.* Ann Surg, 2013. **257**(5): p. 886-93.
181. Bhan, A., M. Soleimani, and S.S. Mandal, *Long Noncoding RNA and Cancer: A New Paradigm.* Cancer Res, 2017. **77**(15): p. 3965-3981.
182. Abraham, J.M. and S.J. Meltzer, *Long Noncoding RNAs in the Pathogenesis of Barrett's Esophagus and Esophageal Carcinoma.* Gastroenterology, 2017. **153**(1): p. 27-34.
183. Kaz, A.M., et al., *Genetic and Epigenetic Alterations in Barrett's Esophagus and Esophageal Adenocarcinoma.* Gastroenterol Clin North Am, 2015. **44**(2): p. 473-89.
184. Grady, W.M. and M. Yu, *Molecular Evolution of Metaplasia to Adenocarcinoma in the Esophagus.* Dig Dis Sci, 2018.
185. Gregson, E.M., J. Bornschein, and R.C. Fitzgerald, *Genetic progression of Barrett's oesophagus to oesophageal adenocarcinoma.* Br J Cancer, 2016. **115**(4): p. 403-10.
186. Reid, B.J., T.G. Paulson, and X. Li, *Genetic Insights in Barrett's Esophagus and Esophageal Adenocarcinoma.* Gastroenterology, 2015. **149**(5): p. 1142-1152 e3.

187. Ross-Innes, C.S., et al., *Whole-genome sequencing provides new insights into the clonal architecture of Barrett's esophagus and esophageal adenocarcinoma*. Nat Genet, 2015. **47**(9): p. 1038-1046.
188. Reid, B.J., et al., *Barrett's esophagus: ordering the events that lead to cancer*. Eur J Cancer Prev, 1996. **5 Suppl 2**: p. 57-65.
189. Wu, T.T., et al., *Genetic alterations in Barrett esophagus and adenocarcinomas of the esophagus and esophagogastric junction region*. Am J Pathol, 1998. **153**(1): p. 287-94.
190. Krishnadath, K.K., et al., *Accumulation of genetic abnormalities during neoplastic progression in Barrett's esophagus*. Cancer Res, 1995. **55**(9): p. 1971-6.
191. Barrett, M.T., et al., *Determination of the frequency of loss of heterozygosity in esophageal adenocarcinoma by cell sorting, whole genome amplification and microsatellite polymorphisms*. Oncogene, 1996. **12**(9): p. 1873-8.
192. Herbst, J.J., et al., *Cell proliferation in esophageal columnar epithelium (Barrett's esophagus)*. Gastroenterology, 1978. **75**(4): p. 683-7.
193. Gray, M.R., et al., *Epithelial proliferation in Barrett's esophagus by proliferating cell nuclear antigen immunolocalization*. Gastroenterology, 1992. **103**(6): p. 1769-76.
194. Reid, B.J., et al., *Barrett's esophagus: cell cycle abnormalities in advancing stages of neoplastic progression*. Gastroenterology, 1993. **105**(1): p. 119-29.
195. Reid, B.J., et al., *Flow-cytometric and histological progression to malignancy in Barrett's esophagus: prospective endoscopic surveillance of a cohort*. Gastroenterology, 1992. **102**(4 Pt 1): p. 1212-9.
196. Galipeau, P.C., et al., *17p (p53) allelic losses, 4N (G2/tetraploid) populations, and progression to aneuploidy in Barrett's esophagus*. Proc Natl Acad Sci U S A, 1996. **93**(14): p. 7081-4.
197. Galipeau, P.C., et al., *Clonal expansion and loss of heterozygosity at chromosomes 9p and 17p in premalignant esophageal (Barrett's) tissue*. J Natl Cancer Inst, 1999. **91**(24): p. 2087-95.
198. Wong, D.J., et al., *p16INK4a promoter is hypermethylated at a high frequency in esophageal adenocarcinomas*. Cancer Res, 1997. **57**(13): p. 2619-22.
199. Maley, C.C., et al., *Selectively advantageous mutations and hitchhikers in neoplasms: p16 lesions are selected in Barrett's esophagus*. Cancer Res, 2004. **64**(10): p. 3414-27.
200. Barrett, M.T., et al., *Evolution of neoplastic cell lineages in Barrett oesophagus*. Nat Genet, 1999. **22**(1): p. 106-9.
201. Wong, D.J., et al., *p16(INK4a) lesions are common, early abnormalities that undergo clonal expansion in Barrett's metaplastic epithelium*. Cancer Res, 2001. **61**(22): p. 8284-9.
202. Jenkins, G.J., et al., *Genetic pathways involved in the progression of Barrett's metaplasia to adenocarcinoma*. Br J Surg, 2002. **89**(7): p. 824-37.
203. Maley, C.C. and B.J. Reid, *Natural selection in neoplastic progression of Barrett's esophagus*. Semin Cancer Biol, 2005. **15**(6): p. 474-83.
204. Contino, G., et al., *The Evolving Genomic Landscape of Barrett's Esophagus and Esophageal Adenocarcinoma*. Gastroenterology, 2017. **153**(3): p. 657-673 e1.
205. Leedham, S.J., et al., *Individual crypt genetic heterogeneity and the origin of metaplastic glandular epithelium in human Barrett's oesophagus*. Gut, 2008. **57**(8): p. 1041-8.
206. Maley, C.C., et al., *Genetic clonal diversity predicts progression to esophageal adenocarcinoma*. Nat Genet, 2006. **38**(4): p. 468-73.
207. Reid, B.J., *Surrogate Markers: Lessons from the Next Gen?* Cancer Prev Res (Phila), 2016. **9**(7): p. 512-7.
208. Stachler, M.D., et al., *Detection of Mutations in Barrett's Esophagus Before Progression to High-Grade Dysplasia or Adenocarcinoma*. Gastroenterology, 2018. **155**(1): p. 156-167.
209. Boonstra, J.J., et al., *Mapping of homozygous deletions in verified esophageal adenocarcinoma cell lines and xenografts*. Genes Chromosomes Cancer, 2012. **51**(3): p. 272-82.
210. Phillips, W.A., et al., *Mutation analysis of PIK3CA and PIK3CB in esophageal cancer and Barrett's esophagus*. Int J Cancer, 2006. **118**(10): p. 2644-6.
211. Dulak, A.M., et al., *Exome and whole-genome sequencing of esophageal adenocarcinoma identifies recurrent driver events and mutational complexity*. Nat Genet, 2013. **45**(5): p. 478-86.

212. Streppel, M.M., et al., *Next-generation sequencing of endoscopic biopsies identifies ARID1A as a tumor-suppressor gene in Barrett's esophagus*. Oncogene, 2014. **33**(3): p. 347-57.
213. Weaver, J.M.J., et al., *Ordering of mutations in preinvasive disease stages of esophageal carcinogenesis*. Nat Genet, 2014. **46**(8): p. 837-843.
214. Stachler, M.D., et al., *Paired exome analysis of Barrett's esophagus and adenocarcinoma*. Nat Genet, 2015. **47**(9): p. 1047-55.
215. Dulak, A.M., et al., *Gastrointestinal adenocarcinomas of the esophagus, stomach, and colon exhibit distinct patterns of genome instability and oncogenesis*. Cancer Res, 2012. **72**(17): p. 4383-93.
216. Nones, K., et al., *Genomic catastrophes frequently arise in esophageal adenocarcinoma and drive tumorigenesis*. Nat Commun, 2014. **5**: p. 5224.
217. Carter, S.L., et al., *Absolute quantification of somatic DNA alterations in human cancer*. Nat Biotechnol, 2012. **30**(5): p. 413-21.
218. Agrawal, N., et al., *Comparative genomic analysis of esophageal adenocarcinoma and squamous cell carcinoma*. Cancer Discov, 2012. **2**(10): p. 899-905.
219. Kastelein, F., et al., *Aberrant p53 protein expression is associated with an increased risk of neoplastic progression in patients with Barrett's oesophagus*. Gut, 2013. **62**(12): p. 1676-83.
220. Li, X., et al., *Temporal and spatial evolution of somatic chromosomal alterations: a case-cohort study of Barrett's esophagus*. Cancer Prev Res (Phila), 2014. **7**(1): p. 114-27.
221. Dunbar, K.B. and R.F. Souza, *Beyond Dysplasia Grade: The Role of Biomarkers in Stratifying Risk*. Gastrointest Endosc Clin N Am, 2017. **27**(3): p. 447-459.
222. Eluri, S. and N.J. Shaheen, *Barrett's esophagus: diagnosis and management*. Gastrointest Endosc, 2017. **85**(5): p. 889-903.
223. Mansour, N.M., S.S. Groth, and S. Anandasabapathy, *Esophageal Adenocarcinoma: Screening, Surveillance, and Management*. Annu Rev Med, 2017. **68**: p. 213-227.
224. Wani, S. and S. Gaddam, *Editorial: Best Practices in Surveillance of Barrett's Esophagus*. Am J Gastroenterol, 2017. **112**(7): p. 1056-1060.
225. Amadi, C. and P. Gatenby, *Barrett's oesophagus: Current controversies*. World J Gastroenterol, 2017. **23**(28): p. 5051-5067.
226. Rajendra, S. and P. Sharma, *Barrett Esophagus and Intramucosal Esophageal Adenocarcinoma*. Hematol Oncol Clin North Am, 2017. **31**(3): p. 409-426.
227. van der Wel, M.J., et al., *What Makes an Expert Barrett's Histopathologist?* Adv Exp Med Biol, 2016. **908**: p. 137-59.
228. Rajendra, S., *Barrett's oesophagus: can meaningful screening and surveillance guidelines be formulated based on new data and rejigging the old paradigm?* Best Pract Res Clin Gastroenterol, 2015. **29**(1): p. 65-75.
229. Lochhead, P. and A.T. Chan, *Screening and surveillance for Barrett esophagus*. JAMA Intern Med, 2015. **175**(2): p. 159-60.
230. Graham, D., et al., *Monitoring the premalignant potential of Barrett's oesophagus'*. Frontline Gastroenterol, 2016. **7**(4): p. 316-322.
231. Sami, S.S., K. Ragunath, and P.G. Iyer, *Screening for Barrett's esophagus and esophageal adenocarcinoma: rationale, recent progress, challenges, and future directions*. Clin Gastroenterol Hepatol, 2015. **13**(4): p. 623-34.
232. Kadri, S.R., et al., *Acceptability and accuracy of a non-endoscopic screening test for Barrett's oesophagus in primary care: cohort study*. BMJ, 2010. **341**: p. c4372.
233. Sharma, P., et al., *Real-time increased detection of neoplastic tissue in Barrett's esophagus with probe-based confocal laser endomicroscopy: final results of an international multicenter, prospective, randomized, controlled trial.* Gastrointest Endosc, 2011. **74**(3): p. 465-72.
234. Martinucci, I., et al., *Barrett's esophagus in 2016: From pathophysiology to treatment*. World J Gastrointest Pharmacol Ther, 2016. **7**(2): p. 190-206.
235. Gregson, E.M. and R.C. Fitzgerald, *Biomarkers for dysplastic Barrett's: ready for prime time?* World J Surg, 2015. **39**(3): p. 568-77.
236. Ong, C.A., P. Lao-Sirieix, and R.C. Fitzgerald, *Biomarkers in Barrett's esophagus and esophageal adenocarcinoma: predictors of progression and prognosis*. World J Gastroenterol, 2010. **16**(45): p. 5669-81.
237. Moyes, L.H. and J.J. Going, *Still waiting for predictive biomarkers in Barrett's oesophagus*. J Clin Pathol, 2011. **64**(9): p. 742-50.

238. Fouad, Y.M., et al., *Biomarkers of Barrett's esophagus.* World J Gastrointest Pathophysiol, 2014. **5**(4): p. 450-6.
239. Mischak, H., et al., *Implementation of proteomic biomarkers: making it work.* Eur J Clin Invest, 2012. **42**(9): p. 1027-36.
240. Huang, Q. and L.J. Hardie, *Biomarkers in Barrett's oesophagus.* Biochem Soc Trans, 2010. **38**(2): p. 343-7.
241. Collins, F.S. and H. Varmus, *A new initiative on precision medicine.* N Engl J Med, 2015. **372**(9): p. 793-5.
242. Ioannidis, J.P.A. and P.M.M. Bossuyt, *Waste, Leaks, and Failures in the Biomarker Pipeline.* Clin Chem, 2017. **63**(5): p. 963-972.
243. Selleck, M.J., M. Senthil, and N.R. Wall, *Making Meaningful Clinical Use of Biomarkers.* Biomark Insights, 2017. **12**: p. 1177271917715236.
244. Ramzan, Z., A.B. Nassri, and S. Huerta, *The use of imaging and biomarkers in diagnosing Barrett's esophagus and predicting the risk of neoplastic progression.* Expert Rev Mol Diagn, 2014. **14**(5): p. 575-91.
245. Bansal, A. and R.C. Fitzgerald, *Biomarkers in Barrett's Esophagus: Role in Diagnosis, Risk Stratification, and Prediction of Response to Therapy.* Gastroenterol Clin North Am, 2015. **44**(2): p. 373-90.
246. Timmer, M.R., et al., *Predictive biomarkers for Barrett's esophagus: so near and yet so far.* Dis Esophagus, 2013. **26**(6): p. 574-81.
247. Reid, B.J., et al., *Predictors of progression to cancer in Barrett's esophagus: baseline histology and flow cytometry identify low- and high-risk patient subsets.* Am J Gastroenterol, 2000. **95**(7): p. 1669-76.
248. Rubenstein, J.H., *Improving the efficiency of Barrett's esophagus management: do biomarkers hit the mark?* Gastrointest Endosc, 2014. **79**(2): p. 257-9.
249. Schulmann, K., et al., *Inactivation of p16, RUNX3, and HPP1 occurs early in Barrett's-associated neoplastic progression and predicts progression risk.* Oncogene, 2005. **24**(25): p. 4138-48.
250. Li, X., et al., *Assessment of Esophageal Adenocarcinoma Risk Using Somatic Chromosome Alterations in Longitudinal Samples in Barrett's Esophagus.* Cancer Prev Res (Phila), 2015. **8**(9): p. 845-56.
251. Falk, G.W., *2017 David Sun Lecture: Screening and Surveillance of Barrett's Esophagus: Where Are We Now and What Does the Future Hold?* Am J Gastroenterol, 2019. **114**(1): p. 64-70.
252. Fels Elliott, D.R. and R.C. Fitzgerald, *Molecular markers for Barrett's esophagus and its progression to cancer.* Curr Opin Gastroenterol, 2013. **29**(4): p. 437-45.
253. Konda, V.J.A. and R.F. Souza, *Barrett's Esophagus and Esophageal Carcinoma: Can Biomarkers Guide Clinical Practice?* Curr Gastroenterol Rep, 2019. **21**(4): p. 14.
254. Zeki, S. and R.C. Fitzgerald, *The use of molecular markers in predicting dysplasia and guiding treatment.* Best Pract Res Clin Gastroenterol, 2015. **29**(1): p. 113-24.
255. Janmaat, V.T., et al., *Use of immunohistochemical biomarkers as independent predictor of neoplastic progression in Barrett's oesophagus surveillance: A systematic review and meta-analysis.* PLoS One, 2017. **12**(10): p. e0186305.
256. Stearns, T. and M. Winey, *The cell center at 100.* Cell, 1997. **91**: p. 303-309.
257. Schatten, H. and Q.Y. Sun, *Functions and dysfunctions of the mammalian centrosome in health, disorders, disease, and aging.* Histochem Cell Biol, 2018. **150**(4): p. 303-325.
258. Gonczy, P., *Centrosomes and cancer: revisiting a long-standing relationship.* Nat Rev Cancer, 2015. **15**(11): p. 639-52.
259. Lerit, D.A. and J.S. Poulton, *Centrosomes are multifunctional regulators of genome stability.* Chromosome Res, 2016. **24**(1): p. 5-17.
260. Joukov, V. and A. De Nicolo, *The Centrosome and the Primary Cilium: The Yin and Yang of a Hybrid Organelle.* Cells, 2019. **8**(7).
261. de Almeida, B.P., et al., *Pan-cancer association of a centrosome amplification gene expression signature with genomic alterations and clinical outcome.* PLoS Comput Biol, 2019. **15**(3): p. e1006832.
262. Sabat-Pospiech, D., et al., *Targeting centrosome amplification, an Achilles' heel of cancer.* Biochem Soc Trans, 2019. **47**(5): p. 1209-1222.
263. Chan, J.Y., *A clinical overview of centrosome amplification in human cancers.* Int J Biol Sci, 2011. **7**(8): p. 1122-44.
264. Godinho, S.A. and D. Pellman, *Causes and consequences of centrosome abnormalities in cancer.* Philos Trans R Soc Lond B Biol Sci, 2014. **369**(1650).

265. Nigg, E.A., D. Schnerch, and O. Ganier, *Impact of Centrosome Aberrations on Chromosome Segregation and Tissue Architecture in Cancer*. Cold Spring Harb Symp Quant Biol, 2017. **82**: p. 137-144.
266. Cosenza, M.R. and A. Kramer, *Centrosome amplification, chromosomal instability and cancer: mechanistic, clinical and therapeutic issues*. Chromosome Res, 2016. **24**(1): p. 105-26.
267. Nano, M. and R. Basto, *The Janus soul of centrosomes: a paradoxical role in disease?* Chromosome Res, 2016. **24**(1): p. 127-44.
268. Raff, J.W. and R. Basto, *Centrosome Amplification and Cancer: A Question of Sufficiency*. Dev Cell, 2017. **40**(3): p. 217-218.
269. Venghateri, J.B., B. Jindal, and D. Panda, *The centrosome: a prospective entrant in cancer therapy*. Expert Opin Ther Targets, 2015. **19**(7): p. 957-72.
270. Rhys, A.D. and S.A. Godinho, *Dividing with Extra Centrosomes: A Double Edged Sword for Cancer Cells*. Adv Exp Med Biol, 2017. **1002**: p. 47-67.
271. Banterle, N. and P. Gonczy, *Centriole Biogenesis: From Identifying the Characters to Understanding the Plot*. Annu Rev Cell Dev Biol, 2017. **33**: p. 23-49.
272. Zyss, D. and F. Gergely, *Centrosome function in cancer: guilty or innocent?* Trends Cell Biol, 2009. **19**(7): p. 334-46.
273. Debec, A., W. Sullivan, and M. Bettencourt-Dias, *Centrioles: active players or passengers during mitosis?* Cell Mol Life Sci, 2010. **67**(13): p. 2173-94.
274. Brito, D.A., S.M. Gouveia, and M. Bettencourt-Dias, *Deconstructing the centriole: structure and number control*. Curr Opin Cell Biol, 2012. **24**(1): p. 4-13.
275. Paintrand, M., et al., *Centrosome organization and centriole architecture: their sensitivity to divalent cations*. J Struct Biol, 1992. **108**(2): p. 107-28.
276. Wu, J. and A. Akhmanova, *Microtubule-Organizing Centers*. Annu Rev Cell Dev Biol, 2017. **33**: p. 51-75.
277. Nigg, E.A. and A.J. Holland, *Once and only once: mechanisms of centriole duplication and their deregulation in disease*. Nat Rev Mol Cell Biol, 2018. **19**(5): p. 297-312.
278. Pihan, G.A., *Centrosome dysfunction contributes to chromosome instability, chromoanagenesis, and genome reprograming in cancer*. Front Oncol, 2013. **3**: p. 277.
279. Loncarek, J. and M. Bettencourt-Dias, *Building the right centriole for each cell type*. J Cell Biol, 2018. **217**(3): p. 823-835.
280. Peneda, C., C.A.M. Lopes, and M. Bettencourt-Dias, *Studying Centriole Duplication and Elongation in Human Cells*. Methods Mol Biol, 2020. **2101**: p. 147-162.
281. Fujita, H., Y. Yoshino, and N. Chiba, *Regulation of the centrosome cycle*. Mol Cell Oncol, 2016. **3**(2): p. e1075643.
282. Firat-Karalar, E.N. and T. Stearns, *The centriole duplication cycle*. Philos Trans R Soc Lond B Biol Sci, 2014. **369**(1650).
283. Brownlee, C.W. and G.C. Rogers, *Show me your license, please: deregulation of centriole duplication mechanisms that promote amplification*. Cell Mol Life Sci, 2013. **70**(6): p. 1021-34.
284. Werner, S., A. Pimenta-Marques, and M. Bettencourt-Dias, *Maintaining centrosomes and cilia*. J Cell Sci, 2017. **130**(22): p. 3789-3800.
285. Varadarajan, R. and N.M. Rusan, *Bridging centrioles and PCM in proper space and time*. Essays Biochem, 2018. **62**(6): p. 793-801.
286. Boveri, T., *Concerning the origin of malignant tumours by Theodor Boveri. Translated and annotated by Henry Harris*. J Cell Sci, 2008. **121 Suppl 1**: p. 1-84.
287. Anderhub, S.J., A. Kramer, and B. Maier, *Centrosome amplification in tumorigenesis*. Cancer Lett, 2012. **322**(1): p. 8-17.
288. Fukasawa, K., et al., *Abnormal centrosome amplification in the absence of p53*. Science, 1996. **271**(5256): p. 1744-7.
289. Bettencourt-Dias, M., et al., *Centrosomes and cilia in human disease*. Trends Genet, 2011. **27**(8): p. 307-15.
290. Nigg, E.A., L. Cajanek, and C. Arquint, *The centrosome duplication cycle in health and disease*. FEBS Lett, 2014. **588**(15): p. 2366-72.
291. Nigg, E.A. and J.W. Raff, *Centrioles, centrosomes, and cilia in health and disease*. Cell, 2009. **139**(4): p. 663-78.
292. Nakajima, T., et al., *Centrosome aberration accompanied with p53 mutation can induce genetic instability in hepatocellular carcinoma*. Mod Pathol, 2004. **17**(6): p. 722-7.

293. Jung, C.K., et al., *Centrosome abnormalities in non-small cell lung cancer: correlations with DNA aneuploidy and expression of cell cycle regulatory proteins*. Pathol Res Pract, 2007. **203**(12): p. 839-47.
294. Pihan, G.A., et al., *Centrosome defects can account for cellular and genetic changes that characterize prostate cancer progression*. Cancer Res, 2001. **61**(5): p. 2212-9.
295. Pihan, G.A., et al., *Centrosome defects and genetic instability in malignant tumors*. Cancer Res, 1998. **58**(17): p. 3974-85.
296. Duensing, S., et al., *Excessive centrosome abnormalities without ongoing numerical chromosome instability in a Burkitt's lymphoma*. Mol Cancer, 2003. **2**: p. 30.
297. Giehl, M., et al., *Centrosome aberrations in chronic myeloid leukemia correlate with stage of disease and chromosomal instability*. Leukemia, 2005. **19**(7): p. 1192-7.
298. Nigg, E.A., *Centrosome aberrations: cause or consequence of cancer progression?* Nat Rev Cancer, 2002. **2**(11): p. 815-25.
299. Kayser, G., et al., *Numerical and structural centrosome aberrations are an early and stable event in the adenoma-carcinoma sequence of colorectal carcinomas*. Virchows Arch, 2005. **447**(1): p. 61-5.
300. Pihan, G.A., et al., *Centrosome abnormalities and chromosome instability occur together in pre-invasive carcinomas*. Cancer Res, 2003. **63**(6): p. 1398-404.
301. Skyldberg, B., et al., *Human papillomavirus infection, centrosome aberration, and genetic stability in cervical lesions*. Mod Pathol, 2001. **14**(4): p. 279-84.
302. Kuo, K.K., et al., *Centrosome abnormalities in human carcinomas of the gallbladder and intrahepatic and extrahepatic bile ducts*. Hepatology, 2000. **31**(1): p. 59-64.
303. Hsu, L.C., et al., *Centrosome abnormalities in ovarian cancer*. Int J Cancer, 2005. **113**(5): p. 746-51.
304. Reiter, R., et al., *Centrosome abnormalities in head and neck squamous cell carcinoma (HNSCC)*. Acta Otolaryngol, 2009. **129**(2): p. 205-13.
305. Koutsami, M.K., et al., *Centrosome abnormalities are frequently observed in non-small-cell lung cancer and are associated with aneuploidy and cyclin E overexpression*. J Pathol, 2006. **209**(4): p. 512-21.
306. Yamamoto, Y., et al., *Centrosome hyperamplification predicts progression and tumor recurrence in bladder cancer*. Clin Cancer Res, 2004. **10**(19): p. 6449-55.
307. Toma, M.I., et al., *Correlation of centrosomal aberrations with cell differentiation and DNA ploidy in prostate cancer*. Anal Quant Cytol Histol, 2010. **32**(1): p. 1-10.
308. Thirthagiri, E., et al., *Spindle assembly checkpoint and centrosome abnormalities in oral cancer*. Cancer Lett, 2007. **258**(2): p. 276-85.
309. Lingle, W.L., et al., *Centrosome amplification drives chromosomal instability in breast tumor development*. Proc Natl Acad Sci U S A, 2002. **99**(4): p. 1978-83.
310. Loh, J.K., et al., *Differential expression of centrosomal proteins at different stages of human glioma*. BMC Cancer, 2010. **10**: p. 268.
311. Schneeweiss, A., et al., *Centrosomal aberrations in primary invasive breast cancer are associated with nodal status and hormone receptor expression*. Int J Cancer, 2003. **107**(3): p. 346-52.
312. Guo, H.Q., et al., *Analysis of the cellular centrosome in fine-needle aspirations of the breast*. Breast Cancer Res, 2007. **9**(4): p. R48.
313. Shimomura, A., et al., *Association of loss of BRCA1 expression with centrosome aberration in human breast cancer*. J Cancer Res Clin Oncol, 2009. **135**(3): p. 421-30.
314. D'Assoro, A.B., et al., *Amplified centrosomes in breast cancer: a potential indicator of tumor aggressiveness*. Breast Cancer Res Treat, 2002. **75**(1): p. 25-34.
315. Gustafson, L.M., et al., *Centrosome hyperamplification in head and neck squamous cell carcinoma: a potential phenotypic marker of tumor aggressiveness*. Laryngoscope, 2000. **110**(11): p. 1798-801.
316. Landen, C.N., Jr., et al., *Overexpression of the centrosomal protein Aurora-A kinase is associated with poor prognosis in epithelial ovarian cancer patients*. Clin Cancer Res, 2007. **13**(14): p. 4098-104.
317. Moskovszky, L., et al., *Centrosome abnormalities in giant cell tumour of bone: possible association with chromosomal instability*. Mod Pathol, 2010. **23**(3): p. 359-66.
318. Syed, M.I., et al., *Gamma tubulin: a promising indicator of recurrence in squamous cell carcinoma of the larynx*. Otolaryngol Head Neck Surg, 2009. **140**(4): p. 498-504.
319. Kramer, A., K. Neben, and A.D. Ho, *Centrosome aberrations in hematological malignancies*. Cell Biol Int, 2005. **29**(5): p. 375-83.

320. Kramer, A., et al., *Centrosome aberrations as a possible mechanism for chromosomal instability in non-Hodgkin's lymphoma*. Leukemia, 2003. **17**(11): p. 2207-13.
321. Chng, W.J., et al., *The centrosome index is a powerful prognostic marker in myeloma and identifies a cohort of patients that might benefit from aurora kinase inhibition*. Blood, 2008. **111**(3): p. 1603-9.
322. Reiter, R., et al., *Aurora kinase A messenger RNA overexpression is correlated with tumor progression and shortened survival in head and neck squamous cell carcinoma*. Clin Cancer Res, 2006. **12**(17): p. 5136-41.
323. Yamamoto, Y., et al., *Centrosome amplification as a putative prognostic biomarker for the classification of urothelial carcinomas*. Hum Pathol, 2011. **42**(12): p. 1923-30.
324. Al-Romaih, K., et al., *Chromosomal instability in osteosarcoma and its association with centrosome abnormalities*. Cancer Genet Cytogenet, 2003. **144**(2): p. 91-9.
325. Vitre, B.D. and D.W. Cleveland, *Centrosomes, chromosome instability (CIN) and aneuploidy*. Curr Opin Cell Biol, 2012. **24**(6): p. 809-15.
326. Arquint, C. and E.A. Nigg, *The PLK4-STIL-SAS-6 module at the core of centriole duplication*. Biochem Soc Trans, 2016. **44**(5): p. 1253-1263.
327. Loncarek, J., et al., *Control of daughter centriole formation by the pericentriolar material*. Nat Cell Biol, 2008. **10**(3): p. 322-8.
328. Fukasawa, K., *Oncogenes and tumour suppressors take on centrosomes*. Nat Rev Cancer, 2007. **7**(12): p. 911-24.
329. Starita, L.M., et al., *BRCA1-dependent ubiquitination of gamma-tubulin regulates centrosome number*. Mol Cell Biol, 2004. **24**(19): p. 8457-66.
330. Karki, M., N. Keyhaninejad, and C.B. Shuster, *Precocious centriole disengagement and centrosome fragmentation induced by mitotic delay*. Nat Commun, 2017. **8**: p. 15803.
331. Maiato, H. and E. Logarinho, *Mitotic spindle multipolarity without centrosome amplification*. Nat Cell Biol, 2014. **16**(5): p. 386-94.
332. Gonczy, P. and G.N. Hatzopoulos, *Centriole assembly at a glance*. J Cell Sci, 2019. **132**(4).
333. Tang, J., et al., *Human cytomegalovirus glycoprotein B variants affect viral entry, cell fusion, and genome stability*. Proc Natl Acad Sci U S A, 2019. **116**(36): p. 18021-18030.
334. Reid, B.J., *Early events during neoplastic progression in Barrett's esophagus*. Cancer Biomark, 2010. **9**(1-6): p. 307-24.
335. Tang, C.J., et al., *CPAP is a cell-cycle regulated protein that controls centriole length*. Nat Cell Biol, 2009. **11**(7): p. 825-31.
336. Kohlmaier, G., et al., *Overly long centrioles and defective cell division upon excess of the SAS-4-related protein CPAP*. Curr Biol, 2009. **19**(12): p. 1012-8.
337. Marteil, G., et al., *Over-elongation of centrioles in cancer promotes centriole amplification and chromosome missegregation*. Nat Commun, 2018. **9**(1): p. 1258.
338. Duensing, S., et al., *Human papillomavirus type 16 E7 oncoprotein-induced abnormal centrosome synthesis is an early event in the evolving malignant phenotype*. Cancer Res, 2001. **61**(6): p. 2356-60.
339. D'Assoro, A.B., W.L. Lingle, and J.L. Salisbury, *Centrosome amplification and the development of cancer*. Oncogene, 2002. **21**(40): p. 6146-53.
340. Ganem, N.J., S.A. Godinho, and D. Pellman, *A mechanism linking extra centrosomes to chromosomal instability*. Nature, 2009. **460**(7252): p. 278-82.
341. Silkworth, W.T., et al., *Multipolar spindle pole coalescence is a major source of kinetochore mis-attachment and chromosome mis-segregation in cancer cells*. PLoS One, 2009. **4**(8): p. e6564.
342. Basto, R., et al., *Centrosome amplification can initiate tumorigenesis in flies*. Cell, 2008. **133**(6): p. 1032-42.
343. Kwon, M., et al., *Mechanisms to suppress multipolar divisions in cancer cells with extra centrosomes*. Genes Dev, 2008. **22**(16): p. 2189-203.
344. Quintyne, N.J., et al., *Spindle multipolarity is prevented by centrosomal clustering*. Science, 2005. **307**(5706): p. 127-9.
345. Kleylein-Sohn, J., et al., *Acentrosomal spindle organization renders cancer cells dependent on the kinesin HSET*. J Cell Sci, 2012. **125**(Pt 22): p. 5391-402.
346. Levine, M.S., et al., *Centrosome Amplification Is Sufficient to Promote Spontaneous Tumorigenesis in Mammals*. Dev Cell, 2017. **40**(3): p. 313-322 e5.
347. Marthiens, V., et al., *Centrosome amplification causes microcephaly*. Nat Cell Biol, 2013. **15**(7): p. 731-40.

348. Godinho, S.A., et al., *Oncogene-like induction of cellular invasion from centrosome amplification*. Nature, 2014. **510**(7503): p. 167-71.
349. Schnerch, D. and E.A. Nigg, *Structural centrosome aberrations favor proliferation by abrogating microtubule-dependent tissue integrity of breast epithelial mammospheres*. Oncogene, 2016. **35**(21): p. 2711-22.
350. Ganier, O., et al., *Structural centrosome aberrations promote non-cell-autonomous invasiveness*. EMBO J, 2018. **37**(9).
351. Arnandis, T., et al., *Oxidative Stress in Cells with Extra Centrosomes Drives Non-Cell-Autonomous Invasion*. Dev Cell, 2018. **47**(4): p. 409-424 e9.
352. Menzl, I., et al., *Loss of primary cilia occurs early in breast cancer development*. Cilia, 2014. **3**: p. 7.
353. Seeley, E.S., et al., *Pancreatic cancer and precursor pancreatic intraepithelial neoplasia lesions are devoid of primary cilia*. Cancer Res, 2009. **69**(2): p. 422-30.
354. Basten, S.G., et al., *Reduced cilia frequencies in human renal cell carcinomas versus neighboring parenchymal tissue*. Cilia, 2013. **2**(1): p. 2.
355. Xiang, W., et al., *HDAC6 inhibition suppresses chondrosarcoma by restoring the expression of primary cilia*. Oncol Rep, 2017. **38**(1): p. 229-236.
356. Li, L., et al., *Sonic Hedgehog promotes proliferation of Notch-dependent monociliated choroid plexus tumour cells*. Nat Cell Biol, 2016. **18**(4): p. 418-30.
357. Higgins, M., I. Obaidi, and T. McMorrow, *Primary cilia and their role in cancer*. Oncol Lett, 2019. **17**(3): p. 3041-3047.
358. Zhao, Y. and X. Wang, *PLK4: a promising target for cancer therapy*. J Cancer Res Clin Oncol, 2019. **145**(10): p. 2413-2422.
359. Fielding, A.B., et al., *A critical role of integrin-linked kinase, ch-TOG and TACC3 in centrosome clustering in cancer cells*. Oncogene, 2011. **30**(5): p. 521-34.
360. Myers, S.M. and I. Collins, *Recent findings and future directions for interpolar mitotic kinesin inhibitors in cancer therapy*. Future Med Chem, 2016. **8**(4): p. 463-89.
361. Lv, J., et al., *Biomarker identification and trans-regulatory network analyses in esophageal adenocarcinoma and Barrett's esophagus*. World J Gastroenterol, 2019. **25**(2): p. 233-244.
362. Reid, B.J., R. Kostadinov, and C.C. Maley, *New strategies in Barrett's esophagus: integrating clonal evolutionary theory with clinical management*. Clin Cancer Res, 2011. **17**(11): p. 3512-9.
363. Timmer, M.R., et al., *Derivation of genetic biomarkers for cancer risk stratification in Barrett's oesophagus: a prospective cohort study*. Gut, 2016. **65**(10): p. 1602-10.
364. Duits, L.C., et al., *The Amsterdam ReBus progressor cohort: identification of 165 Barrett's surveillance patients who progressed to early neoplasia and 723 nonprogressor patients*. Dis Esophagus, 2018.
365. Reid, B.J., et al., *Predictors of progression in Barrett's esophagus II: baseline 17p (p53) loss of heterozygosity identifies a patient subset at increased risk for neoplastic progression*. Am J Gastroenterol, 2001. **96**(10): p. 2839-48.
366. Galipeau, P.C., et al., *NSAIDs modulate CDKN2A, TP53, and DNA content risk for progression to esophageal adenocarcinoma*. PLoS Med, 2007. **4**(2): p. e67.
367. Sato, F., et al., *Three-tiered risk stratification model to predict progression in Barrett's esophagus using epigenetic and clinical features*. PLoS One, 2008. **3**(4): p. e1890.
368. Jin, Z., et al., *A multicenter, double-blinded validation study of methylation biomarkers for progression prediction in Barrett's esophagus*. Cancer Res, 2009. **69**(10): p. 4112-5.
369. Blount, P.L., et al., *Clonal ordering of 17p and 5q allelic losses in Barrett dysplasia and adenocarcinoma*. Proc Natl Acad Sci U S A, 1993. **90**(8): p. 3221-5.
370. Boynton, R.F., et al., *Frequent loss of heterozygosity at the retinoblastoma locus in human esophageal cancers*. Cancer Res, 1991. **51**(20): p. 5766-9.
371. Casson, A.G., et al., *Clinical implications of p53 gene mutation in the progression of Barrett's epithelium to invasive esophageal cancer*. Am J Surg, 1994. **167**(1): p. 52-7.
372. Eads, C.A., et al., *Epigenetic patterns in the progression of esophageal adenocarcinoma*. Cancer Res, 2001. **61**(8): p. 3410-8.
373. Selaru, F.M., et al., *Beyond Field Effect: Analysis of Shrunken Centroids in Normal Esophageal Epithelia Detects Concomitant Esophageal Adenocarcinoma*. Bioinform Biol Insights, 2007. **1**: p. 127-136.
374. Bird-Lieberman, E.L., et al., *Population-based study reveals new risk-stratification biomarker panel for Barrett's esophagus*. Gastroenterology, 2012. **143**(4): p. 927-35 e3.

375. Murray, L., et al., *TP53 and progression from Barrett's metaplasia to oesophageal adenocarcinoma in a UK population cohort*. Gut, 2006. **55**(10): p. 1390-7.
376. Lau, L.F., *CCN1/CYR61: the very model of a modern matricellular protein*. Cell Mol Life Sci, 2011. **68**(19): p. 3149-63.
377. Zanconato, F., M. Cordenonsi, and S. Piccolo, *YAP/TAZ at the Roots of Cancer*. Cancer Cell, 2016. **29**(6): p. 783-803.
378. Chen, C.C. and L.F. Lau, *Functions and mechanisms of action of CCN matricellular proteins*. Int J Biochem Cell Biol, 2009. **41**(4): p. 771-83.
379. Chaqour, B. and M. Goppelt-Struebe, *Mechanical regulation of the Cyr61/CCN1 and CTGF/CCN2 proteins*. FEBS J, 2006. **273**(16): p. 3639-49.
380. Terada, N., P. Kulkarni, and R.H. Getzenberg, *Cyr61 is a potential prognostic marker for prostate cancer*. Asian J Androl, 2012. **14**(3): p. 405-8.
381. Jeong, D., et al., *Cyr61 expression is associated with prognosis in patients with colorectal cancer*. BMC Cancer, 2014. **14**: p. 164.
382. Chen, C.C., F.E. Mo, and L.F. Lau, *The angiogenic factor Cyr61 activates a genetic program for wound healing in human skin fibroblasts*. J Biol Chem, 2001. **276**(50): p. 47329-37.
383. Xie, D., et al., *Levels of expression of CYR61 and CTGF are prognostic for tumor progression and survival of individuals with gliomas*. Clin Cancer Res, 2004. **10**(6): p. 2072-81.
384. Sabile, A.A., et al., *Cyr61 expression in osteosarcoma indicates poor prognosis and promotes intratibial growth and lung metastasis in mice*. J Bone Miner Res, 2012. **27**(1): p. 58-67.
385. Liu, Y., et al., *High expression levels of Cyr61 and VEGF are associated with poor prognosis in osteosarcoma*. Pathol Res Pract, 2017. **213**(8): p. 895-899.
386. O'Kelly, J., et al., *Functional domains of CCN1 (Cyr61) regulate breast cancer progression*. Int J Oncol, 2008. **33**(1): p. 59-67.
387. Jiang, W.G., et al., *Differential expression of the CCN family members Cyr61, CTGF and Nov in human breast cancer*. Endocr Relat Cancer, 2004. **11**(4): p. 781-91.
388. Li, J., et al., *Differential expression of CCN family members CYR611, CTGF and NOV in gastric cancer and their association with disease progression*. Oncol Rep, 2016. **36**(5): p. 2517-2525.
389. Shen, H., et al., *CYR61 overexpression associated with the development and poor prognosis of ovarian carcinoma*. Med Oncol, 2014. **31**(8): p. 117.
390. Lin, Y., et al., *Cysteine-rich, angiogenic inducer, 61 expression in patients with ovarian epithelial carcinoma*. J Int Med Res, 2014. **42**(2): p. 300-6.
391. Kok, S.H., et al., *Expression of Cyr61 (CCN1) in human oral squamous cell carcinoma: An independent marker for poor prognosis*. Head Neck, 2010. **32**(12): p. 1665-73.
392. Haque, I., et al., *Cyr61/CCN1 signaling is critical for epithelial-mesenchymal transition and stemness and promotes pancreatic carcinogenesis*. Mol Cancer, 2011. **10**: p. 8.
393. Nguyen, L.T., Y.W. Song, and S.K. Cho, *Baicalein Inhibits Epithelial to Mesenchymal Transition via Downregulation of Cyr61 and LOXL-2 in MDA-MB231 Breast Cancer Cells*. Mol Cells, 2016. **39**(12): p. 909-914.
394. Huang, X., et al., *Snail/FOXK1/Cyr61 Signaling Axis Regulates the Epithelial-Mesenchymal Transition and Metastasis in Colorectal Cancer*. Cell Physiol Biochem, 2018. **47**(2): p. 590-603.
395. Tsai, M.S., et al., *Cyr61 promotes breast tumorigenesis and cancer progression*. Oncogene, 2002. **21**(53): p. 8178-85.
396. Habel, N., et al., *Cyr61 silencing reduces vascularization and dissemination of osteosarcoma tumors*. Oncogene, 2015. **34**(24): p. 3207-13.
397. Fromigue, O., et al., *CYR61 downregulation reduces osteosarcoma cell invasion, migration, and metastasis*. J Bone Miner Res, 2011. **26**(7): p. 1533-42.
398. Gery, S., et al., *Ovarian carcinomas: CCN genes are aberrantly expressed and CCN1 promotes proliferation of these cells*. Clin Cancer Res, 2005. **11**(20): p. 7243-54.
399. Zhou, X. and Q.Y. Lei, *Regulation of TAZ in cancer*. Protein Cell, 2016. **7**(8): p. 548-61.
400. Dong, X., et al., *YAP/TAZ: a promising target for squamous cell carcinoma treatment*. Cancer Manag Res, 2019. **11**: p. 6245-6252.
401. Moroishi, T., C.G. Hansen, and K.L. Guan, *The emerging roles of YAP and TAZ in cancer*. Nat Rev Cancer, 2015. **15**(2): p. 73-79.

402. Zhao, B., K. Tumaneng, and K.L. Guan, *The Hippo pathway in organ size control, tissue regeneration and stem cell self-renewal*. Nat Cell Biol, 2011. **13**(8): p. 877-83.
403. Piccolo, S., S. Dupont, and M. Cordenonsi, *The biology of YAP/TAZ: hippo signaling and beyond*. Physiol Rev, 2014. **94**(4): p. 1287-312.
404. Bhat, K.P., et al., *The transcriptional coactivator TAZ regulates mesenchymal differentiation in malignant glioma*. Genes Dev, 2011. **25**(24): p. 2594-609.
405. Zhang, H., et al., *TEAD transcription factors mediate the function of TAZ in cell growth and epithelial-mesenchymal transition*. J Biol Chem, 2009. **284**(20): p. 13355-62.
406. Cordenonsi, M., et al., *The Hippo transducer TAZ confers cancer stem cell-related traits on breast cancer cells*. Cell, 2011. **147**(4): p. 759-72.
407. Wang, L., et al., *Overexpression of YAP and TAZ is an independent predictor of prognosis in colorectal cancer and related to the proliferation and metastasis of colon cancer cells*. PLoS One, 2013. **8**(6): p. e65539.
408. Lau, A.N., et al., *Tumor-propagating cells and Yap/Taz activity contribute to lung tumor progression and metastasis*. EMBO J, 2014. **33**(5): p. 468-81.
409. Xu, W., et al., *Up-regulation of the Hippo pathway effector TAZ renders lung adenocarcinoma cells harboring EGFR-T790M mutation resistant to gefitinib*. Cell Biosci, 2015. **5**: p. 7.
410. Bartucci, M., et al., *TAZ is required for metastatic activity and chemoresistance of breast cancer stem cells*. Oncogene, 2015. **34**(6): p. 681-90.
411. Xie, M., et al., *Prognostic significance of TAZ expression in resected non-small cell lung cancer*. J Thorac Oncol, 2012. **7**(5): p. 799-807.
412. Duggan, S.P., et al., *Low pH induces co-ordinate regulation of gene expression in oesophageal cells*. Carcinogenesis, 2006. **27**(2): p. 319-27.
413. Modak, C., et al., *CCN1 is critical for acid-induced esophageal epithelial cell transformation*. Biochem Biophys Res Commun, 2010. **392**(4): p. 533-7.
414. Zhou, Z.Q., et al., *Expression and prognostic significance of THBS1, Cyr61 and CTGF in esophageal squamous cell carcinoma*. BMC Cancer, 2009. **9**: p. 291.
415. Xie, J.J., et al., *Involvement of Cyr61 in the growth, invasiveness and adhesion of esophageal squamous cell carcinoma cells*. Int J Mol Med, 2011. **27**(3): p. 429-34.
416. Di Martino, E., et al., *IGFBP-3 and IGFBP-10 (CYR61) up-regulation during the development of Barrett's oesophagus and associated oesophageal adenocarcinoma: potential biomarkers of disease risk*. Biomarkers, 2006. **11**(6): p. 547-61.
417. Ladwa, R., et al., *Expression of CTGF and Cyr61 in colorectal cancer*. J Clin Pathol, 2011. **64**(1): p. 58-64.
418. Li, Z.Q., et al., *Cyr61/CCN1 is regulated by Wnt/beta-catenin signaling and plays an important role in the progression of hepatocellular carcinoma*. PLoS One, 2012. **7**(4): p. e35754.
419. Xie, J.J., et al., *Expression of cysteine-rich 61 is correlated with poor prognosis in patients with esophageal squamous cell carcinoma*. Eur J Surg Oncol, 2011. **37**(8): p. 669-74.
420. Song, Y.F., et al., *Serum Cyr61 as a potential biomarker for diagnosis of colorectal cancer*. Clin Transl Oncol, 2017. **19**(4): p. 519-524.
421. Lai, D., et al., *Taxol resistance in breast cancer cells is mediated by the hippo pathway component TAZ and its downstream transcriptional targets Cyr61 and CTGF*. Cancer Res, 2011. **71**(7): p. 2728-38.
422. Thiery, J.P., et al., *Epithelial-mesenchymal transitions in development and disease*. Cell, 2009. **139**(5): p. 871-90.
423. Pastushenko, I. and C. Blanpain, *EMT Transition States during Tumor Progression and Metastasis*. Trends Cell Biol, 2019. **29**(3): p. 212-226.
424. Fazilaty, H., et al., *A gene regulatory network to control EMT programs in development and disease*. Nat Commun, 2019. **10**(1): p. 5115.
425. Nieto, M.A., et al., *Emt: 2016*. Cell, 2016. **166**(1): p. 21-45.
426. Lamouille, S., J. Xu, and R. Derynck, *Molecular mechanisms of epithelial-mesenchymal transition*. Nat Rev Mol Cell Biol, 2014. **15**(3): p. 178-96.
427. Petrova, Y.I., L. Schecterson, and B.M. Gumbiner, *Roles for E-cadherin cell surface regulation in cancer*. Mol Biol Cell, 2016. **27**(21): p. 3233-3244.
428. Santamaria, P.G., et al., *EMT: Present and future in clinical oncology*. Mol Oncol, 2017. **11**(7): p. 718-738.

429. Lee, J.Y. and G. Kong, *Roles and epigenetic regulation of epithelial-mesenchymal transition and its transcription factors in cancer initiation and progression.* Cell Mol Life Sci, 2016. **73**(24): p. 4643-4660.
430. Rhim, A.D., et al., *EMT and dissemination precede pancreatic tumor formation.* Cell, 2012. **148**(1-2): p. 349-61.
431. Tomizawa, Y., T.T. Wu, and K.K. Wang, *Epithelial mesenchymal transition and cancer stem cells in esophageal adenocarcinoma originating from Barrett's esophagus.* Oncol Lett, 2012. **3**(5): p. 1059-1063.
432. Hsu, Y.L., et al., *Angiomotin decreases lung cancer progression by sequestering oncogenic YAP/TAZ and decreasing Cyr61 expression.* Oncogene, 2015. **34**(31): p. 4056-68.
433. Segat, D., et al., *Pericentriolar material analyses in normal esophageal mucosa, Barrett's metaplasia and adenocarcinoma.* Histol Histopathol, 2010. **25**(5): p. 551-60.
434. Lingle, W.L., et al., *Centrosome hypertrophy in human breast tumors: implications for genomic stability and cell polarity.* Proc Natl Acad Sci U S A, 1998. **95**(6): p. 2950-5.
435. Lingle, W.L. and J.L. Salisbury, *Altered centrosome structure is associated with abnormal mitoses in human breast tumors.* Am J Pathol, 1999. **155**(6): p. 1941-51.
436. O'Hurley, G., et al., *Garbage in, garbage out: a critical evaluation of strategies used for validation of immunohistochemical biomarkers.* Mol Oncol, 2014. **8**(4): p. 783-98.
437. Robertson, D., et al., *Multiple immunofluorescence labelling of formalin-fixed paraffin-embedded (FFPE) tissue.* BMC Cell Biol, 2008. **9**: p. 13.
438. Hastings, R.J., et al., *Guidelines for cytogenetic investigations in tumours.* Eur J Hum Genet, 2016. **24**(1): p. 6-13.
439. Wong, Y.L., et al., *Cell biology. Reversible centriole depletion with an inhibitor of Polo-like kinase 4.* Science, 2015. **348**(6239): p. 1155-60.
440. LoMastro, G.M. and A.J. Holland, *The Emerging Link between Centrosome Aberrations and Metastasis.* Dev Cell, 2019. **49**(3): p. 325-331.
441. Chowell, D., et al., *Modeling the Subclonal Evolution of Cancer Cell Populations.* Cancer Res, 2018. **78**(3): p. 830-839.
442. Merlo, L.M., et al., *A comprehensive survey of clonal diversity measures in Barrett's esophagus as biomarkers of progression to esophageal adenocarcinoma.* Cancer Prev Res (Phila), 2010. **3**(11): p. 1388-97.
443. Tabassum, D.P. and K. Polyak, *Tumorigenesis: it takes a village.* Nat Rev Cancer, 2015. **15**(8): p. 473-83.
444. Palanca-Wessels, M.C., et al., *Extended lifespan of Barrett's esophagus epithelium transduced with the human telomerase catalytic subunit: a useful in vitro model.* Carcinogenesis, 2003. **24**(7): p. 1183-90.
445. Jaiswal, K.R., et al., *Characterization of telomerase-immortalized, non-neoplastic, human Barrett's cell line (BAR-T).* Dis Esophagus, 2007. **20**(3): p. 256-64.
446. Cuomo, M.E., et al., *p53-Driven apoptosis limits centrosome amplification and genomic instability downstream of NPM1 phosphorylation.* Nat Cell Biol, 2008. **10**(6): p. 723-30.
447. Lambrus, B.G., et al., *p53 protects against genome instability following centriole duplication failure.* J Cell Biol, 2015. **210**(1): p. 63-77.
448. Holland, A.J., et al., *The autoregulated instability of Polo-like kinase 4 limits centrosome duplication to once per cell cycle.* Genes Dev, 2012. **26**(24): p. 2684-9.
449. Rivlin, N., et al., *Mutations in the p53 Tumor Suppressor Gene: Important Milestones at the Various Steps of Tumorigenesis.* Genes Cancer, 2011. **2**(4): p. 466-74.
450. Petitjean, A., et al., *Impact of mutant p53 functional properties on TP53 mutation patterns and tumor phenotype: lessons from recent developments in the IARC TP53 database.* Hum Mutat, 2007. **28**(6): p. 622-9.
451. Tarapore, P., et al., *Difference in the centrosome duplication regulatory activity among p53 'hot spot' mutants: potential role of Ser 315 phosphorylation-dependent centrosome binding of p53.* Oncogene, 2001. **20**(47): p. 6851-63.
452. Noll, J.E., et al., *Mutant p53 drives multinucleation and invasion through a process that is suppressed by ANKRD11.* Oncogene, 2012. **31**(23): p. 2836-48.
453. Palanca-Wessels, M.C., et al., *Genetic analysis of long-term Barrett's esophagus epithelial cultures exhibiting cytogenetic and ploidy abnormalities.* Gastroenterology, 1998. **114**(2): p. 295-304.
454. Zhang, X., et al., *Malignant transformation of non-neoplastic Barrett's epithelial cells through well-defined genetic manipulations.* PLoS One, 2010. **5**(9).

455. McDermott, K.M., et al., *p16(INK4a) prevents centrosome dysfunction and genomic instability in primary cells.* PLoS Biol, 2006. **4**(3): p. e51.
456. Ganem, N.J., et al., *Cytokinesis failure triggers hippo tumor suppressor pathway activation.* Cell, 2014. **158**(4): p. 833-848.
457. Rabinovitch, P.S., et al., *Predictors of progression in Barrett's esophagus III: baseline flow cytometric variables.* Am J Gastroenterol, 2001. **96**(11): p. 3071-83.
458. Thompson, S.L. and D.A. Compton, *Proliferation of aneuploid human cells is limited by a p53-dependent mechanism.* J Cell Biol, 2010. **188**(3): p. 369-81.
459. Davoli, T. and T. de Lange, *The causes and consequences of polyploidy in normal development and cancer.* Annu Rev Cell Dev Biol, 2011. **27**: p. 585-610.
460. Paulson, T.G., et al., *Chromosomal instability and copy number alterations in Barrett's esophagus and esophageal adenocarcinoma.* Clin Cancer Res, 2009. **15**(10): p. 3305-14.
461. Coelho, P.A., et al., *Over-expression of Plk4 induces centrosome amplification, loss of primary cilia and associated tissue hyperplasia in the mouse.* Open Biol, 2015. **5**(12): p. 150209.
462. Sercin, O., et al., *Transient PLK4 overexpression accelerates tumorigenesis in p53-deficient epidermis.* Nat Cell Biol, 2016. **18**(1): p. 100-10.
463. Muller, P.A. and K.H. Vousden, *Mutant p53 in cancer: new functions and therapeutic opportunities.* Cancer Cell, 2014. **25**(3): p. 304-17.
464. Mantovani, F., L. Collavin, and G. Del Sal, *Mutant p53 as a guardian of the cancer cell.* Cell Death Differ, 2019. **26**(2): p. 199-212.
465. Mason, J.M., et al., *Functional characterization of CFI-400945, a Polo-like kinase 4 inhibitor, as a potential anticancer agent.* Cancer Cell, 2014. **26**(2): p. 163-76.
466. http://www.clevelandclinicmeded.com/medicalpubs/diseasemanagement/hematology-oncology/esophageal-cancer/.
467. "Histology of Esophagus," Accessed July 24, 2015, http://classified-blog.com/photogms/histology-of-esophagus..

CHAPTER 7:
Appendixes

APPENDIX 1 – Supporting information for paper: *"CYR61 and TAZ Upregulation and Focal Epithelial to Mesenchymal Transition May Be Early Predictors of Barrett's Esophagus Malignant Progression"*

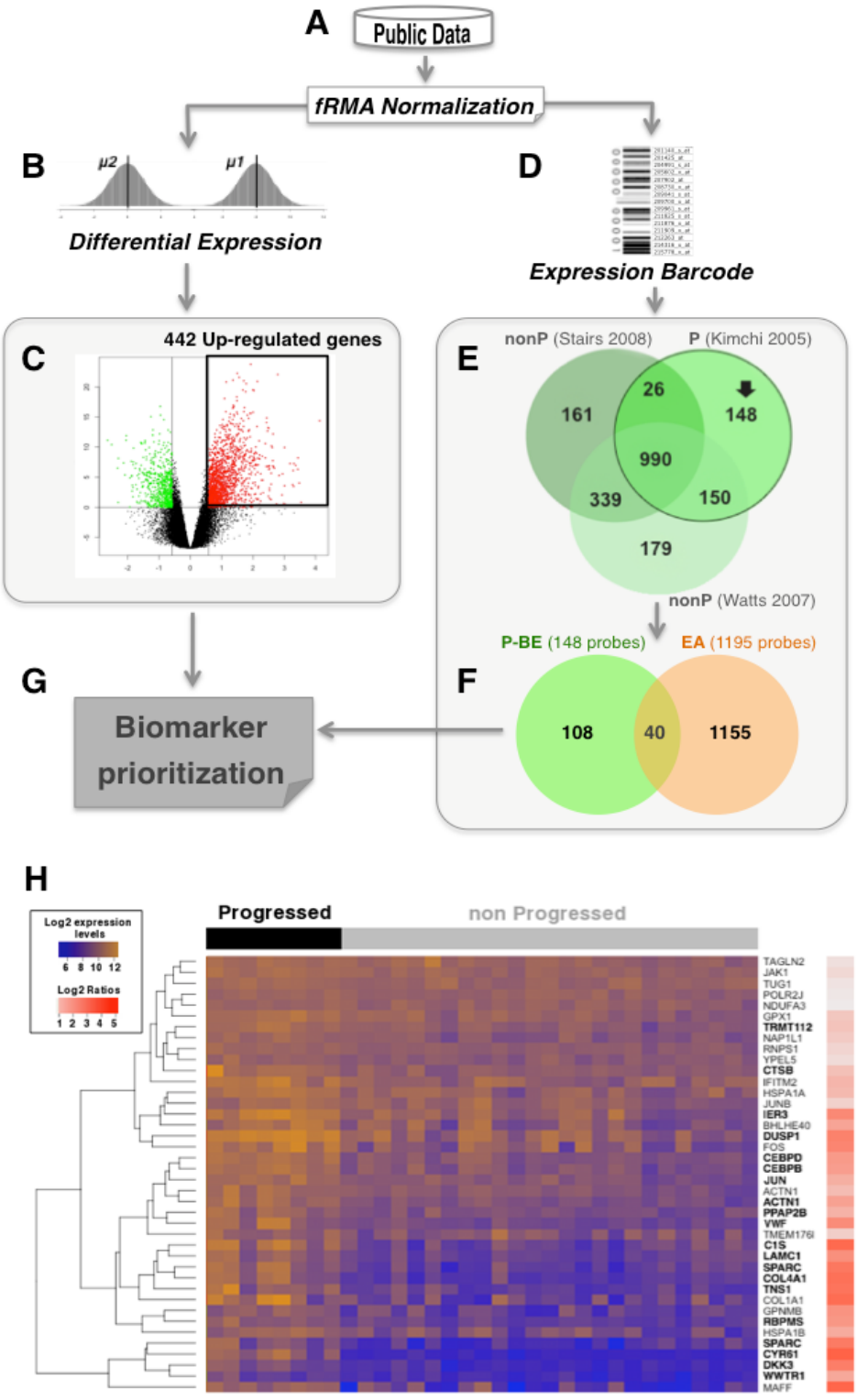

S1 Fig. An original bioinformatics prioritization framework allowed the identification of at risk BE biomarkers. **A.** Publicly available microarray datasets on BE and/or EA were

normalized with the fRMA algorithm. BE samples associated with progression to EA were retrieved from Kimchi *et al.* [1] and assigned to the P-BE group and EA-free BE samples were retrieved from Watts *et al.* [2] and Stairs *et al.* [3] and assigned to nonP-BE group. **B.** Comparison of P-BE versus nonP-BE samples with a differential expression approach which, **C.** resulted in the identification of 442 unique up-regulated genes in P-BE. **D.** Calculation of expression barcodes was performed per individual sample. **E.** P-BE-exclusive probe sets (148) were defined via intersection of P-BE and nonP-BE barcodes. **F.** Forty malignancy-associated progression probe sets were achieved by crossing 148 P-BE barcoded probe sets with EA-associated barcodes. **G.** Integration of barcode and differential expression results to further trim promising candidates for downstream validation. **H.** Combined barcode and differential expression prioritized 20 probe sets associated with BE malignant progression to be validated in downstream experimental settings. In total, 19 unique up-regulated genes (in bold) differentiate P-BE from nonP-BE.

References

1. Kimchi ET, Posner MC, Park JO, Darga TE, Kocherginsky M, Karrison T, et al. Progression of Barrett's metaplasia to adenocarcinoma is associated with the suppression of the transcriptional programs of epidermal differentiation. Cancer Res. 2005;65(8):3146-54. Epub 2005/04/19. doi: 65/8/3146 [pii]
10.1158/0008-5472.CAN-04-2490. PubMed PMID: 15833844.

2. Watts GS, Tran NL, Berens ME, Bhattacharyya AK, Nelson MA, Montgomery EA, et al. Identification of Fn14/TWEAK receptor as a potential therapeutic target in esophageal adenocarcinoma. Int J Cancer. 2007;121(10):2132-9. Epub 2007/06/28. doi: 10.1002/ijc.22898. PubMed PMID: 17594693.

3. Stairs DB, Nakagawa H, Klein-Szanto A, Mitchell SD, Silberg DG, Tobias JW, et al. Cdx1 and c-Myc foster the initiation of transdifferentiation of the normal esophageal squamous epithelium toward Barrett's esophagus. PLoS One. 2008;3(10):e3534. Epub 2008/10/28. doi: 10.1371/journal.pone.0003534. PubMed PMID: 18953412.

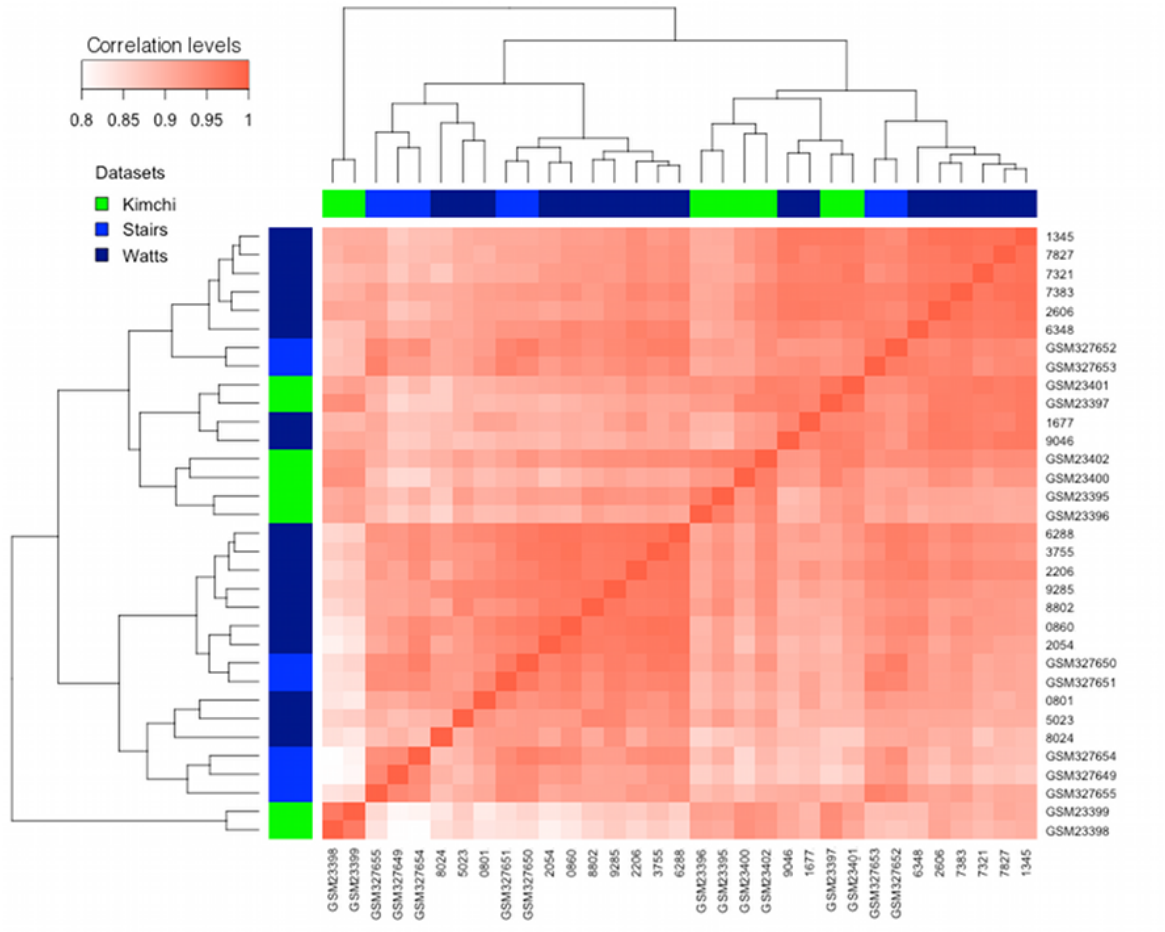

S2 Fig. Microarray data of BE samples from distinct datasets is highly correlated. Pearson's correlations plotted in the heatmap were calculated using fRMA normalized absolute intensity levels and samples were compared through pairwise comparison of all 33 BE samples. Each dataset is represented with a different colour in the coloured side bars.

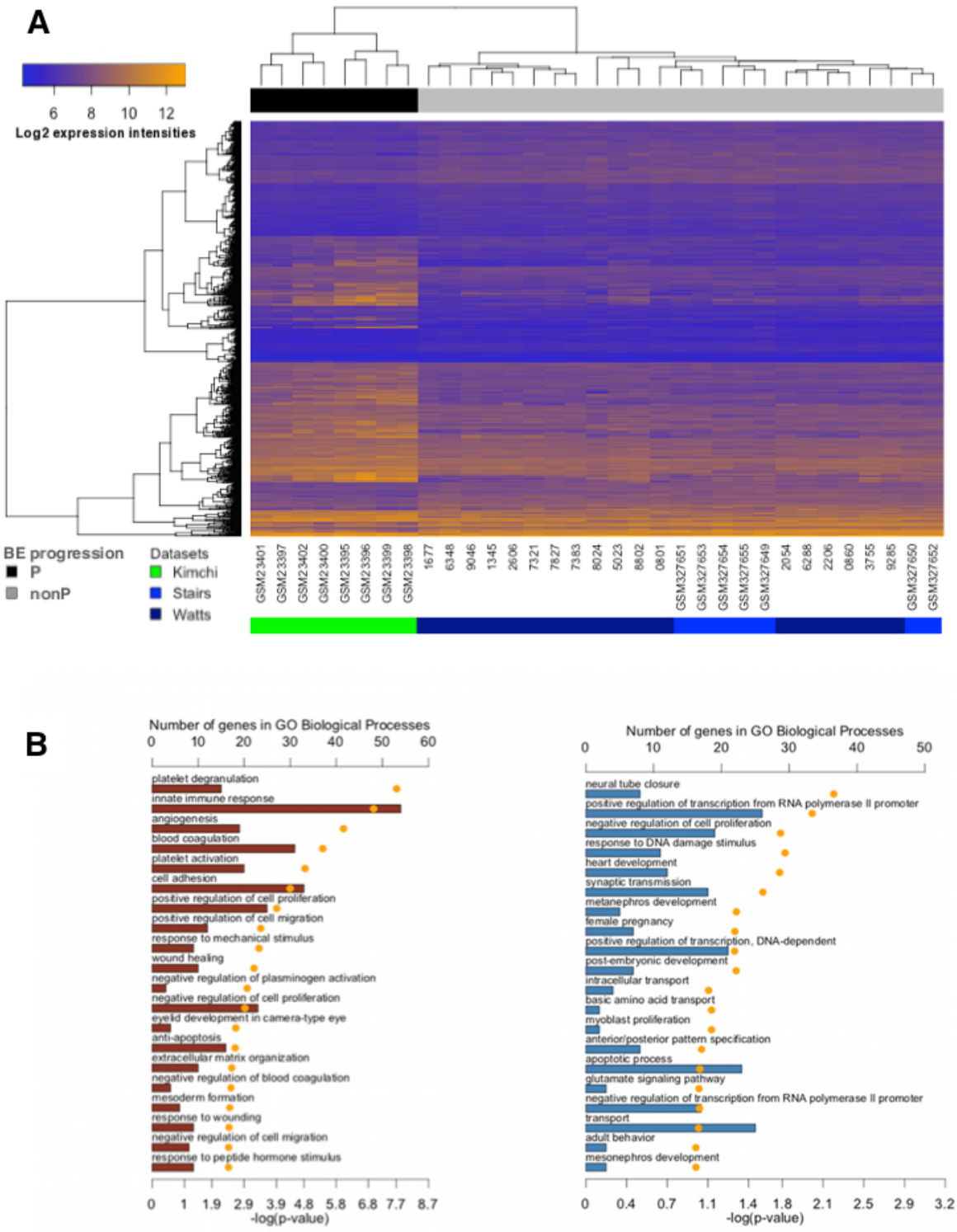

S3 Fig. Differential expression analysis of P-BE and nonP-BE microarray data highlighted more than 700 genes potentially involved in BE malignant progression. A. Heatmap of genes filtered after differential expression analysis with a conservative cutoff (Lods≥5). Each dataset is represented with a different colour in the bottom coloured side bar

and each BE progression group is represented by the upper coloured bar (black and grey). **B.** Top 20 GO Biological Processes (q-value<0.05) over-represented among significantly up-regulated (left plot, in red) and down-regulated (right plot, in blue) genes. Yellow dots illustrate the adjusted Ps for each GO category.

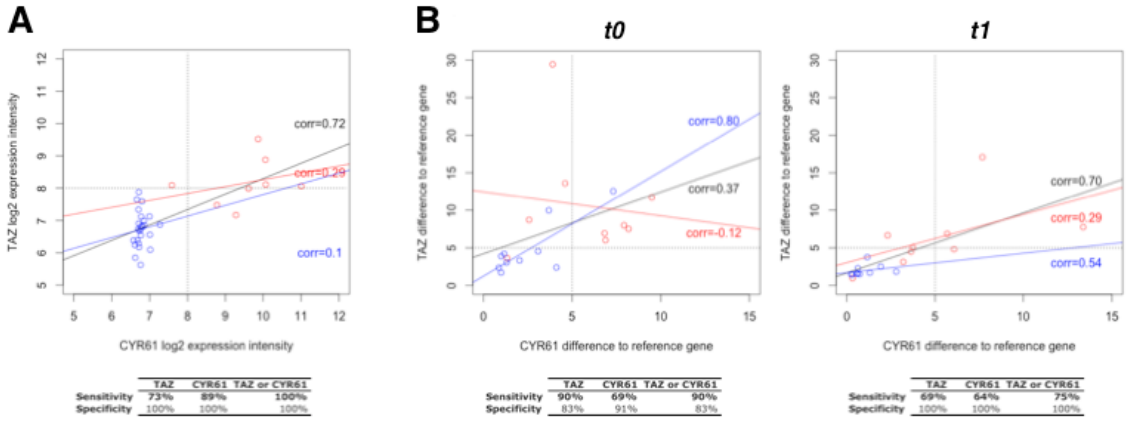

S4 Fig. CYR61 and TAZ expression levels are not correlated. A. Microarray data correlation of CYR61 and TAZ log2 expression intensities. **B.** Correlation of RT-qPCR relative expression levels of CYR61 and TAZ in the index biopsies (t0) and in the recent samples (t1). Results related with P-BE and nonP-BE samples are represented in red and blue, respectively. Black represents results with all samples. A preliminary overview of sensitivity and specificity values for individual or combined usage of biomarkers of at risk BE is shown below each plot.

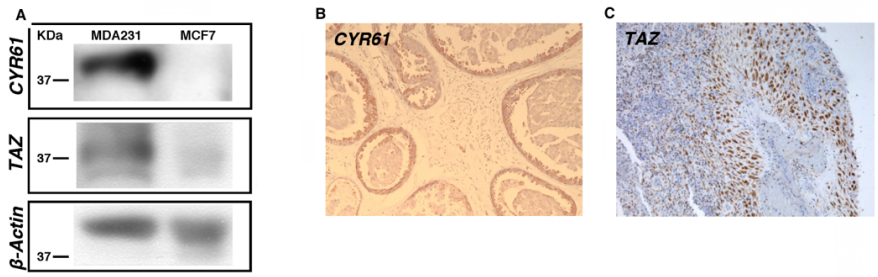

S5 Fig. Validation of CYR61 and TAZ antibodies specificity. A. Western-blot analysis was performed to test the CYR61 and TAZ antibodies specificity on the breast cancer cell lines MDA213 and MCF7. A band of ~42KDa and ~40KDa was observed when using CYR61 and TAZ antibodies, respectively. β–Actin antibody (~50 KDa) was used as a loading control. **B.** Breast cancer and **C.** placenta tissue sections used as used as positive controls of CYR61 and TAZ antibodies, respectively. Magnification 100X.

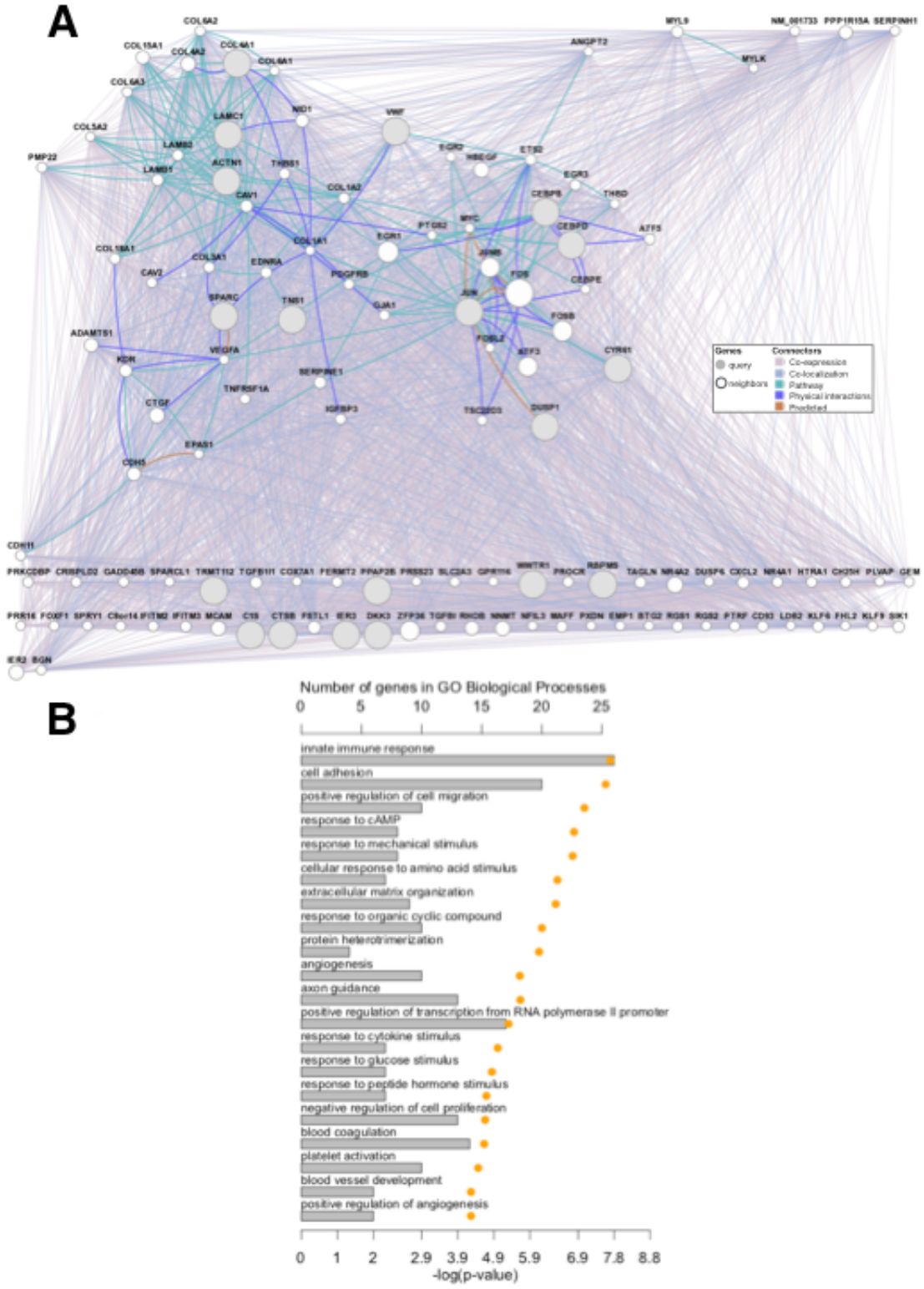

S6 Fig. GeneMania network of the 19 selected candidate biomarkers, network neighbors and associated function showed an enrichment of genes related with cell adhesion, moπ□ptility and response to stimuli. A. The set of 19 genes was use to find

connections with close neighbors according to GeneMania association network algorithm. **B.** Top 20 significant (q-value<0.05) GO Biological Processes were identified by gene set enrichment analysis performed with InnateDB tool. Yellow dots illustrate the adjusted Ps for each GO category.

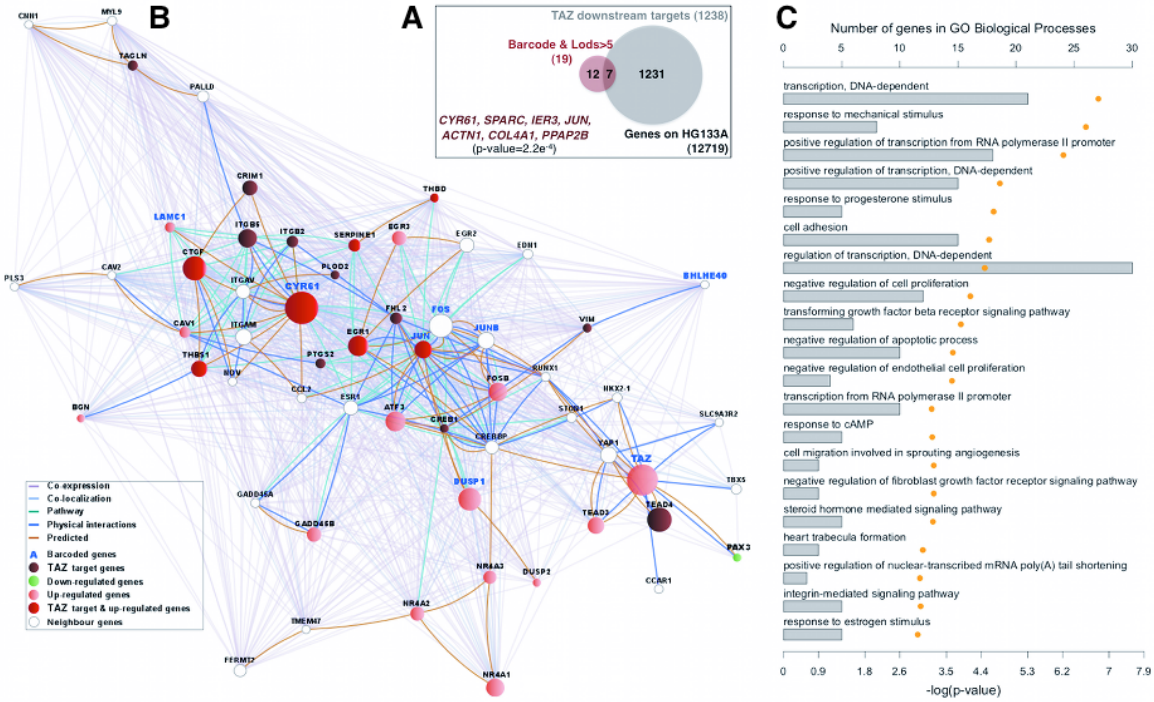

S7 Fig. CYR61 and TAZ are biological linked and share important cellular functions. **A.** TAZ downstream targets represent a category of significantly over-represented genes among the 19 barcode and differentially expressed genes (hypergeometric test pvalue=2.2×10^{-4}, 12719 unique genes represented in the Affymetrix HG-133A GeneChip® platform). **B.** CYR61 and TAZ as query genes in GeneMania network are able to highlight network neighbors which are also TAZ downstream targets, differentially expressed genes and barcode genes. Network genes only connected via co-expression are represented in fig. S4. **C.** Top 20 significantly enriched (q-value<0.05) GO Biological Processes associated with CYR61, TAZ and their 100 GeneMAnia network neighbors. Yellow dots illustrate the adjusted p-values for each GO-BP category.

S1 Table. Clinical data of patients used for the validation set.

Characteristics		*Non Progressed (N=10)*	*Progressed (N=9)*
Age	*Median at t0*	63	51
	Range at t0	32-67	45-71
	Median at t1	69,5	57
	Range at t1	42-81	48-72
Gender	*F*	20% (N=2)	0%
	M	80% (N=8)	100%
Race	*Caucasian*	100%	100%
Alchool history[3]		20% (N=2)	78% (N=7)
Tobacco history[3]		20% (N=2)	44% (N=4)
BMI[3]	*Median*	na	28,6
	Range	na	24.3-31.1
BE-associated high-grade dysplasia/adenocarcino		na	100%
Tumor Grading (TNM)	*T1N0Mx*	na	100%
Follow-up (years)	*Median*	10	4
	Range	3-17	1-13

3. Data not available for all individuals

S2 Table. Primer sequences for target and reference genes.

Symbol	*Forward primer*	*Reverse primer*	*Amplicon length*
CYR61	TGACAACCCTGAGTGCCGCC	TCTTGCCCTTTTTCAGGCTGCTG	95
GAPDH	GGACTCATGACCACAGTCCATGCC	GCGGCCATCACGCCACAGTT	84
MAPKAP2	TACATCCTGCTGTGTGGGTATCCCC	TGGCCCATTCGGATGCGAGTCT	89
TAZ	GCAGGAAGCTGCCCTCTGTCG	TGGGTGGGTTGACAGCAGCC	80
TWIST1	GCCTGGTCCATGTCCGC	GAAACAATGACATCTAGGTCTCCC	82

S3 Table. Differentially expression analysis filtered genes (Lods > 5).

ProbeID	*SYMBOL*	*ENTREZ*	*UNIPROT*	*CHR*	*CHRLOC*	*Log2R*	*Rawpval*	*AdjpvalBH*	*Lods*
201289_at	CYR61	3491	O00622	1	86046443	4,80	5,29E-17	5,90E-13	28,20
202672_s_at	ATF3	467	P18847	1	212738696	3,27	2,57E-17	5,74E-13	28,86
202340_x_at	NR4A1	3164	P22736	12	52445190	2,07	8,23E-16	6,11E-12	25,66
222162_s_at	ADAMTS1	9510	Q8NE26	21	-28208607	3,53	2,54E-15	1,16E-11	24,60
204420_at	FOSL1	8061	P15407	11	-65659691	2,35	2,61E-15	1,16E-11	24,58
201810_s_at	NA	NA	NA	NA	NA	1,86	5,21E-15	1,94E-11	23,93
221031_s_at	APOLD1	81575	A0AVN6	12	12878850	3,24	7,32E-15	2,33E-11	23,61
208078_s_at	NA	NA	NA	NA	NA	2,70	9,99E-15	2,78E-11	23,32
218876_at	TPPP3	51673	Q9BW30	16	-67423713	2,29	2,37E-14	5,88E-11	22,50
211909_x_at	PTGER3	5733	B1AK19	1	-71471537	1,33	3,00E-14	6,67E-11	22,28
38037_at	HBEGF	1839	Q99075	5	-139712428	2,17	7,52E-14	1,52E-10	21,40
217557_s_at	CPM	1368	P14384	12	-69244957	0,86	1,13E-13	2,09E-10	21,02
203066_at	CHST15	51363	B4DHT4	10	-125767185	2,78	2,62E-13	4,49E-10	20,21
222253_s_at	POM121L9P	29774	NA	22	24647588	-0,70	5,32E-13	8,32E-10	19,54
212846_at	RRP1B	23076	Q14684	21	45079431	1,74	5,60E-13	8,32E-10	19,49
202237_at	NNMT	4837	P40261	11	114166534	4,69	9,82E-13	1,37E-09	18,95
201768_s_at	CLINT1	9685	B7Z6F8	5	-157213296	-1,46	1,06E-12	1,39E-09	18,87
200054_at	ZNF259	8882	O75312	11	-116649276	1,46	1,15E-12	1,42E-09	18,80
202768_at	FOSB	2354	A8V1E1	19	45971252	3,32	1,28E-12	1,51E-09	18,69
212864_at	CDS2	8760	O95674	20	5107481	1,27	2,48E-12	2,63E-09	18,06
203044_at	CHSY1	22856	Q86X52	15	-101715928	2,63	2,48E-12	2,63E-09	18,06
202401_s_at	SRF	6722	P11831	6	43138919	1,44	3,24E-12	3,10E-09	17,80
214045_at	LIAS	11019	O43766	4	39460664	-1,14	3,30E-12	3,10E-09	17,79
201207_at	TNFAIP1	7126	Q13829	17	26662547	1,36	3,33E-12	3,10E-09	17,78
212533_at	WEE1	7465	B3KVE1	11	9595227	2,02	4,36E-12	3,75E-09	17,52
204991_s_at	NF2	4771	P35240	22	29999544	1,01	4,38E-12	3,75E-09	17,51
204157_s_at	SIK3	23387	Q9Y2K2	11	-116714119	1,24	4,87E-12	4,02E-09	17,41
213316_at	KIAA1462	57608	Q9P266	10	-30301728	1,18	5,16E-12	4,11E-09	17,35
203821_at	HBEGF	1839	Q99075	5	-139712428	2,33	6,80E-12	5,22E-09	17,09
217686_at	PTPN1	5770	A8K3M3	20	49126890	-0,85	7,43E-12	5,37E-09	17,00
220022_at	ZNF334	55713	Q5XKG8	20	-45129708	-0,63	7,47E-12	5,37E-09	17,00
210764_s_at	CYR61	3491	O00622	1	86046443	3,15	8,92E-12	6,21E-09	16,83
204206_at	MNT	4335	Q99583	17	-2287354	1,50	9,32E-12	6,29E-09	16,78
204597_x_at	STC1	6781	P52823	8	-23699433	3,16	1,06E-11	6,93E-09	16,66
218723_s_at	C13orf15	28984	Q9H4X1	13	42031541	3,27	1,12E-11	7,05E-09	16,60
203119_at	CCDC86	79080	Q9H6F5	11	60609428	1,20	1,15E-11	7,05E-09	16,59
204622_x_at	NR4A2	4929	P43354	2	-157180945	2,42	1,17E-11	7,05E-09	16,56
218708_at	NXT1	29107	Q9UKK6	20	23331372	1,26	1,27E-11	7,46E-09	16,48
212865_s_at	COL14A1	7373	Q05707	8	121137351	1,72	1,37E-11	7,81E-09	16,41
200073_s_at	HNRNPD	3184	Q14103	4	-83274466	1,32	1,46E-11	8,16E-09	16,35
39402_at	IL1B	3553	P01584	2	-113587336	2,52	1,69E-11	8,97E-09	16,21
210529_s_at	FAM115A	9747	Q9Y4C2	7	-143550048	-1,03	1,69E-11	8,97E-09	16,21
209550_at	NDN	4692	Q99608	15	-23930561	1,82	2,74E-11	1,42E-08	15,74
219419_at	RBFA	79863	Q8N0V3	18	77794345	0,97	2,80E-11	1,42E-08	15,72
201693_s_at	EGR1	1958	P18146	5	137801180	2,40	3,47E-11	1,70E-08	15,51
216651_s_at	GAD2	2572	Q05329	10	26505235	-0,64	3,51E-11	1,70E-08	15,50
217210_at	NA	NA	NA	NA	NA	-0,66	3,79E-11	1,79E-08	15,43
202806_at	DBN1	1627	Q16643	5	-176883613	2,15	4,72E-11	2,19E-08	15,22
204642_at	S1PR1	1901	P21453	1	101702304	1,36	5,10E-11	2,32E-08	15,14
216248_s_at	NR4A2	4929	P43354	2	-157180945	2,57	5,80E-11	2,59E-08	15,02
208664_s_at	TTC3	7267	P53804	21	38445570	-1,49	6,65E-11	2,91E-08	14,88
212190_at	SERPINE2	5270	B4DIF2	2	-224839764	2,58	7,13E-11	3,06E-08	14,82
210698_at	NA	NA	NA	NA	NA	-0,64	8,38E-11	3,52E-08	14,66
212884_x_at	APOE	348	P02649	19	45409038	1,33	8,61E-11	3,55E-08	14,63
212646_at	RFTN1	23180	Q14699	3	-16357352	2,66	1,05E-10	4,25E-08	14,44
218754_at	NOL9	79707	Q5SY16	1	-6581408	0,91	1,12E-10	4,40E-08	14,38

ProbeID	*SYMBOL*	*ENTREZ*	*UNIPROT*	*CHR*	*CHRLOC*	*Log2R*	*Rawpval*	*AdjpvalBH*	*Lods*
201811_x_at	SH3BP5	9467	B3KQW6	3	-15296356	2,43	1,13E-10	4,40E-08	14,37
214247_s_at	DKK3	27122	Q9UBP4	11	-11984544	3,00	1,14E-10	4,40E-08	14,36
219619_at	DIRAS2	54769	Q96HU8	9	-93372113	-0,54	1,24E-10	4,67E-08	14,28
201172_x_at	ATP6V0E1	8992	O15342	5	172410762	0,76	1,29E-10	4,79E-08	14,24
206419_at	RORC	6097	P51449	1	-151778547	-1,00	1,39E-10	4,98E-08	14,17
212097_at	CAV1	857	A9XTE5	7	116164838	2,90	1,40E-10	4,98E-08	14,16
202196_s_at	DKK3	27122	Q9UBP4	11	-11984544	2,20	1,43E-10	4,98E-08	14,14
214941_s_at	PRPF40A	55660	O75400	2	-153508108	-1,27	1,43E-10	4,98E-08	14,14
204107_at	NFYA	4800	P23511	6	41040706	-0,96	1,48E-10	5,07E-08	14,11
200810_s_at	CIRBP	1153	Q14011	19	1269266	1,37	1,60E-10	5,39E-08	14,03
212509_s_at	MXRA7	439921	P84157	17	-74675652	2,54	1,70E-10	5,66E-08	13,97
201110_s_at	THBS1	7057	P07996	15	39873279	3,55	1,73E-10	5,66E-08	13,96
204621_s_at	NR4A2	4929	P43354	2	-157180945	2,10	1,82E-10	5,88E-08	13,91
31874_at	GAS2L1	10634	A0A5E8	22	29702996	1,09	1,90E-10	6,06E-08	13,86
210911_at	ID2B	84099	NA	3	-62109160	-0,80	1,94E-10	6,10E-08	13,84
212766_s_at	ISG20L2	81875	Q9H9L3	1	-156692412	1,41	2,04E-10	6,31E-08	13,80
200788_s_at	PEA15	8682	B1AKZ4	1	160175124	2,29	2,18E-10	6,66E-08	13,73
206093_x_at	NA	NA	NA	NA	NA	1,81	2,37E-10	7,13E-08	13,65
202371_at	TCEAL4	79921	Q96EI5	X	102840418	2,15	2,46E-10	7,32E-08	13,61
200694_s_at	DDX24	57062	Q9GZR7	14	-94517268	1,16	2,51E-10	7,33E-08	13,59
204405_x_at	DIMT1L	27292	Q9UNQ2	5	-61684351	1,32	2,53E-10	7,33E-08	13,59
204482_at	CLDN5	7122	D3DX19	22	-19510546	2,31	2,78E-10	7,95E-08	13,49
214406_s_at	SLC7A4	6545	O43246	22	-21383007	-0,91	2,84E-10	8,02E-08	13,47
213069_at	HEG1	57493	Q9ULI3	3	-124684554	2,18	3,11E-10	8,66E-08	13,39
202273_at	PDGFRB	5159	P09619	5	-149493402	1,93	3,23E-10	8,89E-08	13,35
211143_x_at	NR4A1	3164	P22736	12	52445190	1,21	3,28E-10	8,92E-08	13,33
219049_at	CSGALNACT1	55790	Q8TDX6	8	-19261672	2,36	3,50E-10	9,34E-08	13,27
207609_s_at	CYP1A2	1544	P05177	15	75041183	-0,81	3,52E-10	9,34E-08	13,27
217216_x_at	MLH3	27030	Q2M1Z1	14	-75480466	-0,96	3,81E-10	1,00E-07	13,19
214413_at	TAT	6898	P17735	16	-71600753	-0,65	4,08E-10	1,06E-07	13,12
214900_at	ZKSCAN1	7586	P17029	7	99613218	-0,97	4,25E-10	1,09E-07	13,08
201185_at	HTRA1	5654	Q92743	10	124221040	2,04	4,50E-10	1,13E-07	13,03
213823_at	HOXA11	3207	P31270	7	-27220776	-1,17	4,52E-10	1,13E-07	13,02
203973_s_at	CEBPD	1052	P49716	8	-48649475	2,29	4,61E-10	1,14E-07	13,00
215521_at	PHC3	80012	Q8NDX5	3	-169805367	-0,81	4,71E-10	1,15E-07	12,98
37408_at	MRC2	9902	Q9UBG0	17	60704761	0,95	5,02E-10	1,22E-07	12,92
211340_s_at	MCAM	4162	P43121	11	-119179234	2,83	5,16E-10	1,23E-07	12,89
201645_at	TNC	3371	P24821	9	-117782805	3,31	5,17E-10	1,23E-07	12,89
209101_at	CTGF	1490	P29279	6	-132269318	3,47	5,45E-10	1,28E-07	12,84
213905_x_at	BGN	633	P21810	X	152760346	2,12	5,51E-10	1,28E-07	12,83
217481_x_at	NA	NA	NA	NA	NA	-0,62	5,61E-10	1,29E-07	12,81
204677_at	CDH5	1003	P33151	16	66400524	2,25	5,83E-10	1,31E-07	12,77
32541_at	PPP3CC	5533	P48454	8	22298595	0,69	5,85E-10	1,31E-07	12,77
220063_at	GSTCD	79807	Q8NEC7	4	106629940	-0,60	5,88E-10	1,31E-07	12,77
212235_at	PLXND1	23129	Q9Y4D7	3	-129274055	1,68	5,96E-10	1,31E-07	12,75
209087_x_at	MCAM	4162	P43121	11	-119179234	2,86	6,05E-10	1,32E-07	12,74
204472_at	GEM	2669	P55040	8	-95261486	2,47	6,25E-10	1,34E-07	12,71
213568_at	OSR2	116039	Q8N2R0	8	99956630	1,52	6,26E-10	1,34E-07	12,70
202238_s_at	NNMT	4837	P40261	11	114166534	3,29	6,65E-10	1,41E-07	12,65
218368_s_at	TNFRSF12A	51330	Q9NP84	16	3070312	1,45	6,82E-10	1,43E-07	12,62
202087_s_at	CTSL1	1514	P07711	9	90340973	1,63	7,12E-10	1,48E-07	12,58
202994_s_at	FBLN1	2192	P23142	22	45898718	2,22	7,80E-10	1,61E-07	12,49
215308_at	XRCC6	2547	B1AHC8	22	42017294	-0,53	7,96E-10	1,63E-07	12,47
211980_at	COL4A1	1282	P02462	13	-110801310	3,34	8,10E-10	1,64E-07	12,45
217445_x_at	GART	2618	P22102	21	-34896315	-0,70	8,15E-10	1,64E-07	12,45
217547_x_at	ZNF675	171392	Q8TD23	19	-23835708	-0,54	8,40E-10	1,67E-07	12,42
208249_s_at	TGDS	23483	O95455	13	-95226308	-1,15	9,01E-10	1,78E-07	12,35

ProbeID	*SYMBOL*	*ENTREZ*	*UNIPROT*	*CHR*	*CHRLOC*	*Log2R*	*Rawpval*	*AdjpvalBH*	*Lods*
203065_s_at	CAV1	857	A9XTE5	7	116164838	1,72	9,34E-10	1,82E-07	12,32
213269_at	ZNF248	57209	A2RUI7	10	-38117898	-0,84	9,39E-10	1,82E-07	12,31
203723_at	ITPKB	3707	B2R9J0	1	-226819391	1,47	1,12E-09	2,16E-07	12,14
210896_s_at	ASPH	444	B4DIC9	8	-62587818	-2,28	1,17E-09	2,22E-07	12,10
201980_s_at	RSU1	6251	A8KA46	10	-16632618	1,12	1,18E-09	2,22E-07	12,09
217532_x_at	NA	NA	NA	NA	NA	-0,66	1,21E-09	2,27E-07	12,06
208298_at	EVI5	7813	O60447	1	-92974254	-0,61	1,29E-09	2,39E-07	12,00
216834_at	RGS1	5996	Q08116	1	192544856	2,38	1,31E-09	2,39E-07	11,99
201148_s_at	TIMP3	7078	P35625	22	33196801	1,44	1,31E-09	2,39E-07	11,99
212430_at	RBM38	55544	Q9H0Z9	20	55966462	1,01	1,33E-09	2,39E-07	11,97
204686_at	IRS1	3667	P35568	2	-227596033	1,71	1,34E-09	2,39E-07	11,96
218239_s_at	GTPBP4	23560	D2CFK9	10	1034348	1,08	1,34E-09	2,39E-07	11,96
209850_s_at	CDC42EP2	10435	O14613	11	65082330	0,94	1,37E-09	2,41E-07	11,95
201842_s_at	EFEMP1	2202	Q12805	2	-56093102	3,07	1,39E-09	2,43E-07	11,93
201261_x_at	BGN	633	P21810	X	152760346	1,90	1,40E-09	2,44E-07	11,92
200804_at	TMBIM6	7009	P55061	12	50135292	-1,20	1,45E-09	2,50E-07	11,89
218468_s_at	GREM1	26585	A6XAA7	15	33010204	4,67	1,50E-09	2,57E-07	11,85
209702_at	FTO	79068	B3KU60	16	53737874	1,11	1,53E-09	2,58E-07	11,84
209487_at	RBPMS	11030	Q93062	8	30241943	2,31	1,53E-09	2,58E-07	11,84
212119_at	RHOQ	23433	P17081	2	46769866	1,92	1,62E-09	2,71E-07	11,78
215475_at	NA	NA	NA	NA	NA	-0,51	1,63E-09	2,71E-07	11,77
202689_at	RBM15B	29890	Q8NDT2	3	51428730	0,84	1,68E-09	2,78E-07	11,74
208030_s_at	ADD1	118	A2A3N8	4	2845583	1,10	1,72E-09	2,83E-07	11,72
201694_s_at	EGR1	1958	P18146	5	137801180	2,69	1,74E-09	2,83E-07	11,71
206946_at	HCN4	10021	Q9Y3Q4	15	-73612200	-0,66	1,77E-09	2,84E-07	11,69
200702_s_at	DDX24	57062	Q9GZR7	14	-94517268	1,14	1,77E-09	2,84E-07	11,69
210326_at	AGXT	189	P21549	2	241808161	-0,95	1,79E-09	2,84E-07	11,68
208226_x_at	ADAM22	53616	Q08AL8	7	87563701	-0,79	1,80E-09	2,84E-07	11,68
218199_s_at	NOL6	65083	Q9H6R4	9	-33461351	1,03	1,84E-09	2,89E-07	11,66
202878_s_at	CD93	22918	Q9NPY3	20	-23059993	2,95	1,95E-09	3,03E-07	11,60
220880_at	NA	NA	NA	NA	NA	-0,53	1,96E-09	3,03E-07	11,59
212747_at	ANKS1A	23294	Q05CP0	6	34857037	1,23	1,98E-09	3,04E-07	11,59
201783_s_at	RELA	5970	Q04206	11	-65421067	0,90	2,02E-09	3,09E-07	11,56
203574_at	NFIL3	4783	Q16649	9	-94171328	2,29	2,06E-09	3,12E-07	11,55
208789_at	PTRF	284119	Q6NZI2	17	-40554468	2,12	2,10E-09	3,16E-07	11,53
208361_s_at	POLR3D	661	P05423	8	22102618	0,80	2,17E-09	3,22E-07	11,50
218035_s_at	RBM47	54502	A0AV96	4	-40425271	-1,94	2,17E-09	3,22E-07	11,50
214071_at	GNAL	2774	A8K1Y9	18	11689135	1,28	2,20E-09	3,25E-07	11,48
212723_at	JMJD6	23210	Q6NYC1	17	-74714526	1,42	2,33E-09	3,41E-07	11,43
218641_at	C11orf95	65998	C9JLR9	11	-63527364	1,27	2,37E-09	3,45E-07	11,41
204376_at	VPRBP	9730	Q9Y4B6	3	-51433297	-0,53	2,44E-09	3,53E-07	11,38
222146_s_at	TCF4	6925	B3KVA4	18	-52889561	1,84	2,54E-09	3,65E-07	11,34
219155_at	PITPNC1	26207	Q9UKF7	17	65373923	1,37	2,61E-09	3,73E-07	11,31
219562_at	RAB26	25837	Q3L6K5	16	2198650	-1,35	2,63E-09	3,73E-07	11,31
209012_at	TRIO	7204	O75962	5	14143828	0,85	2,67E-09	3,76E-07	11,29
211327_x_at	HFE	3077	Q30201	6	26087508	-1,00	2,71E-09	3,80E-07	11,28
213127_s_at	MED8	112950	Q96G25	1	-43850397	0,99	2,85E-09	3,97E-07	11,23
208191_x_at	PSG4	5672	B3KQL2	19	-43696855	-1,03	3,03E-09	4,19E-07	11,17
50221_at	TFEB	7942	P19484	6	-41651715	1,12	3,06E-09	4,21E-07	11,16
216142_at	NA	NA	NA	NA	NA	1,02	3,08E-09	4,21E-07	11,15
65591_at	WDR48	57599	Q8TAF3	3	39093506	-0,79	3,12E-09	4,23E-07	11,14
202624_s_at	CABIN1	23523	Q9Y6J0	22	24407764	-0,85	3,13E-09	4,23E-07	11,14
209074_s_at	FAM107A	11170	O95990	3	-58549846	2,18	3,32E-09	4,44E-07	11,08
221737_at	GNA12	2768	B3KXS2	7	-2767742	0,79	3,33E-09	4,44E-07	11,08
219868_s_at	ANKFY1	51479	B3KPZ0	17	-4097774	-0,81	3,43E-09	4,55E-07	11,05
219028_at	HIPK2	28996	Q9H2X6	7	-139246316	1,11	3,57E-09	4,71E-07	11,01
202565_s_at	SVIL	6840	O95425	10	-29746276	1,81	3,62E-09	4,74E-07	11,00

ProbeID	*SYMBOL*	*ENTREZ*	*UNIPROT*	*CHR*	*CHRLOC*	*Log2R*	*Rawpval*	*AdjpvalBH*	*Lods*
214075_at	NENF	29937	Q9UMX5	1	212606228	0,69	3,71E-09	4,78E-07	10,97
217044_s_at	PLEKHG3	26030	A1L390	14	65171192	-0,95	3,71E-09	4,78E-07	10,97
221359_at	GDNF	2668	P39905	5	-37812778	-0,56	3,73E-09	4,78E-07	10,97
207574_s_at	GADD45B	4616	O75293	19	2476122	2,16	3,73E-09	4,78E-07	10,97
216675_at	NA	NA	NA	NA	NA	-0,64	3,87E-09	4,90E-07	10,93
200096_s_at	ATP6V0E1	8992	O15342	5	172410762	0,81	3,87E-09	4,90E-07	10,93
215438_x_at	GSPT1	2935	B2RCT6	16	-11961986	1,11	3,95E-09	4,97E-07	10,91
210994_x_at	TRIM23	373	P36406	5	-64885508	-0,62	4,02E-09	5,03E-07	10,89
207188_at	CDK3	1018	Q00526	17	73966986	-0,74	4,31E-09	5,36E-07	10,83
214784_x_at	XPO6	23214	Q96QU8	16	-28109315	0,84	4,38E-09	5,43E-07	10,81
216333_x_at	NA	NA	NA	NA	NA	1,76	4,52E-09	5,57E-07	10,78
208636_at	ACTN1	87	B3V8S3	14	-69340840	2,16	4,55E-09	5,57E-07	10,77
211554_s_at	APAF1	317	O14727	12	99039077	-0,94	4,59E-09	5,58E-07	10,76
202577_s_at	DDX19A	55308	Q9NUU7	16	70380823	0,83	4,69E-09	5,68E-07	10,74
201961_s_at	RNF41	10193	A6NFW0	12	-56598285	0,69	4,74E-09	5,71E-07	10,73
222176_at	PTEN	5728	P60484	10	89623194	-0,56	4,98E-09	5,97E-07	10,68
216406_at	NA	NA	NA	NA	NA	-0,50	5,05E-09	6,02E-07	10,67
210455_at	C10orf28	27291	Q4KMY3	10	99894380	-0,58	5,34E-09	6,33E-07	10,62
209145_s_at	CBFA2T2	9139	O43439	20	32077927	-0,67	5,40E-09	6,37E-07	10,60
203886_s_at	FBLN2	2199	B7Z9C5	3	13590624	1,62	5,46E-09	6,40E-07	10,59
212136_at	ATP2B4	493	B1APW5	1	203595927	2,23	5,51E-09	6,41E-07	10,59
210771_at	PPARA	5465	Q07869	22	46546498	-0,42	5,53E-09	6,41E-07	10,58
214807_at	NA	NA	NA	NA	NA	1,04	5,57E-09	6,43E-07	10,58
214813_at	ZNF75D	7626	A6NK62	X	-134419723	-0,71	5,64E-09	6,48E-07	10,56
208763_s_at	TSC22D3	1831	Q5JRJ2	X	-106956459	2,24	5,69E-09	6,48E-07	10,55
213249_at	FBXL7	23194	Q9UJT9	5	15500304	0,95	5,70E-09	6,48E-07	10,55
209007_s_at	C1orf63	57035	Q9BUV0	1	-25568740	-1,93	5,77E-09	6,53E-07	10,54
218356_at	FTSJ2	29960	Q9UI43	7	-2273927	1,05	5,82E-09	6,54E-07	10,53
202686_s_at	AXL	558	P30530	19	41725107	2,35	5,84E-09	6,54E-07	10,53
217672_x_at	EIF1	10209	P41567	17	39845126	0,72	5,91E-09	6,58E-07	10,52
207770_x_at	CSH2	1443	A6NIT4	17	-61949372	-0,74	6,00E-09	6,65E-07	10,50
211863_x_at	HFE	3077	Q30201	6	26087508	-0,72	6,13E-09	6,76E-07	10,48
217106_x_at	DIMT1L	27292	Q9UNQ2	5	-61684351	1,28	6,57E-09	7,18E-07	10,41
218469_at	GREM1	26585	A6XAA7	15	33010204	4,10	6,67E-09	7,25E-07	10,40
203753_at	TCF4	6925	B3KVA4	18	-52889561	1,72	6,76E-09	7,31E-07	10,39
221127_s_at	DKK3	27122	Q9UBP4	11	-11984544	1,22	7,09E-09	7,63E-07	10,34
212172_at	AK2	204	P54819	1	-33478582	-0,72	7,39E-09	7,91E-07	10,30
204917_s_at	MLLT3	4300	P42568	9	-20344967	-1,68	7,45E-09	7,94E-07	10,29
213451_x_at	NA	NA	NA	NA	NA	1,90	7,53E-09	7,98E-07	10,28
220874_at	NA	NA	NA	NA	NA	-0,55	7,55E-09	7,98E-07	10,28
221681_s_at	DSPP	1834	Q9NZW4	4	88529680	1,03	7,78E-09	8,18E-07	10,25
218181_s_at	MAP4K4	9448	O95819	2	102314487	1,49	8,20E-09	8,58E-07	10,20
208723_at	USP11	8237	P51784	X	47092313	1,31	8,52E-09	8,85E-07	10,16
205432_at	OVGP1	5016	Q12889	1	-111956937	-0,77	8,56E-09	8,85E-07	10,16
204489_s_at	CD44	960	O95370	11	35160416	1,55	8,58E-09	8,85E-07	10,15
214028_x_at	TDRD3	81550	Q9H7E2	13	60970590	-0,51	8,87E-09	9,03E-07	10,12
209082_s_at	COL18A1	80781	D3DSM4	21	46825096	1,85	8,87E-09	9,03E-07	10,12
211426_x_at	GNAQ	2776	P50148	9	-80335199	-0,85	8,90E-09	9,03E-07	10,12
212886_at	CCDC69	26112	A6NI79	5	-150560613	1,95	8,92E-09	9,03E-07	10,12
210793_s_at	NUP98	4928	P52948	11	-3733058	1,73	9,88E-09	9,97E-07	10,02
210311_at	FGF5	2250	P12034	4	81187741	-0,70	9,93E-09	9,97E-07	10,01
204513_s_at	ELMO1	9844	A4D1X5	7	-36893960	1,60	1,00E-08	1,00E-06	10,00
208782_at	FSTL1	11167	Q12841	3	-120113061	2,98	1,03E-08	1,03E-06	9,97
201446_s_at	TIA1	7072	P31483	2	-70436576	-1,30	1,04E-08	1,03E-06	9,97
207686_s_at	CASP8	841	Q14790	2	202098165	-1,05	1,06E-08	1,04E-06	9,95
217209_at	CEACAM3	1084	P40198	19	42300533	-1,36	1,10E-08	1,08E-06	9,91
218233_s_at	NA	NA	NA	NA	NA	1,09	1,11E-08	1,08E-06	9,90

ProbeID	SYMBOL	ENTREZ	UNIPROT	CHR	CHRLOC	Log2R	Rawpval	AdjpvalBH	Lods
209214_s_at	EWSR1	2130	B0QYK1	22	29663997	0,77	1,15E-08	1,12E-06	9,87
202732_at	PKIG	11142	Q549H9	20	43160435	2,44	1,17E-08	1,13E-06	9,85
204115_at	GNG11	2791	P61952	7	93551015	2,56	1,18E-08	1,14E-06	9,84
218670_at	PUS1	80324	E5KMT5	12	132413744	0,95	1,20E-08	1,14E-06	9,83
34063_at	RECQL5	9400	A5YM55	17	-73646444	-0,63	1,20E-08	1,14E-06	9,83
202241_at	TRIB1	10221	Q96RU8	8	126442562	1,85	1,23E-08	1,17E-06	9,80
201787_at	FBLN1	2192	P23142	22	45898718	1,76	1,24E-08	1,17E-06	9,79
220052_s_at	TINF2	26277	Q9BSI4	14	-24708852	0,96	1,24E-08	1,17E-06	9,79
221752_at	SSH1	54434	Q8WYL5	12	-109185695	1,10	1,27E-08	1,19E-06	9,77
215022_x_at	ZNF33B	7582	Q06732	10	-43084554	-0,88	1,27E-08	1,19E-06	9,77
213338_at	TMEM158	25907	Q8WZ71	3	-45265956	2,21	1,31E-08	1,22E-06	9,74
206115_at	EGR3	1960	B4DH80	8	-22545173	1,19	1,34E-08	1,23E-06	9,72
202291_s_at	MGP	4256	P08493	12	-15034114	3,81	1,34E-08	1,23E-06	9,72
204955_at	SRPX	8406	B3KWP8	X	-38008588	2,78	1,35E-08	1,24E-06	9,71
213763_at	HIPK2	28996	Q9H2X6	7	-139246316	-0,86	1,37E-08	1,26E-06	9,69
179_at	PMS2P11	441263	NA	7	76610138	-0,71	1,39E-08	1,26E-06	9,68
209118_s_at	TUBA1A	7846	Q71U36	12	-49578584	2,43	1,40E-08	1,26E-06	9,67
201431_s_at	DPYSL3	1809	B3SXQ8	5	-146770370	2,82	1,41E-08	1,26E-06	9,67
211866_x_at	HFE	3077	Q30201	6	26087508	-0,76	1,41E-08	1,26E-06	9,67
220623_s_at	TSGA10	80705	Q9BZW7	2	-99613724	-0,59	1,43E-08	1,28E-06	9,65
216934_at	NA	NA	NA	NA	NA	-0,70	1,47E-08	1,31E-06	9,63
206086_x_at	HFE	3077	Q30201	6	26087508	-0,73	1,53E-08	1,35E-06	9,59
214955_at	TMPRSS6	164656	Q8IU80	22	-37461478	-0,69	1,53E-08	1,35E-06	9,59
215222_x_at	MACF1	23499	Q96PK2	1	39547117	0,76	1,56E-08	1,37E-06	9,57
211490_at	ADRA1A	148	B0ZBD3	8	-26627221	-0,73	1,56E-08	1,37E-06	9,57
200986_at	SERPING1	710	P05155	11	57365026	2,72	1,64E-08	1,43E-06	9,52
221839_s_at	UBAP2	55833	Q5T6F2	9	-33921690	0,67	1,64E-08	1,43E-06	9,52
219935_at	ADAMTS5	11096	Q9UNA0	21	-28290231	1,54	1,68E-08	1,46E-06	9,50
214880_x_at	CALD1	800	A8K0X1	7	134464163	1,00	1,71E-08	1,47E-06	9,48
210195_s_at	PSG1	5669	P11464	19	-43371357	-0,78	1,71E-08	1,47E-06	9,48
222264_at	HNRNPUL2	221092	Q1KMD3	11	-62482221	0,94	1,71E-08	1,47E-06	9,48
203650_at	PROCR	10544	Q9UNN8	20	33759773	1,23	1,72E-08	1,47E-06	9,47
204475_at	MMP1	4312	B4DN15	11	-102660640	4,70	1,73E-08	1,47E-06	9,47
204027_s_at	METTL1	4234	Q53FS9	12	-58162351	1,03	1,76E-08	1,49E-06	9,45
220914_at	NA	NA	NA	NA	NA	-0,51	1,76E-08	1,49E-06	9,45
220350_at	ZNF235	9310	Q14590	19	-44790501	-0,76	1,78E-08	1,50E-06	9,44
206069_s_at	ACADL	33	P28330	2	-211052717	-0,58	1,80E-08	1,51E-06	9,43
210781_x_at	GRIN1	2902	Q05586	9	140033608	-0,72	1,83E-08	1,53E-06	9,41
216343_at	PCDHGA3	56112	Q9Y5H0	5	140723600	-0,93	1,87E-08	1,55E-06	9,39
216856_s_at	DLEU2	8847	NA	13	-50556687	-0,44	1,91E-08	1,59E-06	9,37
211753_s_at	RLN1	6013	P04808	9	-5334968	-0,73	1,93E-08	1,60E-06	9,36
209174_s_at	QRICH1	54870	A1L3Z9	3	-49067143	0,53	1,99E-08	1,63E-06	9,33
210506_at	FUT7	2529	Q11130	9	-139924625	-0,87	2,05E-08	1,68E-06	9,30
208275_x_at	UTF1	8433	Q5T230	10	135043777	-0,77	2,08E-08	1,70E-06	9,29
202391_at	BASP1	10409	P80723	5	17217749	2,49	2,12E-08	1,73E-06	9,27
200600_at	MSN	4478	P26038	X	64887510	3,19	2,20E-08	1,79E-06	9,23
213450_s_at	ICOSLG	23308	A0N0L8	21	-45646723	-0,75	2,31E-08	1,86E-06	9,19
220929_at	GALNT8	26290	Q9NY28	12	4829751	-1,14	2,44E-08	1,96E-06	9,13
210995_s_at	TRIM23	373	P36406	5	-64885508	-0,67	2,51E-08	2,01E-06	9,10
203307_at	GNL1	2794	B4DYK6	6	-30509155	1,15	2,56E-08	2,04E-06	9,09
202450_s_at	CTSK	1513	P43235	1	-150768686	2,19	2,56E-08	2,04E-06	9,09
214662_at	WDR43	23160	Q15061	2	29117532	1,04	2,71E-08	2,15E-06	9,03
205067_at	IL1B	3553	P01584	2	-113587336	1,99	2,78E-08	2,19E-06	9,01
218586_at	C20orf20	55257	A8C4L5	20	61427804	0,93	2,80E-08	2,20E-06	9,00
218713_at	NARG2	79664	Q659A1	15	-60711808	-0,87	2,83E-08	2,21E-06	8,99
201040_at	GNAI2	2771	B3KP24	3	50273646	1,07	2,83E-08	2,21E-06	8,99
221325_at	KCNK13	56659	B5TJL8	14	90528107	-0,62	2,89E-08	2,24E-06	8,97

ProbeID	SYMBOL	ENTREZ	UNIPROT	CHR	CHRLOC	Log2R	Rawpval	AdjpvalBH	Lods
212067_s_at	C1R	715	P00736	12	-7187516	2,61	2,89E-08	2,24E-06	8,97
205039_s_at	IKZF1	10320	Q13422	7	50344377	-0,53	2,93E-08	2,26E-06	8,95
212464_s_at	FN1	2335	P02751	2	-216279384	4,24	2,93E-08	2,26E-06	8,95
212813_at	JAM3	83700	Q9BX67	11	133938819	1,80	2,96E-08	2,27E-06	8,95
209967_s_at	CREM	1390	A8K014	10	35415800	0,95	2,99E-08	2,29E-06	8,93
205100_at	GFPT2	9945	O94808	5	-179727699	1,11	3,09E-08	2,36E-06	8,90
200771_at	LAMC1	3915	P11047	1	182992594	2,49	3,11E-08	2,36E-06	8,90
208431_s_at	TUB	7275	P50607	11	8060179	-0,64	3,12E-08	2,37E-06	8,89
203502_at	BPGM	669	A4D1N9	7	134331530	1,30	3,17E-08	2,40E-06	8,88
217565_at	GRIA3	2892	P42263	X	122318095	-0,69	3,20E-08	2,41E-06	8,87
218313_s_at	GALNT7	51809	Q86SF2	4	174089903	-2,60	3,26E-08	2,45E-06	8,85
216982_x_at	NA	NA	NA	NA	NA	0,70	3,28E-08	2,45E-06	8,84
212755_at	MON2	23041	Q7Z3U7	12	62860596	-0,58	3,31E-08	2,47E-06	8,84
219091_s_at	MMRN2	79812	Q9H8L6	10	-88695299	1,40	3,52E-08	2,61E-06	8,78
203063_at	PPM1F	9647	P49593	22	-22273791	1,10	3,53E-08	2,62E-06	8,77
56197_at	PLSCR3	57048	Q9NRY6	17	-7293054	0,99	3,65E-08	2,69E-06	8,74
221748_s_at	TNS1	7145	A1L0S7	2	-218664511	3,32	3,67E-08	2,70E-06	8,73
219805_at	CXorf56	63932	A8MPX7	X	-118672112	0,62	3,73E-08	2,72E-06	8,72
219822_at	MTRF1	9617	O75570	13	-41790516	-0,96	3,74E-08	2,72E-06	8,72
202112_at	VWF	7450	P04275	12	-6058039	2,53	3,75E-08	2,72E-06	8,71
211748_x_at	PTGDS	5730	P41222	9	139871955	2,14	3,75E-08	2,72E-06	8,71
204345_at	COL16A1	1307	Q07092	1	-32117847	1,31	3,76E-08	2,72E-06	8,71
211534_x_at	PTPRN2	5799	Q92932	7	-157331750	-0,75	3,82E-08	2,75E-06	8,70
202613_at	CTPS	1503	P17812	1	41445006	1,13	3,83E-08	2,75E-06	8,69
200931_s_at	VCL	7414	B3KXA2	10	75757871	1,37	3,85E-08	2,76E-06	8,69
200859_x_at	FLNA	2316	P21333	X	-153576899	2,38	3,87E-08	2,76E-06	8,68
213348_at	CDKN1C	1028	P49918	11	-2904449	1,87	3,89E-08	2,77E-06	8,68
201339_s_at	SCP2	6342	A6NM69	1	53392900	-1,95	3,90E-08	2,77E-06	8,67
213254_at	TNRC6B	23112	Q9UPQ9	22	40440820	0,79	3,92E-08	2,77E-06	8,67
201253_s_at	CDIPT	10423	A8K3L7	16	-29869678	1,23	3,98E-08	2,80E-06	8,66
220539_at	C10orf92	54777	NA	10	NA	-0,55	4,01E-08	2,80E-06	8,65
203737_s_at	PPRC1	23082	Q5VV67	10	103892786	1,29	4,01E-08	2,80E-06	8,65
208393_s_at	RAD50	10111	A5D6Y3	5	131892615	-1,03	4,02E-08	2,80E-06	8,65
217916_s_at	FAM49B	51571	Q9NUQ9	8	-130853717	0,72	4,03E-08	2,80E-06	8,64
201522_x_at	NA	NA	NA	NA	NA	1,78	4,03E-08	2,80E-06	8,64
211535_s_at	FGFR1	2260	P11362	8	-38280848	1,73	4,05E-08	2,80E-06	8,64
217563_at	CLOCK	9575	O15516	4	-56298659	-0,65	4,08E-08	2,81E-06	8,63
213884_s_at	TRIM3	10612	O75382	11	-6469843	-0,93	4,10E-08	2,82E-06	8,63
211588_s_at	NA	NA	NA	NA	NA	-0,76	4,15E-08	2,84E-06	8,61
217214_s_at	SLC6A2	6530	B4DX48	16	55689541	-0,59	4,16E-08	2,84E-06	8,61
201042_at	TGM2	7052	P21980	20	-36766352	1,77	4,27E-08	2,91E-06	8,59
203477_at	COL15A1	1306	P39059	9	101706137	4,06	4,42E-08	3,00E-06	8,55
207017_at	RAB27B	5874	O00194	18	52495839	-1,22	4,53E-08	3,07E-06	8,53
203173_s_at	C16orf62	57020	Q7Z3J2	16	19567039	0,83	4,56E-08	3,08E-06	8,52
220861_at	NA	NA	NA	NA	NA	-0,56	4,63E-08	3,11E-06	8,51
215798_at	ALDH1L1	10840	O75891	3	-125822407	-0,71	4,63E-08	3,11E-06	8,51
212744_at	BBS4	585	Q96RK4	15	72978525	-0,65	4,67E-08	3,13E-06	8,50
202729_s_at	LTBP1	4052	B7ZLY3	2	33172368	1,90	4,74E-08	3,16E-06	8,49
211599_x_at	MET	4233	A1L467	7	116312458	-1,18	4,75E-08	3,16E-06	8,48
214752_x_at	FLNA	2316	P21333	X	-153576899	2,49	4,77E-08	3,16E-06	8,48
202084_s_at	SEC14L1	6397	A5PLM6	17	75137004	1,21	4,94E-08	3,26E-06	8,44
208526_at	OR2F1	26211	Q13607	7	143657019	-0,69	4,94E-08	3,26E-06	8,44
210869_s_at	MCAM	4162	P43121	11	-119179234	2,29	4,98E-08	3,27E-06	8,44
203237_s_at	NOTCH3	4854	Q9UM47	19	-15270444	-0,56	4,99E-08	3,27E-06	8,43
207679_at	PAX3	5077	P23760	2	-223158348	-0,50	5,13E-08	3,35E-06	8,41
222043_at	CLU	1191	P10909	8	-27454450	2,42	5,26E-08	3,43E-06	8,38
207836_s_at	RBPMS	11030	Q93062	8	30241943	1,65	5,29E-08	3,43E-06	8,38

ProbeID	SYMBOL	ENTREZ	UNIPROT	CHR	CHRLOC	Log2R	Rawpval	AdjpvalBH	Lods
222297_x_at	RPL18	6141	Q07020	19	-49118587	0,67	5,30E-08	3,43E-06	8,38
206947_at	B3GALT5	10317	Q9Y2C3	21	41029253	-1,04	5,43E-08	3,51E-06	8,35
214518_at	PDHA2	5161	P29803	4	96761238	-0,81	5,56E-08	3,58E-06	8,33
203068_at	KLHL21	9903	Q9UJP4	1	-6650784	1,59	5,67E-08	3,64E-06	8,31
204083_s_at	TPM2	7169	P07951	9	-35682923	4,02	5,77E-08	3,69E-06	8,29
211719_x_at	FN1	2335	P02751	2	-216279384	4,51	5,78E-08	3,69E-06	8,29
205140_at	FPGT	8790	A6NMH3	1	74663925	-1,31	5,81E-08	3,69E-06	8,29
209144_s_at	CBFA2T2	9139	O43439	20	32077927	-0,66	5,83E-08	3,69E-06	8,28
210386_s_at	MTX1	4580	Q13505	1	155178489	1,05	5,83E-08	3,69E-06	8,28
207164_s_at	ZNF238	10472	Q99592	1	244214560	-0,57	5,85E-08	3,69E-06	8,28
211565_at	SH3GL3	6457	Q99963	15	84116090	-0,55	5,88E-08	3,69E-06	8,27
204030_s_at	SCHIP1	29970	Q9P0W5	3	158991543	1,36	5,90E-08	3,69E-06	8,27
208335_s_at	DARC	2532	Q16570	1	159174509	2,79	5,90E-08	3,69E-06	8,27
202332_at	CSNK1E	1454	P49674	22	-38686697	1,17	5,94E-08	3,71E-06	8,26
203526_s_at	APC	324	B7Z2B6	5	112043217	-0,68	5,98E-08	3,72E-06	8,26
212072_s_at	CSNK2A1	1457	B4DYS6	20	-463337	0,52	5,99E-08	3,72E-06	8,26
211349_at	SLC15A1	6564	B2CQT6	13	-99336056	-0,50	6,02E-08	3,73E-06	8,25
217830_s_at	NSFL1C	55968	A2A2L1	20	-1422812	0,63	6,21E-08	3,83E-06	8,22
206590_x_at	DRD2	1813	P14416	11	-113280317	-0,64	6,25E-08	3,84E-06	8,22
219025_at	CD248	57124	Q9HCU0	11	-66081957	1,31	6,31E-08	3,87E-06	8,20
37152_at	PPARD	5467	B4E3V3	6	35310334	1,33	6,40E-08	3,91E-06	8,19
202283_at	SERPINF1	5176	P36955	17	1665258	2,38	6,54E-08	3,99E-06	8,17
220473_s_at	ZCCHC4	29063	Q9H5U6	4	25314395	-0,40	6,59E-08	4,01E-06	8,16
213679_at	TTC30A	92104	Q86WT1	2	-178479026	-0,47	6,60E-08	4,01E-06	8,16
210367_s_at	PTGES	9536	O14684	9	-132500615	1,54	6,64E-08	4,02E-06	8,16
209313_at	GPN1	11321	B4DQJ5	2	27851514	0,76	6,65E-08	4,02E-06	8,15
219635_at	ZNF606	80095	Q8WXB4	19	-58488446	-0,69	6,78E-08	4,08E-06	8,14
212187_x_at	PTGDS	5730	P41222	9	139871955	2,05	6,89E-08	4,14E-06	8,12
218310_at	RABGEF1	27342	Q9UJ41	7	66205642	0,79	6,93E-08	4,15E-06	8,11
213656_s_at	KLC1	3831	Q07866	14	104095524	1,79	6,97E-08	4,16E-06	8,11
200839_s_at	CTSB	1508	P07858	8	-11700035	1,53	7,03E-08	4,19E-06	8,10
208089_s_at	TDRD3	81550	Q9H7E2	13	60970590	-0,66	7,08E-08	4,21E-06	8,09
220715_at	NA	NA	NA	NA	NA	-0,64	7,11E-08	4,21E-06	8,09
211125_x_at	GRIN1	2902	Q05586	9	140033608	-0,81	7,12E-08	4,21E-06	8,09
209039_x_at	EHD1	10938	B2R5U3	11	-64620207	0,83	7,18E-08	4,24E-06	8,08
212349_at	POFUT1	23509	Q9H488	20	30795695	0,75	7,23E-08	4,25E-06	8,07
209609_s_at	MRPL9	65005	Q9BYD2	1	-151732124	1,43	7,24E-08	4,25E-06	8,07
220841_s_at	AHI1	54806	Q8N157	6	-135708921	-0,75	7,29E-08	4,26E-06	8,06
212501_at	CEBPB	1051	P17676	20	48807375	2,27	7,33E-08	4,28E-06	8,06
221915_s_at	RANBP1	5902	P43487	22	20105023	-0,72	7,39E-08	4,30E-06	8,05
209519_at	NCBP1	4686	Q09161	9	100395704	-0,44	7,41E-08	4,30E-06	8,05
212977_at	CXCR7	57007	P25106	2	237478379	2,43	7,70E-08	4,45E-06	8,01
211086_x_at	NEK1	4750	Q5JXL9	4	-170314428	-0,48	7,79E-08	4,50E-06	8,00
41553_at	OSGIN2	734	Q9Y236	8	90914095	-0,44	7,83E-08	4,51E-06	7,99
207459_x_at	GYPB	2994	P06028	4	-144917256	-0,68	7,84E-08	4,51E-06	7,99
216693_x_at	HDGFRP3	50810	Q9Y3E1	15	-83806815	1,10	7,88E-08	4,51E-06	7,99
222179_at	NA	NA	NA	NA	NA	-0,60	8,14E-08	4,63E-06	7,96
212354_at	SULF1	23213	Q8IWU6	8	70378858	1,87	8,14E-08	4,63E-06	7,96
220770_s_at	C5orf54	63920	Q8IZ13	5	-159820154	-0,65	8,15E-08	4,63E-06	7,95
221541_at	CRISPLD2	83716	Q9H0B8	16	84853586	2,50	8,21E-08	4,66E-06	7,95
203719_at	ERCC1	2067	B2RC01	19	-45916692	0,87	8,33E-08	4,71E-06	7,93
204595_s_at	STC1	6781	P52823	8	-23699433	2,16	8,48E-08	4,78E-06	7,92
203888_at	THBD	7056	P07204	20	-23026270	1,18	8,52E-08	4,79E-06	7,91
216145_at	NA	NA	NA	NA	NA	-0,76	8,65E-08	4,86E-06	7,90
216953_s_at	WT1	7490	B3KSA5	11	-32409324	-0,84	8,70E-08	4,86E-06	7,89
218574_s_at	LMCD1	29995	Q9NZU5	3	8543510	1,27	8,71E-08	4,86E-06	7,89
205017_s_at	MBNL2	10150	A2A3S3	13	97874573	-0,97	8,75E-08	4,87E-06	7,89

ProbeID	SYMBOL	ENTREZ	UNIPROT	CHR	CHRLOC	Log2R	Rawpval	AdjpvalBH	Lods
216368_s_at	COL4A3	1285	Q01955	2	228029280	-0,62	9,11E-08	5,06E-06	7,85
204539_s_at	CELSR1	9620	Q9NYQ6	22	-46756730	-0,56	9,14E-08	5,07E-06	7,84
216442_x_at	FN1	2335	P02751	2	-216279384	3,99	9,32E-08	5,15E-06	7,82
45297_at	EHD2	30846	Q9NZN4	19	48216600	1,16	9,39E-08	5,17E-06	7,82
210976_s_at	PFKM	5213	P08237	12	48499655	0,97	9,40E-08	5,17E-06	7,82
219676_at	ZSCAN16	80345	Q9H4T2	6	28092386	-0,76	9,56E-08	5,25E-06	7,80
203529_at	PPP6C	5537	B7Z2W9	9	-127908852	0,88	9,61E-08	5,26E-06	7,79
214894_x_at	MACF1	23499	Q96PK2	1	39547117	1,10	9,69E-08	5,29E-06	7,79
217897_at	FXYD6	53826	Q9H0Q3	11	-117707692	1,23	9,73E-08	5,30E-06	7,78
201464_x_at	JUN	3725	P05412	1	-59246463	1,86	9,89E-08	5,38E-06	7,77
213290_at	COL6A2	1292	P12110	21	47518032	1,11	9,98E-08	5,41E-06	7,76
202019_s_at	LANCL1	10314	B2R602	2	-211295973	-0,82	1,01E-07	5,46E-06	7,75
219003_s_at	MANEA	79694	Q5SRJ9	6	96025412	-0,51	1,02E-07	5,49E-06	7,74
206473_at	MBTPS2	51360	O43462	X	21857655	-0,59	1,03E-07	5,53E-06	7,72
221198_at	SCT	6343	P09683	11	-626312	1,13	1,03E-07	5,53E-06	7,72
204615_x_at	IDI1	3422	Q13907	10	-1085965	-1,79	1,03E-07	5,53E-06	7,72
208747_s_at	C1S	716	P09871	12	7167979	3,38	1,04E-07	5,53E-06	7,72
221466_at	P2RY4	5030	P51582	X	-69478015	-0,64	1,05E-07	5,60E-06	7,71
201908_at	DVL3	1857	Q92997	3	183873283	0,99	1,06E-07	5,62E-06	7,70
203568_s_at	TRIM38	10475	O00635	6	25963070	-0,70	1,06E-07	5,62E-06	7,70
206205_at	MPHOSPH9	10198	Q99550	12	-123640947	-0,54	1,06E-07	5,62E-06	7,70
216477_at	NA	NA	NA	NA	NA	-0,55	1,07E-07	5,65E-06	7,69
205602_x_at	PSG7	5676	Q13046	19	-43428285	-0,69	1,07E-07	5,65E-06	7,69
206968_s_at	NFRKB	4798	Q6P4R8	11	-129733670	-0,61	1,08E-07	5,68E-06	7,68
217118_s_at	KIAA0930	23313	Q6ICG6	22	-45588122	1,37	1,10E-07	5,75E-06	7,66
221012_s_at	TRIM8	81603	Q9BZR9	10	104404251	1,21	1,10E-07	5,77E-06	7,66
213004_at	ANGPTL2	23452	Q8NCH7	9	-129849627	1,13	1,11E-07	5,77E-06	7,66
218982_s_at	NA	NA	NA	NA	NA	1,11	1,11E-07	5,77E-06	7,65
216624_s_at	MLL	4297	Q03164	11	118307204	-0,62	1,11E-07	5,77E-06	7,65
214670_at	ZKSCAN1	7586	P17029	7	99613218	-1,63	1,12E-07	5,78E-06	7,65
216234_s_at	PRKACA	5566	P17612	19	-14202508	-0,65	1,12E-07	5,78E-06	7,65
202891_at	NIT1	4817	B1AQP4	1	161087861	-0,71	1,14E-07	5,90E-06	7,62
200005_at	EIF3D	8664	O15371	22	-36906897	0,84	1,15E-07	5,90E-06	7,62
220890_s_at	DDX47	51202	Q9H0S4	12	12966279	0,94	1,15E-07	5,90E-06	7,62
215388_s_at	NA	NA	NA	NA	NA	1,88	1,16E-07	5,94E-06	7,61
205854_at	TULP3	7289	B7Z1E7	12	3000032	1,02	1,21E-07	6,17E-06	7,57
216874_at	DKFZp686O1327	401014	NA	2	145425533	-0,57	1,22E-07	6,24E-06	7,56
200675_at	CD81	975	P60033	11	2398546	1,79	1,24E-07	6,29E-06	7,55
209081_s_at	COL18A1	80781	D3DSM4	21	46825096	1,64	1,25E-07	6,35E-06	7,54
215496_at	SAMD4A	23034	Q8WW19	14	55034636	-0,85	1,26E-07	6,35E-06	7,53
215813_s_at	PTGS1	5742	P23219	9	125133228	2,06	1,26E-07	6,35E-06	7,53
216955_at	TAF1	6872	P21675	X	70586113	-0,64	1,26E-07	6,35E-06	7,53
204252_at	CDK2	1017	O75100	12	56360555	0,98	1,27E-07	6,37E-06	7,53
51176_at	MED27	9442	Q6P2C8	9	-134735498	0,70	1,27E-07	6,38E-06	7,52
202266_at	TDP2	51567	O95551	6	-24650205	-2,68	1,28E-07	6,40E-06	7,52
208459_s_at	XPO7	23039	Q9UIA9	8	21777179	-1,28	1,28E-07	6,40E-06	7,51
209748_at	SPAST	6683	E5KRP5	2	32288679	-0,93	1,28E-07	6,40E-06	7,51
212642_s_at	HIVEP2	3097	P31629	6	-143072604	0,80	1,29E-07	6,40E-06	7,51
206137_at	RIMS2	9699	B3KX91	8	104512975	-0,58	1,29E-07	6,40E-06	7,51
216623_x_at	TOX3	27324	B4DRD0	16	-52471917	-3,29	1,29E-07	6,41E-06	7,50
204871_at	MTERF	7978	Q99551	7	-91502020	-0,60	1,31E-07	6,48E-06	7,49
210845_s_at	PLAUR	5329	Q03405	19	-44152731	1,71	1,33E-07	6,54E-06	7,48
206058_at	SLC6A12	6539	B3KWG3	12	-299251	-0,89	1,34E-07	6,59E-06	7,47
222311_s_at	SCAF4	57466	O95104	21	-33043312	-0,91	1,35E-07	6,62E-06	7,46
218828_at	PLSCR3	57048	Q9NRY6	17	-7293054	0,93	1,36E-07	6,64E-06	7,46
217904_s_at	BACE1	23621	P56817	11	-117156416	1,18	1,36E-07	6,64E-06	7,46
201993_x_at	HNRPDL	9987	O14979	4	-83344348	1,10	1,37E-07	6,66E-06	7,45

ProbeID	SYMBOL	ENTREZ	UNIPROT	CHR	CHRLOC	Log2R	Rawpval	AdjpvalBH	Lods
218782_s_at	ATAD2	29028	Q6PL18	8	-124332092	-0,80	1,37E-07	6,67E-06	7,45
207902_at	IL5RA	3568	Q01344	3	-3133493	-0,64	1,38E-07	6,72E-06	7,44
216130_at	NA	NA	NA	NA	NA	-0,59	1,39E-07	6,74E-06	7,43
200665_s_at	SPARC	6678	P09486	5	-151041018	3,20	1,40E-07	6,79E-06	7,42
216264_s_at	LAMB2	3913	P55268	3	-49158547	1,38	1,41E-07	6,79E-06	7,42
202374_s_at	RAB3GAP2	25782	A6H8V0	1	-220321609	-0,65	1,42E-07	6,84E-06	7,41
216919_at	TP53I11	9537	O14683	11	-44953899	-0,72	1,43E-07	6,85E-06	7,41
214820_at	BRWD1	54014	Q6P2D1	21	-40668365	-0,63	1,43E-07	6,85E-06	7,40
202499_s_at	SLC2A3	6515	P11169	12	-8071824	1,99	1,44E-07	6,87E-06	7,40
243_g_at	MAP4	4134	P27816	3	-48014569	0,76	1,44E-07	6,87E-06	7,40
203230_at	DVL1	1855	O14640	1	-1270658	1,41	1,45E-07	6,88E-06	7,39
221142_s_at	PECR	55825	Q9BVY49	2	-216903110	-1,08	1,45E-07	6,88E-06	7,39
220292_at	ZNF434	54925	Q9NX65	16	-3432085	-0,77	1,46E-07	6,92E-06	7,38
215146_s_at	TTC28	23331	Q96AY4	22	-28374003	0,75	1,51E-07	7,11E-06	7,35
208429_s_at	HNF4A	3172	P41235	20	42984440	-1,03	1,51E-07	7,11E-06	7,35
211563_s_at	C19orf2	8725	O94763	19	30433424	-0,78	1,51E-07	7,12E-06	7,35
202628_s_at	SERPINE1	5054	B7Z4S0	7	100770378	2,04	1,53E-07	7,18E-06	7,34
214496_x_at	MYST4	23522	Q8WYB5	10	76586378	-0,91	1,54E-07	7,19E-06	7,34
211160_x_at	ACTN1	87	B3V8S3	14	-69340840	1,45	1,54E-07	7,20E-06	7,33
201105_at	LGALS1	3956	P09382	22	38071612	2,92	1,55E-07	7,20E-06	7,33
205665_at	TSPAN9	10867	O75954	12	3186520	0,70	1,55E-07	7,20E-06	7,33
209651_at	TGFB1I1	7041	O43294	16	31483475	2,88	1,57E-07	7,27E-06	7,32
219520_s_at	WWC3	55841	Q9ULE0	X	9983794	1,16	1,57E-07	7,27E-06	7,31
215212_at	NA	NA	NA	NA	NA	0,41	1,57E-07	7,27E-06	7,31
205382_s_at	CFD	1675	P00746	19	859664	2,38	1,60E-07	7,37E-06	7,30
201174_s_at	TERF2IP	54386	Q9NYB0	16	75681634	0,76	1,61E-07	7,41E-06	7,29
207986_x_at	CYB561	1534	B3KTA1	17	-61509665	-0,67	1,62E-07	7,44E-06	7,28
220501_at	ACTL7A	10881	Q9Y615	9	111624602	-0,73	1,62E-07	7,45E-06	7,28
213034_at	SIK3	23387	Q9Y2K2	11	-116714119	1,19	1,63E-07	7,45E-06	7,28
212372_at	MYH10	4628	P35580	17	-8377531	1,77	1,63E-07	7,45E-06	7,28
218470_at	YARS2	51067	Q9Y2Z4	12	-32899478	0,62	1,66E-07	7,55E-06	7,26
204896_s_at	PTGER4	5734	A0PJF5	5	40680031	-1,31	1,66E-07	7,56E-06	7,26
204619_s_at	VCAN	1462	P13611	5	82767492	1,36	1,67E-07	7,60E-06	7,25
221304_at	NA	NA	NA	NA	NA	-1,07	1,69E-07	7,65E-06	7,24
214938_x_at	HMGB1	3146	P09429	13	-31032880	-0,59	1,69E-07	7,65E-06	7,24
217015_at	RBBP4	5928	Q09028	1	33116748	-0,51	1,70E-07	7,65E-06	7,24
213800_at	CFH	3075	P08603	1	196621007	1,96	1,70E-07	7,65E-06	7,24
211665_s_at	SOS2	6655	Q07890	14	-50583846	-0,90	1,73E-07	7,76E-06	7,22
210495_x_at	FN1	2335	P02751	2	-216279384	3,76	1,73E-07	7,76E-06	7,22
204682_at	LTBP2	4053	Q14767	14	-74964888	1,76	1,77E-07	7,94E-06	7,19
214801_at	NA	NA	NA	NA	NA	0,82	1,78E-07	7,94E-06	7,19
217351_at	NA	NA	NA	NA	NA	-0,73	1,79E-07	7,98E-06	7,19
216431_at	NA	NA	NA	NA	NA	-0,87	1,80E-07	8,01E-06	7,18
219243_at	GIMAP4	55303	Q9NUV9	7	150264457	1,26	1,82E-07	8,04E-06	7,17
219979_s_at	C11orf73	51501	Q53FT3	11	86013252	0,86	1,82E-07	8,04E-06	7,17
207744_at	NA	NA	NA	NA	NA	-0,39	1,82E-07	8,04E-06	7,17
217966_s_at	FAM129A	116496	Q9BZQ8	1	-184760166	2,00	1,83E-07	8,04E-06	7,17
215923_s_at	PSD4	23550	Q8NDX1	2	113931559	-1,18	1,83E-07	8,04E-06	7,17
212915_at	PDZRN3	23024	Q9UPQ7	3	-73431651	1,98	1,83E-07	8,04E-06	7,16
217057_s_at	GNAS	2778	A6NI00	20	57414794	-0,75	1,83E-07	8,04E-06	7,16
208730_x_at	RAB2A	5862	P61019	8	61429558	1,92	1,84E-07	8,04E-06	7,16
57715_at	CALHM2	51063	Q9HA72	10	-105206544	0,94	1,84E-07	8,04E-06	7,16
202644_s_at	TNFAIP3	7128	P21580	6	138188580	1,97	1,91E-07	8,30E-06	7,12
217441_at	USP33	23032	Q8TEY7	1	-78177339	-0,77	1,91E-07	8,30E-06	7,12
202887_s_at	DDIT4	54541	Q9NX09	10	74033676	2,05	1,92E-07	8,30E-06	7,12
212429_s_at	GTF3C2	2976	Q8WUA4	2	-27548720	0,80	1,92E-07	8,30E-06	7,12
209454_s_at	TEAD3	7005	Q99594	6	-35441375	0,84	1,92E-07	8,30E-06	7,12

ProbeID	SYMBOL	ENTREZ	UNIPROT	CHR	CHRLOC	Log2R	Rawpval	AdjpvalBH	Lods
207476_at	NA	NA	NA	NA	NA	0,72	1,92E-07	8,31E-06	7,12
219462_at	TMEM53	79639	Q6P2H8	1	-45119501	-0,75	1,93E-07	8,31E-06	7,11
213183_s_at	CDKN1C	1028	P49918	11	-2904449	0,60	1,94E-07	8,35E-06	7,11
202681_at	USP4	7375	Q08AK7	3	-49314576	0,75	1,98E-07	8,51E-06	7,09
221710_x_at	FAM176B	55194	Q9NVM1	1	-36787631	1,16	2,00E-07	8,57E-06	7,08
210990_s_at	LAMA4	3910	Q16363	6	-112574985	-0,57	2,01E-07	8,61E-06	7,07
209765_at	ADAM19	8728	Q8TBU7	5	-156904312	0,87	2,02E-07	8,61E-06	7,07
203917_at	CXADR	1525	P78310	21	18885329	-1,74	2,03E-07	8,65E-06	7,06
201494_at	PRCP	5547	A8MU24	11	-82535409	1,43	2,04E-07	8,65E-06	7,06
217762_s_at	RAB31	11031	Q13636	18	9708227	2,69	2,04E-07	8,68E-06	7,06
211587_x_at	CHRNA3	1136	P32297	15	-78887646	-0,64	2,11E-07	8,93E-06	7,03
201345_s_at	UBE2D2	7322	P62837	5	138940750	1,12	2,16E-07	9,15E-06	7,00
214994_at	APOBEC3F	200316	Q6ICH3	22	39436672	0,87	2,18E-07	9,22E-06	6,99
219043_s_at	NA	NA	NA	NA	NA	0,96	2,20E-07	9,25E-06	6,99
218294_s_at	NUP50	10762	Q9UKX7	22	45559725	-1,33	2,20E-07	9,25E-06	6,99
216414_at	NA	NA	NA	NA	NA	-0,61	2,21E-07	9,26E-06	6,98
206932_at	CH25H	9023	O95992	10	-90965695	0,94	2,21E-07	9,26E-06	6,98
207364_at	TEX28	1527	O15482	X	-153498932	-0,82	2,22E-07	9,26E-06	6,98
204291_at	ZNF518A	9849	Q6AHZ1	10	97889471	-1,07	2,22E-07	9,26E-06	6,98
221974_at	IPW	3653	NA	15	25361691	0,78	2,25E-07	9,35E-06	6,96
201792_at	AEBP1	165	Q8IUX7	7	44143959	1,91	2,26E-07	9,41E-06	6,96
205128_x_at	PTGS1	5742	P23219	9	125133228	1,70	2,27E-07	9,43E-06	6,95
216200_at	PLEKHM1	9842	Q9Y4G2	17	-43513266	0,79	2,28E-07	9,45E-06	6,95
218351_at	COMMD8	54951	Q9NX08	4	-47452814	-1,38	2,29E-07	9,45E-06	6,95
209777_s_at	SLC19A1	6573	P41440	21	-46934628	-0,82	2,29E-07	9,45E-06	6,95
207780_at	CYLC2	1539	Q14093	9	105757592	-0,49	2,31E-07	9,51E-06	6,94
202995_s_at	FBLN1	2192	P23142	22	45898718	2,61	2,32E-07	9,52E-06	6,93
202741_at	PRKACB	5567	B2RB89	1	84543744	-2,32	2,35E-07	9,63E-06	6,92
201359_at	COPB1	1315	P53618	11	-14479048	-1,08	2,37E-07	9,71E-06	6,91
212423_at	ZCCHC24	219654	Q8N2G6	10	-81142084	1,31	2,38E-07	9,73E-06	6,91
221781_s_at	DNAJC10	54431	Q8IXB1	2	183580998	-1,28	2,38E-07	9,73E-06	6,91
208179_x_at	KIR2DL3	3804	E3NZD8	19	55249973	-0,71	2,40E-07	9,77E-06	6,90
202082_s_at	SEC14L1	6397	A5PLM6	17	75137004	1,99	2,43E-07	9,87E-06	6,89
202202_s_at	LAMA4	3910	Q16363	6	-112574985	2,60	2,46E-07	1,00E-05	6,87
201684_s_at	TOX4	9878	O94842	14	21945334	0,78	2,50E-07	1,01E-05	6,86
209524_at	HDGFRP3	50810	Q9Y3E1	15	-83806815	1,52	2,50E-07	1,01E-05	6,86
221301_at	C6orf27	80737	Q9Y334	6	-31733371	-0,55	2,52E-07	1,02E-05	6,85
217737_x_at	C20orf43	51507	Q9BY42	20	55043646	0,88	2,55E-07	1,02E-05	6,84
201601_x_at	IFITM1	8519	P13164	11	313990	2,25	2,55E-07	1,02E-05	6,84
208971_at	UROD	7389	P06132	1	45477804	0,75	2,55E-07	1,02E-05	6,84
213907_at	EEF1E1	9521	C9JLK5	6	-8079635	-0,50	2,56E-07	1,02E-05	6,84
212379_at	GART	2618	P22102	21	-34896315	-0,60	2,58E-07	1,03E-05	6,83
58696_at	EXOSC4	54512	Q9NPD3	8	145133521	0,91	2,58E-07	1,03E-05	6,83
214541_s_at	QKI	9444	Q8WY44	6	163835674	-0,67	2,60E-07	1,03E-05	6,82
211331_x_at	HFE	3077	Q30201	6	26087508	-0,61	2,60E-07	1,03E-05	6,82
64064_at	GIMAP5	55340	Q96F15	7	150434450	0,66	2,60E-07	1,03E-05	6,82
220303_at	PDZD3	79849	B0YJ61	11	119056165	-1,46	2,62E-07	1,04E-05	6,81
206249_at	MAP3K13	9175	O43283	3	185080969	-0,86	2,63E-07	1,04E-05	6,81
221319_at	PCDHB8	56128	Q9UN66	5	140557429	-0,50	2,63E-07	1,04E-05	6,81
213541_s_at	ERG	2078	B4DN83	21	-39751951	1,13	2,64E-07	1,04E-05	6,81
206071_s_at	EPHA3	2042	P29320	3	89156673	-0,48	2,66E-07	1,04E-05	6,80
220591_s_at	EFHC2	80258	Q5JST6	X	-44007128	-0,75	2,66E-07	1,04E-05	6,80
210421_s_at	SLC24A1	9187	O60721	15	65914269	-0,50	2,66E-07	1,04E-05	6,80
208156_x_at	EPPK1	83481	P58107	8	-144939911	1,05	2,69E-07	1,05E-05	6,79
40687_at	GJA4	2701	P35212	1	35258598	0,96	2,69E-07	1,05E-05	6,79
204432_at	SOX12	6666	O15370	20	306238	0,57	2,69E-07	1,05E-05	6,79
210762_s_at	DLC1	10395	A8K119	8	-13162117	2,25	2,69E-07	1,05E-05	6,79

ProbeID	SYMBOL	ENTREZ	UNIPROT	CHR	CHRLOC	Log2R	Rawpval	AdjpvalBH	Lods
215570_s_at	NA	NA	NA	NA	NA	-0,62	2,70E-07	1,05E-05	6,79
204796_at	EML1	2009	O00423	14	100259744	0,81	2,70E-07	1,05E-05	6,78
209818_s_at	HABP4	22927	Q5JVS0	9	99212413	0,55	2,70E-07	1,05E-05	6,78
221241_s_at	BCL2L14	79370	Q9BZR8	12	12223877	-1,56	2,72E-07	1,05E-05	6,78
218993_at	RNMTL1	55178	Q9HC36	17	685512	0,96	2,73E-07	1,06E-05	6,77
210411_s_at	GRIN2B	2904	Q13224	12	-13714409	-0,57	2,76E-07	1,06E-05	6,76
221421_s_at	ADAMTS12	81792	P58397	5	-33527286	-0,75	2,79E-07	1,07E-05	6,75
207026_s_at	ATP2B3	492	Q16720	X	152801579	-0,89	2,82E-07	1,08E-05	6,74
222136_x_at	ZNF43	7594	P17038	19	-21987752	-0,51	2,86E-07	1,10E-05	6,73
205619_s_at	MEOX1	4222	A8MWF9	17	-41717766	1,39	2,89E-07	1,11E-05	6,72
213793_s_at	HOMER1	9456	Q5U5K4	5	-78669786	1,25	2,90E-07	1,11E-05	6,72
220765_s_at	LIMS2	55679	B3KNZ3	2	-128395996	1,31	2,90E-07	1,11E-05	6,72
217298_at	NA	NA	NA	NA	NA	-0,77	2,92E-07	1,11E-05	6,71
209320_at	ADCY3	109	B3KT86	2	-25042040	0,73	2,93E-07	1,11E-05	6,71
218157_x_at	CDC42SE1	56882	Q9NRR8	1	-151023448	1,48	2,94E-07	1,12E-05	6,70
216271_x_at	SYDE1	85360	Q6ZW31	19	15218213	-0,81	2,95E-07	1,12E-05	6,70
201809_s_at	ENG	2022	P17813	9	-130577291	1,75	2,95E-07	1,12E-05	6,70
204099_at	SMARCD3	6604	Q6STE5	7	-150936059	0,99	2,95E-07	1,12E-05	6,70
204160_s_at	ENPP4	22875	Q9Y6X5	6	46097700	-2,01	2,96E-07	1,12E-05	6,70
218962_s_at	TMEM168	64418	Q9H0V1	7	-112405788	-1,46	2,98E-07	1,12E-05	6,69
212238_at	ASXL1	171023	Q498B9	20	30946146	0,72	2,99E-07	1,12E-05	6,69
215482_s_at	EIF2B4	8890	Q9UI10	2	-27587220	0,87	2,99E-07	1,12E-05	6,68
203859_s_at	PALM	5064	O75781	19	708952	0,87	3,03E-07	1,14E-05	6,67
215734_at	IZUMO4	113177	A7RA93	19	2096867	-0,73	3,06E-07	1,14E-05	6,66
210028_s_at	ORC3	23595	B4E025	6	88299842	-0,76	3,10E-07	1,16E-05	6,65
208516_at	MTNR1B	4544	P49286	11	92702788	-0,62	3,10E-07	1,16E-05	6,65
217769_s_at	POMP	51371	D6MXU3	13	29233240	0,67	3,13E-07	1,16E-05	6,64
203853_s_at	GAB2	9846	A7MD36	11	-77926336	0,74	3,14E-07	1,16E-05	6,64
207731_at	NA	NA	NA	NA	NA	-0,59	3,14E-07	1,16E-05	6,64
203240_at	FCGBP	8857	Q9Y6R7	19	-40353963	-3,39	3,18E-07	1,18E-05	6,63
217764_s_at	RAB31	11031	Q13636	18	9708227	2,62	3,20E-07	1,18E-05	6,62
207767_s_at	EGR4	1961	B2RAE3	2	-73518057	-0,84	3,22E-07	1,19E-05	6,61
215833_s_at	SPPL2B	56928	Q8TCT7	19	2328628	-1,27	3,24E-07	1,19E-05	6,61
209335_at	DCN	1634	P07585	12	-91539035	2,45	3,26E-07	1,20E-05	6,60
47571_at	ZNF236	7776	Q9UL36	18	74536115	-0,61	3,27E-07	1,20E-05	6,60
205800_at	SLC3A1	6519	Q07837	2	44502596	-0,48	3,28E-07	1,20E-05	6,59
208330_at	ALX4	60529	Q9H161	11	-44282277	-0,65	3,32E-07	1,21E-05	6,58
204794_at	DUSP2	1844	Q05923	2	-96808916	1,16	3,36E-07	1,23E-05	6,57
209536_s_at	EHD4	30844	A8K9B9	15	-42191640	1,29	3,36E-07	1,23E-05	6,57
211754_s_at	SLC25A17	10478	O43808	22	-41165640	0,75	3,37E-07	1,23E-05	6,57
204890_s_at	LCK	3932	P06239	1	32716839	-0,84	3,38E-07	1,23E-05	6,57
205239_at	AREG	374	P15514	4	75310852	2,50	3,38E-07	1,23E-05	6,56
214410_at	TRPM1	4308	Q6PE48	15	-31293552	-0,57	3,40E-07	1,23E-05	6,56
203957_at	E2F6	1876	O75461	2	-11584501	0,77	3,42E-07	1,24E-05	6,56
219548_at	ZNF16	7564	P17020	8	-146155745	0,54	3,43E-07	1,24E-05	6,55
207147_at	DLX2	1746	Q07687	2	-172964166	-0,39	3,43E-07	1,24E-05	6,55
210022_at	PCGF1	84759	Q9BSM1	2	-74732177	-0,61	3,47E-07	1,25E-05	6,54
221357_at	CHRM4	1132	P08173	11	-46406639	-0,84	3,51E-07	1,26E-05	6,53
214427_at	NOP2	4839	P46087	12	-6666036	0,84	3,52E-07	1,26E-05	6,53
201859_at	SRGN	5552	P10124	10	70847827	2,74	3,52E-07	1,26E-05	6,53
219196_at	SCG3	29106	B4DK99	15	51973549	-0,38	3,52E-07	1,26E-05	6,53
205811_at	POLG2	11232	E5KS15	17	-62473903	-0,50	3,52E-07	1,26E-05	6,53
201162_at	IGFBP7	3490	Q16270	4	-57897245	2,49	3,53E-07	1,26E-05	6,52
221585_at	CACNG4	27092	Q9UBN1	17	64961012	-0,54	3,54E-07	1,26E-05	6,52
211663_x_at	PTGDS	5730	P41222	9	139871955	1,59	3,55E-07	1,26E-05	6,52
205371_s_at	DBT	1629	P11182	1	-100652478	-0,67	3,59E-07	1,27E-05	6,51
209959_at	NR4A3	8013	Q92570	9	102584136	1,13	3,59E-07	1,27E-05	6,51

ProbeID	SYMBOL	ENTREZ	UNIPROT	CHR	CHRLOC	Log2R	Rawpval	AdjpvalBH	Lods
216770_at	NA	NA	NA	NA	NA	-0,45	3,59E-07	1,27E-05	6,51
217767_at	C3	718	P01024	19	-6677846	2,68	3,65E-07	1,29E-05	6,49
209477_at	EMD	2010	P50402	X	153607596	1,36	3,66E-07	1,29E-05	6,49
221034_s_at	TEX13B	56156	Q9BXU2	X	-107224093	-0,68	3,66E-07	1,29E-05	6,49
203887_s_at	THBD	7056	P07204	20	-23026270	2,91	3,66E-07	1,29E-05	6,49
208474_at	CLDN6	9074	P56747	16	-3064713	-0,78	3,68E-07	1,29E-05	6,48
214417_s_at	FETUB	26998	Q9UGM5	3	186358148	-0,56	3,69E-07	1,29E-05	6,48
219315_s_at	TMEM204	79652	Q9BSN7	16	1584230	1,38	3,69E-07	1,29E-05	6,48
201885_s_at	CYB5R3	1727	B7Z7L3	22	-43013846	0,62	3,76E-07	1,31E-05	6,46
208633_s_at	MACF1	23499	Q96PK2	1	39547117	0,93	3,80E-07	1,32E-05	6,45
217471_at	NA	NA	NA	NA	NA	-0,65	3,87E-07	1,35E-05	6,43
212521_s_at	PDE8A	5151	O60658	15	85525204	-0,82	3,87E-07	1,35E-05	6,43
210848_at	NA	NA	NA	NA	NA	-0,62	3,92E-07	1,36E-05	6,42
201150_s_at	TIMP3	7078	P35625	22	33196801	3,30	3,98E-07	1,38E-05	6,41
211260_at	BMP7	655	A8K571	20	-55743808	-0,60	4,05E-07	1,40E-05	6,39
205233_s_at	PAFAH2	5051	Q99487	1	-26286259	-1,08	4,06E-07	1,40E-05	6,39
213891_s_at	TCF4	6925	B3KVA4	18	-52889561	1,95	4,13E-07	1,42E-05	6,37
203785_s_at	DDX28	55794	Q9NUL7	16	-68055178	0,90	4,13E-07	1,42E-05	6,37
204958_at	PLK3	1263	Q9H4B4	1	45266035	1,29	4,20E-07	1,44E-05	6,35
204894_s_at	AOC3	8639	Q16853	17	41003200	2,10	4,20E-07	1,44E-05	6,35
212144_at	SUN2	25777	B0QY62	22	-39130734	0,92	4,21E-07	1,44E-05	6,35
217035_at	SKAP2	8935	A4D173	7	-26706689	-0,53	4,22E-07	1,44E-05	6,35
200728_at	ACTR2	10097	P61160	2	65454828	-1,17	4,23E-07	1,44E-05	6,35
200924_s_at	SLC3A2	6520	P08195	11	62623517	0,97	4,24E-07	1,44E-05	6,35
208858_s_at	ESYT1	23344	Q9BSJ8	12	56521985	1,12	4,24E-07	1,44E-05	6,34
210962_s_at	AKAP9	10142	Q5GIA7	7	91570188	-1,87	4,25E-07	1,44E-05	6,34
204904_at	GJA4	2701	P35212	1	35258598	0,86	4,25E-07	1,44E-05	6,34
208245_at	RAB9BP1	9366	NA	5	104435174	-0,36	4,26E-07	1,44E-05	6,34
213807_x_at	MET	4233	A1L467	7	116312458	-0,85	4,26E-07	1,44E-05	6,34
205112_at	PLCE1	51196	A8K1D7	10	95753745	-1,62	4,26E-07	1,44E-05	6,34
34478_at	RAB11B	9230	Q15907	19	8455204	-0,77	4,31E-07	1,45E-05	6,33
220441_at	DNAJC22	79962	Q8N4W6	12	49741040	-1,42	4,31E-07	1,45E-05	6,33
219170_at	FSD1	79187	Q9BTV5	19	4304590	-0,57	4,32E-07	1,45E-05	6,33
212387_at	TCF4	6925	B3KVA4	18	-52889561	1,70	4,33E-07	1,45E-05	6,32
201677_at	C3orf37	56941	Q96FZ2	3	128997683	0,75	4,34E-07	1,46E-05	6,32
214616_at	HIST1H3E	8353	P68431	6	26225382	-0,86	4,38E-07	1,47E-05	6,31
203339_at	SLC25A12	8604	O75746	2	-172639914	0,74	4,42E-07	1,48E-05	6,30
205882_x_at	ADD3	120	Q5VU08	10	111765725	-1,87	4,43E-07	1,48E-05	6,30
48659_at	MIIP	60672	Q5JXC2	1	12079511	-0,47	4,48E-07	1,49E-05	6,29
202796_at	SYNPO	11346	Q8N3V7	5	149980641	1,26	4,50E-07	1,50E-05	6,29
207827_x_at	SNCA	6622	P37840	4	-90645250	1,15	4,55E-07	1,51E-05	6,28
215992_s_at	RAPGEF2	9693	Q9Y4G8	4	160188997	-0,59	4,57E-07	1,52E-05	6,27
220965_s_at	RSPH6A	81492	Q9H0K4	19	-46298968	-0,80	4,58E-07	1,52E-05	6,27
212687_at	LIMS1	3987	B7Z483	2	109150856	0,97	4,62E-07	1,53E-05	6,26
204079_at	TPST2	8459	O60704	22	-26921715	1,30	4,62E-07	1,53E-05	6,26
213746_s_at	FLNA	2316	P21333	X	-153576899	2,55	4,64E-07	1,53E-05	6,26
218486_at	KLF11	8462	B4DZE7	2	10183681	1,08	4,68E-07	1,54E-05	6,25
207493_x_at	NA	NA	NA	NA	NA	-0,79	4,68E-07	1,54E-05	6,25
210810_s_at	SLC6A5	9152	Q4VAM4	11	20620945	-0,58	4,70E-07	1,54E-05	6,24
222321_at	AGTR2	186	P50052	X	115301957	-0,55	4,72E-07	1,55E-05	6,24
201041_s_at	DUSP1	1843	B4DU40	5	-172195094	2,89	4,78E-07	1,57E-05	6,23
202010_s_at	ZNF410	57862	Q86VK4	14	74353585	0,56	4,79E-07	1,57E-05	6,22
201465_s_at	JUN	3725	P05412	1	-59246463	1,43	4,82E-07	1,58E-05	6,22
217618_x_at	HUS1	3364	A4D2F2	7	-48003782	-0,57	4,88E-07	1,59E-05	6,21
208982_at	PECAM1	5175	P16284	17	-62399863	2,43	4,89E-07	1,59E-05	6,20
203203_s_at	KRR1	11103	A0JLP0	12	-75891420	-0,67	4,89E-07	1,59E-05	6,20
202409_at	NA	NA	NA	NA	NA	1,84	4,91E-07	1,60E-05	6,20

ProbeID	SYMBOL	ENTREZ	UNIPROT	CHR	CHRLOC	Log2R	Rawpval	AdjpvalBH	Lods
214655_at	GPR6	2830	P46095	6	110300297	-0,50	4,93E-07	1,60E-05	6,20
217652_at	MAU2	23383	Q9Y6X3	19	19431629	-0,53	4,95E-07	1,60E-05	6,19
207126_x_at	NA	NA	NA	NA	NA	-2,20	5,06E-07	1,64E-05	6,17
212452_x_at	MYST4	23522	Q8WYB5	10	76586378	-0,79	5,12E-07	1,65E-05	6,16
211463_at	ZIC4	84107	B4DF89	3	-147103834	-0,53	5,14E-07	1,66E-05	6,16
220229_s_at	AP4E1	23431	Q9UPM8	15	51200945	-0,44	5,19E-07	1,67E-05	6,15
202261_at	VPS72	6944	Q15906	1	-151148933	0,84	5,24E-07	1,69E-05	6,14
37079_at	NUS1P3	11049	NA	13	NA	-0,53	5,27E-07	1,69E-05	6,13
219024_at	PLEKHA1	59338	B3KQ55	10	124134219	-1,35	5,29E-07	1,70E-05	6,13
201109_s_at	THBS1	7057	P07996	15	39873279	2,03	5,30E-07	1,70E-05	6,13
217991_x_at	SSBP3	23648	Q9BWW4	1	-54692195	-0,87	5,35E-07	1,71E-05	6,12
206724_at	CBX4	8535	O00257	17	-77806955	-0,74	5,37E-07	1,71E-05	6,11
217180_at	NA	NA	NA	NA	NA	-0,63	5,42E-07	1,73E-05	6,10
208788_at	ELOVL5	60481	Q9NYP7	6	-53132195	2,24	5,48E-07	1,74E-05	6,09
212386_at	TCF4	6925	B3KVA4	18	-52889561	1,93	5,49E-07	1,74E-05	6,09
206942_s_at	PMCH	5367	P20382	12	-102590238	-0,61	5,53E-07	1,75E-05	6,09
222122_s_at	THOC2	57187	Q8NI27	X	-122734412	-1,15	5,55E-07	1,76E-05	6,08
40420_at	STK10	6793	O94804	5	-171469073	0,82	5,56E-07	1,76E-05	6,08
212777_at	SOS1	6654	Q07889	2	-39208691	-0,74	5,57E-07	1,76E-05	6,08
208227_x_at	ADAM22	53616	Q08AL8	7	87563701	-0,69	5,58E-07	1,76E-05	6,08
214124_x_at	FGFR1OP	11116	O95684	6	167412815	-0,98	5,59E-07	1,76E-05	6,07
220048_at	EDAR	10913	Q9UNE0	2	-109510930	-0,65	5,63E-07	1,77E-05	6,07
201147_s_at	TIMP3	7078	P35625	22	33196801	1,95	5,65E-07	1,78E-05	6,06
204054_at	PTEN	5728	P60484	10	89623194	-0,84	5,67E-07	1,78E-05	6,06
209161_at	PRPF4	9128	O43172	9	116037973	0,76	5,70E-07	1,78E-05	6,06
221258_s_at	KIF18A	81930	Q8NI77	11	-28042162	-0,42	5,70E-07	1,78E-05	6,06
213075_at	OLFML2A	169611	Q6BBL7	9	127539436	1,13	5,71E-07	1,78E-05	6,05
205510_s_at	FLJ10038	55056	NA	15	-50641136	0,69	5,71E-07	1,78E-05	6,05
209067_s_at	HNRPDL	9987	O14979	4	-83344348	1,33	5,75E-07	1,79E-05	6,05
211851_x_at	BRCA1	672	P38398	17	-41196312	-0,70	5,76E-07	1,79E-05	6,05
215242_at	PIGC	5279	Q92535	1	-172410597	-0,43	5,80E-07	1,80E-05	6,04
218573_at	MAGEH1	28986	Q9H213	X	55478537	1,13	5,81E-07	1,80E-05	6,04
220773_s_at	GPHN	10243	Q9NQX3	14	66974124	-0,86	5,82E-07	1,80E-05	6,03
203427_at	ASF1A	25842	Q9Y294	6	119215240	-1,30	5,87E-07	1,82E-05	6,03
218656_s_at	LHFP	10186	Q9Y693	13	-39917029	2,19	5,88E-07	1,82E-05	6,03
215499_at	MAP2K3	5606	P46734	17	21187967	1,19	5,89E-07	1,82E-05	6,02
201430_s_at	DPYSL3	1809	B3SXQ8	5	-146770370	1,82	5,93E-07	1,83E-05	6,02
219192_at	UBAP2	55833	Q5T6F2	9	-33921690	1,25	5,95E-07	1,83E-05	6,01
222192_s_at	C2orf43	60526	Q9H6V9	2	-20884818	-1,08	5,98E-07	1,84E-05	6,01
214774_x_at	TOX3	27324	B4DRD0	16	-52471917	-3,24	5,99E-07	1,84E-05	6,01
201288_at	ARHGDIB	397	P52566	12	-15094949	1,65	5,99E-07	1,84E-05	6,01
212722_s_at	JMJD6	23210	Q6NYC1	17	-74714526	0,81	6,01E-07	1,84E-05	6,00
215755_at	NA	NA	NA	NA	NA	-0,45	6,02E-07	1,84E-05	6,00
212226_s_at	PPAP2B	8613	O14495	1	-56960432	1,82	6,03E-07	1,84E-05	6,00
200982_s_at	ANXA6	309	B7Z8A7	5	-150480269	1,92	6,04E-07	1,84E-05	6,00
214022_s_at	IFITM1	8519	P13164	11	313990	2,17	6,06E-07	1,85E-05	6,00
212362_at	ATP2A2	488	P16615	12	110719031	-0,78	6,10E-07	1,85E-05	5,99
215971_at	NA	NA	NA	NA	NA	-0,65	6,11E-07	1,85E-05	5,99
213659_at	ZNF75D	7626	A6NK62	X	-134419723	-0,67	6,11E-07	1,85E-05	5,99
202133_at	WWTR1	25937	Q9GZV5	3	-149235021	2,07	6,12E-07	1,85E-05	5,99
215354_s_at	PELP1	27043	Q8IZL8	17	-4574679	0,87	6,15E-07	1,86E-05	5,98
203005_at	LTBR	4055	P36941	12	6493356	1,14	6,15E-07	1,86E-05	5,98
209804_at	DC1RE1A	9937	Q6PJP8	10	-115594483	-0,74	6,24E-07	1,88E-05	5,97
217939_s_at	AFTPH	54812	Q53GW0	2	64751438	-0,63	6,25E-07	1,88E-05	5,97
211245_x_at	KIR2DL4	3805	Q99706	19	55315066	-0,63	6,30E-07	1,89E-05	5,96
201941_at	CPD	1362	B7ZAU4	17	28705983	-1,88	6,33E-07	1,90E-05	5,95
216337_at	NA	NA	NA	NA	NA	-0,59	6,33E-07	1,90E-05	5,95

ProbeID	SYMBOL	ENTREZ	UNIPROT	CHR	CHRLOC	Log2R	Rawpval	AdjpvalBH	Lods
203519_s_at	UPF2	26019	Q9HAU5	10	-11962021	-0,92	6,35E-07	1,90E-05	5,95
217018_at	NA	NA	NA	NA	NA	-0,76	6,37E-07	1,91E-05	5,95
204667_at	FOXA1	3169	P55317	14	-38059192	-1,02	6,40E-07	1,91E-05	5,94
219769_at	INCENP	3619	Q9NQS7	11	61891444	-0,49	6,41E-07	1,91E-05	5,94
222295_x_at	NA	NA	NA	NA	NA	-0,37	6,43E-07	1,92E-05	5,94
209304_x_at	GADD45B	4616	O75293	19	2476122	1,24	6,44E-07	1,92E-05	5,94
215520_at	PYGO1	26108	Q9Y3Y4	15	-55838220	-0,53	6,46E-07	1,92E-05	5,93
220325_at	TAF7L	54457	Q5H9L4	X	-100523241	-0,52	6,49E-07	1,93E-05	5,93
32209_at	FAM89B	23625	Q8NSH3	11	65339819	0,83	6,50E-07	1,93E-05	5,93
222085_at	FAM174B	400451	Q3ZCQ3	15	-93160680	-0,51	6,52E-07	1,93E-05	5,92
201748_s_at	SAFB	6294	Q15424	19	5623163	0,87	6,55E-07	1,93E-05	5,92
212644_x_at	MAPK1IP1L	93487	Q8NDC0	14	55518361	0,90	6,56E-07	1,93E-05	5,92
203052_at	C2	717	B4DPF3	6	31868775	0,74	6,56E-07	1,93E-05	5,92
214438_at	HLX	3142	Q14774	1	221052742	1,14	6,62E-07	1,95E-05	5,91
209961_s_at	HGF	3082	P14210	7	-81380216	-0,64	6,65E-07	1,95E-05	5,91
209754_s_at	TMPO	7112	P42166	12	98909350	-1,48	6,82E-07	2,00E-05	5,88
209723_at	SERPINB9	5272	P50453	6	-2887505	2,72	6,82E-07	2,00E-05	5,88
212561_at	DENND5A	23258	Q6IQ26	11	-9160376	1,29	6,85E-07	2,00E-05	5,88
823_at	CX3CL1	6376	A0N0N7	16	57406413	0,82	6,85E-07	2,00E-05	5,88
207594_s_at	SYNJ1	8867	B9EGN3	21	-34001068	-0,65	6,91E-07	2,02E-05	5,87
219544_at	C13orf34	79866	Q6PGQ7	13	73302041	-0,77	6,92E-07	2,02E-05	5,87
211518_s_at	BMP4	652	P12644	14	-54416456	-0,95	6,94E-07	2,02E-05	5,86
208991_at	STAT3	6774	P40763	17	-40465342	1,06	6,98E-07	2,03E-05	5,86
204536_s_at	REST	5978	Q13127	4	57774041	-0,55	7,00E-07	2,03E-05	5,86
205479_s_at	PLAU	5328	P00749	10	75670861	2,12	7,07E-07	2,05E-05	5,85
213943_at	TWIST1	7291	Q15672	7	-19155092	1,06	7,10E-07	2,06E-05	5,84
208069_x_at	NA	NA	NA	NA	NA	-0,78	7,10E-07	2,06E-05	5,84
218638_s_at	SPON2	10417	Q9BUD6	4	-1160721	1,40	7,24E-07	2,09E-05	5,82
202260_s_at	STXBP1	6812	P61764	9	130374485	1,13	7,25E-07	2,09E-05	5,82
200838_at	CTSB	1508	P07858	8	-11700035	1,64	7,27E-07	2,09E-05	5,82
219817_at	C12orf47	51275	NA	12	-112277572	-0,59	7,27E-07	2,09E-05	5,82
216317_x_at	RHCE	6006	P18577	1	-25688740	-0,51	7,32E-07	2,10E-05	5,81
214245_at	RPS14	6208	P62263	5	-149823793	-0,53	7,33E-07	2,10E-05	5,81
215239_x_at	ZNF273	10793	Q14593	7	64363619	-0,78	7,33E-07	2,10E-05	5,81
220835_s_at	ZNF407	55628	Q9C0G0	18	72342918	-0,53	7,34E-07	2,10E-05	5,81
206359_at	SOCS3	9021	O14543	17	-76352858	1,26	7,38E-07	2,11E-05	5,80
210259_s_at	DLX4	1748	Q92988	17	48046561	-0,67	7,41E-07	2,12E-05	5,80
204446_s_at	ALOX5	240	P09917	10	45869628	1,61	7,58E-07	2,16E-05	5,78
49327_at	NA	NA	NA	NA	NA	-0,52	7,64E-07	2,18E-05	5,77
210013_at	HPX	3263	P02790	11	-6452267	-0,64	7,67E-07	2,18E-05	5,77
212910_at	THAP11	57215	Q96EK4	16	67876212	0,66	7,71E-07	2,19E-05	5,76
221538_s_at	PLXNA1	5361	Q9UIW2	3	126707436	1,35	7,71E-07	2,19E-05	5,76
217408_at	MRPS18B	28973	B0S7P4	6	30585485	1,12	7,73E-07	2,19E-05	5,76
202763_at	CASP3	836	P42574	4	-185548851	-1,54	7,78E-07	2,20E-05	5,75
220613_s_at	SYTL2	54843	Q9HCH5	11	-85405266	-1,44	7,80E-07	2,20E-05	5,75
204140_at	TPST1	8460	A4D2M0	7	65670258	0,74	7,81E-07	2,21E-05	5,75
221419_s_at	NA	NA	NA	NA	NA	1,46	7,83E-07	2,21E-05	5,75
221371_at	TNFSF18	8995	Q9UNG2	1	-173010359	-0,59	7,85E-07	2,21E-05	5,74
221196_x_at	BRCC3	79184	P46736	X	154299709	-1,02	8,00E-07	2,25E-05	5,72
221900_at	COL8A2	1296	P25067	1	-36560844	1,13	8,04E-07	2,26E-05	5,72
208654_s_at	CD164	8763	Q04900	6	-109687717	-2,16	8,04E-07	2,26E-05	5,72
206561_s_at	AKR1B10	57016	O60218	7	134212343	-1,14	8,06E-07	2,26E-05	5,72
46167_at	NA	NA	NA	NA	NA	0,99	8,14E-07	2,28E-05	5,71
215463_at	OR7E24	26648	Q6IFN5	19	9361719	-0,52	8,19E-07	2,29E-05	5,70
212028_at	RBM25	58517	P49756	14	73525220	-0,87	8,21E-07	2,29E-05	5,70
201690_s_at	TPD52	7163	A6NCF2	8	-80947104	-1,83	8,34E-07	2,33E-05	5,68
206017_at	KIAA0319	9856	B7ZML3	6	-24544331	-0,63	8,42E-07	2,35E-05	5,67

ProbeID	SYMBOL	ENTREZ	UNIPROT	CHR	CHRLOC	Log2R	Rawpval	AdjpvalBH	Lods
206253_at	DLG2	1740	Q15700	11	-83166055	-0,53	8,55E-07	2,38E-05	5,66
213463_s_at	FAM149B1	317662	Q96BN6	10	74927876	-0,48	8,59E-07	2,39E-05	5,66
222108_at	AMIGO2	347902	Q86SJ2	12	-47470382	1,38	8,61E-07	2,39E-05	5,65
201741_x_at	SRSF1	6426	Q07955	17	-56078281	-0,53	8,63E-07	2,39E-05	5,65
202382_s_at	GNPDA1	10007	P46926	5	-141380237	0,86	8,65E-07	2,39E-05	5,65
216575_at	NA	NA	NA	NA	NA	-0,38	8,67E-07	2,40E-05	5,65
207601_at	SULT1B1	27284	O43704	4	-70592687	-1,89	8,71E-07	2,40E-05	5,64
206308_at	TRDMT1	1787	O14717	10	-17184982	-0,55	8,73E-07	2,41E-05	5,64
219968_at	ZNF589	51385	Q86UQ0	3	48282595	-0,82	8,78E-07	2,42E-05	5,63
204179_at	MB	4151	P02144	22	-36002811	-0,80	8,86E-07	2,44E-05	5,63
218297_at	FAM188A	80013	Q9H8M7	10	-15820174	-0,69	9,03E-07	2,48E-05	5,61
213330_s_at	STIP1	10963	P31948	11	63953586	1,31	9,08E-07	2,49E-05	5,60
207061_at	ERN1	2081	O75460	17	-62120389	-0,70	9,09E-07	2,49E-05	5,60
206094_x_at	NA	NA	NA	NA	NA	-1,94	9,19E-07	2,52E-05	5,59
213310_at	EIF2C2	27161	A4FVC0	8	-141541264	0,95	9,22E-07	2,52E-05	5,59
222082_at	ZBTB7A	51341	O95365	19	-4045217	-0,74	9,23E-07	2,52E-05	5,58
202239_at	PARP4	143	Q9UKK3	13	-24995074	-1,30	9,26E-07	2,52E-05	5,58
208551_at	HIST1H4G	8369	Q99525	6	-26246839	-0,78	9,27E-07	2,52E-05	5,58
206702_at	TEK	7010	Q02763	9	27109146	1,06	9,28E-07	2,52E-05	5,58
219982_s_at	NA	NA	NA	NA	NA	0,73	9,29E-07	2,52E-05	5,58
204907_s_at	BCL3	602	P20749	19	45251977	-1,28	9,35E-07	2,54E-05	5,57
205045_at	AKAP10	11216	O43572	17	-19808751	-0,51	9,38E-07	2,54E-05	5,57
217502_at	IFIT2	3433	P09913	10	91061705	-0,78	9,40E-07	2,55E-05	5,57
210517_s_at	AKAP12	9590	A6NEC7	6	151561133	2,21	9,44E-07	2,55E-05	5,56
220827_at	NA	NA	NA	NA	NA	-0,66	9,52E-07	2,57E-05	5,56
201265_at	NA	NA	NA	NA	NA	-0,67	9,56E-07	2,58E-05	5,55
219064_at	ITIH5	80760	Q86UX2	10	-7613367	1,43	9,59E-07	2,58E-05	5,55
208538_at	ANP32C	23520	O43423	4	-165118159	0,59	9,59E-07	2,58E-05	5,55
214376_at	NA	NA	NA	NA	NA	-0,72	9,59E-07	2,58E-05	5,55
216595_at	FAM186A	121006	A6NE01	12	-50721094	-0,64	9,65E-07	2,59E-05	5,54
202157_s_at	CELF2	10659	O95319	10	11047258	1,84	9,74E-07	2,61E-05	5,53
204695_at	CDC25A	993	P30304	3	-48198667	0,88	9,78E-07	2,62E-05	5,53
202497_x_at	SLC2A3	6515	P11169	12	-8071824	1,13	9,78E-07	2,62E-05	5,53
219489_s_at	NA	NA	NA	NA	NA	2,18	9,85E-07	2,63E-05	5,52
212964_at	HIC2	23119	Q96JB3	22	21771692	0,86	9,87E-07	2,63E-05	5,52
218660_at	DYSF	8291	O75923	2	71680752	1,01	9,88E-07	2,63E-05	5,52
201069_at	MMP2	4313	P08253	16	55513080	2,43	1,00E-06	2,67E-05	5,50
216400_at	NA	NA	NA	NA	NA	-0,67	1,01E-06	2,67E-05	5,50
207358_x_at	MACF1	23499	Q96PK2	1	39547117	1,40	1,01E-06	2,67E-05	5,50
210288_at	KLRG1	10219	Q96E93	12	9142220	-0,71	1,01E-06	2,68E-05	5,50
36829_at	PER1	5187	O15534	17	-8043788	0,66	1,01E-06	2,68E-05	5,50
205750_at	BPHL	670	Q86WA6	6	3118925	-0,91	1,01E-06	2,68E-05	5,50
203990_s_at	KDM6A	7403	O15550	X	44732422	-0,78	1,01E-06	2,68E-05	5,49
217885_at	IPO9	55705	Q96P70	1	201798287	0,86	1,02E-06	2,69E-05	5,49
211504_x_at	ROCK2	9475	O75116	2	-11321777	-0,80	1,03E-06	2,72E-05	5,48
212822_at	HEG1	57493	Q9ULI3	3	-124684554	0,92	1,04E-06	2,74E-05	5,47
204222_s_at	GLIPR1	11010	P48060	12	75874512	1,28	1,05E-06	2,75E-05	5,46
215158_s_at	DEDD	9191	O75618	1	-161090770	0,48	1,05E-06	2,76E-05	5,46
206097_at	SLC22A18AS	5003	Q8N1D0	11	-2909327	-1,13	1,05E-06	2,76E-05	5,46
211981_at	COL4A1	1282	P02462	13	-110801310	2,40	1,06E-06	2,79E-05	5,45
61732_r_at	IFT74	80173	A0PJM7	9	26947036	-0,38	1,07E-06	2,80E-05	5,44
218229_s_at	POGK	57645	Q5TIJ1	1	166808723	1,02	1,07E-06	2,81E-05	5,44
215834_x_at	NA	NA	NA	NA	NA	-0,50	1,08E-06	2,82E-05	5,43
208524_at	GPR15	2838	B6V9G9	3	98250877	-0,59	1,09E-06	2,83E-05	5,43
208311_at	GPR50	9248	Q13585	X	150345055	-0,55	1,09E-06	2,83E-05	5,43
203168_at	ATF6B	1388	Q6AZW6	6	-32083046	0,79	1,09E-06	2,84E-05	5,42
221747_at	TNS1	7145	A1L0S7	2	-218664511	1,85	1,09E-06	2,84E-05	5,42

ProbeID	SYMBOL	ENTREZ	UNIPROT	CHR	CHRLOC	Log2R	Rawpval	AdjpvalBH	Lods
220515_at	DUSP21	63904	Q9H596	X	44703248	-0,70	1,09E-06	2,84E-05	5,42
215778_x_at	NA	NA	NA	NA	NA	1,47	1,10E-06	2,85E-05	5,41
211242_x_at	KIR2DL4	3805	Q99706	19	55315066	-0,90	1,10E-06	2,85E-05	5,41
202992_at	C7	730	P10643	5	40909598	1,59	1,11E-06	2,87E-05	5,41
204532_x_at	NA	NA	NA	NA	NA	-2,10	1,12E-06	2,89E-05	5,40
203617_x_at	ELK1	2002	P19419	X	-47494920	0,54	1,12E-06	2,89E-05	5,40
206948_at	NEU3	10825	A8K327	11	74699949	-0,66	1,12E-06	2,89E-05	5,39
201405_s_at	COPS6	10980	Q7L5N1	7	99686582	1,12	1,12E-06	2,89E-05	5,39
212667_at	SPARC	6678	P09486	5	-151041018	3,08	1,13E-06	2,91E-05	5,39
212405_s_at	METTL13	51603	C4B4C6	1	171750760	0,65	1,15E-06	2,95E-05	5,37
203162_s_at	KATNB1	10300	Q9BVA0	16	57769659	0,52	1,15E-06	2,96E-05	5,37
207337_at	CTAG2	30848	O75638	X	-153880245	0,59	1,16E-06	2,96E-05	5,37
209687_at	CXCL12	6387	P48061	10	-44872510	2,46	1,16E-06	2,98E-05	5,36
207733_x_at	PSG9	5678	Q00887	19	-43757435	-0,85	1,16E-06	2,98E-05	5,36
218103_at	FTSJ3	117246	Q8IY81	17	-61896794	0,68	1,17E-06	2,99E-05	5,35
202229_s_at	CHERP	10523	Q8IWX8	19	-16628699	-0,62	1,17E-06	2,99E-05	5,35
220277_at	CXXC4	80319	Q9H2H0	4	-105393344	-0,37	1,19E-06	3,04E-05	5,34
212203_x_at	IFITM3	10410	Q01628	11	-319672	1,70	1,19E-06	3,04E-05	5,33
219366_at	AVEN	57099	Q9NQS1	15	-34158428	0,95	1,20E-06	3,04E-05	5,33
212137_at	LARP1	23367	Q6PKG0	5	154092461	1,01	1,20E-06	3,04E-05	5,33
205805_s_at	ROR1	4919	Q01973	1	64239689	-0,80	1,20E-06	3,05E-05	5,33
201631_s_at	IER3	8870	P46695	6	-30710976	2,56	1,21E-06	3,07E-05	5,32
206140_at	LHX2	9355	B3KNJ5	9	126773888	-0,38	1,21E-06	3,07E-05	5,32
211514_at	DSTYK	25778	Q6XUX3	1	-205111631	-0,47	1,21E-06	3,07E-05	5,32
222033_s_at	FLT1	2321	B0LPF1	13	-28973181	1,15	1,22E-06	3,07E-05	5,31
215327_at	NA	NA	NA	NA	NA	-0,60	1,22E-06	3,07E-05	5,31
209496_at	RARRES2	5919	Q7LE02	7	-150035407	1,72	1,22E-06	3,08E-05	5,31
219384_s_at	ADAT1	23536	Q9BUB4	16	-75632246	-0,63	1,22E-06	3,08E-05	5,31
202276_at	SHFM1	7979	P60896	7	-96318080	0,69	1,23E-06	3,10E-05	5,30
202957_at	HCLS1	3059	P14317	3	-121350246	1,94	1,25E-06	3,15E-05	5,29
214947_at	FAM105A	54491	Q9NUL6	5	14581890	-0,67	1,26E-06	3,15E-05	5,28
219838_at	TTC23	64927	Q5W5X9	15	-99676528	-0,74	1,26E-06	3,15E-05	5,28
206481_s_at	LDB2	9079	O43679	4	-16503166	1,90	1,26E-06	3,15E-05	5,28
219355_at	CXorf57	55086	Q6NSI4	X	105855159	-0,60	1,26E-06	3,16E-05	5,28
213239_at	PIBF1	10464	Q8WXW3	13	73356229	-0,70	1,27E-06	3,16E-05	5,28
222145_at	NA	NA	NA	NA	NA	-0,78	1,28E-06	3,18E-05	5,27
204134_at	PDE2A	5138	O00408	11	-72287185	0,98	1,28E-06	3,18E-05	5,27
217774_s_at	TRMT112	51504	Q9UI30	11	-64084167	1,41	1,29E-06	3,22E-05	5,26
206828_at	TXK	7294	P42681	4	-48068411	-0,41	1,29E-06	3,22E-05	5,25
215288_at	TRPC2	7221	NA	11	3647713	-0,71	1,30E-06	3,22E-05	5,25
221443_x_at	PRLH	51052	P81277	2	238475216	-0,77	1,30E-06	3,22E-05	5,25
206775_at	CUBN	8029	O60494	10	-16865965	-0,59	1,30E-06	3,22E-05	5,25
221306_at	GPR27	2850	Q9NS67	3	71803200	-0,63	1,31E-06	3,25E-05	5,24
200610_s_at	NCL	4691	B3KM80	2	-232319459	0,81	1,32E-06	3,25E-05	5,24
218966_at	MYO5C	55930	Q9NQX4	15	-52484516	-1,78	1,33E-06	3,28E-05	5,23
1494_f_at	CYP2A6	1548	P11509	19	-41349443	-0,67	1,34E-06	3,30E-05	5,22
208609_s_at	TNXB	7148	O95680	6	-32008931	1,48	1,34E-06	3,30E-05	5,22
211959_at	IGFBP5	3488	P24593	2	-217536828	2,93	1,35E-06	3,31E-05	5,22
207211_at	USP2	9099	O75604	11	-119225925	-0,77	1,35E-06	3,32E-05	5,21
212086_x_at	LMNA	4000	P02545	1	156084460	1,21	1,35E-06	3,32E-05	5,21
207049_at	SCN8A	6334	Q9UQD0	12	51985019	-0,69	1,37E-06	3,37E-05	5,20
209621_s_at	PDLIM3	27295	Q53GG5	4	-186421816	2,24	1,38E-06	3,37E-05	5,20
202555_s_at	MYLK	4638	Q15746	3	-123331144	3,33	1,39E-06	3,40E-05	5,19
219851_at	ZNF613	79898	Q6PF04	19	52430687	0,44	1,39E-06	3,40E-05	5,19
204400_at	EFS	10278	O43281	14	-23825611	2,60	1,39E-06	3,40E-05	5,18
205232_s_at	PAFAH2	5051	Q99487	1	-26286259	-1,17	1,39E-06	3,40E-05	5,18
212950_at	GPR116	221395	Q8IZF2	6	-46820241	1,83	1,40E-06	3,40E-05	5,18

ProbeID	*SYMBOL*	*ENTREZ*	*UNIPROT*	*CHR*	*CHRLOC*	*Log2R*	*Rawpval*	*AdjpvalBH*	*Lods*
212728_at	DLG3	1741	B4E0H1	X	69664704	-0,83	1,41E-06	3,42E-05	5,17
221958_s_at	WLS	79971	Q5JRS7	1	-68591040	1,36	1,41E-06	3,43E-05	5,17
205594_at	ZNF652	22834	A8K9F2	17	-47366568	-1,60	1,42E-06	3,44E-05	5,17
204468_s_at	TIE1	7075	P35590	1	43766663	1,54	1,42E-06	3,44E-05	5,17
204628_s_at	ITGB3	3690	P05106	17	45331207	0,81	1,42E-06	3,44E-05	5,16
221987_s_at	TSR1	55720	Q2NL82	17	-2225991	0,88	1,43E-06	3,44E-05	5,16
217644_s_at	SOS2	6655	Q07890	14	-50583846	-0,55	1,43E-06	3,44E-05	5,16
202722_s_at	GFPT1	2673	Q06210	2	-69546904	-1,39	1,44E-06	3,47E-05	5,15
220134_x_at	FAM176B	55194	Q9NVM1	1	-36787631	1,09	1,44E-06	3,47E-05	5,15
213626_at	CBR4	84869	Q8N4T8	4	-169908743	-1,17	1,45E-06	3,49E-05	5,14
216943_at	NA	NA	NA	NA	NA	-0,63	1,45E-06	3,49E-05	5,14
207584_at	LPA	4018	P08519	6	-160952515	-0,36	1,45E-06	3,49E-05	5,14
222303_at	NA	NA	NA	NA	NA	2,24	1,47E-06	3,53E-05	5,13
210511_s_at	INHBA	3624	A4D1W7	7	-41728602	1,90	1,47E-06	3,54E-05	5,13
221579_s_at	NUDT3	11165	O95989	6	-34256001	0,84	1,48E-06	3,54E-05	5,13
50965_at	RAB26	25837	Q3L6K5	16	2198650	-0,83	1,49E-06	3,57E-05	5,12
214424_s_at	ALDOB	229	P05062	9	-104182841	-0,63	1,49E-06	3,57E-05	5,12
212095_s_at	MTUS1	57509	B4DH03	8	-17501303	-1,66	1,50E-06	3,58E-05	5,11
207552_at	ATP5G2	517	Q06055	12	-54058944	-0,79	1,50E-06	3,58E-05	5,11
221039_s_at	ASAP1	50807	B2RNV3	8	-131064352	0,71	1,52E-06	3,62E-05	5,10
221730_at	COL5A2	1290	P05997	2	-189896641	2,38	1,53E-06	3,63E-05	5,09
202141_s_at	COPS8	10920	A8K1H6	2	237994083	0,69	1,53E-06	3,63E-05	5,09
212077_at	CALD1	800	A8K0X1	7	134464163	3,23	1,53E-06	3,63E-05	5,09
212971_at	CARS	833	B4DPV7	11	-3022159	0,94	1,53E-06	3,63E-05	5,09
214340_at	ALOX12P2	245	NA	17	6756894	-0,76	1,53E-06	3,63E-05	5,09
204234_s_at	ZNF195	7748	O14628	11	-3380010	-1,22	1,53E-06	3,63E-05	5,09
206147_x_at	SCML2	10389	Q9UQR0	X	-18257432	-0,52	1,54E-06	3,63E-05	5,09
213745_at	ATRNL1	26033	Q5VV63	10	116853123	-0,32	1,54E-06	3,64E-05	5,08
208402_at	IL17A	3605	Q16552	6	52051184	-0,46	1,55E-06	3,65E-05	5,08
205642_at	CEP110	11064	Q7Z7A1	9	123850573	-0,78	1,55E-06	3,66E-05	5,08
221011_s_at	LBH	81606	Q53QV2	2	30454396	2,13	1,56E-06	3,68E-05	5,07
209236_at	SLC23A2	9962	Q9UGH3	20	-4833001	1,00	1,58E-06	3,71E-05	5,06
201076_at	NHP2L1	4809	P55769	22	-42069937	1,02	1,58E-06	3,71E-05	5,06
203729_at	EMP3	2014	P54852	19	48828628	2,18	1,59E-06	3,73E-05	5,06
212856_at	GRAMD4	23151	Q6IC98	22	47022657	-1,03	1,59E-06	3,73E-05	5,05
218029_at	FAM65A	79567	B4DEQ9	16	67562716	0,63	1,60E-06	3,74E-05	5,05
204715_at	PANX1	24145	Q96RD7	11	93862093	0,89	1,60E-06	3,74E-05	5,05
206285_at	NPHP1	4867	O15259	2	-110880915	-0,32	1,60E-06	3,75E-05	5,05
208136_s_at	MGC3771	81854	NA	16	-3160460	-0,55	1,61E-06	3,77E-05	5,04
216925_s_at	TAL1	6886	P17542	1	-47681962	-0,59	1,62E-06	3,78E-05	5,04
204778_x_at	HOXB7	3217	P09629	17	-46684602	-1,09	1,64E-06	3,82E-05	5,03
219382_at	SERTAD3	29946	Q9UJW9	19	-40946748	1,09	1,65E-06	3,84E-05	5,02
208063_s_at	CAPN9	10753	O14815	1	230883129	-2,66	1,66E-06	3,87E-05	5,01
219102_at	RCN3	57333	Q96D15	19	50030874	0,94	1,67E-06	3,87E-05	5,01
221623_at	BCAN	63827	Q96GW7	1	156611739	-0,49	1,67E-06	3,89E-05	5,00
208550_x_at	KCNG2	26251	Q9UJ96	18	77623667	0,82	1,68E-06	3,89E-05	5,00
221672_s_at	TRAPPC9	83696	Q96Q05	8	-140742585	0,80	1,68E-06	3,89E-05	5,00

S4 Table. Barcode genes exclusively associated with P-BE.

UNIPROT	*SYMBOLS*	*Entrez*	*ENSEMBL*	*Chr*	*CHRLOC*
D3DU92	RNPS1	10921	ENSG00000205937	16	-2303120
Q15287	HNRNPD	3184	ENSG00000138668	4	-83274466
Q14103	SPARC	6678	ENSG00000113140	5	-151041018
P09486	GOT2	2806	ENSG00000125166	16	-58741034
P00505	ARF3	377	ENSG00000134287	12	-49329991
P61204	GPX1	2876	ENSG00000233276	3	-49394610
P07203	TPP1	1200	ENSG00000166340	11	-6633996
O14773	LAMC1	3915	ENSG00000135862	1	182992594
P11047	PEA15	8682	ENSG00000162734	1	160175124
Q6NVY8	MCL1	4170	ENSG00000143384	1	-150547036
B1AKZ4	HSPA1A	3303	ENSG00000204388	6	31783290
Q15121	CIRBP	1153	ENSG00000099622	19	1269266
C8YZ26	CIRBP	1153	ENSG00000099622	19	1269266
Q07820	CTSB	1508	ENSG00000164733	8	-11700035
A8K5I0	TAGLN2	8407	ENSG00000158710	1	-159887902
B3KTT5	VCL	7414	ENSG00000035403	10	75757871
P08107	DCTN2	10540	ENSG00000175203	12	-57924093
Q14011	LDHB	3945	ENSG00000111716	12	-21788274
Q53XX5	DUSP1	1843	ENSG00000120129	5	-172195094
Q14011	STOM	2040	ENSG00000148175	9	-124101356
Q53XX5	GPNMB	10457	ENSG00000136235	7	23286315
P07858	CSDA	8531	ENSG00000060138	12	-10851677
P37802	BHLHE40	8553	ENSG00000134107	3	5021096
B3KXA2	CYR61	3491	ENSG00000142871	1	86046443
P18206	IFITM2	10581	ENSG00000185201	11	308106
B2RBK5	EMP1	2012	ENSG00000134531	12	13349601
Q13561	ETS2	2114	ENSG00000157557	21	40177848
P07195	COPS6	10980	ENSG00000168090	7	99686582
Q5U077	CNN3	1266	ENSG00000117519	1	-95362508
B4DU40	JUN	3725	ENSG00000177606	1	-59246463
P28562	JUNB	3726	ENSG00000171223	19	12902309
B1AM77	PPP4R1	9989	ENSG00000154845	18	-9546791
P27105	RRAGA	10670	ENSG00000155876	9	19049371
Q9H376	IER3	8870	ENSG00000137331	6	-30710976
Q14956	JAK1	3716	ENSG00000162434	1	-65298905
Q96F58	KRT5	3852	ENSG00000186081	12	-52908360
P16989	PLAT	5327	ENSG00000104368	8	-42032235
O14503	VWF	7450	ENSG00000110799	12	-6058039
Q6IB83	WWTR1	25937	ENSG00000018408	3	-149235021
O00622	TRIB1	10221	ENSG00000173334	8	126442562
Q6FI18	COL1A1	1277	ENSG00000108821	17	-48261458
Q01629	ST5	6764	ENSG00000166444	11	-8714899
P54849	SVIL	6840	ENSG00000197321	10	-29746276
P15036	NA	NA	NA	NA	NA
Q7L5N1	LEPROTL1	23484	ENSG00000104660	8	29952921
Q15417	SNRPD1	6632	ENSG00000167088	18	19192259
Q6FHA7	DRG1	4733	ENSG00000185721	22	31795538
P05412	AMOTL2	51421	ENSG00000114019	3	-134074189
P17275	NDUFS8	4728	ENSG00000110717	11	67798083
Q5U079	HDDC2	51020	ENSG00000111906	6	-125596495
Q8TF05	CAV2	858	ENSG00000105971	7	116139443
Q7L523	PPL	5493	ENSG00000118898	16	-4932507
P46695	COL15A1	1306	ENSG00000204291	9	101706137
P23458	EPHA2	1969	ENSG00000142627	1	-16450831
P13647	S100A9	6280	ENSG00000163220	1	153330329
P00750	PI3	5266	ENSG00000124102	20	43803539
P04275	CEBPD	1052	ENSG00000221869	8	-48649475
Q9GZV5	S100A2	6273	ENSG00000196754	1	-153533586
Q96RU8	TRIM16	10626	ENSG00000221926	17	-15531280
P02452	KRT15	3866	ENSG00000171346	17	-39669997
P78524	MAL	4118	ENSG00000172005	2	95691478
O95425	SPRR1B	6699	ENSG00000169469	1	153003678
Q569J5	KRT17	3872	ENSG00000128422	17	-39775691
NA	SPINK5	11005	ENSG00000133710	5	147443534
O95214	S100A7	6278	ENSG00000143556	1	-153430219
Q6FHL7	NA	NA	NA	NA	NA
P62314	SCEL	8796	ENSG00000136155	13	78109808
Q9Y295	CSRP2	1466	ENSG00000175183	12	-77252495
Q9Y2J4	SF1	7536	ENSG00000168066	11	-64532075
O00217	NA	NA	NA	NA	NA
Q7Z4H3	ACTN1	87	ENSG00000072110	14	-69340840
P51636	ACTN1	87	ENSG00000072110	14	-69340840
Q53X57	C1S	716	ENSG00000182326	12	7167979
O60437	NAP1L1	4673	ENSG00000187109	12	-76438671

UNIPROT	*SYMBOLS*	*Entrez*	*ENSEMBL*	*Chr*	*CHRLOC*
P39059	TSC22D3	1831	ENSG00000157514	X	-106956459
P29317	PSMB5	5693	ENSG00000100804	14	-23495060
P06702	PTK2	5747	ENSG00000169398	8	-141668501
P19957	STAT3	6774	ENSG00000168610	17	-40465342
P49716	NA	NA	NA	NA	NA
P29034	KRT6A	3853	ENSG00000205420	12	-52880958
O95361	KRT6B	3854	ENSG00000185479	12	-52840436
B3KVF5	FOS	2353	ENSG00000170345	14	75745480
P19012	TUBB6	84617	ENSG00000176014	18	12308256
P21145	CRYAB	1410	ENSG00000109846	11	-111779349
Q6FH77	KRT14	3861	ENSG00000186847	17	-39738532
P22528	RBPMS	11030	ENSG00000157110	8	30241943
Q04695	SERPINB3	6317	ENSG00000057149	18	-61322432
Q14666	SERPINB3	6317	ENSG00000057149	18	-61322432
Q9NQ38	KLK10	5655	ENSG00000129451	19	-51516000
P31151	KRT16	3868	ENSG00000186832	17	-39766032
NA	CARD10	29775	ENSG00000100065	22	-37886400
B7Z797	CD47	961	ENSG00000196776	3	-107761940
O95171	CSRP2	1466	ENSG00000175183	12	-77252495
Q16527	HSPA2	3306	ENSG00000126803	14	65007185
B7Z1Q1	HOPX	84525	ENSG00000171476	4	-57514153
Q15637	DYNC1H1	1778	ENSG00000197102	14	102430864
NA	COL4A1	1282	ENSG00000187498	13	-110801310
B3V8S3	FKBP9	11328	ENSG00000122642	7	32997004
P12814	PPAP2B	8613	ENSG00000162407	1	-56960432
Q1HE25	KRT17	3872	ENSG00000128422	17	-39775691
B3V8S3	SLC7A1	6541	ENSG00000139514	13	-30083551
P12814	CEBPB	1051	ENSG00000172216	20	48807375
Q1HE25	WEE1	7465	ENSG00000166483	11	9595227
P09871	SPARC	6678	ENSG00000113140	5	-151041018
P55209	POLR2J	5439	ENSG00000005075	7	-102113547
Q5JRJ2	C9orf3	84909	ENSG00000148120	9	97488885
Q99576	CARS	833	ENSG00000110619	11	-3022159
B4DUM9	AHNAK2	113146	ENSG00000185567	14	-105403590
P28074	KANK1	23189	ENSG00000107104	9	504702
B4E2N6	ARHGEF18	23370	ENSG00000104880	19	7459998
Q05397	YAP1	10413	ENSG00000137693	11	101981191
Q59GM6	KAZ	23254	ENSG00000189337	1	14925212
Q658W2	KRT6B	3854	ENSG00000185479	12	-52840436
P40763	SPRR1A	6698	ENSG00000169474	1	152956556
P29972	MINK1	50488	ENSG00000141503	17	4736634
P02538	DKK3	27122	ENSG00000050165	11	-11984544
P04259	SPRR1A	6698	ENSG00000169474	1	152956556
P01100	NA	NA	NA	NA	NA
Q6FG41	MAP2K3	5606	ENSG00000034152	17	21187967
Q9BUF5	HDGF	3068	ENSG00000143321	1	-156711899
P02511	TRMT112	51504	ENSG00000173113	11	-64084167
P02533	YPEL5	51646	ENSG00000119801	2	30369749
Q93062	BAG3	9531	ENSG00000151929	10	121410881
P29508	DYNLRB1	83658	ENSG00000125971	20	33104203
P29508	NGFRAP1	27018	ENSG00000166681	X	102631267
O43240	PHLDA1	22822	ENSG00000139289	12	-76419227
P08779	SLC38A2	54407	ENSG00000134294	12	-46751971
Q9BWT7	NDUFA3	4696	ENSG00000170906	19	54606159
Q08722	OSBPL10	114884	ENSG00000144645	3	-31702317
Q16527	SLC24A3	57419	ENSG00000185052	20	19193289
P54652	TMEM45A	55076	ENSG00000181458	3	100211462
B7WNL2	NA	NA	NA	NA	NA
Q9BPY8	RHCG	51458	ENSG00000140519	15	-90014637
Q14204	CRNN	49860	ENSG00000143536	1	-152381718
P02462	AIM1L	55057	ENSG00000176092	1	-26648349
A7YQ73	TMEM176B	28959	ENSG00000106565	7	-150488377
O95302	CRCT1	54544	ENSG00000169509	1	152486977
O14495	SPRR2C	6702	NA	1	-153112594
Q04695	SLC38A2	54407	ENSG00000134294	12	-46751971
Q14666	HSPB8	26353	ENSG00000152137	12	119616594
P30825	TNS1	7145	ENSG00000079308	2	-218664511
P17676	TUG1	55000	NA	22	31365633
B3KVE1	NA	NA	NA	NA	NA
P30291	MAFF	23764	ENSG00000185022	22	38597938
Q86V29	AQP3	360	ENSG00000165272	9	-33441161
P09486	PI3	5266	ENSG00000124102	20	43803539
P52435	SPSB3	90864	ENSG00000162032	16	-1826713
Q8N6M6	PLSCR3	57048	ENSG00000187838	17	-7293054

Supplementary Results

CYR61 and *TAZ* upregulation and focal epithelial to mesenchymal transition may be early predictors of Barrett's esophagus malignant progression

Joana Cardoso, Marta Mesquita, António Dias Pereira, Mónica Bettencourt-Dias, Paula Chaves, José B. Pereira-Leal

Two main reasons motivated us to develop a new bioinformatics pipeline to search for early biomarkers of BE malignant progression using publicly available transcriptome microarray data. First, while several datasets on BE are in the public domain, none of them simultaneously contained samples from EA, P-BE and nonP-BE that could be directly compared. This issue required us to merge the existing samples from distinct datasets and compare them by DEA. However, inter-dataset DEA is very sensitive to technical noise. Methods such as ComBat and SVA remove batch-associated noise (reviewed in (1)) but due to the reduced number of available BE samples these methods also removed most of the meaningful biological signal. To better deal with the inter-dataset noise and to take advantage of genes with bimodal expression, which are in principle more easily translated to protein level differences and thus the ideal biomarker candidates, we included the Gene Expression Barcode 2.0 binarization algorithm developed by McCall *et al.* (2, 3). The produced barcodes are very robust against random sources of noise because their calculation relies on the usage of a large amount of annotated public data as a reference to binarize the expression of each gene (1=expressed, 0=not expressed) per individual sample.

In the context of our pipeline framework (S1 Fig), we curated three publicly available datasets of BE data on the Affymetrix HG-133A GeneChip® microarray platform. Overall, these three datasets contained a total of 33 BE samples. Samples described as collected in the

context of a clinically diagnosed EA (4) were assigned to the P-BE group (n=8) and samples not associated with EA at the time of analysis (5, 6) were assigned to the nonP-BE group (n=25). After frozen robust multi-array (fRMA) sample normalization (2, 3) we verified that individual samples in the merged set displayed highly correlated expression profiles (Parson's correlation mean=0.92, min=0.80) (S2 Fig). This is indicative that despite the three distinct data sources and associated batch noise, the biological signal of BE samples was very comparable.

We next identified differential gene expression (DGE) between P-BE and nonP-BE samples using a Bayesian DEA, as illustrated in S1 Fig C. Under the very conservative statistical criteria logarithm of the odds (Lods)≥5, probability DGE>99.33%) and a false discovery rate (FDR) of 3.9×10-5 for DGE, we identified 958 independent probe sets mapping to 799 unique ENTREZ id genes (S3 Table). Among the unique genes, we have found up-regulation for 442 (S1 Fig C) and down-regulation for 357 genes. The 799 genes are able to correctly segregate P-BE from nonP-BE samples (S3 Fig A). As anticipated (see Materials and Methods section), no significant probe sets were found after testing of EA samples across distinct datasets (Kimchi *et al.* (4) vs. Watts *et al.* (6)). Barcode binarization of fRMA normalized BE and EA data (S1 Fig D) and the subsequent intersection of P-BE and nonP-BE barcodes allowed us to find a set of 148 probe sets (S4 Table) expressed in the P-BE samples (barcode=1) but oppositely marked as non-expressed (barcode=0) in the nonP-BE samples (S1 Fig E). To find candidates more likely associated with malignancy we assumed that P-BE-specific probe sets should overlap with probe sets expressed in EA (barcode=1). Thus, we have next intersected the 148 and 1195 probe sets, respectively from P-BE and EA barcodes. This procedure resulted in the filtering of malignancy-linked barcode candidates to 40 probe sets, corresponding to 38 unique genes (S1 Fig F), up-regulated in P-BE and EA samples as compared to nonP-BE samples. To maximize the discovery of BE early

progression biomarkers that most likely could be translated into routine clinical practice, we defined our top candidates as genes up-regulated according to DGE results and with barcode values set to 1 (S1 Fig G). With this final step we slimed down the final list of candidates to 20 probe sets, corresponding to 19 unique genes over-expressed in P-BE (S1 Fig H).

Systems biology approach for biomarker prioritization

To improve biomarker prioritization we thought of integrating biological functions of filtered genes with functions potentially relevant for BE malignant progression, by uncovering the gene GO-BP categories over-represented among the 19 filtered biomarkers. First, we used a guilt-by-association GeneMANIA tool (7) to build a functional association network between the set of 19 genes and 100 network neighbors (S6 Fig A). Secondly we used all network players to evaluate the enriched GO-BP categories by GSEA. We have used this alternative strategy instead of directly applying GSEA to the set of 19 genes due its reduced number. GSEA on GeneMania network genes (biomarkers and neighbors) highlighted that the significant (FDR<0.05) GO-BP top categories related with cell adhesion/motility, inflammation, differentiation/wounding, vasculature development, extracellular-matrix and response to stimulus among others (S6 Fig B, S5 Table).

To further increase the odds of success of downstream validation efforts, we have used knowledge-driven biomarker prioritization criteria. To be included, candidates must be functionally linked to 1) top biological functions detected by GSEA and to 2) phenotype features that characterizes BE (e.g. differentiation/wounding responses) and finally 3) candidates must have been previously associated to cancer progression in other tumors. Thus, we have searched the literature for functional characterization of the set of 19 genes and selected two potential biomarkers for proof-of-principle experimental validation. CYR61 (alias CCN1) was the most significantly over-expressed gene in our DGE analysis (S3 Table) and according to barcode analysis is expressed in >93 % of EA samples. Its over-expression

is involved in the malignant progression and prognosis of major tumors (breast, prostate, colorectal and others outlined in Table 1). CYR61 was recently identified in the context of breast cancer (8) as a downstream target of WWTR1 (alias TAZ), one of the barcode and differentially expressed genes. TAZ up-regulation is also implicated in the progressive phenotype of malignant tumors such as breast, colorectal and glioma, among others (Table 1) and was expressed according to barcode in 87% of the EA tumors in our dataset. In addition to CYR61, six other TAZ downstream target genes (SPARC, IER3, JUN, ACTN1, COL4A1, PPAP2B) were significantly enriched (*P*-value=2.2×10-4) among our group of 19 candidates (S7 Fig A), suggesting that specific pathways where CYR61, TAZ and likely other functionally-linked genes operate are deregulated during BE-associated EA progression. To further test this functional link hypothesis we explored CYR61 and TAZ interacting genes with gene GeneMania networking algorithm (S7 Fig B). Among network genes we identified barcode genes (e.g. FOS, JUN, LAMC1), significantly up-regulated genes (e.g. TEAD3, FOSB, ATF3) of which some are TAZ downstream targets (e.g. CTFG, JUN, EGR1). Analysis of top GO-BP categories (FDR<0.01) over-represented among CYR61, TAZ and neighbors (S7 Fig C) pointed to biological functions involving cell adhesion/migration, transcription and response to stimulus (S6 Table). One hypothesis suggested by the data is that P-BE samples have deregulated transcriptional responses to diverse stimuli, including an up-regulation of cell adhesive and migratory properties which will ultimately contribute to the malignant phenotype of BE cells.

References

1. Chen C, Grennan K, Badner J*, et al.* Removing batch effects in analysis of expression microarray data: an evaluation of six batch adjustment methods. *PLoS One* 2011; 6(2): e17238.

2. McCall MN, Uppal K, Jaffee HA, Zilliox MJ, Irizarry RA. The Gene Expression Barcode: leveraging public data repositories to begin cataloging the human and murine transcriptomes. *Nucleic Acids Res* 2011 Jan; 39(Database issue): D1011-5.
3. Zilliox MJ, Irizarry RA. A gene expression bar code for microarray data. *Nat Methods* 2007 Nov; 4(11): 911-3.
4. Kimchi ET, Posner MC, Park JO, *et al.* Progression of Barrett's metaplasia to adenocarcinoma is associated with the suppression of the transcriptional programs of epidermal differentiation. *Cancer Res* 2005 Apr 15; 65(8): 3146-54.
5. Stairs DB, Nakagawa H, Klein-Szanto A, *et al.* Cdx1 and c-Myc foster the initiation of transdifferentiation of the normal esophageal squamous epithelium toward Barrett's esophagus. *PLoS One* 2008; 3(10): e3534.
6. Watts GS, Tran NL, Berens ME, *et al.* Identification of Fn14/TWEAK receptor as a potential therapeutic target in esophageal adenocarcinoma. *Int J Cancer* 2007 Nov 15; 121(10): 2132-9.
7. Montojo J, Zuberi K, Rodriguez H, *et al.* GeneMANIA Cytoscape plugin: fast gene function predictions on the desktop. *Bioinformatics* 2010 Nov 15; 26(22): 2927-8.
8. Zhang H, Liu CY, Zha ZY, *et al.* TEAD transcription factors mediate the function of TAZ in cell growth and epithelial-mesenchymal transition. *J Biol Chem* 2009 May 15; 284(20): 13355-62.

APPENDIX 2 – Supplementary material for paper: *"Centrosome amplification arises before neoplasia and increases upon p53 loss in tumorigenesis"*

Supplemental material

Lopes et al., https://doi.org/10.1083/jcb.201711191

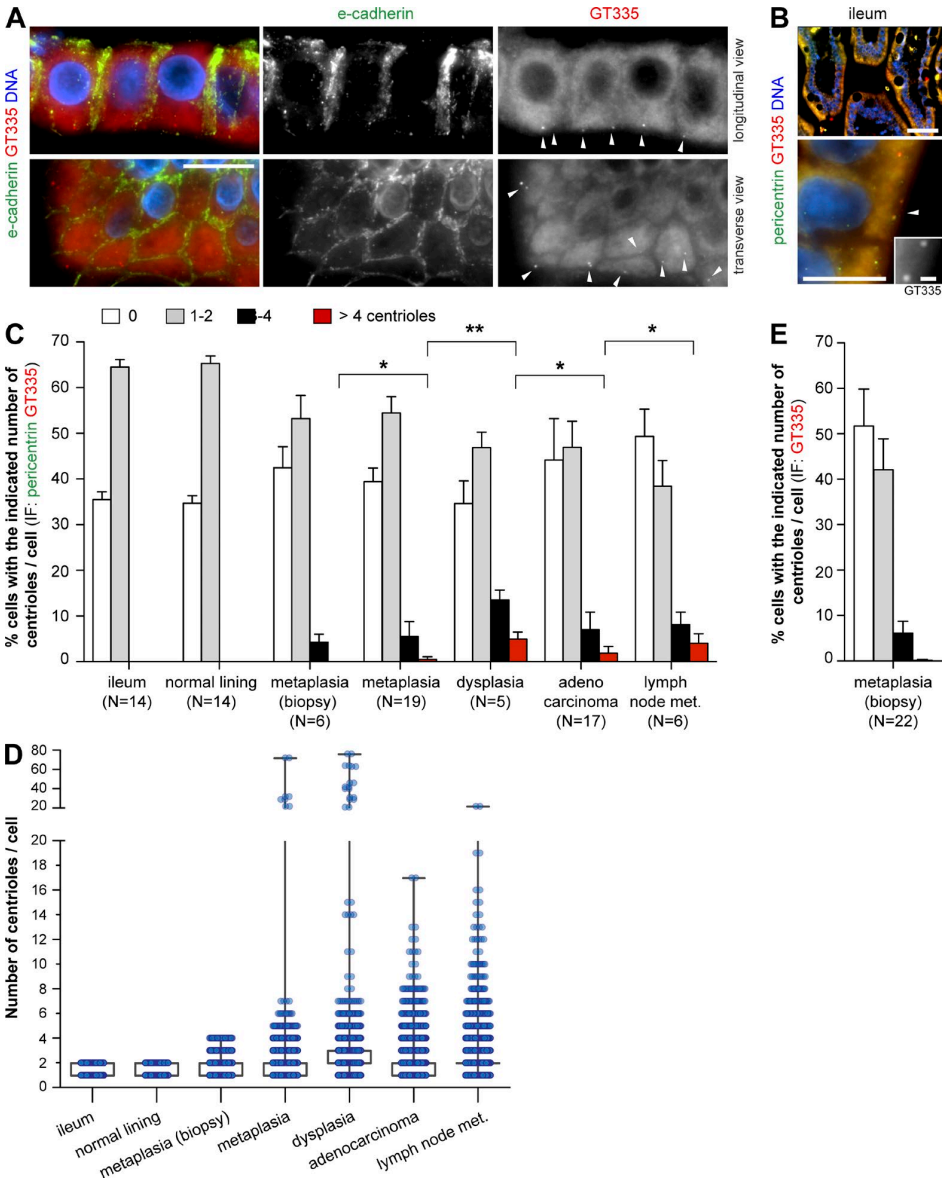

Figure S1. **Analysis of centriole numbers in patient samples. (A and B)** Tissue samples of the normal ileum were stained for the cell membrane (E-cadherin), centrioles (GT335), and DNA (A) or for PCM (pericentrin), centrioles (GT335), and DNA (B). **(A)** Representative images show that the cell's limits, defined by E-cadherin staining, are easily distinguished using solely the GT335 background staining. Arrowheads indicate centrioles. Bar, 10 µm. **(B)** Representative images with enlargements of cells and centrioles in a single cell (arrowhead). Bars: (top) 50 µm; (bottom, main image) 10 µm; (bottom, inset) 1 µm. **(C and D)** The number of centrioles in each cell was analyzed in samples of the normal ileum, of the normal lining of the esophagus, and of the different stages of BE multistep tumorigenesis progression: metaplasia from biopsies of patients that have not progressed to this date (cohort 1) and areas of metaplasia, dysplasia, adenocarcinoma, and lymph node metastasis (met.) from cohorts 2 and 3. Samples were stained for PCM (pericentrin), centrioles (GT335), and DNA. **(C)** Quantification of cells with the indicated centriole number content for the tissue samples present in each case analyzed. $n \geq 200$ cells/tissue/patient. N, number of cases analyzed. Cells with more than four centrioles: *, $P < 0.05$; **, $P < 0.01$ (two-sample Wilcoxon rank-sum [Mann-Whitney]; independent samples; two sided; p-values were adjusted for multiple testing using the Benjamini and Hochberg method). **(D)** Number of centrioles per cell (individual circles) for the tissue samples present in each case analyzed. $n = 200$ cells/tissue/patient; number of cases was analyzed as in C. Individual data points are plotted over the box plots. **(E)** The number of centrioles in each cell was analyzed in metaplasia samples from biopsies of another 22 patients that have not progressed to this date. Samples were stained for centrioles (GT335) only and DNA. Quantification of cells with the indicated centriole number content. $n \geq 200$ cells/patient. N, number of cases analyzed. Error bars show means ± SD.

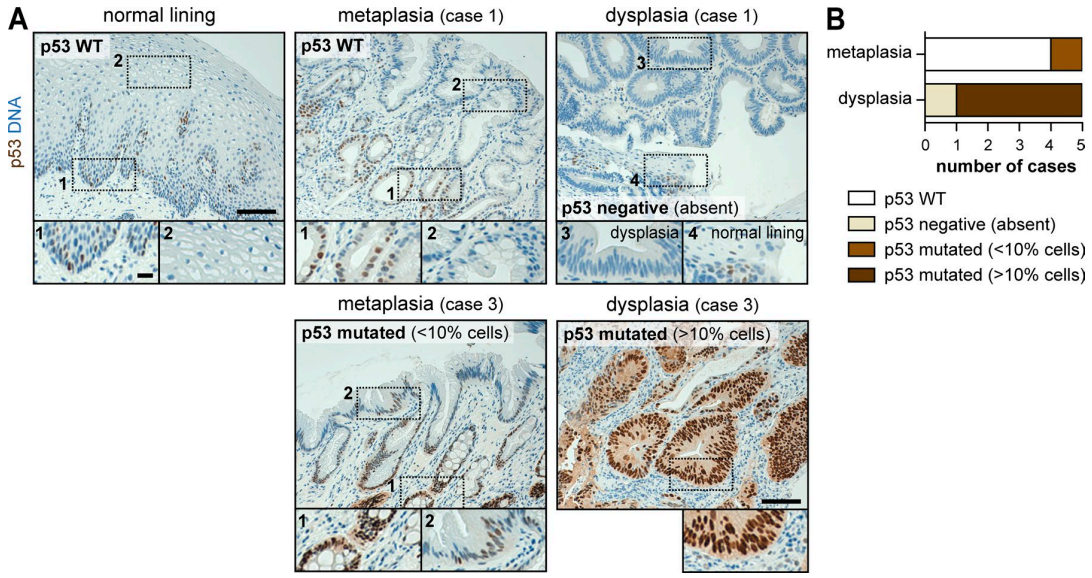

Figure S2. **Analysis of p53 status in patient samples by IHC. (A and B)** p53 expression was analyzed by IHC in tissue samples of the normal lining and in metaplasia and dysplasia samples from the same patient (cohort 2). **(A)** Representative images of p53 protein expression in the different tissue samples. DNA is shown in blue. Insets show 2× magnification of indicated areas. As WT p53 protein has a short half-life, it is only weakly detected in the nucleus of some proliferating cells (1) and not in differentiated areas (2). Altered p53 protein expression, indicative of p53 mutation, was considered when there was either a strong accumulation within the nucleus (scored as focal or diffuse if there were <10% or >10% of positive cells, respectively) caused by prolonged half-life of p53 mutants (p53 mutated) or absence of p53 staining (3) within a context of WT staining (metaplasia or native epithelium [4]) caused by p53 mutations, leading to truncation or epigenetic silencing, in which case p53 was not detected by IHC (p53 negative [absent]). Bars: (main images) 100 µm; (insets) 20 µm. **(B)** Histogram showing the summary of p53 status in metaplasia and dysplasia areas of each case analyzed.

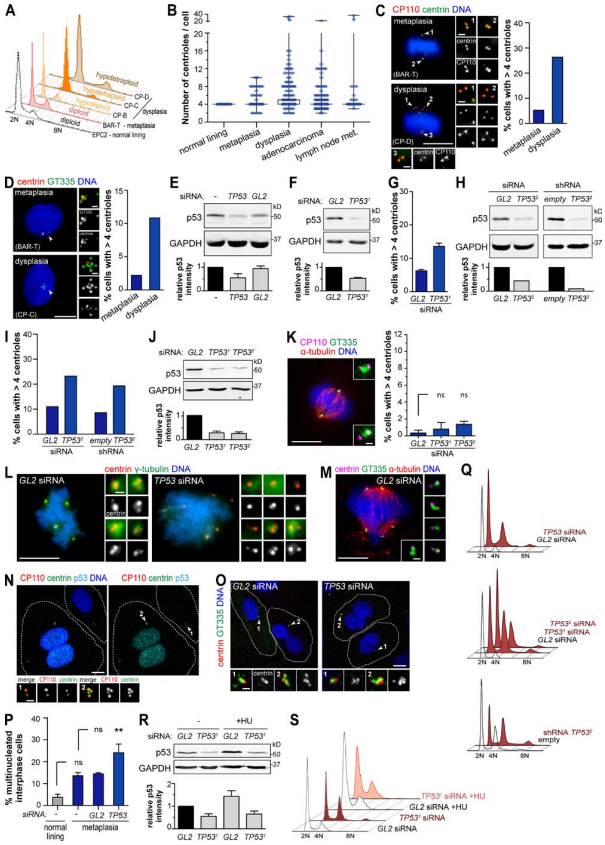

Figure S3. **Centriole number and ploidy in cell lines. (A)** Flow cytometry analysis of cells derived from the normal lining, metaplasia, and dysplasia. **(B)** Cells derived from the normal lining and from all stages of BE progression were stained for centrioles (centrin and GT335) and DNA. The number of centrioles was analyzed in each individual mitotic cell (individual circles, $n \geq 60$/cell line) of the indicated tissue of origin. Individual data points are plotted over the box plots. Met., metastasis. **(C and D)** Left: Metaplasia and dysplasia cells were stained for centrioles (centrin and CP110 in C, and centrin and GT335 in D) and DNA. Representative images with enlargements of centrioles (arrowheads) are shown. **(C)** Right: Quantification of mitotic cells with centriole amplification. $n \geq 50$/cell line. **(D)** Right: Quantification of mononucleated interphase cells with centriole amplification. $n \geq 90$/cell line. **(E)** Metaplasia cells were transfected with control (*GL2*) siRNA or siRNA against endogenous p53 (*TP53*). Top: Depletion of p53 was confirmed by WB. Bottom: Quantification of p53 relative to the loading control (GAPDH) is shown; ratios were normalized to the untreated cells. Three independent experiments. **(F and G)** Metaplasia cells were transfected with control (*GL2*) or p53 ($TP53^1$) siRNA. **(F)** Top: Depletion of p53 was confirmed by WB. Bottom: Quantification of p53 relative to the loading control (GAPDH) is shown; ratios were normalized to the control. Two independent experiments. **(G)** Cells were stained for centrioles (centrin and GT335) and DNA. Quantification of mitotic cells with centriole amplification. $n \geq 60$ cells/condition/experiment. Two independent experiments. **(H and I)** Centriole number was analyzed in metaplasia-derived cells containing pSUPER-p53RNAi (shRNA $TP53^2$) or the empty pSUPER vector (*empty*) as well as in metaplasia cells transfected with control (*GL2*) siRNA or siRNA against p53 with the same sequence against p53 ($TP53^2$) as the one used to generate the pSUPER-p53RNAi plasmid. **(H)** Top: Depletion of p53 was confirmed by WB. Data are from one experiment. Bottom: Quantification of p53 relative to the loading control (GAPDH) is shown; ratios were normalized to the controls. **(I)** Cells were stained for centrioles (centrin and GT335) and DNA. Quantification of mitotic cells with centriole amplification. $n \geq 100$ cells/condition. One experiment. **(J and K)** Normal lining cells were transfected with control (*GL2*) siRNA or two independent siRNAs against p53 ($TP53^1$ and $TP53^2$). **(J)** Top: Depletion of p53 was confirmed by WB. Bottom: Quantification of p53 relative to the loading control (GAPDH) is shown; ratios were normalized to the control. Three independent experiments. **(K)** Left: Cells were stained for centrioles (CP110 and GT335), microtubules (α-tubulin), and DNA. Representative images with enlargements of centrioles are shown. Right: Quantification of mitotic cells with centriole amplification. $n \geq 80$/condition/experiment. Three independent experiments. **(L and M)** Metaplasia cells transfected with control (GL2) or p53 (*TP53*) siRNA were stained for centrioles (centrin), PCM (γ-tubulin), and DNA (L) or for centrioles (centrin and GT335), microtubules (α-tubulin), and DNA (M). Representative images with enlargements of centrioles are shown. **(N)** Metaplasia cells were stained for p53, centrioles (centrin and CP110), and DNA. Dashed lines denote individual cell outlines given by the CP110/centrin background signal. Insets show centrioles (arrowheads) in p53-negative (1) and p53-positive (2) cells. **(O and P)** Metaplasia cells transfected with control (*GL2*) or p53 (*TP53*) siRNA were stained for centrioles (centrin and GT335) and DNA. **(O)** Dashed lines denote individual cell outlines given by the centrin/GT335 background signal. Insets show centrioles (arrowheads) in mononucleated (1) and multinucleated (2) cells. Bars: (main images) 10 µm; (insets) 1 µm. **(P)** Quantification of multinucleated interphase cells. Untreated metaplasia and normal lining cells were also analyzed. $n \geq 700$ cells/condition/experiment. Three independent experiments. **(K and P)** **, $P < 0.01$ (ANOVA). **(Q)** Flow cytometry analysis of metaplasia cells transfected with control (GL2) siRNA or three independent siRNAs against p53 (endogenous p53, *TP53*; total p53, $TP53^1$ or $TP53^2$) and of metaplasia-derived cells containing pSUPER-p53RNAi (shRNA $TP53^2$) or the empty pSUPER vector (*empty*). **(R and S)** Metaplasia cells transfected with control (*GL2*) or p53 (*TP53*) siRNA were either treated with (S phase blocked and hydroxyurea [+HU]) or without hydroxyurea (DMSO, asynchronous, and –). **(R)** Top: Depletion of p53 was confirmed by WB. Bottom: Quantification of p53 relative to the loading control (GAPDH) is shown; ratios were normalized to the control. Three independent experiments. Error bars show means ± SEM. **(S)** S phase blocking of cells upon hydroxyurea treatment was assessed by flow cytometry analysis.

Table S1. **Centriole number analysis in paraffin-embedded tissue**

Tissue areas	**Centriole number per cell (min–max)**				**Cells with centriole amplification**			
					%			
Normal lining – esophagus								
Cases 1–14	0–2				0.0			
Normal lining – ileum								
Case 1–14	0–2				0.0			
	M	**DYS**	**ADC**	**LNM**	**M**	**DYS**	**ADC**	**LNM**
Cohort 1								
Case 1	1–4	-	-	-	0.0	-	-	-
Case 2	1–3	-	-	-	0.0	-	-	-
Case 3	1–4	-	-	-	0.0	-	-	-
Case 4	1–4	-	-	-	0.0	-	-	-
Case 5	1–4	-	-	-	0.0	-	-	-
Case 6	1–4	-	-	-	0.0	-	-	-
Cohort 2								
Case 1	1–5	1–7	-	-	1.5	8.5	-	-
Case 2	1–5	1–5	-	-	1.5	4.0	-	-
Case 3	1–6	1–7	1–7	-	1.5	9.5	7.5	-
Case 4	1–72	1–76	1–6	-	3.5	9.0	5.0	-
Case 5	1–6	1–14	1–17	-	1.5	7.0	7.0	-
Cohort 3								
Case 1	1–5	-	1–8	-	0.5	-	3.0	-
Case 2	1–6	-	1–13	1–22	1.0	-	5.5	13.0
Case 3	1–4	-	1–7	1–7	0.0	-	0.5	2.5
Case 4	1–4	-	1–8	-	0.0	-	2.0	-
Case 5	1–4	-	1–7	1–8	0.0	-	1.0	6.5
Case 6	1–5	-	1–7	-	0.5	-	1.5	-
Case 7	1–4	-	1–12	-	0.0	-	2.0	-
Case 8[a]	1–5	-	1–5	1–15	0.5	-	2.5	9.5
Case 9	1–4	-	1–10	1–19	0.0	-	0.5	13.0
Case 10	1–7	-	1–5	-	2.5	-	6.5	-
Case 11	1–4	-	1–8	1–7	0.0	-	1.5	5.0
Case 12	1–5	-	1–8	-	0.5	-	3.0	-
Case 13	1–5	-	1–6	-	1.0	-	3.0	-
Case 14	1–4	-	1–5	-	0.0	-	2.0	-

ADC, adenocarcinoma; DYS, dysplasia; LNM, lymph node metastasis; M, metaplasia.
[a]The cell line ESO51 used in this study was derived from the primary tumor of this case.

Table S2. **Analysis of TP53 status**

Case/cell line	Experiment	Metaplasia			Dysplasia		
		Coding	Protein	% Reads	Coding	Protein	% Reads
Patient tissue samples – cohort 2							
Case 1	NGS	216delC	V73fs	22.5			
					586C>T	R196*	60.4
					569_570insC	P191fs	32.0
					86_87insA	N29fs	1.6
		751A>C	I251L	3.5	751A>C	I251L	4.4
		153_154insA	Q52fs	24.2	153_154insA	Q52fs	28.1
		215C>G	*P72R*	*60.9*	*215C>G*	*P72R*	*74.5*
	IHC	WT			Negative (absent)		
Case 2	NGS	n.d.			n.d.		
	IHC	WT			Intensity: moderate		
					>10% cells mutated		
Case 3	NGS				455delC	P152fs	96.6
					452C>A	P151H	3.4
		751A>C	I251L	3.0	751A>C	I251L	4.2
		404G>T	C135F	36.9	404G>T	C135F	49.9
		215C>G	*P72R*	*62.3*	*215C>G*	*P72R*	*76.5*
	IHC	Intensity: weak			Intensity: strong		
		<10% cells mutated			>10% cells mutated		
Case 4	NGS	733G>A	G245S	3.4			
					799C>T	R267W	17.6
					153_154insA	Q52fs	22.9
		751A>C	I251L	3.3	751A>C	I251L	6.0
		215C>G	*P72R*	*62.3*	*215C>G*	*P72R*	*76.5*
	IHC	WT			Intensity: strong		
					>10% cells mutated		
Case 5	NGS				638G>A	R213Q	3.3
					524G>A	R175H	6.6
					153_154insA	Q52fs	30.1
		215C>G	*P72R*	*51.5*	*215C>G*	*P72R*	*45.8*
	IHC	WT			Intensity: moderate		
					>10% cells mutated		
Cell line							
BAR-T	NGS	*215C>G*	*P72R*	*98.3*			

*, nonsense mutation; fs, frameshift mutation; n.d., not determined due to insufficient amount of quality DNA; text in italics indicate known polymorphism in p53.

Table S3 is an attached Excel file showing cell line information and centriole analysis.

Table S3. Cell line information and centriole analysis

		Centriole number		Ploidy	Genetic alterations		
Tissue of origin	**Cell line**	**Centrioles/cell** (min-max)	**Amplification** (%)		**p53 status**	**p16 status**	**References**
Retinal pigment Epithelium	RPE1	2 - 4	0.0	diploid	p53 functionally intact	p16 functionally intact	
Normal lining esophagus	EPC2	2 - 4	0.0	diploid	p53 functionally intact	p16 functionally intact	Harada et al. 2003
Metaplasia	BAR-T	4 - 10	8.4	diploid (minimal chromosomal abnormalities)	p53 functionally intact	p16 expression is lost	Jaiswal et al. 2007
	BAR-T10	4 - 10	15.2	diploid (minimal chromosomal abnormalities)	p53 functionally intact	p16 expression is lost	Zhang et al. 2010
Dysplasia	CP-B	2 - 12	27.4	aneuploid (hypodiploid)	17p LOH/missense mutation (c.524G>A) p.R175H	9p LOH/mutation	Palanca-Wessels et al. 1998, ATCC
	CP-C	1 - 34	36.6	aneuploid (hypotetraploid)	17p LOH/missense mutation (c.724C>T) p.R248W	9p LOH	Palanca-Wessels et al. 1998, ATCC
	CP-D	3 - 15	31.3	aneuploid (hypotetraploid)	17p LOH/missense mutation (frameshift 302)	9p LOH/mutation	Palanca-Wessels et al. 1998, ATCC
Adenocarcinoma	SK-GT-4	2 - 12	15.6	aneuploid (hyperdiploid)	nonsense mutation (c.298C>T) p.Q100*	no mutation	Boonstra et al. 2010, EACC
	OE19	2 - 6	1.2	aneuploid (hyperdiploid)	frameshift c.929dupA	-	Boonstra et al. 2010, EACC
	OACP4	3 - 5	1.5	aneuploid (hyperdiploid)	nonsense mutation (c.574C>T) p.192*	-	Boonstra et al. 2010, EACC
	FLO-1	3 - 8	5.9	aneuploid (hypotetraploid)	missense mutation (c.830G>T) p. C277F	-	Boonstra et al. 2010, EACC
	ESO26	3 - 8	9.9	aneuploid (hypodiploid)	missense mutation (c.742C>T) p.R248W	-	Boonstra et al. 2010, EACC
	ESO51*	3 - 12	10.0	aneuploid (hypotetraploid)	missense mutation (c.524G>A) p.R175H	-	Boonstra et al. 2010, EACC
	OE33	3 - 22	31.8	aneuploid (hypotetraploid)	missense mutation (c.404G>A) p.C135Y	mutated	Boonstra et al. 2010, EACC
Lymph node metastasis	OACM5.1	4 - 37	11.3	aneuploid (hypodiploid)	missense mutation (c.164delC/c.743G>A)	-	Boonstra et al. 2010, EACC

*The cell line ESO51 used in this study was derived from the primary tumor of Case 8 from Cohort 3 (see Table S1).

References

Boonstra, J.J., R. van Marion, D.G. Beer, L. Lin, P. Chaves, C. Ribeiro, A.D. Pereira, L. Roque, S.J. Darnton, N.K. Altorki, et al. 2010. Verification and unmasking of widely used human esophageal adenocarcinoma cell lines. J. Natl. Cancer Inst. 102:271–274.

Harada, H., H. Nakagawa, K. Oyama, M. Takaoka, C.D. Andl, B. Jacobmeier, A. von Werder, G.H. Enders, O.G. Opitz, and A.K. Rustgi. 2003. Telomerase induces immortalization of human esophageal keratinocytes without p16INK4a inactivation. *Mol. Cancer Res.* 1:729–738.

Jaiswal, K.R., C.P. Morales, L.A. Feagins, K.G. Gandia, X. Zhang, H.Y. Zhang, K. Hormi-Carver, Y. Shen, F. Elder, R.D. Ramirez, et al. 2007. Characterization of telomerase-immortalized, non-neoplastic, human Barrett's cell line (BAR-T). *Dis. Esophagus*. 20:256–264.

Palanca-Wessels, M.C.A., A. Klingelhutz, B.J. Reid, T.H. Norwood, K.E. Opheim, T.G. Paulson, Z. Feng, and P.S. Rabinovitch. 2003. Extended lifespan of Barrett's esophagus epithelium transduced with the human telomerase catalytic subunit: a useful in vitro model. *Carcinogenesis*. 24:1183–1190.

Zhang, X., C. Yu, K. Wilson, H.Y. Zhang, S.D. Melton, X. Huo, D.H. Wang, R.M. Genta, S.J. Spechler, and R.F. Souza. 2010. Malignant transformation of non-neoplastic Barrett's epithelial cells through well-defined genetic manipulations. *PLoS One*. 5:1–11.